MATHEMATICAL METHODS FOR ACCIDENT RECONSTRUCTION

A FORENSIC ENGINEERING PERSPECTIVE

HAROLD FRANCK DARREN FRANCK

CRC Press
Taylor & Francis Group

MATHEMATICAL METHODS FOR ACCIDENT RECONSTRUCTION

A FORENSIC ENGINEERING PERSPECTIVE

MATHEMATICAL METHODS FOR ACCIDENT RECONSTRUCTION

A FORENSIC ENGINEERING PERSPECTIVE

HAROLD FRANCK   DARREN FRANCK

CRC Press
Taylor & Francis Group
Boca Raton   London   New York

CRC Press is an imprint of the
Taylor & Francis Group, an **informa** business

CRC Press
Taylor & Francis Group
6000 Broken Sound Parkway NW, Suite 300
Boca Raton, FL 33487-2742

Printed in the United States of America on acid-free paper
10 9 8 7 6 5 4 3 2 1

International Standard Book Number: 978-1-4200-8897-7 (Hardback)

Library of Congress Cataloging-in-Publication Data

Franck, Harold.
Mathematical methods for accident reconstruction : a forensic engineering perspective / Harold Franck and Darren Franck.
p. cm.
Includes bibliographical references and index.
ISBN 978-1-4200-8897-7 (alk. paper)
1. Forensic engineering--Mathematics. 2. Traffic accidents. I. Franck, Darren. II. Title.

TA219.F73 2009
363.12'5650151--dc22 2009013022

Visit the Taylor & Francis Web site at
http://www.taylorandfrancis.com

and the CRC Press Web site at
http://www.crcpress.com

Acknowledgments

The authors wish to acknowledge the diligent conscientious efforts of Janice Franck, their wife and mother, in the long process of the preparation of this book. Her patience, insight, constructive criticism, and extensive computer and grammatical skills proved invaluable. The authors also wish to acknowledge the invaluable help from Taylor & Francis.

Table of Contents

Symbols and Units

Commonality in nomenclature makes studying technical and scientific subjects easier. Noncommon nomenclature is usually a result of disjointed and haphazard organization. Every attempt has been made in this book to carry a common nomenclature. It is with this concept in mind that we introduce the following symbols. In all cases bold lettering represents vector quantities and nonbold lettering represents scalar quantities.

Coordinates

x, y, z	rectangular coordinate points in space
ρ, θ, z	cylindrical coordinate points in space
r, θ, φ	spherical coordinate points in space
X, Y, ψ	vehicle-fixed coordinates

Unit vectors

$\mathbf{a}_x$, $\mathbf{a}_y$, $\mathbf{a}_z$	unit vectors in rectangular coordinates
$\mathbf{a}_\rho$, $\mathbf{a}_\varphi$, $\mathbf{a}_z$	unit vectors in cylindrical coordinates
$\mathbf{a}_r$, $\mathbf{a}_\theta$, $\mathbf{a}_\varphi$	unit vectors in spherical coordinates

Symbols

F	vector force measured in lbs
PDOF	principal direction of force
$\mathbf{a}_\mathbf{F}$	unit vector of **F**=PDOF
Γ	vector moment measured in ft-lbs
r	radial moment arm of force **F**
$\mathbf{a}_\mathbf{r}$	unit vector of vector moment
$\boldsymbol{v}$	velocity vector measured in ft/sec or
$\mathbf{a}_\mathrm{v}$	unit vector of velocity vector
a	acceleration vector measured in ft/sec^2
$\mathbf{a}_\mathrm{a}$	unit vector of acceleration vector
m	mass
w	weight measure in lbs
g	acceleration due to gravity=32.2
μ	coefficient of frication or drag factor

μ_k	coefficient of kinetic friction
μ_s	coefficient of static friction
CG	center of gravity or center of mass
T	torque measured in ft-lb
K_e	kinetic energy
K_p	potential energy
E_{ep}	elastic potential energy
W	work
D	distance measured in ft
t	time measured in seconds
A_i	precollision angle
A_f	postcollision angle
V_i	initial speed
V_f	final speed
I	moment of inertia
$\mathbf{w}$	angular velocity
$\mathbf{L}$	angular momentum
Γ	torque
Ω	vector angular velocity of procession
e	coefficient of restitution
$\mathbf{H}$	vector angular momentum
ρ	density
WB	wheel base
$\mathbf{P}$	power

Preface

Scope

This book is intended for engineers and scientists who perform vehicular accident reconstructions. Accident reconstructions involving moving vehicles include automobiles, small and large trucks, bicycles, motorcycles, all terrain vehicles, pedestrians, trains, and a variety of construction equipment. Construction equipment may include motorized hoists and cranes, tracked or rubber tired dozers, scoops, and hoes. The book is anchored on basic principles of physics that may be applied to any of the above-named vehicles or equipment. An important component of the book is aimed at providing the limits of applicability of the various physical methods employed in accident reconstruction. This book has developed over the course of the last 25 years as the authors have been involved in the investigation of a variety of accident scenarios. Included in the hundreds of reconstructions, a variety of similarities and differences in accident scenarios have been noted. Many reconstructions can be classified by types, such as head-on collisions between two vehicles, T-bone collisions, loss of control, mechanical failure, and other accident types. However, from a fundamental standpoint, all of the accident types must obey fundamental laws of motion. The laws of motion are generally covered in engineering studies in courses in physics, dynamics, or kinematics. Generally, theses courses are taken through the sophomore year in a traditional engineering education. Additional engineering courses that aid in the reconstruction of accidents include, statics, strength of materials, and thermodynamics. It is assumed that the reader has a traditional engineering or scientific education so that great emphasis is not placed on prerequisite knowledge. However, some emphasis is placed on the more subtle details of basic physical principles because that is where nontraditionally trained reconstructionists make errors or fail to perform calculations.

Standardization in Forensic Engineering

The main goals of a forensic engineer are to safeguard the life, health, property, and welfare of the public and to establish and maintain a high standard of integrity, skill, and practice in the profession of forensic engineering. The rules of professional conduct for engineers dictate that the forensic engineer shall be completely objective, truthful, and shall include all relevant and pertinent information in all professional reports, statements, and testimony. When serving as expert or technical witness before any court, commission, or any other tribunal, the engineer shall express an opinion only when it is founded upon adequate knowledge of the facts in issue, upon a background of technical competence in the subject matter, and upon honest connection of accuracy and propriety of his testimony. These statements or similar ones are generally found in the rules of conduct for engineers in the United States and Canada.

The courts of the United States have recognized that bad science or unproven theories are often offered through expert testimony. Historically, unproven theories or "junk science" have been presented in federal, state, and local jurisdictions. The requirements for expert testimony are often more stringent at the federal level than at the state level and less so at the local level. However, the requirements to offer expert testimony at all levels have become more rigorous in the past few years. This pattern has resulted from recent cases such as Daubert vs. Merrell Dow Pharmaceuticals and the Kumho tire case. These cases have reaffirmed the Frye standard that was established at the federal level almost a century ago. These more stringent requirements are welcome because they tend to rid the court system of expert opinions based on bad or questionable science.

The nature of the court systems is adversarial. Engineering experts are subject to *voir dire* and strong attacks on their methodologies and conclusions. Under such pressure, the testimony of the expert may be considered outside the mainstream laws of physics, mathematics, and applied engineering principles. In contrast, when the engineering expert's opinions are based on a solid foundation of the physical principles and laws, the expert's testimony generally withstands the challenges that are presented by the opposing attorneys. Forensic engineers practice in many diverse fields, which include the four basic engineering disciplines of civil, chemical, electrical, and mechanical engineering. Additionally, there are many practitioners who specialize within each of the engineering disciplines. For example, there are environmental experts that may arise from civil engineering or metallurgists from mechanical engineering. In a forensic engineering analysis, all of the disciplines must determine the cause and the aspects of a failure. The failure may have been produced by nature, substandard design or construction, or human error or carelessness.

Engineering design of systems most often incorporates rigorous industrial standards such as the Society of Automotive Engineers (SAE), American Society of Testing and Materials (ASTM), National Fire Protection Association (NFPA), American National Standards Institute (ANSI), and Underwriters Laboratories (UL) to name a few. In the practice of forensic engineering, an assessment of the applicable standards is often made in order to determine whether failure to follow recognized standards contributed to the incident. The mission of ASTM, NFPA, SAE, and others is to develop and promulgate guides and standards so that our environments are safer and recognized scientific principles are adhered to in testing. The Code of Federal Regulations (CFR) governs many areas that apply to forensic engineering and in particular accident reconstruction. These areas include the design and safety of vehicles, tractor trailers, trains, roads, and construction equipment. You may ask the question "what does testing have to do with forensic engineering?" In fact, forensic engineering encompasses a wide range of tests and methods in order to arrive at answer for the failure or incident. These tests and methods include electrical, mechanical, chemical, and laboratory analysis as well as mathematical formulations based on recognized principles of physics. For example, in a vehicular crash, tests may be performed to determine if a component failure caused the loss. The black box recorder may be interrogated so that brake activation, throttle position, or precrash velocity can be determined. Calculations may be performed utilizing recognized principles of conservation of energy and momentum. Parametric studies may be performed in order to zero in on a logical solution. Crush damage may be compared to damage produced in controlled tests. All of these procedures and countless others may be incorporated in a vehicular incident reconstruction. Similar scenarios can be developed for all the areas of forensic engineering. The common threads that bind these investigations are observeability, repeatability, and the scientific method. As such, forensic engineering investigations lend themselves to detailed systematic procedures, guides, and standards.

The study and the practice of engineering revolve around recognized procedures and methodologies. As engineering students we learn the proper rules of integration and differentiation, the methods of solution of various types of differential equations, the method of images in electromagnetic fields, moment methods in structural analysis, test procedures for soils, concrete, and steel, and many others. In fact, the list of tests and procedures we learn and utilize for the practice of engineering is almost infinitely exhaustive. Forensic engineering is no different because it utilizes the natural laws and mathematics, the language of science, to describe the event or failure.

Science and engineering are responsible for today's advancements. When systems fail and engineers are called to determine the cause, the failure mode is determined from the application of the scientific method. Forensic engineers are the purveyors of the facts based on natural laws and scientific reasoning. Therefore, logical, orderly, forensic engineering investigations are perfectly suited for guidance from recognized practices. As an added benefit, when a forensic investigation is conducted within the framework of a recognized standard guide, the challenges to the methodology, calculations, and conclusions are severely diminished if not eliminated. Standard guides have a dual purpose. The first purpose is to educate the practitioners. The second purpose is to ensure conformity and thereby provide a level playing field for those involved. In this context, Chapter 15 of the book deals with most of the pertinent standards normally encountered in accident reconstructions. Chapter 15 also includes a broad guide that may be used when conducting an accident reconstruction.

Synopsis

The book is divided into 16 chapters. Chapter 1 gives a brief introduction. Chapter 2 emphasizes the need for proper measurement, calculations, and the application of basic physics principles used in accident reconstructions within engineering and scientific certainty. Chapter 2 discusses the mathematical thrust of the book and the basic skills needed for the thorough understanding of the concepts that are introduced. Attention is paid to the interrelationship between physics and mathematics. Chapter 2 introduces the basic coordinate systems and principles employed in standard three dimensional analyses of vector functions as well as specialized coordinate systems that are sometimes used in accident reconstruction. Complex reconstructions using a multitude of data require complex computer techniques that involve coordinate transformations in order to properly model the accident scenario. This chapter includes the basic physical principles utilized in accident reconstruction. The basic foundations of measurement, photography, and computer techniques are introduced in Chapter 3.

Chapter 4 derives various energy methods used in reconstructions from first principles. Basic derivations are used to contradict certain assumptions that violate first principles. The concepts of potential and kinetic energy and their relationship to work and power are used to derive pertinent reconstruction equations. Crush energy methods are developed in this chapter with their relationship to speed. Special attention is paid to friction, one of the most abused topics in reconstructions.

Chapter 5 is devoted to momentum methods. Momentum is the most widely misunderstood physical principle by nonengineering or nonscientific reconstructionists. Special attention is devoted to elastic, inelastic, linear, and rotational momentum principles. The concept of restitution is introduced. Comparison is made between momentum and energy methods that were developed in Chapter 4.

Chapter 6 deals with vehicle specifications. By simply knowing engine displacement, acceleration characteristics, gear ratios, and braking performance, various accident scenarios can be included or discounted. Steering and off-tracking dynamics of vehicles are analyzed. Chapter 6 includes accident scenarios involving the center of mass, rollover or tip-over accidents, and accidents where vehicles or passengers lose contact with the road surface or vehicle.

Failure analysis and testing of components are included in Chapter 7. Chapter 8 deals with bicycles, motorcycles, all terrain vehicles, and pedestrians.

Chapter 9 deals with the geometrical characteristics of highways. In many accidents, road characteristics are responsible or are blamed for the collision or loss of control. Basic design characteristics of roadways are discussed.

Chapter 10 deals with train accidents and re-emphasizes the concept of the sight distance triangle introduced in Chapter 9 as it applies to train-vehicle collisions.

Chapter 11 discusses the basic characteristics of large vehicles and off road equipment. The primary large vehicle in the United States is the tractor trailer combination. These vehicles, although larger than standard passenger vehicles, must still obey the laws of physics. The necessary assumptions used in this type of reconstruction are introduced and analyzed.

Chapter 12 deals with softer scientific issues such as visibility, perception, and reaction. These issues cannot conclusively be quantified in hard scientific terms as velocity and acceleration often are. Uncertainty for these factors is much broader but can be narrowed to acceptable ranges. Vehicle design strategies can sometimes be used to contradict some reaction times propounded by certain investigators.

Chapter 13 summarizes many of the concepts introduced in the preceding chapters in its discussion of computer methods. Emphasis is placed on the retrieval of data from crash data recorders and similar devices. Some commercially available computer programs are introduced as well as the use of spread sheets for calculations.

Chapter 14 deals with low speed impacts. Included are the methods of analysis and the biomechanics of injury. Staged collisions are analyzed and discussed.

Chapter 15 is devoted to standards and protocols and closes the introduction of the theme of the book. A final Chapter 16 has been added on sensitivity and uncertainty of the equations used throughout the book. MATLAB® is a registered trademark of The MathWorks, Inc. For product information, please contact: The MathWorks, Inc., 3 Apple Hill Drive, Natick, MA 01760-2098 USA. Tel: 508 647 7000; Fax: 508-647-7001; E-mail: info@mathworks.com; Web: www.mathworks.com

Introduction

1

Modern accident reconstruction uses basic principles of physics dating to the time of Sir Isaac Newton. These basic physical principles require a relatively sophisticated knowledge of mathematics. The mathematical principles involve algebra, trigonometry, calculus, differential equations, and some advanced topics for certain complex events. The theme of the book involves extensive use of mathematics in the development of the equations because it is very important that the practitioner understand the foundation principles of the equations that are used. The understanding of the mathematical development of the equations is also important for the reconstructionist because, in depositions or in court testimony, the expert is sometimes called to show the derivation of a particular equation. The extensive use of mathematics in the book also serves as a reference in the style of a textbook. The reader can refer to a particular section and solidify his or her understanding of the physical principles.

This book is geared toward engineers and scientists involved in the analysis of accident reconstruction. It is assumed that the reader has a basic understanding of the physical principles used in reconstruction work and has a thorough background in mathematics through the undergraduate level achieved by engineers or science students. Knowledge of mathematics and physical principals, coupled with the latest developments in computational tools, allow the practitioners to solve complex problems. Today's rapid development and power of the personal computer dictates that investigators involved in accident reconstruction avail themselves of this powerful tool. The combination of laser technology and the microprocessor allows engineers and scientific investigators to measure and input data for analysis at an unbelievable rate with unprecedented precision.

Accidents involving vehicles are as old as the automobile. There are three main culprits that cause accidents, the road, the vehicle, and the driver. Soon after the American people fell in love with the automobile, their quest for adventure, freedom, and speed led them down the path of destruction. By far, the main contributor to accidents or collisions is the action of the driver. However, the evolution of the automobile has not been without problems. Safety features for automobiles evolved only after cars were well developed, fast and quite maneuverable. The seat belt, air bag, and antilock braking systems have contributed to safer vehicles. It took more than half a century for these safety features to become commonplace. Some vehicles have been improperly designed and have caused many severe accidents. The two most widely recognized problematic cars were the Pínto and the Corvair. In general, vehicles have not been very crash-worthy in the past although a trend toward safer, more impact survivable vehicles has been evolving over the past 10–20 years. Improper or deficient design of automobiles is probably the second most common contributor to accidents. Many accidents are caused by vehicle system failures. These failures may include blown tires, brake failures, steering or suspension problems, or simply broken parts. Some accidents are caused by inadequate or improper repairs or maintenance. In other instances roadway defects or geometry may play a significant role in an accident. The wide use of electronic systems and computer control of vehicles will increase accidents caused by such system failures. However, by and large, accidents caused by vehicle system failures are very small in comparison to the main causes of accidents, speed, alcohol/drugs, and failure to obey the rules of the road. Sometimes visibility, perception, and general inattentiveness cause accidents.

In this book, we will address the physical processes and measurable quantities that are defensible in a court of law to a high degree of engineering and scientific certainty. Certain topics such as perception and reaction are covered in terms of widely accepted standards. Human perception of events varies widely and in most instances, is extremely biased. Such "soft" concepts cannot be accurately measured, observed, and quantified in "hard" scientific terms. A theme carried throughout the book is to model accidents with basic, defensible principles. Engineers and scientists observe, measure, calculate, and properly model physical processes involved in vehicular accidents. Reconstructions of accidents are merely models of events based on known, measurable, and observable principles. Whenever possible, an accident should be modeled by two or more methods. Often momentum methods, energy methods, and test comparison data can be used to properly model the accident. In all cases, the vehicle trajectories must obey Newtonian mechanics. In many instances, dynamic behavior of vehicles and participants can be restricted to varying ranges of possibilities. These dynamic models can predict possible scenarios and omit others. Usually this type of parametric analysis is performed with the aid of computer programs that are commercially available or simply programmed into commercial software by capable investigators. Parametric analysis can be used to disprove other reconstructionists' opinions or verify.

As with any scientific investigation, engineers and scientists performing accident reconstructions use the scientific method. Consequently, it is important to outline and remind the reader of the logical steps involved in the scientific method. First, based on observation of the available data (i.e., topography, road geometry, road and weather conditions, physical evidence such as skid or gouge marks, crush deformation of the vehicles, etc.) a hypothesis is formulated relative to the accident scenario. This hypothesis includes factors such as pre- and postimpact angles, impact point, and pre- and postimpact travel distances of the vehicles. The hypothesis is then tested by performing calculations using a variety of methods such as momentum and energy analysis, crush analysis, etc. Based on the hypothesis testing, the accident scenario is refined and parametric analysis is performed to include uncertainties. In all cases, the methodology is outlined, the assumptions are explained, and the analysis is performed. If the analysis does not support the hypothesis, then the hypothesis must be modified or discarded and the process repeated. In all cases, the hypothesis must be supported by the physical evidence. Investigators cannot simply ignore certain physical evidence that does not support the hypothesis and only incorporate the evidence that supports their view. When evidence is ignored, the scientific method is not followed and the investigation is not proper in engineering or scientific terms. This type of analysis is recognized as deductive reasoning and is the cornerstone of the scientific method. A key point is the repeatability of the analysis by other investigators. To do less does not meet the criteria required by the courts in light of the Daubert decision and the rules followed by the legal procedure.

The Daubert decision stems from a case concerning birth defects that were allegedly caused by the mothers' use of an antinausea drug, Bendectin. This drug was used during the first trimester of pregnancy and allegedly caused severe birth defects. The drug manufacturer, Merrill-Dow, moved for summary judgment claiming that the drug could not have caused injury to the children. In support of its motion, Merrill-Dow submitted an affidavit from a prominent epidemiologist, Dr. Steven H. Lamar. Dr. Lamar reviewed 30 published studies of 130,000 patients that found no evidence that Bendectin caused birth defects. Daubert, responding to Merrill-Dow's motion, submitted affidavits from eight experts who found a link between the use of Bendectin and birth defects based on animal studies. Merrill-Dow's motion was granted by the court because Daubert's experts relied on evidence that was not established and did not have general acceptance in the field. Furthermore, the court ruled that Daubert's evidence was not admissible because the findings had not been published or subjected to peer review. The appellate court affirmed the lower court's decision based on the Frye standard.

The Frye standard stems from a 1923 case that established the minimum standard required for the admission of expert testimony in federal cases. The Frye standard required the expert to use data and methodology "generally accepted" by other experts. In the Daubert case, the evidence presented by the plaintiff was considered novel scientific evidence or "junk science." Therefore, such novel science did not qualify under the Frye standard as admissible expert testimony. Upon appeal to the U.S. Supreme Court, the lower court rulings were overturned and a new standard was developed. This new standard for admissibility of expert testimony is based on the criteria that the evidence be reliable and relevant. Pertaining to the reliability of evidence, the court established a separate, nonexclusive four part test as follows:

1. Can the theory or technique be tested?
2. Has the theory or technique been subjected to peer review and publication?
3. Is there a known or potential rate of error?
4. Is there a general acceptance in the scientific community similar to the Frye standard?

Many reconstructionists offer testimony that does not meet the Daubert criterion or the Frye standard. They make statements such as, "In my opinion, the car was traveling 35 miles per hour" or "The collision occurred in the southbound lane because that is where the gouges on the road were found." A common ploy is to average or decrease the coefficient of friction based on the number of skid marks. The examples above as well as many others are routinely offered by experts. The important point to consider is that these types of statements and alleged analysis do not meet the Daubert challenge or the Frye standard. It is simply "junk science." The methodology is never presented, the underlying assumptions are never addressed, the computations and results cannot be verified, and the reconstruction cannot be duplicated or tested.

A new "junk science" has emerged from nonscientific reconstructions reflected in the following statements: "I don't trust dynamic simulation computer programs." "You can take these computer programs and you can plug in variables and have that computer kick out answers that are directly in conflict with Sir Isaac Newton and Albert Einstein." "The laws of physics were developed by Sir Isaac Newton 400 years ago and the only one to ever find that Sir Isaac Newton made a mathematical error was Albert Einstein and that was so minute that it meant a hill of beans." Obviously, the statements above, made by reconstructionists in actual cases, were from investigators who were not trained in the classic sense and who have a deep fear and distrust of the use of a computer in a reconstruction. "Junk scientists" do not follow the scientific method in their investigations. They perform few, if any, calculations. A common argument employed is to say that there is insufficient data to compute speeds or to say that techniques such as conservation of momentum cannot be employed in the particular accident scenario. Of course, these experts fail to use standard, well recognized, sophisticated techniques because their calculations may be easily challenged or they fail to understand some concepts. For example, their training may not allow them to differentiate the subtle point that energy may not always be conserved but that momentum is always conserved.

The reader, through the progression of the book, will acquire a sense for the adherence to the scientific method as it applies to accident reconstructions. The mathematical tools and scientific principles will be developed. These principles will be discussed within the limiting assumptions that must be made to properly model the accident. Through knowledge and experience, the reader will be properly equipped to appropriately use the concepts and to use a variety of methods in the analysis. The application of various methods that reach similar conclusions is of paramount importance when defending the reconstruction in court. The best way to defeat an opposing expert is to reconstruct the accident using two or three different methods all yielding similar results. The methodology and calculations with accompanying equations, graphs, and results should be clearly explained so that they may be readily reproduced by trained investigators. The analysis should be sophisticated, concise, and mathematically rigorous. In this manner, the opinions of other reconstructionists can be easily discounted or verified through the discovery process.

If the discussion presented above seems adversarial, it is meant to be. The court system in the United States is adversarial in nature. Furthermore, a reconstructionist can expect challenges to his work not only because of the adversarial nature of the court system but also because less sophisticated experts and reconstructionists will attempt to degrade scientific-based analysis in order to cover up their own deficiencies. Needless to say, reconstructions performed by parties representing opposing sides of a collision should obtain similar results if recognized analysis techniques, pertinent standards, and comparable data are used. The calculated values should be within engineering accuracy, i.e., vary by not more than 5 or 10%.

Basic Principles

2

2.1 Introduction

Mechanics, when applied to accident reconstructions, deals with the relationships between forces, bodies, and motion. The forces are produced by a combination of the relative motion of the vehicles, occupants, or systems. The method used to describe motion from a mathematical standpoint is called kinematics.

The motion of the particular body is defined as its continuous change in position relative to a coordinate system. For most applications in accident reconstruction, the preferred coordinate system is the Cartesian system. Some applications require cylindrical or spherical coordinate systems. In any of these coordinate systems, the position of the body is specified by its projection into the three axes of a rectangular coordinate system. As the bodies move along a path, the projections of the path to the respective axes move in straight lines. Thus, the motion of the bodies is reconstructed from the motions produced by the projections on the coordinate system. We begin this section with a discussion of the coordinate systems and their interrelationships.

2.2 Coordinate Systems

The language of science is mathematics—a statement often repeated in a traditional engineering or science curriculum. The mathematics of science include a thorough knowledge of trigonometry, algebra, differential and integral calculus, differential equations, vector algebra, analysis of complex variables, and advanced topics for the solutions of boundary value problems whose solutions may be defined by infinite series. Each of these math topics is directly applicable to accident reconstructions, and a basic understanding of these topics is crucial in obtaining proper solutions to the accidents we model.

As a first example, let us consider a common Cartesian coordinate system as described in Figure 2.1.

The point $P(x_1,y_1)$ is recognized to be located in the first quadrant and is trigonometrically described as

$$x_1 = |r_1| \cos \theta; \qquad y_1 = |r_1| \sin \theta \tag{2.1}$$

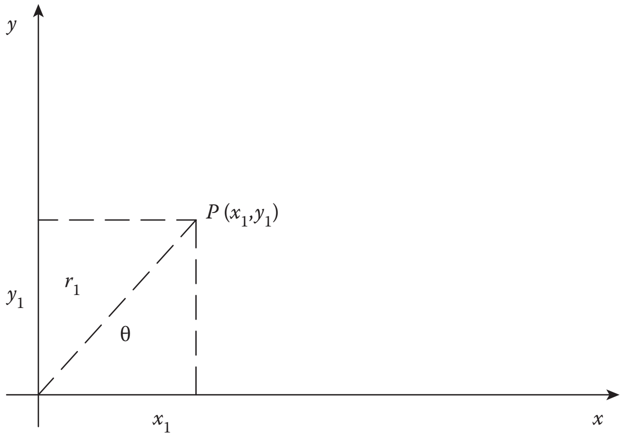

Figure 2.1 Cartesian coordinates.

It should be obvious that when θ is positive, x_1 and y_1 are positive. However, when θ is negative and located in the fourth quadrant, x_1 remains positive but y_1 becomes negative. If the reconstructionist does not realize the importance of a simple switch between a positive and negative angle, in terms of a recognized coordinate system, the solution involving trigonometric functions can be significantly altered. If r_1 represents a velocity, it must be properly described by its magnitude and direction. Many solutions can be shown to be incorrect by an appropriate description of the vector function in relation to a standard coordinate system. The reconstructionist may obtain a correct solution for the magnitude but an incorrect direction or conversely assume an incorrect direction and yet obtain a correct value for the magnitude. Throughout this book, we will assume solutions based on a standard or modified Cartesian coordinate system, which may readily be converted to cylindrical or spherical coordinates. A set of standard Cartesian coordinates in three dimensions is shown in Figure 2.2.

The Cartesian or rectangular coordinates describing the point P_1, are

$$P_1(x_1, y_1, z_1) \tag{2.2}$$

In cylindrical coordinates, the point P_1 is described as

$$P_1(\rho, \theta, z_1) \tag{2.3}$$

where

$$x_1 = \rho \cos \theta \tag{2.4}$$

$$y_1 = \rho \sin \theta \tag{2.5}$$

$$z_1 = z_1 \tag{2.6}$$

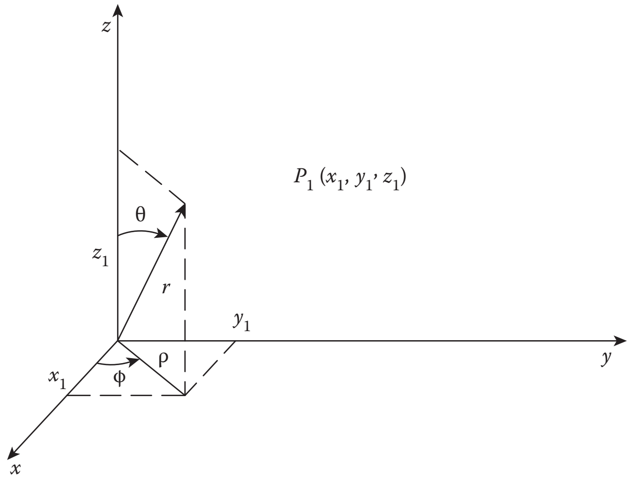

Figure 2.2 Coordinate system.

In spherical coordinates the point P_1, is described by

$$P_1(r, \theta, \varphi) \tag{2.7}$$

where

$$x_1 = r \sin\theta \cos\varphi \tag{2.8}$$

$$y_1 = r \sin\theta \sin\varphi \tag{2.9}$$

$$z_1 = r \cos\theta \tag{2.10}$$

Most accidents can be described by the two dimensional coordinate system of Figure 2.1. In such cases, the vertical velocity component is negligible and can be ignored or corrected for by appropriate substitutions into the frictional coefficient. In other instances, such as in ballistic motion, the lateral component of velocity is zero and the problem reduces to two dimensions. When solutions to reconstructions require curvilinear motion such as rotational momentum or centripetal acceleration, then the cylindrical coordinate system is best suited to describe a proper solution. Complex geometries sometimes require three dimensional coordinates to model the accident. In those cases, any of the three coordinate systems described by Equations 2.2 through 2.10 may be used.

The main reason for introducing the three dimensional coordinate systems is predicated by the manner in which data are gathered. Standard surveying techniques, whether using traditional optical devices or computerized laser transits, gather data with respect to azimuth, elevation, and distance.

More simply, this data are collected in spherical coordinates and may need to be converted to a rectangular coordinate system. Modern laser transits, commonly referred to as total stations, will perform the necessary conversions between coordinate systems internally and automatically so that they may be downloaded into standard drawing software, such as AutoCAD or 3D Studio. However, if the data from certain laser ranging devices is stored in terms of azimuth, elevation, and distance, then the necessary coordinate transformations based on Equations 2.3 through 2.10 are required.

The Society of Automotive Engineers (SAE) has adopted a coordinate system convention known as SAE J670e-Vehicle Dynamics Terminology (1976). The SAE convention defines two individual coordinate systems—one that describes the dynamics of the vehicle with respect to its own coordinates and the other that describes the motion of the vehicle with respect to its location and dynamics with respect to the earth. These coordinate systems are simply modified forms of standard coordinate systems which are more aptly suited to the dynamics of a vehicle and the reconstruction of an accident. The first is the vehicle-fixed coordinate system, and the second is referred to as the earth-fixed coordinate system. Figure 2.3 describes the vehicle-fixed coordinate system according to the SAE J670e convention.

For the vehicle-fixed coordinate system, the x-axis points straight ahead of the vehicle and originates at the center of mass of the vehicle. Accordingly, the y-axis points to the right or passenger's side of the vehicle, while the z-axis points downward toward the center of the earth. The vehicle-fixed coordinate system is attached to the vehicle's center of mass and moves along with the vehicle with respect to the earth-fixed coordinate system shown in Figure 2.4.

Note that in both the vehicle and earth-fixed coordinate systems, the z-axis points toward the center of the earth and is therefore shifted by 180

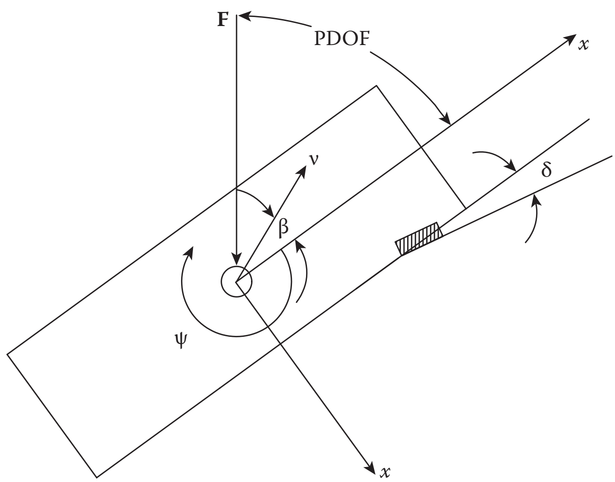

Figure 2.3 Vehicle based coordinate system (x, y, ψ).

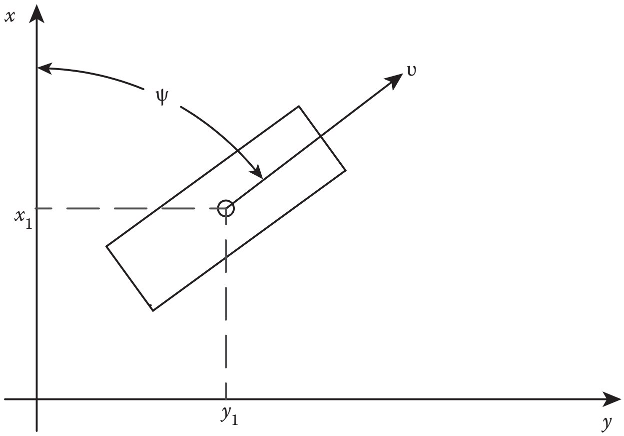

Figure 2.4 Earth-fixed coordinate system (x, y, ψ).

degrees from the conventional coordinate system described in Equations 2.1 through 2.10. Care should be taken when converting data from standard coordinate systems to earth- or vehicle-fixed coordinate systems with respect to the orientation of the z-axis. It is important to introduce the various coordinate systems at the point because they are commonly interchanged in a reconstruction depending on the type of analysis performed.

2.3 Basic Principles of Physics

Classical mechanics are based on three natural laws that are attributed to Sir Isaac Newton (1643–1727). Newton published in 1686, his "*Philosophiae Naturalis Principia Mathematica*" in which he described these laws. Engineers and scientists recognize these three basic principles as laws because they have never been disproved. Keep in mind that Newton's laws do not take into account relativistic effects described by Albert Einstein. It suffices to say that relativistic effects are not encountered in accident reconstructions because the velocities are far below the speed of light and because Newton's first law is based on an inertial reference system. The basic equations are,

$$\mathbf{v} = \frac{dx}{dt}; \qquad \mathbf{a} = \frac{d\boldsymbol{v}}{dt} \tag{2.11}$$

where

$\mathbf{v}$ = velocity
$\mathbf{a}$ = acceleration
x = displacement
t = time.

2.4 Uniformly Accelerated Linear Motion

Many paths taken by vehicles involved in collisions take straight lines before and after the collision. Sometimes the paths are not quite straight but can be approximated by straight lines. The straight line approximations may be piece-wise, i.e., the curved path broken down into linear pieces that closely approximate the actual path. Such piece-wise approximations are common in engineering analysis and have a sound mathematical underpinning. This type of motion is then considered linear because it follows straight line paths. If the acceleration of the bodies in question is constant and linear, it is referred to as uniformly accelerated linear motion. For example, the acceleration or deceleration of an automobile is nearly constant when the brakes are applied or when the accelerator is activated. Generally, as a first approximation for most reconstructions, it is proper to assume constant acceleration. From Equation 2.11 we may write $\mathbf{a} = \mathbf{a}(t)$ = constant, or

$$\mathbf{v} = \int \mathbf{a}(t)dt + c_1 = \mathbf{a}t + c_1 \tag{2.12}$$

If we know the initial velocity of the vehicle or body, the constant c_1, becomes $\boldsymbol{v}_0$, the initial velocity, thus,

$$\mathbf{v} = \mathbf{v}_0 + \mathbf{a}t = v(t) \tag{2.13}$$

Equation 2.12 yields the velocity as a function of time $\boldsymbol{v}(t)$. Thus, again from Equation 2.11 we may write,

$$x = \int \mathbf{v}(t)dt + c_2 = \mathbf{v}_0 + \frac{1}{2}\mathbf{a}t^2 + c_2 \tag{2.14}$$

If we know the initial position x_0 at time $t = 0$, then $x_0 = c_2$ and

$$x = x_0 + \mathbf{v}_0 t + \frac{1}{2}\mathbf{a}t^2 \tag{2.15}$$

If we consider the acceleration as a function of the displacement or distance we may write from Equation 2.11

$$\mathbf{a} = \frac{d\mathbf{v}}{dt} = \mathbf{v}\frac{d\mathbf{v}}{dx} \tag{2.16}$$

$$\int \mathbf{v}d\mathbf{v} = \int \mathbf{a}dx + c_3 \tag{2.17}$$

which yields

$$\frac{\mathbf{v}^2}{2} = \mathbf{a}x + c_3 \tag{2.18}$$

If $\mathbf{v}_0$ is the velocity when the displacement is x_0, the constant of integration can be solved,

$$\mathbf{v}^2 = \mathbf{v}_0^2 + 2\mathbf{a}\,(x - x_0) \tag{2.19}$$

Thus, for uniformly accelerated linear motion the equations may be summarized as follows.

$$\text{Acceleration} \quad \mathbf{a} = \mathbf{a}(t) = \mathbf{a}(x) = \text{constant} \tag{2.20}$$

$$\text{Velocity} \quad \mathbf{v} = \mathbf{v}(t) = \mathbf{v}_0 + \mathbf{a}t \tag{2.21}$$

$$\text{Displacement} \quad x = x(t) = x_0 + \mathbf{v}_0 t + \frac{1}{2}\mathbf{a}t^2 \tag{2.22}$$

$$\text{Velocity} \quad \mathbf{v} = \mathbf{v}(x) = \sqrt{\mathbf{v}_0{}^2 + 2\mathbf{a}(x - x_0)} \tag{2.23}$$

2.5 Motion in a Plane

Up to this point we have only considered motion along a straight line. The equations we have presented are used in accident reconstructions to describe the motions of vehicles as they are accelerating or decelerating (known as braking) or skidding. As we shall see at the end of the chapter in the sections of impulse and momentum and from our discussion of Newton's laws, vehicles skidding out of control tend to follow straight or slightly curved paths. Consider the vehicle in motion in Figure 2.5.

The velocity components are given by

$$\mathbf{v}_x = \frac{dx}{dt}; \qquad \mathbf{v}_y = \frac{dy}{dt} \tag{2.24}$$

Similarly, the acceleration components become

$$\mathbf{a}_x = \frac{d\mathbf{v}_x}{dt} = \frac{d^2x}{dt^2}; \qquad \mathbf{a}_y = \frac{d\mathbf{v}_y}{dt} = \frac{d^2y}{dt^2} \tag{2.25}$$

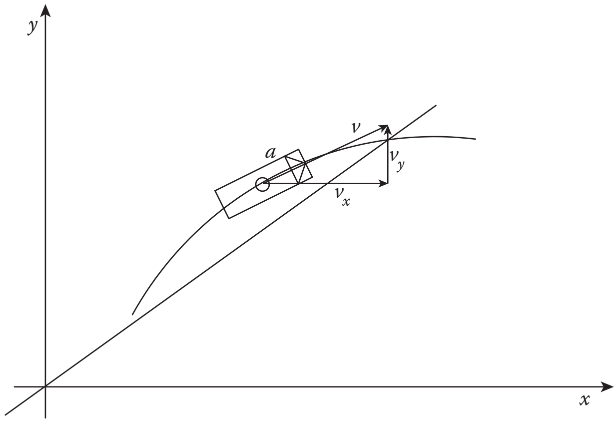

Figure 2.5 Motion in a plane.

The velocity and acceleration vectors then become

$$\mathbf{v} = \mathbf{v}_x \bar{\mathbf{a}}_x + \mathbf{v}_y \bar{\mathbf{a}}_y \tag{2.26}$$

$$\mathbf{a} = a_x \bar{\mathbf{a}}_x + a_y \bar{\mathbf{a}}_y \tag{2.27}$$

generally: $\bar{\boldsymbol{a}}_x ; \bar{\boldsymbol{a}}_y ; \bar{\boldsymbol{a}}_z$ represent unit Cartesian coordinate vectors.

2.6 Projectile Motion

A special case of uniformly accelerated linear motion occurs when a baseball is thrown, a gun is fired, a person jumps from a building, or a car drives off a cliff. In the absence of air resistance and near the surface of the earth, objects fall with almost constant acceleration. Figure 2.6 represents in a general manner the motion of a projectile. The *x-y* plane represents the surface of the earth or the reference plane and the *z*-axis represents the elevation relative to the reference plane.

The trajectory is the motion of the projectile. The projectile is the object with initial velocity that is acted upon by the acceleration due to gravity. In this analysis we neglect air resistance and the rotational motion of the earth. Strictly speaking, since the system is not inertial, it is not completely correct to use Newton's second law to relate the force on the projectile to its acceleration. Please refer to the section on Newton's second law for a more complete description. Based on the coordinates chosen in Figure 2.6, we may write

$$\boldsymbol{v}_x = \boldsymbol{v}_0 \cos\theta \tag{2.28}$$

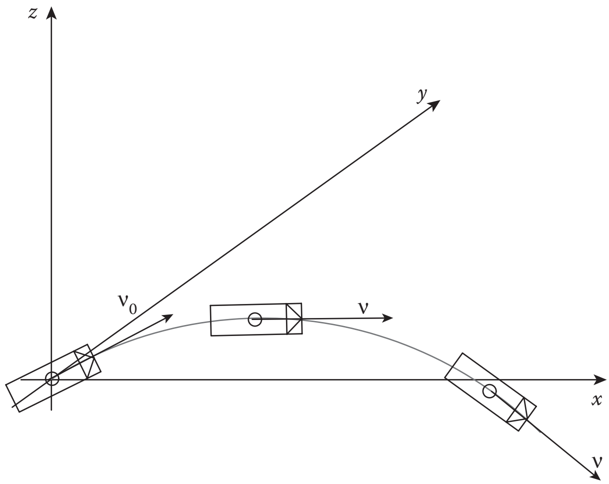

Figure 2.6 Projectile trajectory.

$$\mathbf{v}_z = \mathbf{v}_0 \sin\theta - gt \tag{2.29}$$

Note that these components can be added vectorially as

$$\mathbf{v} = \mathbf{v}_x \bar{\mathbf{a}}_x + \mathbf{v}_z \bar{\mathbf{a}}_z \tag{2.30}$$

$$\boldsymbol{v} = \sqrt{\boldsymbol{v}_x^2 + \boldsymbol{v}_z^2} \tag{2.31}$$

The coordinates of the projectile at any time can be found from the equations of uniformly accelerated linear motion. These are given by,

$$x = \mathbf{v}_0 \cos\theta t \tag{2.32}$$

$$z = \mathbf{v}_0 \sin\theta t - \frac{1}{2} g t^2 \tag{2.33}$$

In the equations above g is the acceleration due to gravity, t is the time, and θ is the angle of departure of the projectile relative to the reference plane. Equations 2.32 and 2.33 produce the trajectory in terms of time t. Eliminating t from the above equations we obtain,

$$z = \tan\theta x - \frac{g x^2}{2 \boldsymbol{v}_0^2 \cos^2\theta} \tag{2.34}$$

Equation 2.34 can be solved for the departure velocity given by

$$\mathbf{v}_0 = \sqrt{\frac{gx^2}{2\cos^2\theta(x\tan\theta + z)}} \tag{2.35}$$

A special case of projectile motion occurs when an object falls freely. In terms of the coordinate system utilized in the previous discussion, Equation 2.22 may be written as

$$z = z_0 + \mathbf{v}_0 t + \frac{1}{2}\mathbf{a}t^2 \tag{2.36}$$

but $z_0 = v_0 = 0$ and $\boldsymbol{a} = g$, then

$$z = -\frac{1}{2}gt^2 \tag{2.37}$$

2.7 Uniformly Accelerated Curvilinear Motion

Curvilinear motion involves rotation and translation. Thus far we have only considered translational motion along a straight line or along a curve. Before we discuss the equations of curvilinear motion we will investigate rotation without translation. Figure 2.7 represents a rigid body, in this example a vehicle, that is undergoing rotation without translation about a fixed axis through point 0.

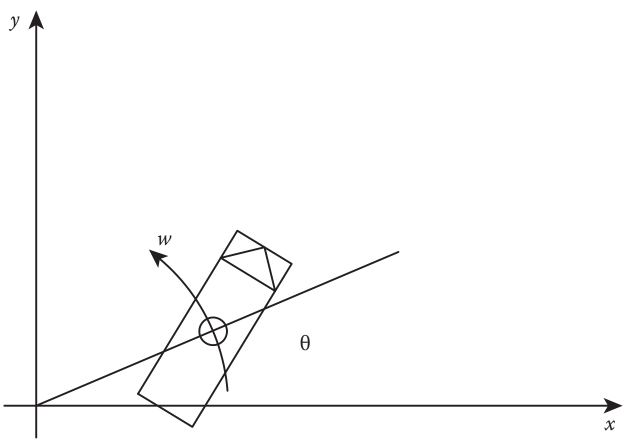

Figure 2.7 Vehicle rotation.

The instantaneous angular velocity **w** and the angular acceleration $\boldsymbol{\alpha}$ are given by,

$$\mathbf{w} = \frac{d\theta}{dt}; \qquad \boldsymbol{\alpha} = \frac{d\mathbf{w}}{dt} \tag{2.38}$$

For rotation with constant angular acceleration

$$\boldsymbol{\alpha} = \frac{d\mathbf{w}}{dt} = \text{constant} \tag{2.39}$$

we may write,

$$\mathbf{w} = \int \boldsymbol{\alpha}\, dt + c_1 \tag{2.40}$$

if $\boldsymbol{w}_0$ is the angular velocity when $t = 0$, the integration constant c_1 becomes the angular velocity

$$\mathbf{w} = \mathbf{w}_0 + \boldsymbol{\alpha}\, t \tag{2.41}$$

In a similar manner since $\boldsymbol{w} = d\theta/dt$ we may write,

$$\theta = \int \mathbf{w}_0 dt + \int \boldsymbol{\alpha} t\, dt + c_2 \tag{2.42}$$

Evaluating c_2 at θ_0 when $t = 0$ we obtain,

$$\theta = \theta_0 + \mathbf{w}_0 t + \frac{1}{2}\boldsymbol{\alpha} t^2 \tag{2.43}$$

Since $\alpha = \boldsymbol{w}d\boldsymbol{w}/d\theta$ by the chain rule, then

$$\int \boldsymbol{\alpha}\, d\theta = \int \mathbf{w}\, d\mathbf{w} + c_3 \tag{2.44}$$

If $\theta = \theta_0$ when $t = 0$ and $\mathbf{w} = \mathbf{w}_0$ is the initial angular velocity, then the constant of integration can be solved as

$$\mathbf{w}^2 = \mathbf{w}_0 + 2\boldsymbol{\alpha}(\theta - \theta_0) \tag{2.45}$$

2.8 Relation between Angular and Linear Velocity and Acceleration

In many reconstructions of accidents, a vehicle loses control rounding a curve and deposits yaw marks on the road surface. The arc produced by the yaw marks can be used to determine to a first approximation the velocity of the vehicle when loss of control occurred. This method of analysis is the subject of much debate. In subsequent sections of the book we will pose our arguments for the accuracy and validity of this analysis. Consider Figure 2.8 which represents a vehicle losing control rounding a curve and producing a nearly circular path.

The radius of the circle and the arc length are given by

$$s = r\theta \tag{2.46}$$

If the radius is constant upon differentiation we obtain,

$$\frac{ds}{dt} = r\frac{d\theta}{dt} \tag{2.47}$$

In Equation 2.47 ds/dt represents the magnitude of the linear velocity ν and $d\theta/dt$ is the angular velocity **w**, so

$$v = rw \tag{2.48}$$

If we differentiate again with respect to time,

$$\frac{dv}{dt} = r\frac{dw}{dt} \tag{2.49}$$

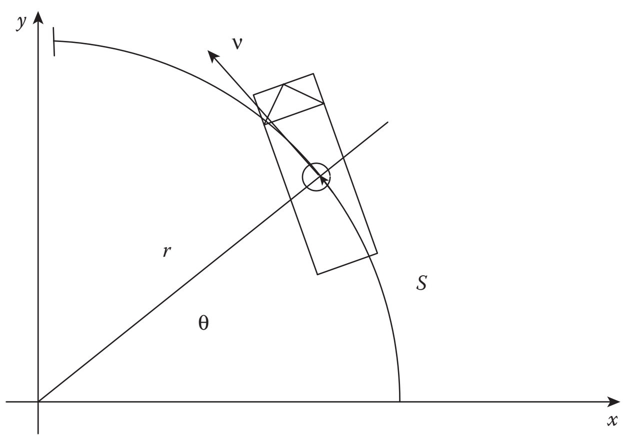

Figure 2.8 Vehicle loss of control.

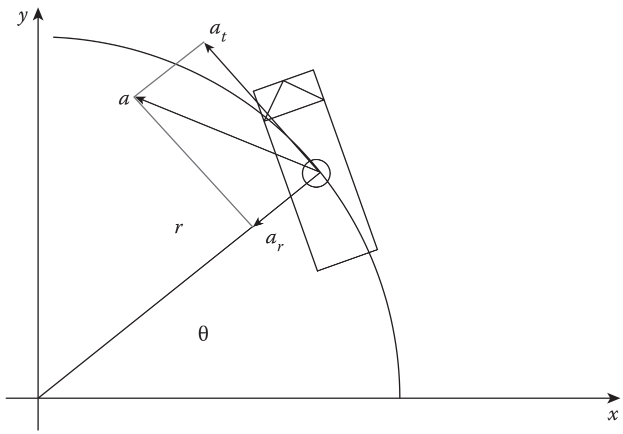

Figure 2.9 Angular acceleration.

In Equation 2.49 the term *dv/dt* is the magnitude of the tangential component of the acceleration $\mathbf{a}_T$ and *dw/dt* is the angular acceleration $\boldsymbol{\alpha}$, so

$$\boldsymbol{a}_T = r\boldsymbol{\alpha}\mathbf{a}_t \tag{2.50}$$

The radial component of the acceleration is then

$$\mathbf{a}_R = \frac{v^2}{r}\mathbf{a}_r = w^2 r\mathbf{a}_r = wv\mathbf{a}_r \tag{2.51}$$

In general, the acceleration can be expressed in terms of the tangential and radial or normal components

$$\mathbf{a} = \mathbf{a}_T + \mathbf{a}_N \tag{2.52}$$

or for the case in question

$$\mathbf{a} = r\boldsymbol{\alpha}\mathbf{a}_t + \frac{v^2}{r}\mathbf{a}_r \tag{2.53}$$

$\mathbf{a}_t$; $\mathbf{a}_r$ represent unit tangential, radial vectors.

Figure 2.9 represents the accelerations discussed above.

2.9 Newton's First Law

At first glance, Newton's first law appears simple and self-evident. However, upon analysis, the first law has subtle points that need to be clarified. The first law deals with forces on bodies such as passenger vehicles. In an accident, forces alter the shape or dimensions of the vehicles, and they change the state of motion of these vehicles. The motion of a vehicle consists of its translational motion and its rotational motion. When forces balance any translational and rotational motion, the vehicle is in equilibrium. A body or vehicle in equilibrium is therefore at rest or moves in a straight line with constant speed, and the body is either not rotating or rotating at a constant rate. In mathematical terms, we may refer to the vehicle representation of the vehicle-fixed coordinate system of Figure 2.4. We define the following for the earth-fixed system.

V = velocity of the vehicle relative to the earth

Ψ_1 = vehicle heading relative to the earth

X_1 and Y_1 = coordinate positions at any instant of time t. Similarly, for the vehicle-fixed system we define

ν = velocity of the vehicle relative to its coordinates

β = sideslip angle of the vehicle

δ = steering angle of the vehicle

ψ = relative rotations of the vehicle

F = external force acting on the vehicle through a relative angle referred to as the principal direction of force (PDOF)

Thus, the vehicle in equilibrium would meet the following criteria

$$\mathbf{V} = \mathbf{v} = \psi = 0 \text{ or a constant} \tag{2.54}$$

It is possible that the vehicle is in translational but not rotational equilibrium or vice versa. For the case of translational but not rotational equilibrium, the lines of action affecting the vehicle would not align and the vehicle would then form a couple. This motion is sometimes seen at the end of a skid when a vehicle tends to rotate about its center of mass. In other cases, the vehicle first rotates upon impact and then rolls or slides to its rest position. In mathematical form, the resultant forces for a vehicle in equilibrium must cancel, so that

$$\sum \mathbf{F}_x = 0 \quad \text{and} \quad \sum \mathbf{F}_y = 0 \tag{2.55}$$

Equation 2.55 in two dimensions is called the first condition of equilibrium. The second condition of equilibrium can be expressed in terms of the moments of the forces acting on the vehicle. Recall that the vector moment Γ of a force **F** about an arbitrary axis is defined as

$$\Gamma = \boldsymbol{r} \times \mathbf{F} \tag{2.56}$$

where

$\boldsymbol{r}$ = radial moment arm of the force **F**

$|\Gamma| = \Gamma = r\mathbf{F} \sin\theta$ = magnitude of the torque

In order to eliminate the condition of a couple, i.e., the forces acting on the vehicle, have the same line of action, the magnitude of the resultant moment about the perpendicular axis to the plane must be zero. Thus, for the equations described in Equation 2.55 the condition must be

$$\sum T_z = 0 \tag{2.57}$$

Therefore, in order to meet both conditions of equilibrium, the resultant force **F** and the resultant vector moment Γ about any axis must be zero or

$$\mathbf{F} = 0; \qquad \Gamma = 0 \tag{2.58}$$

A statement of Newton's first law is generally expressed as "Every body continues in its state of rest or in uniform motion in a straight line unless acted upon by external forces." An inertial reference system is defined as one relative to which a body remains at rest or moves uniformly in a straight line when no external force acts on it. For the purpose of accident reconstruction, a reference system attached to the earth can be considered an inertial system if we disregard the earth's rotation. Thus, the earth-fixed coordinate systems of Figures 2.1, 2.2, and 2.4 satisfy Newton's first law.

2.10 Newton's Second Law

The second law is a direct consequence of Newton's first law. The first law states that if the force on a body is zero, then the acceleration on the body must be zero. Recall from basic physics that acceleration is the time derivative of velocity. If velocity is a constant with respect to time, then the acceleration or time derivative of a constant must be zero. Newton's second law states that if the resultant force on a body is not zero, the body must move with accelerated motion. Furthermore, the acceleration produced by the force depends on the mass of the object. In equation form Newton's second law is stated as

$$\sum \mathbf{F} = m\frac{d\boldsymbol{v}}{dt} = m\boldsymbol{a} \tag{2.59}$$

Newton's second law, as stated above, applies to rectilinear as well as curvilinear motion for a particle. In the context of a body such as a vehicle in an accident reconstruction, it is recognized that all the particles that comprise the vehicle are not rotating with the same acceleration if the vehicle is in curvilinear motion. It is sufficient, however, to consider the acceleration at the center of mass of the vehicle.

Accident reconstructions generally involve solutions to physical phenomena within the study of "mechanics." Mechanics include the study of motion and the forces that produce the motion. More specifically, the study of motion is referred to as "dynamics" while in the special case where the acceleration is zero, it is known as "statics." Some authors use the term "kinematics" to describe systems in motion. It is again worthwhile to emphasize that the velocities encountered in accident reconstruction are very small compared to the velocity of light so that relativistic concepts need not be considered. All the velocities and accelerations are measured relative to an inertial reference system, namely, the earth. The above discussion reveals that Newton's first law is a special case of a more general phenomenon, which is recognized as Newton's second law.

In the introduction, we refered to statements that fall into the category of "junk science" perpetrated by reconstructionists without formal engineering or scientific training. Recall the statement about Newton making a mathematical error that was discovered by Einstein. We, of course, know that Newtonian mechanics are a special case of relativistic effects formulated by Albert Einstein. Suffice it to say that the assumptions made in mechanics are valid and yield quite accurate solutions to the problems modeled in an accident reconstruction.

Before we depart from Newton's second law, we need to include a final word about mass and its center. A discussion of finding the center of mass or gravity, as it is sometimes referred to, will follow in a later section. In accident reconstructions, it is sufficient to track the motion of the center of mass of the vehicle whether the motion is rectilinear, curvilinear, or a combination of both is immaterial. Newton's second law, as expressed in Equation 2.16 is general. Knowing the acceleration vector $\mathbf{a}$ at any point in time and the corresponding force vectors $\sum \mathbf{F}$, a sufficient description of the accident event can be formulated.

2.11 Newton's Third Law

A single isolated force is physically impossible. Consider the case of an object resting on a table. If we only consider the force of gravity on the object, then the object should be accelerated toward the center of the earth. It is obvious that a resistive force, applied through the structure of the table, must be exerting a force equal in magnitude and opposite in direction. We see then that when a body exerts a force on another body, the second must always exert on the first an equal and opposite force through the same line of action in order to keep the object on the table. These two forces describing the interaction between two bodies are often called the action and reaction with no delineation as to which is the cause and which is the effect. Accident reconstruction analysis of crush energy deformation makes use of Newton's third law as a method of checks and balances for speed calculations. The general statement of Newton's third law is "for every action there is always an equal and opposite reaction." Mathematically, we represent Newton's third law for a force **F** and its reaction **F′** as

$$\mathbf{F} = -\mathbf{F}' \tag{2.60}$$

Newton's third law describes the equilibrium of a particle or an object. In nature, the forces acting on an object or vehicle do not all pass through one point such as the center of mass. Thus, the forces are noncurrent so that the vehicle, which is a relatively rigid body, undergoes rotational and translational motion. There are many accident scenarios where the rotation of the vehicle has a relatively small consequence on the accident reconstruction and can therefore be ignored. In these cases, translational linear motion suffices as an accurate description of the accident scenario. In other instances, the effects of rotation cannot be ignored and must be accounted for in the analysis. Several examples in subsequent chapters will highlight the various techniques and appropriate assumptions employed by the authors.

Nature is deceptively complicated. Most processes are very complex. Take, for example, the motion of a pedestrian struck by an automobile. Knowing the approximate point of impact and where the pedestrian landed, we might want to calculate the speed of the vehicle at impact. To do so, several simplifying assumptions may need to be made. First we consider the pedestrian to be an ideal object like a rigid smooth sphere. Second, we ignore the rotation of the body and the effects of air resistance including the buoyancy effects of air. The idealized problem is then quite different from the original problem. However, at relatively low velocities, the simplifying assumptions yield manageable calculations that solve the problem within engineering accuracy.

2.12 Center of Gravity or Mass

In a vehicle, every particle of that vehicle is attracted toward the center of the earth. Since the center of the earth is at a far distance, the forces attracting all the particles in the vehicle are essentially parallel. The sum of all the forces is the total weight of the vehicle or

$$\sum w_i = w_T \tag{2.61}$$

Since the resultant moment of the weight about any axis through the center of gravity is zero, the line of action of the weight of the vehicle passes through the center of mass. This concept allows the accident reconstructionist to track the path of the vehicles through their centers of mass irrespective of the orientation of the vehicle when considering translational effects. Consequently, significant emphasis need not be placed on the relative shape of the skid marks deposited by the tires in a collision. The line of action of the weight of a vehicle in the respective rectangular coordinates can be expressed as

$$\bar{x} = \frac{\sum x_i w_i}{w_T} \tag{2.62}$$

$$\bar{y} = \frac{\sum y_i w_i}{w_T} \tag{2.63}$$

and

$$\bar{z} = \frac{\sum z_i w_i}{w_T} \tag{2.64}$$

Center of gravity calculations are sometimes necessary in accident reconstructions. Certain accident scenarios require the computations in order to determine the propensity for rollover or flip of the vehicle. Loading conditions on tractor trailers can significantly affect the center of mass, which sometimes causes these large vehicles to overturn. Similarly, hoists, man lifts, and cranes all operate on the premise that the center of gravity will dominate the loading conditions. Therefore, these devices have limits of operation that must be followed. Misapplication of loading conditions on cranes generally results in catastrophic failure. Construction equipment, such as bulldozers, backhoes, and loaders, have safe ranges of operation all dealing with the center of mass. Sport utility vehicles and all terrain vehicles have relatively high centers of mass, making then more prone to overturning. These high centers of gravity for particular vehicles can influence the reconstruction and may lead to product liability considerations.

2.13 Impulse and Momentum

Newton's laws of motion give rise to the concepts of work and energy and the concepts of impulse and momentum. We will first consider impulse and momentum and then work and energy. Both concepts are similarly derived from Newton's second law.

$$\mathbf{F} = m\boldsymbol{a} = m\frac{d\boldsymbol{v}}{dt} \tag{2.65}$$

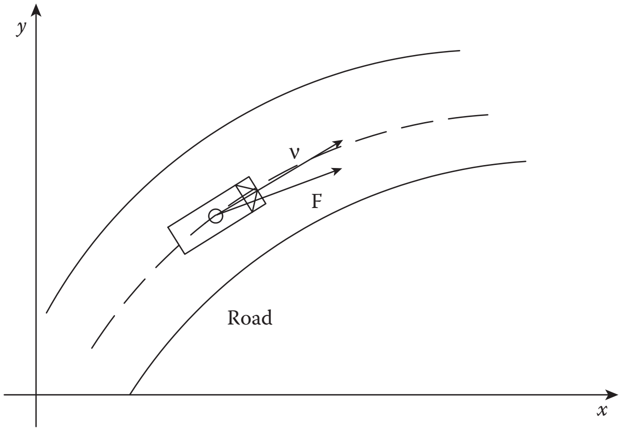

Figure 2.10 Vehicle in a curved path.

Figure 2.10 represents a vehicle moving along a roadway with coordinate axes x and y.

Rearranging Equation 2.65 and providing limits of integration we observe

$$\int_{t_1}^{t_2} \mathbf{F} dt = \int_{v_1}^{v_2} m d\mathbf{v} \tag{2.66}$$

The quantity on the left side of Equation 2.66 is called the impulse of the force **F** over the time interval $t_2 - t_1$. So by definition

$$\text{Impulse} = \int_{t_1}^{t_2} \mathbf{F} dt \tag{2.67}$$

The impulse is a vector quantity that can only be evaluated when the force **F** is known as a function of time t. In vehicular collisions or events, the force is simply not known as a function of time. In some instances the force may be calculated based on the results of the right side of Equation 2.66. The integral on the right side of Equation 2.66 yields the result

$$\int_{v_1}^{v_2} m dv = mv_2 - mv_1 \tag{2.68}$$

The product of the mass of the vehicle and its velocity is a vector quantity and is called the linear momentum

$$\text{Linear momentum} = m\boldsymbol{v} \tag{2.69}$$

We may thus rewrite Equation 2.66 as

$$\int_{t_1}^{t_2} \mathbf{F} dt = m\mathbf{v}_2 - m\mathbf{v}_1 \tag{2.70}$$

Equation 2.70 expresses a subtle yet very important concept that applies to collisions between vehicles as will soon be discussed. First we wish to state the significant fact of Equation 2.70: the "vector impulse" of the resultant force on a vehicle or particle, over the time interval, is equal in magnitude and direction to the "vector change" in momentum of the vehicle or particle. This is the impulse momentum principle that is often violated in the reconstruction of vehicular collisions. The impulse momentum principle is chiefly applied to short duration forces arising from explosive events or collisions. These types of forces are often referred to as impulsive forces.

We will soon see that work and energy are scalar quantities where the development of impulse and momentum reveal that they are vector quantities. As such, the impulse and momentum may be broken down into component parts in the *x*-*y* plane of Figure 2.10 to yield

$$\int_{t_1}^{t_2} \mathbf{F}_x \, dt = mv_{x2} - mv_{x1} \tag{2.71}$$

$$\int_{t_1}^{t_2} \mathbf{F}_y \, dt = mv_{y2} - mv_{y1} \tag{2.72}$$

It follows that in a three dimensional problem when the forces and velocities have a component in the *z* direction,

$$\int_{t_1}^{t_2} \mathbf{F}_z dt = mv_{z2} - mv_{z1} \tag{2.73}$$

Consider Figure 2.11 where the force produced in a collision decreases over time. The area under the curve between the times t_1 and t_2 is equal to the impulse of the force in the time interval. For vehicular collisions, the time interval is in the range of 100 milliseconds. The force exerted on one vehicle may vary according to the stiffness of the vehicle. The stiffer the vehicle, the shorter the duration of the impulse. Accordingly, the more flexible the vehicle, the longer the duration of the pulse. Figure 2.12 shows the plot of the force on two vehicles with equal impulses but over different time elements.

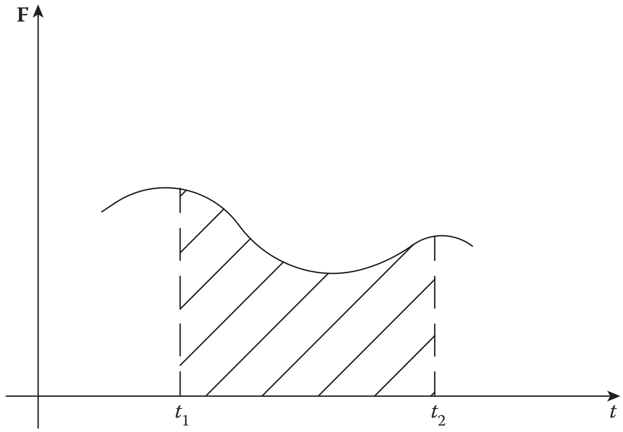

Figure 2.11 Force decreases over time.

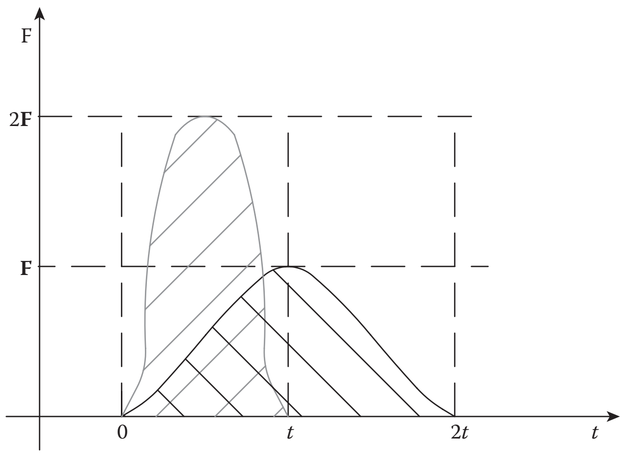

Figure 2.12 Equal areas.

The curves of Figure 2.12 represent the different designs exhibited by a stiff vehicle and a more crash worthy or flexible vehicle. The newer design in vehicles allows for the energy or in particular the impulse pulse, to be spread out over a longer time span which reduces the forces exerted on the occupants. In a collision, the change in momentum of the vehicle is dictated by the mass of the vehicle and the corresponding change in the velocity. The center of the mass of the vehicle is totally unimportant. Keep in mind that vehicles are relatively stiff structures even though the newer models contain crumple zones that help absorb the energy. Even in a relatively violent collision, the center of mass of the vehicle does not move appreciably. We will come back to the concept of center of mass when discussing objections to the use of momentum techniques.

2.14 Conservation of Momentum

In a general sense, we now explain the concept of conservation of linear momentum. In later sections of the book, we will discuss the specific applications of various momentum methods. These include elastic and plastic collisions, restitution, and rotational momentum techniques.

When two vehicles, bodies, or particles interact and produce forces, the momentum of each body is changed because of the forces that each exert on the other. Thus, by Newton's Third Law the force that is exerted on each body is equal in magnitude and opposite in direction to that which is exerted on the other. Notice that in this discussion we say that the vehicles, bodies, or particles are involved in the adherence to Newton's third law. A vehicle or body is simply a conglomeration of various particles or smaller bodies. Each portion of the vehicle is subject to the same law. Since these objects generally remain together as a result of the collision, it is useful to describe the behavior pre- and postcollision in terms of the center of mass of the object, machine, or vehicle. Even if a portion of a vehicle separates from the other portion, Newton's third law applies as does conservation of momentum. It is important to note that the impulses of the forces are equal in magnitude and opposite in direction.

This topic is very important and needs further clarification. Since the impulses of the forces are equal and opposite, the vector change in momentum of either vehicle, in any time interval, is also equal in magnitude and opposite in direction to the vector change in momentum of the other. Thus, the net change in momentum of the colliding bodies, the system, must be zero. Since the pair of action/reaction forces are internal forces of the system, since the total momentum of the system cannot be changed by internal forces, since the only forces acting on the system are internal forces, the total momentum of the system must remain constant in magnitude and direction. Keep in mind that in such a collision there are no appreciable external forces acting on the system. Thus, when no external force acts on the system, the total momentum of the system must remain constant in magnitude and direction.

This is the principle of conservation of linear momentum. This principle is also misunderstood by some accident reconstructionists. Typical arguments against the use of conservation of linear momentum fall into four basic categories. One category involves collinear collisions. That is, both vehicles are traveling in the same or opposite directions. In such instances, many reconstructions fail at a solution because of their inability to understand the problem and their lack of mathematical sophistication. Another category involves low velocity impacts. Some people state that momentum does not hold true for low velocity impact. However, conservation of linear momentum places no restrictions on initial conditions, and conservation of momentum can be used at any speed. A third category involves vehicles of significantly different masses such as a tractor trailer and a passenger vehicle. Again the development of conservation of linear momentum places no restrictions on masses, i.e., initial conditions for the collision. In actuality, before the advent of sophisticated measurement techniques in the last century, the muzzle velocity of a bullet was measured using the concept of conservation of linear momentum. That is, a small mass, the bullet, traveling at a high velocity, was fired into a large block of wood and the deflection of the wood from the impact was measured. The block of wood was a large mass at rest. This standard test was used successfully to accurately determine the muzzle velocity of bullets. Note that this test set up involved greatly varying masses and velocities, two arguments used against the use of momentum. A final category of argument against the use of conservation of linear momentum is that it does not hold true for shallow angle collisions. Again there are no restrictions on initial conditions, i.e., shallow angles, in the development of the theoretical arguments of momentum. It is true, however, that shallow angle collisions are very sensitive to the preimpact angles. These types of collisions lend themselves readily to computer solutions. It should be obvious that if two vehicles sideswipe and keep on going, it is not possible to utilize momentum to determine vehicle velocities. However, if they collide at shallow angles and skid to rest, there is no restriction on the use of momentum to determine the vehicle velocities. This is an example where engineering judgement, skill, and sophistication allow the problem to be solved.

In conclusion, it must be stated that the principle of conservation of momentum, whether linear or rotational, is extremely fundamental and powerful. Conservation of momentum is more fundamental and general than the principle of conservation of mechanical energy. Momentum methods have a wider application than energy methods. Conservation of momentum holds true no matter what the nature of the internal forces acting on the bodies, particles, or vehicles. In contrast, mechanical energy is conserved only when the internal forces are themselves conservative. We will discuss conservation of energy and work in the next section.

On a final note, momentum is generally applied to T-bone type collisions because those are the easiest to solve and are not sensitive to pre- and postcollision angles.

2.15 Conservation of Energy and Work

In order to determine how energy and work affect a vehicle in motion, we consider the diagram shown in Figure 2.13. The curved path represents the trajectory of the vehicle of mass m moving in the *x*-*y* plane and acted on by a force **F**. This force may be produced by the driver's input or resulting from

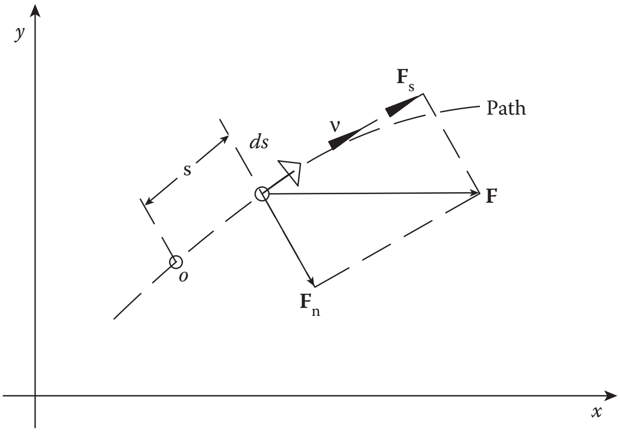

Figure 2.13 Vehicle in motion.

a collision and may vary from point to point along the path. We choose to resolve the force into its components $\mathbf{F}_s$ and $\mathbf{F}_n$ along and normal to the path. The normal component of the path, $\mathbf{F}_n$, is the centripetal force and its effect is to change the direction of the velocity $\boldsymbol{v}$. The effect of the component, $\mathbf{F}_s$, is to change the magnitude of the velocity.

In general terms, the magnitude of $\mathbf{F}_s$ will be a function of the path s, where s is the distance that the vehicle has traveled from a fixed reference point O. Applying Newton's second law

$$\mathbf{F}_s = m\frac{d\mathbf{v}}{dt} \tag{2.74}$$

Since $\mathbf{F}_s$ is a function of the path s, we may apply the chain rule, so

$$\frac{dv}{dt} = \frac{dv}{ds}\frac{ds}{dt} = v\frac{dv}{ds} \tag{2.75}$$

then

$$\mathbf{F}_s = mv\frac{dv}{ds} \tag{2.76}$$

If v_1 is the velocity when $s = s_1$ and v_2 is the velocity when $s = s_2$, we may integrate Equation 2.76.

$$\int_{s_1}^{s_2} \mathbf{F}_s d_s = \int_{v_1}^{v_2} mvdv \tag{2.77}$$

The integral on the left of Equation 2.77 is the work W of the force **F** and is defined as

$$W = \int_{s_1}^{s_2} \mathbf{F}_s d_s \tag{2.78}$$

The integral given by Equation 2.78 can only be integrated when $\mathbf{F}_s$ is known as a function of s or when $\mathbf{F}_s$ and s are related by another variable. In accident reconstructions, this is seldom the case. However, the integral on the right side can always be evaluated.

$$\int_{v_1}^{v_2} mvdv = \frac{1}{2}mv_2^2 - \frac{1}{2}mv_1^2 \tag{2.79}$$

Equation 2.79 represents the kinetic energy of the vehicle and is represented as

$$E_k = \frac{1}{2}mv^2 \tag{2.80}$$

Equation 2.77 is generally written as

$$W = E_{k2} - E_{k1} \tag{2.81}$$

stating that the work of the resultant force exerted on the vehicle equals the change in the kinetic energy, and is known as the work-energy principle.

Some explanatory material is in order at this point so that work and energy are properly applied to vehicles and the resulting collisions. Work on a vehicle is only done when the forces are exerted while the components move along the line of motion "at the same time." If the component of the force is in the same direction as the displacement, the work is positive. If the force is opposite to the displacement, the work is negative. If the force is perpendicular to the displacement, the work is zero. If the car or a component of the car is lifted, the work of the lifting force is positive as when a spring is stretched or when the gas in a shock absorber is compressed. When the car skids on a road, the work of the frictional force exerted on the tires is negative along the path since the force is opposite the displacement of the vehicle. No work is done on the road by the frictional forces because there is no motion of the road.

In computing the work of a force, we multiply the magnitude of the vector **F** in the direction of the vector $d\mathbf{s}$. This is the scalar product of the vectors. Thus, in general terms, care must be taken in computing the work as

$$W = \int_{s_1}^{s_2} \mathbf{F} \cdot d\mathbf{s} = \int_{s_1}^{s_2} \mathbf{F}\cos\theta d\mathbf{s} \tag{2.82}$$

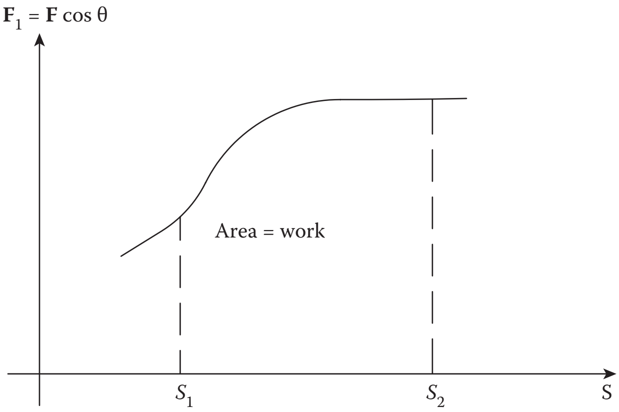

Figure 2.14 Work diagram.

In the special case where $\cos\theta = \pm 1$

$$W = \pm\, \mathbf{F}\mathbf{s} \tag{2.83}$$

Only in this special case is work equal to force times distance. Figure 2.14 is a generalized diagram representing work according to Equation 2.82.

The resultant force **F** acting on the vehicle may be made up of several forces acting "on it," such as the individual frictional forces on the tires as the vehicle skids out of control. Each of these may be computed from the basic definition of work. Since work is a scalar quantity, the total work is the algebraic sum of the individual works. These concepts are fully analyzed in the section on friction and the speed of a vehicle in the energy methods of Chapter 4. Note that only the total work is equal to the change in kinetic energy of the vehicle.

2.16 Kinetic Energy

A review of Equation 2.81 reveals that kinetic energy and work are scalar quantities. The magnitude of the velocity of a moving vehicle is the only parameter that establishes the amount of kinetic energy. The process that produced the motion nor the direction of the motion establishes the value of the kinetic energy. The work energy principle states that the change in the kinetic energy does not depend on the individual values of the force **F** and the path *s*. Kinetic energy increases if the work is positive and decreases if the work is negative. As a vehicle accelerates, the work is positive and as it decelerates, the work is negative. A vehicle traveling at a constant velocity does no work and the change in kinetic energy is zero.

2.17 Potential Energy due to Gravity

In accident reconstructions the bodies in motion, whether vehicles, humans, or equipment, are near or on the surface of the earth so that variations in the gravitational force can be neglected. Figure 2.15 represents a body moving vertically along an arbitrary path.

The downward force on the body is produced by its weight w and P is the resultant of all the other forces acting on the body. The work of the gravitational force is

$$W_g = \int_{s_1}^{s_2} w \cos\theta \, ds \tag{2.84}$$

Since ϕ is the angle between ds and the vertical component dy, then $dy = ds \cos \phi$, and $dy = -\cos \theta \, ds$, thus

$$W_g = -\int_{y_1}^{y_2} w\,dy = w(y_2 - y_1) = (mgy_2 - mgy_1) \tag{2.85}$$

Therefore, the work of the gravitational force depends only on the initial and final elevations and not on the path. Since the total work is equal to the change in kinetic energy,

$$W_T = W_p + W_g = E_{k2} - E_{k1} \tag{2.86}$$

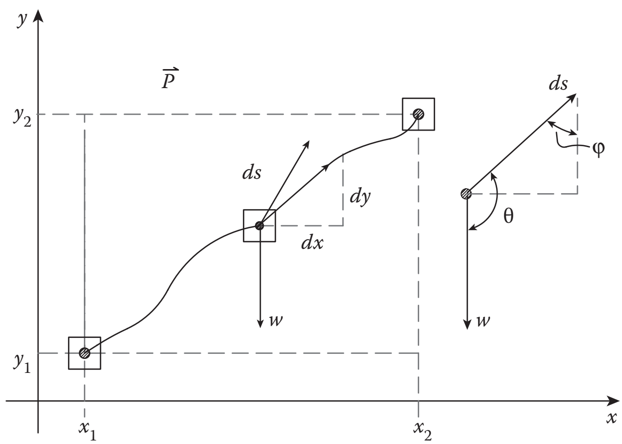

Figure 2.15 Gravitational potential energy.

where

$W_{T=}$ total work

W_p = work of the force **P**

W_R = work due to gravitational effects

E_{k2} = final kinetic energy

E_{k1} = initial kinetic energy

Generally, it is convenient to express Equation 2.86 in terms of the work of the force **P** so that

$$W_{\mathbf{P}} = \left(\frac{1}{2}mv_2^2 - \frac{1}{2}mv_1^2\right) + (mgy_2 - mgy_1) \tag{2.87}$$

or

$$W_{\mathbf{P}} = \left(\frac{1}{2}mv_2^2 + mgy_2\right) - \left(\frac{1}{2}mv_1^2 + mgy_1\right) \tag{2.88}$$

where

$$E_{\mathbf{P}} = mgy \tag{2.89}$$

is the gravitational potential energy.

The sum of the kinetic and potential energy is called the total mechanical energy. The work of all the forces acting on the body, except for the gravitational force, equals the change in the mechanical energy. If the work $W_{\mathbf{P}}$ is positive, the mechanical energy increases; if negative, it decreases. In the special case in which the only force on the body is the gravitational force, the work $W_{\mathbf{P}}$ is zero. Then

$$\frac{1}{2}mv_2^2 + mgy_2 = \frac{1}{2}mv_1^2 + mgy_1 \tag{2.90}$$

2.18 Elastic Potential Energy

Another concept that is utilized in accident reconstruction is that of elastic potential energy. This principle is introduced in the modeling of the crush deformation of a vehicle during a collision and is based on Hooke's law, which states that the elastic force is proportional to the displacement of the spring. Consider Figure 2.16.

When an external force P stretches or compresses the spring so as not to permanently deform it, the elastic force is given by

$$F = kx \tag{2.91}$$

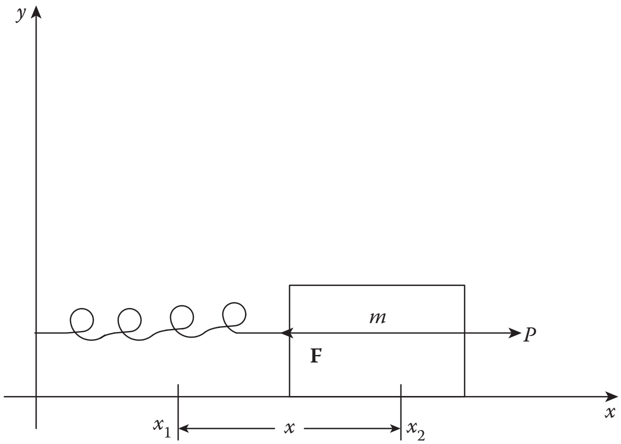

Figure 2.16 Hooke's law.

where k is the stiffness constant of the spring and x is the displacement. The work of the elastic force is given by

$$W_e = \int \mathbf{F} \cdot d\mathbf{s} = \int_{x_1}^{x_2} \mathrm{F} \cos\theta \, dx \tag{2.92}$$

since the force **F** is opposite the direction of dx, $\cos\theta = -1$ and

$$W_e = -\int_{x_1}^{x_2} \mathbf{F} dx = -\int_{x_1}^{x_2} kx dx \tag{2.93}$$

$$W_e = -\left(\frac{1}{2}kx_2^2 - \frac{1}{2}kx_1^2\right) \tag{2.94}$$

As in the previous section, we will let W_P be the work of the applied force P so that the total work is equal to the change in the kinetic energy, and

$$W_T = W_p + W_e = E_{k2} - E_{k1} \tag{2.95}$$

or

$$W_P = \left(\frac{1}{2}mv_2^2 - \frac{1}{2}mv_1^2\right) + \left(\frac{1}{2}kx_2^2 - \frac{1}{2}kx_1^2\right) \tag{2.96}$$

where

$$E_{ep} = \frac{1}{2}kx^2 \tag{2.97}$$

is the elastic potential energy. Equation 2.96 may also be written similarly to Equation 2.88 as

$$W_P = \left(\frac{1}{2}mv_2^2 + \frac{1}{2}kx_2^2\right) - \left(\frac{1}{2}mv_1^2 + \frac{1}{2}kx_1^2\right) \tag{2.98}$$

In this case, the total mechanical energy is the sum of the kinetic and elastic potential energies. The work of all the forces acting on the body, except for the elastic force, equals the change in the mechanical energy. If W_P is positive, mechanical energy increases; if negative, it decreases. In the special case when W_P is zero, the mechanical energy is conserved and constant.

2.19 Dissipation and Conservation of Forces

The work of the gravitational force is independent of the path and purely dependent on the vertical displacement. Thus, when an object such as a vehicle or a person falls and is subject to the motion of a projectile, for the same initial speed, irrespective of the angle of departure, the speed is the same at all points at the same elevation. If the gravitational force acts alone on the object, the total mechanical energy is conserved. If the object first rises and then descends to its original position, the work is completely recovered.

Similarly, in the extension and contraction of a spring to the original location, the elastic potential energies are conserved and the work is recovered. Thus, conservative forces as outlined above are characterized by independence of path, equality of the difference between initial and final energy functions, and are completely recoverable. In contrast, the force produced by friction depends on the path. When a vehicle skids for 50 ft or for 75 ft from one point to another, the energy expended differs. The skid of 50 ft may be a straight line between two points, whereas the skid of 75 ft may be a curved path between the two points. Much erroneous significance is often placed on which wheel produced which skid by many reconstructionists. Later sections of the book outline the fallacy in these arguments based on basic principles. If a vehicle skids to one location and then skids back to its original position, the work is not recovered and thus the total mechanical energy is not conserved. Care must always be taken when applying conservation of energy principles. That is why in an earlier section, we stated that energy is not always conserved but momentum is always conserved and is therefore a more fundamental principle. Friction involves dissipative forces rather than conservative forces in classical Newtonian mechanics.

2.20 Internal Work, Energy, Power, and Velocity

Consider a vehicle undergoing acceleration as shown in Figure 2.17.

The external forces on the automobile are the weight W and the normal forces N_1 and N_2. The work of these external forces is zero because they are perpendicular to the motion of the vehicle. The forces P_1 and P_2, depending on whether the vehicle is rear, front, or all wheel drive are the unbalanced forces which produce the acceleration and velocity. The work of P_1 and P_2 is zero at the point of application and is not equal to the increase in kinetic energy of the system. Therefore, the internal work is responsible for the motion that is produced, in a more general sense, both internal and external forces produce the change in the total kinetic energy of the system. Thus

$$W_T = W_o + W_i = \Delta E_k \tag{2.99}$$

where

W_T = total work
W_o = external work
W_i = internal work
ΔE_k = kinetic energy change

A more general representation for the work produced by external and internal forces is then,

$$W_P = W_T + \Delta E_{ep} + \Delta E_{ip} \tag{2.100}$$

where

W_t = total kinetic energy change
ΔE_{ep} = external potential energy
ΔE_{ip} = internal potential energy

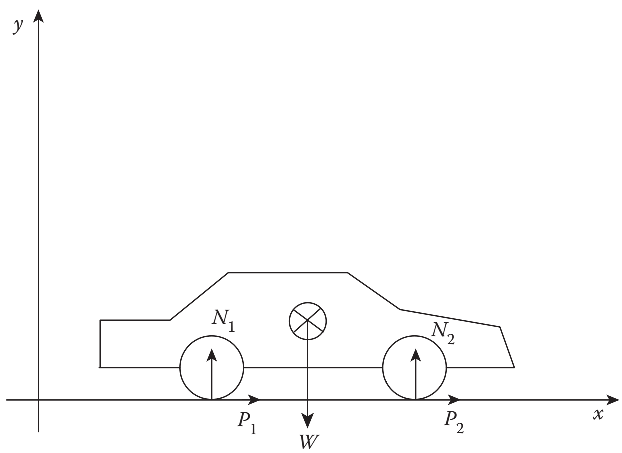

Figure 2.17 Accelerating vehicle.

In Equation 2.100 the total mechanical energy of the system includes the external and internal potential energies and the kinetic energy. The total mechanical energy is conserved only when W_P is zero.

The rate of doing work is defined as the power of the system so that the instantaneous power is given by

$$P = \frac{dW}{dt} \tag{2.101}$$

and the average power is

$$P_{\text{av}} = \frac{\Delta W}{\Delta t} \tag{2.102}$$

Figure 2.18 represents a force on a vehicle causing a displacement Δs along a path.

The tangential component F_t of the force **F** is related to the power by the velocity ν as

$$P_{av} = \frac{\Delta W}{\Delta t} = F_t \frac{\Delta s}{\Delta t} = F_t \mathbf{v} \tag{2.103}$$

In general we may write

$$P = \mathbf{F} \cdot \mathbf{v} \tag{2.104}$$

Equation 2.104 states that the instantaneous power is the product of the instantaneous velocity ν and the tangential component of the force F_t.

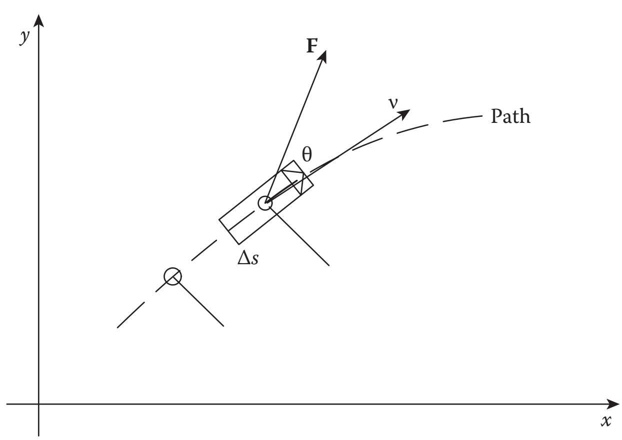

Figure 2.18 Forces on a vehicle.

Equations 2.99 through 2.104 are used to compute the relationship between velocity and horsepower of a given vehicle if the gear ratio of the transmission is known.

2.21 Change in Velocity

When vehicles collide they undergo a change in their velocities. The change in their velocities is a result of the conservation of energy and conservation of momentum which we discussed in the previous sections. Change in velocity is a concept which is simple in concept but often misunderstood. In order to properly define change in velocity, sometimes improperly referred to as change in speed, and commonly described as ΔV, we refer to Figure 2.19.

In a statement, change in velocity is defined as the change in the magnitude and the change in the direction of the velocity of a vehicle resulting from a collision. Thus, the change in velocity of a vehicle is a measure of the velocity vector preimpact and the velocity vector postimpact. In terms of equations we define:

$$\Delta V = [(V_{ix} - (V_{fx})^2 + (V_{iy} - V_{fy})^2)]^{1/2} \tag{2.105}$$

Equation 2.105 represents the basic definition of the velocity change where

ΔV = change in velocity
V_{ix} = initial velocity in the x-direction
V_{fx} = final velocity in the x-direction
V_{iy} = initial velocity in the y-direction
V_{fy} = final velocity in the y-direction

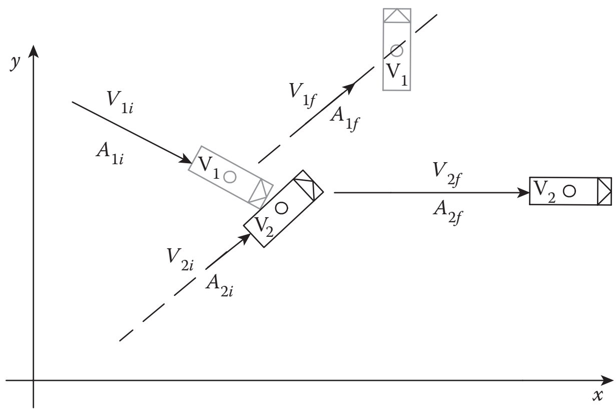

Figure 2.19 Change in velocity.

Thus, by definition, the velocity change is the vector from the tip of the initial velocity vector to the tip of the final velocity vector. This definition completely and accurately describes the velocity change. Furthermore, when vehicles are instrumented for crash testing, the equipment that measures the velocity change does so in accordance with the equation described above. For two vehicles we can then define the velocity change equations as,

$$\Delta V_1 = \sqrt{(V_{1i}\cos A_{1i} - V_{1f}\cos A_{1f})^2 + (V_{1i}\sin A_{1i} - V_{1f}\sin A_{1f})^2} \tag{2.106}$$

$$\Delta V_2 = \sqrt{(V_{2i}\cos A_{2i} - V_{2f}\cos A_{2f})^2 + (V_{2i}\sin A_{2i} - V_{2f}\sin A_{2f})^2} \tag{2.107}$$

In the above equations V_{1i} and V_{2i} represent the initial velocities and V_{1f} and V_{2f} represent the final velocities of the vehicles. The initial and the final angles are represented by A_{1i} and A_{2i} and A_{1f} and A_{2f}, respectively.

The astute observer will have noticed that depending on the direction of the initial and final angles of the vehicles, the change in velocity vector may lie in one of the four quadrants of a standard Cartesian set of coordinates in the *x*-*y* plane. The angle of the velocity change, ΔA, is therefore defined as follows:

First quadrant: $\Delta A = a \tan \theta$
Second quadrant: $\Delta A = 180 - a \tan \theta$
Third quadrant: $\Delta A = 180 + a \tan \theta$
Fourth quadrant: $\Delta A = 360 - a \tan \theta$
where θ is the angle of ΔV with respect to the *x*-axis.

Evidence Gathering

3

3.1 Introduction

In order to properly reconstruct or model a collision, an accident, or an event, it is important to gather all the information that is available. The more information that is gathered, the more accurate the model of the event becomes. As with any forensic engineering investigation, while the evidence is being gathered, it is often unknown which evidence, measurement, or facts will be more important. Sometimes evidence is overlooked or simply ignored. Careful investigators are methodical and generally slow in their approach. Through experience, they have learned that the use of check lists or set procedures is very helpful in conducting forensic investigations.

There is a movement among some forensic engineers to avoid and discourage the use and development of standards or guides in forensic engineering. A typical argument against the use and development of standards is to rely on engineering judgment when conducting a forensic engineering investigation. Engineering judgment or more properly stated, scientific judgment, deals with the selection of scientific methods in the analysis of an event. For example, when measuring a road and the markings produced in a collision, there are several perfectly acceptable methods that may be used. The investigator may choose to use an optical surveying instrument, a total station, a rolling tape, a simple tape, or may resort to photography when necessary. Under these conditions, scientific, or engineering judgment is allowed. Alternatively, engineering judgment may be allowed in the use of the methods for the calculations. It is perfectly acceptable to use conservation of momentum or conservation of energy methods to find the solution for the velocities of the vehicles. When properly applied, under justifiable assumptions, both methods produce comparable results. What is not allowed under engineering or scientific judgment is to disregard key evidence, skew the information, or selectively choose the information that only fits the client's perspective. For example, a common ploy is to average skid marks or significantly reduce the coefficient of friction based on the number of skids deposited on the road surface. Such tactics are not engineering or scientific judgment but simply misapplication of the laws of physics and violations of the scientific method and the canons of ethics in engineering. Keep in mind that the thrust of this book is toward a forensic engineering perspective. The views expressed in the book may not be in accord with other types of investigators or reconstructionists. The methods and techniques used by these other investigators may not be deeply rooted in science and mathematics.

In this light, the development of standards or guides is an invaluable tool to aid the investigating engineer in gathering all of the available facts or data. The three most important areas of measurement or data gathering are the site, the vehicles or equipment, and the pertinent components that may be involved in the event. Each of these topics will be discussed in greater detail in the following sections.

3.2 Measurements

A simple ruler, tape measure, or roller tape is invaluable in measuring many characteristics of an accident site or vehicle dimension. In certain instances, a ruler is used to measure undercarriage components that may have caused gouges on the road. There are various commercially available devices used to measure crush depth profiles of vehicles. Crush profiles may also be measured with a simple string and a ruler. In fact, crush profile measuring instruments are sophisticated strings and rulers. Another method of measuring crush profiles is to use a laser transit. This method, although realistically no more accurate than a string and ruler, may be preferred because the input data is easily stored and available for reproduction. The measurements can be compared to photographs through photogrammetry. The systematic storage and reproducibility of the data are of utmost importance in light of the Daubert decision and the scientific method. As the analysis tools used by reconstructionists become more sophisticated, the importance of storage and preservation of the evidence becomes more pronounced.

Today's reconstructionists have at their disposal large data bases for vehicle dimensions. Several companies throughout the country provide vehicle specifications, dimensions, and performance data for automobiles, trucks, and all terrain vehicles. In many instances, the performance parameters of vehicles can be used to validate or refute an accident scenario. Based on a real case, I will describe the following accident scenario. A van pulled out of an access road after stopping and noting a large dump truck some distance down the road. The van pulled out, made a right turn, and traveled more than 100 ft before being rear-ended by the dump truck. The speed limit on this section of road was 25 mph. Standard analysis revealed that the dump truck was traveling at least 45 mph at impact and that the van's speed was approximately 20 mph. Performance data on the van's acceleration indicated that the computed speed of the van was within its performance parameters. The dump truck driver stated that the van pulled out in front of him and that he could not stop. He stated that he was traveling 25 mph, and his truck was in 13^{th} gear. After impact the dump ruck required almost 500 ft to come to a stop. Subsequent discovery revealed that the truck's braking system was inoperable and that braking was mainly performed through the engine retarder. Furthermore, performance data on the dump truck revealed that the vehicle could not travel at 25 mph in 13^{th} gear. Essentially, the engine would have shaken and chugged violently at that speed and gearing. The 13^{th} gear performance of the truck was verified through calculations. Of course, the opposing expert testified that the dump truck was not traveling faster than 25 mph and that the van pulled out suddenly and was responsible for the accident. The opposing expert used a common ploy to decrease the speed by decreasing the frictional coefficient in his calculations. This ploy will be revealed in a later section and will be mathematically shown to violate the laws of physics.

"Measure twice and cut once" is heard with respect to carpentry and the construction trades. Engineers as accident reconstructionists apply the statement as they gather facts of an accident based on sound engineering and physical principles. They are not allowed to rebuild the accident unless all the pieces of the puzzle fit together. Therefore, we must measure, remeasure, calculate, recalculate, and use multiple methods to ensure that all the pieces fit. This data must be properly stored and available for verification by other investigators. The data and analysis must be reproducible and defensible in a court of law.

Many times measurements can only be made from the available data such as photographs. Often reconstructionists are asked to analyze an accident months or years after the occurrence. Sometimes the vehicles are no longer available or the road surface has been re-paved. In such cases, more sophisticated techniques involving computers are used to measure and gather data. These techniques are referred to as photogrammetry and three-dimensional analysis. There are various computer programs available that aid the reconstructionist in this type of analysis, which will be discussed in Chapter 11.

"A picture is worth a thousand words" is heard often and rings true. One of the most powerful measurement tools is the camera. Good quality single lens reflex (SLR) cameras are available today at reasonable prices. Versatile variable lenses including macro features work best to document the accident site and the vehicles.

3.2.1 Site Inspection

The first question that arises concerning the site inspection is "should the site always be inspected?" The simple answer is yes whenever possible. Let us discuss two different scenarios that may arise when the site may or may not be inspected. The first case is when the site has been modified after the event. Generally roadways are not completely altered, i.e., the site is bulldozed or covered with 20 ft of soil and a new highway constructed. What often may happen is that the road surface is repaved or repainted. Perhaps signage has been changed. The second case is when the client, because of monetary constraints is not willing to spend the money on a site inspection. Such a scenario arises in what is referred to as paper or desk-top reconstructions. These reconstructions generally involve low velocity impacts or staged collisions. In these cases the injuries claimed are soft tissue injuries with no discernible medical pathology. Please refer to the chapter on low speed impacts for a detailed analysis and characteristics of staged collisions.

In the first case, when the site has been altered, an inspection and detailed measurements can reveal the information that has been covered up or lost. The basic geometry of the site is seldom altered. The road curvature, superelevation, width, curbs, drainage, and many other features are seldom altered. In the case where police or adjuster photographs are available, photogrammetric techniques can be employed to uncover the lost information. In complex cases, a virtual scene reconstruction in conjunction with photogrammetry and survey data can reveal the hidden, covered up, or lost data. Such exhaustive analysis and site inspection techniques are seldom necessary and are time consuming and therefore beyond the budget of the standard reconstruction.

Another important reason for inspecting the site, taking photographs, and measuring the basic geometry is to answer the opposing attorney. Then the answer is simply, "Yes I was there, here are my photographs, and this is my site diagram and full notes." At that point, considerable wind is removed from the attorney's sails.

When the site is not personally inspected by the forensic investigator, there are viable alternatives. Often the insurance adjuster visited the site and took photographs or basic measurements. The investigating officer may have also taken basic or complex measurements and photographs. These alternate methods of site recognition and analysis are acceptable in most low impact and staged collisions. Aerial photographs or satellite photographs may be available that show sufficient detail to make valuable engineering judgments.

The next question to be answered is how much do I measure? Again, this is a question for engineering judgment. Only the information pertinent to the reconstruction needs to be measured. This information would include road widths, lanes, curbs, signage, skids, gouges, etc. To what accuracy should these measurements be taken? For most reconstructions, the accuracy of the measurements needs only to be to ½ of a foot. In many instances accuracy to the nearest foot is sufficient. For example, if a skid mark measures 74 ft 4½ inches, a measurement of between 74 and 75 ft is sufficient because the accuracy of the calculation will be within 2% which is well within engineering accuracy of between 5 and 10%. The accuracy of the frictional coefficient cannot be known to any degree greater than 5% or 10% of the actual value. Thus, the measurement of the skid between 74 and 75 ft does not produce a calculation outside of engineering accuracy.

When measurements are taken with more accurate instruments such a total stations, the measurements can easily be rounded to the nearest foot or can be used as recorded. Just remember that when velocity calculations are carried out, it is preposterous to state that a particular vehicle was traveling 63.45 mph. Realistically, it is more accurate to state a range of speeds, perhaps between 61 and 65 mph or approximately 63 mph. Also remember, that if different methods are used to perform the calculations, the answers obtained will not be exactly the same. Thus, the authors prefer to use a range of values or an approximate value within engineering or scientific accuracy.

The accuracy of the site measurements is less significant. Very seldom is it necessary to measure the site to greater accuracy than to the nearest foot. One exception is when it is important to determine what portion of a vehicle's structure caused a particular gouge. For example, two gouges in close proximity may have been produced by a particularly violent collision. One may be due to a lower control arm on a vehicle's suspension and the other produced by a wheel rim. Other experts may opine that one of the gouges was produced by the drain plugs of the oil pan. Such questions arise in left of center collisions, when the extent of intrusion into the opposing lane is important. In such a scenario, measurements to within one inch of accuracy may be necessary. This range of accuracy leads to the inspection of the vehicle.

3.2.2 Vehicle Inspection

Vehicle inspections can take two forms similar to the site inspection. One type of inspection involves a review of vehicle specifications and photographs. The other type of inspection involves an actual visit to the vehicle with detailed measurements and photographs. A review of vehicle specifications and photographs taken by other entities is sufficient of low impact or staged collisions. Often such collisions involve minor damage or mismatched damage. One vehicle may show relatively no damage and the other vehicle may show much more significant damage. More significant collisions generally require that the vehicle be inspected, photographed, and measured. Of course, if the vehicles are no longer available, the investigator must rely on the other methods of analysis.

Vehicle specifications can be obtained from different sources. There are several commercially available sources for vehicle specifications. Virtually any domestic or foreign passenger vehicle's specifications can be obtained in this manner. These types of specifications also include light duty trucks and tractors. Specialty vehicles, such as motor homes or conversion type vehicles specifications can generally only be obtained from the manufacturer. This is also true for trailers hauled by tractors. Specifications for some commercial or specialty vehicles can only be determined by inspections. Obviously, some form of engineering judgment enters into this phase of the investigation. It goes without saying that if the vehicle specifications have been obtained from the manufacturer, the validity of those specifications and measurements cannot be questioned by an opposing attorney. Figure 3.1 shows the measured crush profiles of two vehicles involved in a collision. Figure 3.2 shows a typical measurement of the crush on a vehicle as it is conducted in the field under adverse conditions. Figure 3.3 shows the accident road marks after the collision. Figure 3.4 shows a large truck as it is readied for analysis

When it is deemed necessary to inspect the vehicle, measurements and photographs should be taken. It is generally helpful to have the vehicle

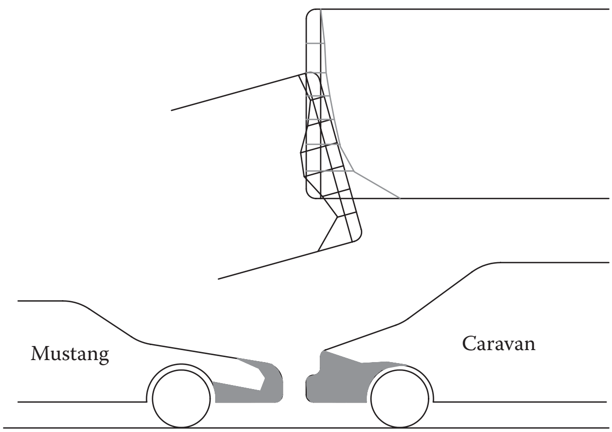

Figure 3.1 Crush profiles.

Figure 3.2 Crush measurement.

Figure 3.3 Accident site.

Figure 3.4 Truck.

specifications when conducting the measurements. For example, the collision may have produced a shortening of the wheel base. Knowing the relative position of the front axle with respect to the rear axle can aid in measuring the crush deformation. The Society of Automotive Engineers (SAE) has developed standards for the measurement of the crush profiles of passenger vehicles and trucks. A recurring theme of this book is the use of standards and guides so that the authors encourage the use of this information. There are some commercially available aids for the measurements of crush. These may be used or you may simply choose to use some tape, a string, and a couple of rulers to conduct your measurements. Either technique yields sufficiently accurate and acceptable measurements. The accuracy for these measurements needs only to be to the nearest inch. Greater accuracy is unnecessary and generally unattainable because of the conditions under which the measurements are taken. Seldom are these measurements taken in a garage faculty with a concrete floor without other vehicles obstructing the measurements. The typical salvage yard is dirty, muddy, overgrown with weeds, and littered with vehicles and parts. Sometimes the salvage yards are helpful and they will move the vehicles to inspection sites where conditions are more favorable. However, do not count on it and always be prepared for the worst of conditions.

One of the measurements that can be taken on certain vehicles is the interrogation of the air bag module. Please refer to Chapter 13 for a detailed discussion of the retrieval of the crash data.

Figure 3.5 shows the retrieval of the crash data from the air-bag module of a vehicle. The accompanying graph of the data is shown in Figure 3.6 and the crush on the vehicle is depicted in Figure 3.7. A standard for the interrogation of the crash information has been developed by ASTM (ASTM E2493-07) which should be followed when this data is retrieved. Please refer to Chapter 15 for the standard.

3.2.3 Component Inspection

Whenever possible, component inspections should be undertaken under controlled conditions. If a component is suspected to have failed and caused a collision or an accident, the inspection needs to be performed in accordance with recognized or approved protocols. Under these circumstances, the accuracy of the measurements increases. Where the site measurement accuracy may be to the nearest foot and the vehicle crush deformation to the

Figure 3.5 Crash data retrieval.

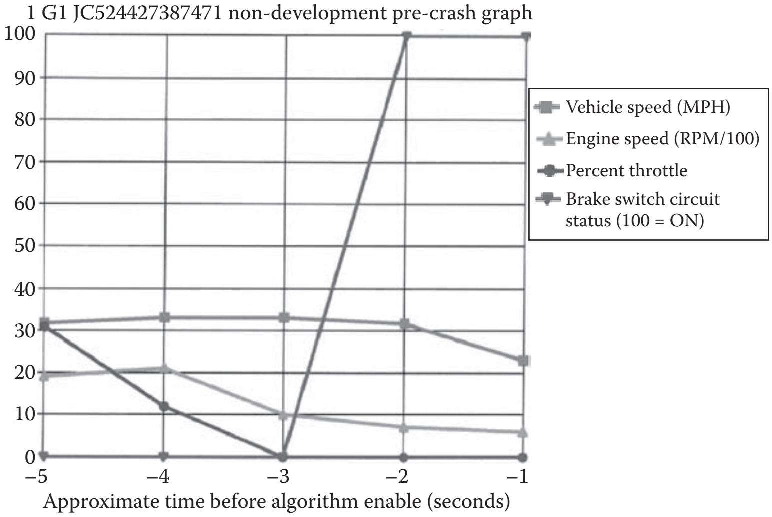

Figure 3.6 CDR graph.

Figure 3.7 Crush on vehicle.

nearest inch, the accuracy of the component measurement may be significantly greater.

At this point it is noteworthy to mention that standard guides for the inspection of suspected failed components are available. These standards are included in Chapter 15. Following these guides will certainly keep detractors at bay but also ensure that the evidence is preserved.

If during a vehicle inspection, a particular component is suspected of having played a part in the incident, the component should be carefully documented and photographed. Preferably, the component should not be removed until the interested parties are notified and an agreed upon protocol for the inspection can be established. Please refer to Chapter 15 on standards and protocols. In some instances, in order to preserve the evidence, the suspected component must be removed. For example, the inspection of the vehicle may reveal that the Pitman arm on a steering box indicates cyclic fatigue failure and may become detached. This component should be preserved even though some disassembly may be required. All that needs to be done is to carefully and systematically document the removal, tagging, and packaging of the component. This process is easily immortalized through photographs or video documentation.

Once the component has been removed and preserved, a chain of custody form should be filled out. The chain of custody form contains basic information on the particulars for the retention and safe keeping of the evidence. Any time the evidence changes hands or locations, a chain of evidence form should be filled out for proper documentation and trail of the evidence. Included below is a typical chain of custody form containing the necessary information.

Chain of Custody

Client/company:	Insured:	Control #:
Date:	Time:	
Evidence taken from:	____________________ Name printed	____________________ Signature
Evidence taken by:	____________________ Name printed	____________________ Signature

List of evidence:
1. a
2. b
3. c
4. d

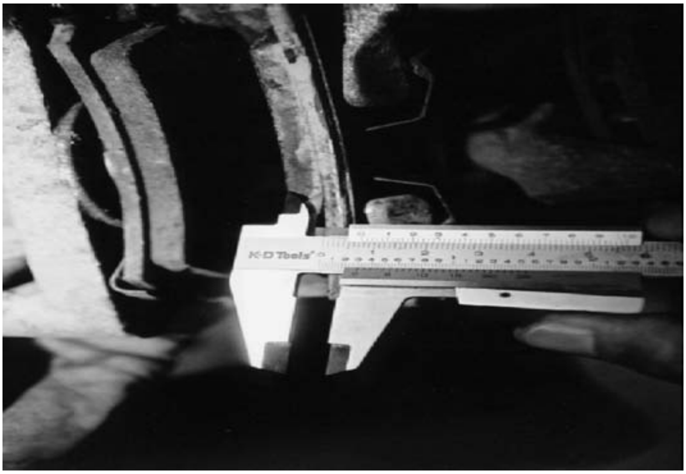

Figure 3.8 Brake inspection.

It is suggested that some photographs be taken as the evidence changes hands or location. In this manner, the parties involved cannot be accused of tampering with or modifying the evidence. Figure 3.8 shows the inspection of a brake pad after it was removed.

3.3 Photography

Photographs are probably some of the most important pieces of data gathering that a reconstructionist can obtain. In some cases the vehicles are no longer available for inspection so that photographs cannot be taken. However, often the investigating adjuster for the respective insurance company may have taken photographs. In some instances the repair facility may have photographs of the vehicle. Many progressive body repair shops have started taking photographs in order to minimize their exposure in case problems arise as a result of their work. Commercial companies such as hauling outfits, trucking companies, contracting companies, etc., will send their personnel to the accident site in order to photograph the conditions at the scene or of their vehicles. Some investigating police departments take photographs as a matter of course especially when serious injuries or death occurs as a result of the collision.

The equipment used and the quality of the photographs taken by other individuals cannot be controlled by the investigating forensic engineer. Those photographs must be taken at face value and the available evidence extracted accordingly. Some of the information expected from the photographs cannot be obtained because of the quality of the photograph that is being analyzed.

The azimuth and elevation angles of the photograph may not reveal the information that is being sought. Similarly, the framing of the subject, lighting conditions, shadows, and obstructions may be such that the photograph is devoid of the information. Sometimes the photographs, if taken with a low resolution digital camera, will yield printed images that are lacking in quality. Most of the problems outlined above are beyond the control of the engineer and must be dealt with accordingly.

What is under the direct control of the investigating forensic engineer is the quality of the photographs he or she takes. Some investigators make use of a professional photographer. This approach is certainly very acceptable as long as the investigator directs the shots that are taken. In our experience the preferred method is to become sufficiently adept at photography. Fortunately, today's technology can make the novice and not so experienced photographer look very good. Camera technology has advanced to the point that most features are automatic so that the photographer need only to point and shoot.

3.4 Computer Techniques

Today's technology affords the accident investigator a wealth of resources from which to gather information. These resources may be governmental or private resources. Some examples of private resources include the SAE, the *Accident Reconstruction Journal*, the *Accident Reconstruction Quarterly*, *Expert Auto Stats*, and *Motor Vehicle Data* to name a few. An example of a governmental agency that provides vehicle crash data is the National Highway Traffic Safety Administration. The government also publishes vehicle recalls through various web addresses.

In some instances, the accident site is not visited, inspected, measured, or photographed. Similarly, the vehicles involved in the collision may not be so inspected or available for inspection. In those instances, the data bases available can produce significant information. Global mapping programs have a large portion of the world photographed to excellent detail in most instances to the extent that accurate dimensions and significant features can be gleaned. Global positioning systems can also be used in order to locate accident sites in rural areas. A considerable amount of information can be gathered through the world wide web.

3.5 Photogrammetry

Reconstruction methods often use terrestrial photogrammetric methods in order to determine distances and general measurements. The American

Society of Photogrammetry defines the process as "the art, science, and technology of obtaining reliable information about physical objects through the recording, measuring, and interpreting photographic images." Metric photogrammetry using terrestrial photos consists of making precise measurements from photographs in order to locate the relative location of points in a real world environment.

When a photograph of an accident scene is taken, the orientation of the camera axis is generally oblique. When oblique terrestrial photographs are taken, the camera axis is inclined either up or down at the time of exposure. Generally, when accident reconstruction photographs are taken, the camera axis is tilted down so that the angle of inclination is negative. A typical oblique photograph with horizontal and vertical displacement is shown in Figure 3.9. It should be denoted that although the representation of Figure 3.9 includes a negative angle of inclination, the procedure for a positive angle of inclination is exactly the same.

From Figure 3.9 we can define the following geometric points relative to the photograph

θ = angle of inclination (depression angle if negative, elevation angle if positive)
v_1, v_2 = vanishing points at horizon
a = point of interest on photograph
x_a, y_a = photograph coordinates of point "a" relative to the oblique coordinates established by the photograph
f = focal distance of the camera
W, H = enlarged photograph dimensions
e_a = enlargement adjustment from negative to photographic positive

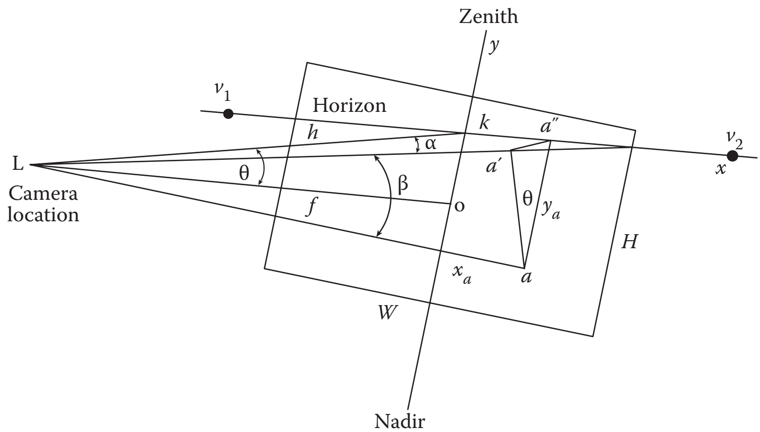

Figure 3.9 Oblique terrestrial photograph.

The angle of inclination may be determined in two ways

$$\theta = \tan^{-1}\left[\frac{k_o}{f'}\right] = \tan^{-1}\left[\frac{y_o}{f'}\right] \tag{3.1}$$

where

$$f' = e_a f \tag{3.2}$$

alternatively

$$t = \tan^{-1}\left[\frac{\text{on}}{f'}\right] \tag{3.3}$$

thus

$$\theta = t - 90^\circ \tag{3.4}$$

The horizontal and vertical angles may be referred to as the azimuth and depression angles, respectively. Thus,

$$\alpha_a = \tan^{-1}\left[\frac{ha'}{Lk - hk}\right] = \tan^{-1}\left[\frac{x_a}{f'\sec\theta - y_a\sin\theta}\right] \tag{3.5}$$

$$\begin{aligned}\beta_a &= \tan^{-1}\left[\frac{aa'}{La'}\right] = \tan^{-1}\left[\frac{aa'}{(Lk - hk)\sec\alpha_a}\right] \\ &= \tan^{-1}\left[\frac{y_a \cos\,\theta}{(f'\sec\theta - y_a\sin\theta)\sec\alpha_a}\right]\end{aligned} \tag{3.6}$$

where
a_a = azimuth angle and β_a = depression angle.
Given θ, α_a, β_a we can determine dimensions on a photograph as follows:

I. Locate the center of the photograph, point 0, see example.
II. Establish horizon or zenith lines.
III. Draw the photograph axis and locate the points of interest on the photograph (points, *a*, *b*, etc.).
IV. Record the coordinates of the points x_a, x_b, etc.

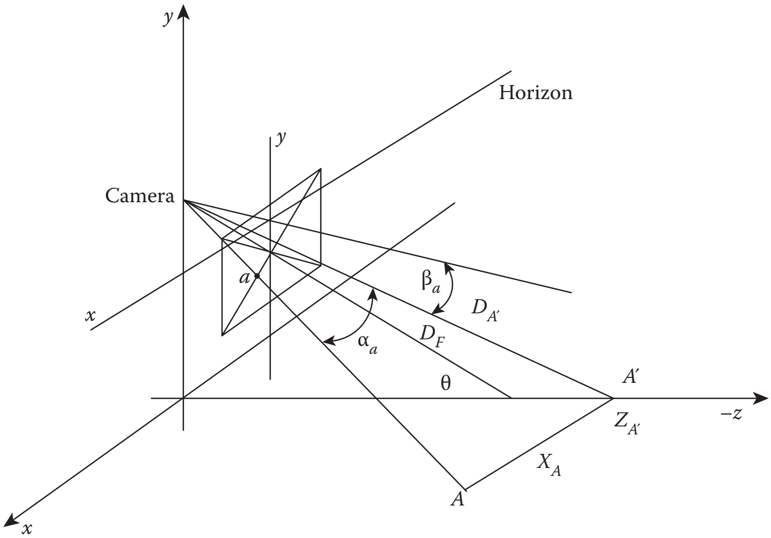

Figure 3.10 Camera and real world.

After the data are gathered and plotted, the oblique photograph may be resolved into its azimuth and elevation views as follows. Consider Figure 3.10, which shows a three dimensional view of the camera, the oblique photograph, and the real world line. For consistency, lowercase letters and symbols are used on the photograph and uppercase notation for the geometry of the real world.

On the elevation plane the geometry resolves as in Figure 3.11 for two points a and b. While the azimuth plane is as shown in Figure 3.12.

From the geometry, the following equations may be obtained

$$Z_R = \frac{H_c}{\tan\theta} \tag{3.7}$$

$$D_F = \sqrt{Z_R^2 + H_C^2} \tag{3.8}$$

$$D'_A = D + F\sin\theta/\sin\beta_a \tag{3.9}$$

$$Z'_A = D'_A\cos\beta_a \tag{3.10}$$

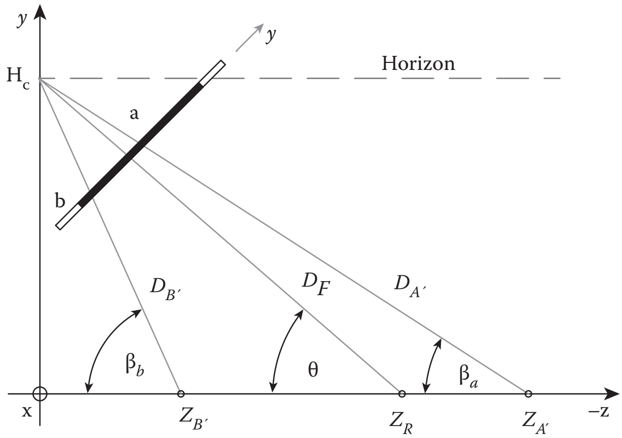

Figure 3.11 Camera view—elevation.

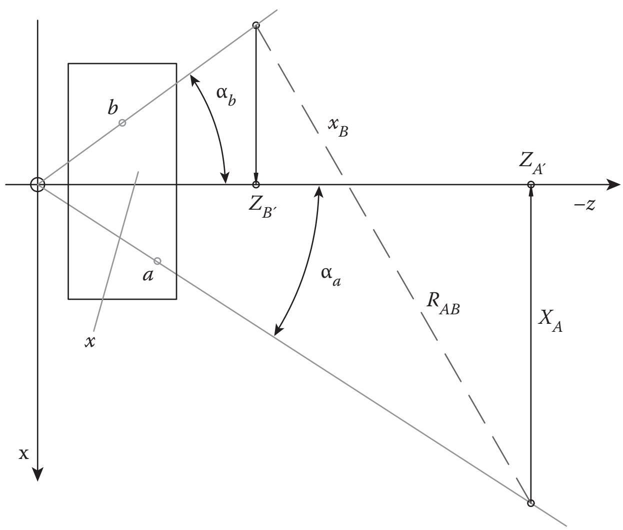

Figure 3.12 Camera view—azimuth.

$$X_A = D'_A \tan\alpha_a \tag{3.11}$$

$$D'_B = D_F \sin\theta/\sin\beta_b \tag{3.12}$$

$$Z'_B = D'_B \cos\beta_b \tag{3.13}$$

$$X_B = D'_B \tan\alpha_b \tag{3.14}$$

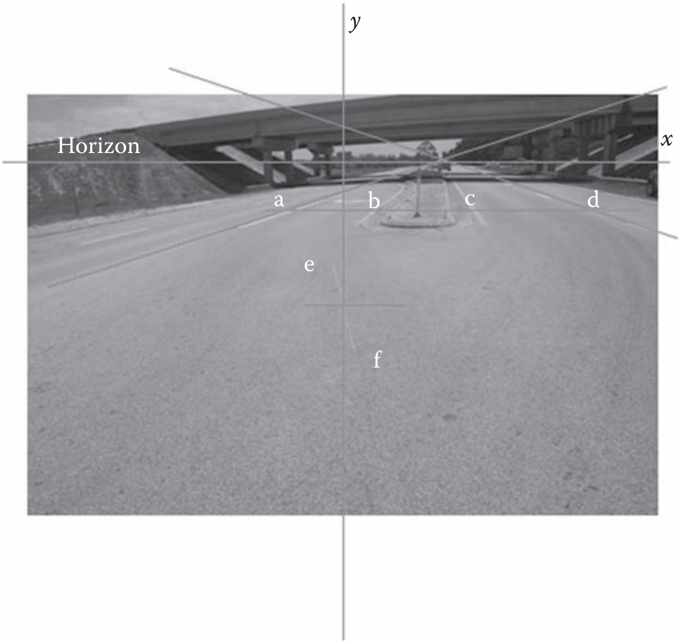

Figure 3.13 Photogrammetry.

$$R_{AB} = \sqrt{(Z'_A - Z'_B)^2 + (X_A - X_B)^2} \tag{3.15}$$

Given the dimensions of two or three points, the camera focal length f, and the camera height H_c may need to be adjusted. Depending on the size of the photograph, the enlargement adjustment e_a needs to be precisely determined. Figure 3.13 shows an example of photogrammetry to determine lane widths and length of a gouge. The lane widths are used as accuracy checks a–b and c–d. The gouge length is e–f. Table 3.1 shows the results of the photogrammetric measurements.

From Table 3.1 the calculated distance R_{AB} is 10.7 ft. This lane was actually measured to be 11.0 ft. The calculated distance R_{CD} is 11.99 ft. The lane is a measured standard 12 ft lane. The calculated gouge from photogrammetry is R_{EF} = 18.27 ft. The actual measurement at the accident site was 18 ft 4 inches. Thus, this example shows how accurate photogrammetric methods are when properly implemented. Note that the size of the photograph and the location of the points on the photograph along with the determination of the horizon determine the accuracy of the measurements from the photograph. In conclusion, it can be stated that the measurements from the photograph are well within engineering accuracy.

Table 3.1 Photogrammetry

Description	Symbol	Value	Units	Symbol	Value	Units	Symbol	Value	Units
Camera focal length	f	55.00	mm	f	55.00	mm	f	55.00	mm
Enlargement adjustment	e_a	417	none	e_a	4.17	none	e_a	4.17	none
Adjusted camera focal length	f	229.13	mm	f	229.13	mm	f	229.13	mm
Depression distance	y_0	−46.50	mm	y0	−46.50	mm	y_0	−46.50	mm
Angle of inclination	Ai	−11.47	deg	Ai	−11.47	deg	A_i	−11.47	deg
Camera height	H_c	5.40	ft	Hc	5.40	ft	H_c	5.40	ft
X-coordinate (point a,c,e)	X_a	−17.00	mm	Xc	44.00	mm	X_e	−4.00	mm
Y-coordinate (point a,c,e)	Y_a	−15.00	mm	Yc	−15.00	mm	Y_e	−33.00	mm
X-coordinate (point b,d,f)	X_b	12.00	mm	Xd	77.00	mm	X_f	4.00	mm
Y-coordinate (point b,d,f)	Y_b	−15.00	mm	Yd	−15.00	mm	Y_f	−62.50	mm
Point a azimuth angle	A_a	−4.21	deg	Ac	10.79	deg	A_e	−1.01	deg
Point a depression angle	B_a	−363	deg	Bc	−358	deg	B_e	−8.10	deg
Point b azimuth angle	A_b	2.98	deg	Ad	18.45	deg	A_f	1.04	deg
Point b depression angle	B_b	−3.64	deg	Bd	−3.64	deg	B_f	−15.32	deg
Ground focal distance	Z_R	26.61	ft	ZR	−26.61	ft	Z_R	−26.61	ft
Focal distance to ground	D_F	27.15	ft	DF	27.15	ft	D_F	27.15	ft
Focal distance to A′,C′,E′	$D_{A'}$	85.19	ft	DC	86.48	ft	$D_{E'}$	38.33	ft
Ground focal distance to A′,C′,E′	$Z_{A'}$	85.02	ft	ZC	86.31	ft	$Z_{E'}$	37.95	ft
X-ground distance to A,C,E	X_A	−6.27	ft	XC	16.49	ft	X_E	−0.67	ft
Focal distance to B′,D′,F′	$D_{B'}$	85.13	ft	DD^1	85.13	ft	$D_{F'}$	20.44	ft
Ground focal distance to B′,D′,F′	Z_B	84.96	ft	ZD^1	84.95	ft	$Z_{F'}$	19.71	ft
X-ground distance to B,D_1F	X_B	4.43	ft	XD	28.40	ft	X_F	0.37	ft
Distance from A to B_1C to D,E to F	R_{AB}	10.70	ft	RCD	11.99	ft	R_{EF}	18.27	ft

4 Energy Methods

4.1 Introduction

The path represented in Figure 4.1 is that of trajectory of a mass *m* moving arbitrarily in the *x*-*y* plane. The motion of the mass *m* is acted upon by a force **F** that can vary in magnitude and direction from point to point along the path. This force may represent the resultant velocity, acceleration, or any other measurement of a particular parameter of a vehicle in an accident reconstruction. The path of the mass may, in fact, represent the center of mass of a vehicle, the path of a pedestrian after being struck by an automobile, or the interval motions of a vehicle such as steering or braking inputs. Irrespective of the actual descriptions of the force **F**, certain basic principles are derived as follows.

S is the path length or distance that the mass travels as it is measured along the path. $\mathbf{F}_s$ is the force along the path creating the motion. Associated with this force is the velocity vector **v**. From Newton's second law we know

$$F_s = ma = m\frac{dv}{dt} \tag{4.1}$$

From the chain rule we express

$$\frac{dv}{dt} = \frac{dv}{ds}\frac{ds}{dt} = v\frac{dv}{ds} \tag{4.2}$$

Then

$$F_s = mv\frac{dv}{ds} \tag{4.3}$$

$$F_s ds = mvdv \tag{4.4}$$

or

over appropriate limits we may integrate Equation 4.4 to obtain

$$\int_{s_1}^{s_2} F_s ds = \int_{v_1}^{v_2} mvdv \tag{4.5}$$

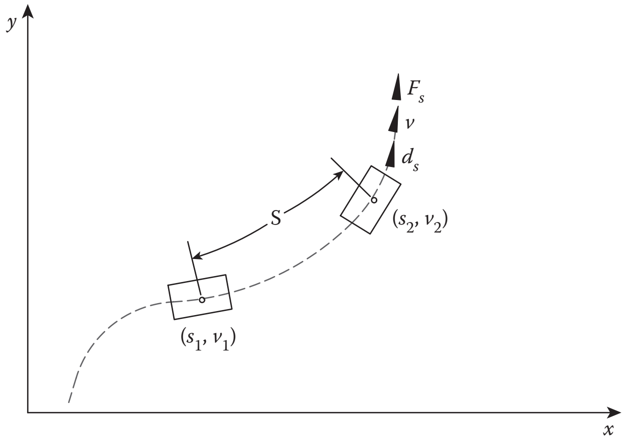

Figure 4.1 Path of mass *m*.

The integral on the left side is called the work W of the force **F** and can be integrated only when F_s is known as a function of s or when F_s and s are known as function of another variable such as friction. In other instances, when such relationships are not known, the left side of Equation 4.5 may not be classifiable. As we will see in the next section on friction, the work performed during braking or skidding can yield solutions to many reconstruction problems. However, the integral on the right side of Equation 4.5 can always be evaluated as

$$\int_{v_1}^{v_2} mv\,dv = \frac{1}{2}mv_2^2 - \frac{1}{2}mv_1^2 \tag{4.6}$$

The kinetic energy of a mass is defined as

$$E_k = \frac{1}{2}mv^2 \tag{4.7}$$

We can now properly express the work energy principle in equation form as

$$W = \int_{s_1}^{s_2} F_s(s)\,ds = \int_{v_1}^{v_2} mv\,dv = E_{k2} - E_{k1} \tag{4.8}$$

Equation 4.8 states that the work performed by the force that acts on a body equals the change in the kinetic energy. Equation 4.8 is known as the work energy principle. A more general form of Equation 4.8 presents itself when the force $\mathbf{F}_s(s)$ is not directed along the path ds. Consequently, the proper vector notation for the work energy principle is

$$W = \int_{s_1}^{s_2} F_s(s) \cdot ds = \Delta E_k \tag{4.9}$$

In this discussion the force **F** represents the resultant of all forces that externally may affect a body. Such a force may be produced by friction or the impact forces resulting from a vehicular collision. Often it is necessary to consider the work produced by separate forces. Each of these may be computed from the general definition as introduced by Equation 4.9. Since the work is a scalar quantity, the total work is the algebraic sum of all the individual components of work. In contrast, the individual forces are vectors and must be considered as such. As a consequence, the change in kinetic energy is equal to the total work. This subtle concept can be introduced when friction is considered on a nonlevel surface as will be seen in the various discussions of friction.

4.2 Friction

When two bodies slide over each other, they exert a frictional force on each other. The force is parallel to the surfaces and opposite in the direction of motion. Traditionally, friction is represented by drawing a free body diagram of a block sliding over a surface as shown in Figure 4.2.

Figure 4.2 represents a block resting on a horizontal surface. The block is in equilibrium as long as $N = W$ and $\mathbf{F} = f$. The block will remain in equilibrium until the force **F** is greater than the frictional force f. A similar condition exists when the block rests on an incline as shown in Figure 4.3.

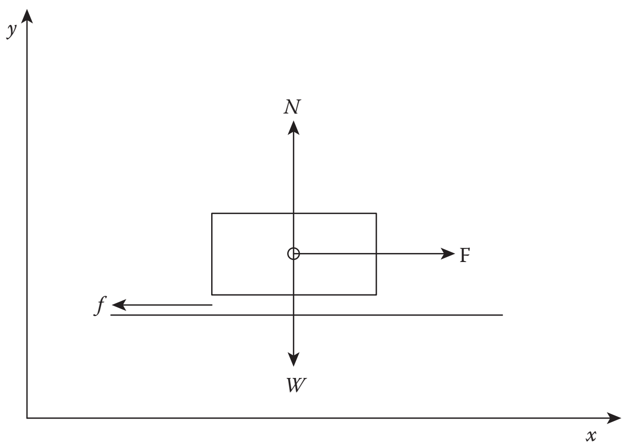

Figure 4.2 Frictional forces.

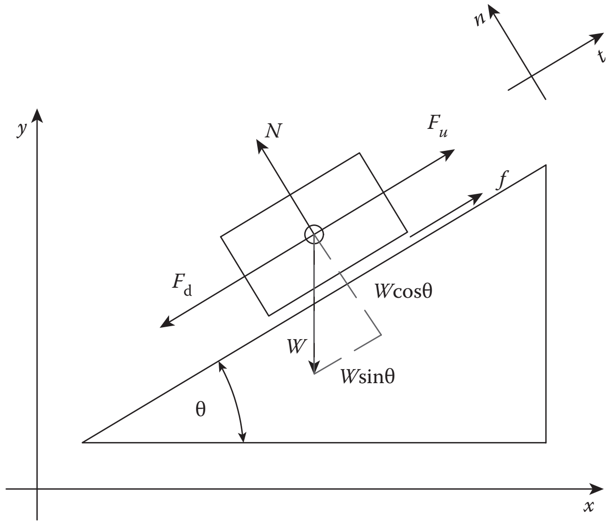

Figure 4.3 Frictional forces on an incline.

It is obvious that for the conditions represented in Figure 4.3, the block will remain at rest as long as $W \sin\theta < f$. Furthermore, an external force may be introduced to move the block up the slope (F_u) or to move it down the slope (F_d). Therefore, depending on the motion of the block, the total frictional force will be greater or lesser depending on the angle of incline and the relative motion of the block. The correction for friction on a slope follows from the free body diagram of Figure 4.3. Summing forces, we obtain for movement down the slope

$$\sum F_n = 0: N - W\cos\theta = 0$$
$$\sum F_t = 0: F_d + W\sin\theta - f = 0 \tag{4.10}$$

Summing forces for movement up the slope

$$\sum F_u = 0: N - W\cos\theta = 0$$
$$\sum F_t = 0: -F_u + W\sin\theta - f = 0 \tag{4.11}$$

The coefficient of friction is defined as the ratio of the tangential to the normal forces. On a horizontal surface as depicted in Figure 4.2, the coefficient of friction would be

$$\mu = \frac{F}{W} = \frac{f}{N} \tag{4.12}$$

Solving Equation 4.10 yields

$$\frac{F_d}{W\cos\theta} = \frac{f}{W\cos\theta} - \frac{W\sin\theta}{W\cos\theta} \tag{4.13}$$

or

$$\mu_{\text{CORR}} = \mu - S \tag{4.14}$$

where

S = slope = tan θ

θ = angle of incline.

In general, a solution for Equations 4.10 or 4.11 yields a corrected value of the frictional coefficient on an incline as

$$\mu_{\text{CORR}} = \mu_{\text{Normal}} \pm S \tag{4.15}$$

where μ_{Normal} = coefficient of friction on a horizontal roadway, S = slope of the road. The + sign is used if the vehicle travels up the slope and the − sign if it travels down the slope. At this point, it is warranted to derive two simple equations relating vehicle speeds and skid marks. Generally, a vehicle may deposit skid marks on the road surface when the brakes are applied in a relatively straight trajectory or may deposit skid marks in a yaw while rounding a curve. During the accident investigation, the skid marks may have been documented and measured. Let us consider the two cases separately.

4.3 Critical Speed-Straight Trajectory

The forces acting on the vehicle are the force of gravity *W*, the normal force *N* (the component of the reaction force on the surface of the vehicle's tires perpendicular to the road surface), the applied force **F** (produced by the vehicle's speed), and the frictional force *f* (the component of the reaction force on the vehicle's wheels parallel to the road surface). At this point, we will assume that the entire weight of the vehicle is distributed evenly over the tires. The following development, as represented by Figure 4.4, is based on the movement of the center of mass of the vehicle and is not dependent on the length or number of skid marks. Figure 4.4 represents a vehicle in which the brakes are suddenly applied.

If we attempt to push a vehicle at rest with all wheels locked, we must overcome the static coefficient of friction. Once the vehicle is moving, again with locked wheels, the functional forces are dependent on the kinetic coefficient of friction. Let us discuss kinetic friction first since it is the simplest of

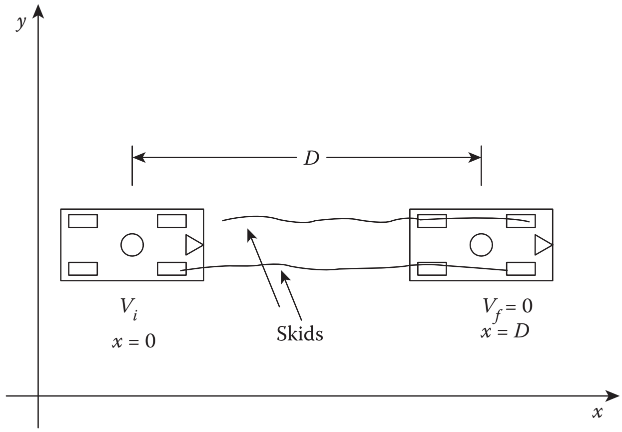

Figure 4.4 Straight skids.

the two forces. Kinetic friction has been found to have the following properties according to classical mechanics:

1. The force of kinetic friction is proportional to the normal force. The constant of proportionality is called the coefficient of kinetic friction and is denoted by μ_k. We write Equation 4.16.

$$f_k = \mu_k N \tag{4.16}$$

2. The coefficient of kinetic friction is independent of the surface area of contact.
3. The coefficient of kinetic friction is independent of the relative speed between the surfaces in contact.

The actual value of the coefficient of kinetic friction depends on the nature of the two surfaces in contact, for example wood on steel, rubber on concrete, etc. However, for a given pair of materials, the above three rules are found to be valid to a reasonable degree of engineering certainty. In most cases we are dealing with automobile tire rubber on concrete or asphalt so that the kinetic coefficient of friction is about 0.8 on a good dry surface and as low as 0.3 on a slippery wet surface. On ice the kinetic coefficient of friction may drop to a dangerously slippery value of 0.1 or less. In some instances, when a vehicle overturns, the coefficient of friction of metal on the road surface may need to be considered. Tables 4.1 and 4.2, reproduced from a multitude of sources including the authors' experiments, list typical values of the frictional coefficient. Note that some of the values vary according to the speed of a vehicle. These adjustments to the values of μ are based on numerous skid tests performed by a variety of investigators and may seem to violate

Table 4.1 Coefficient of Friction

Solids	Static (μ_s)	Kinetic (μ_k)
Steel on steel	0.74	0.57
Brass on steel	0.51	0.44
Copper on cast iron	1.05	0.29
Glass on glass	0.94	0.40
Rubber on concrete	0.73	–
Rubber on carpet	0.66	–
Rubber on tile	0.39	–
Leather on concrete	0.60	–

Table 4.2 Coefficient of Friction

	Dry		Wet	
Tires on Roads (μ_k)	<30 mph	>30 mph	<30 mph	>30 mph
New concrete	0.080–1.20	0.70–1.00	0.50–0.80	0.40–0.75
Old concrete	0.55–0.80	0.50–0.75	0.45–0.70	0.45–0.65
New asphalt	0.80–1.20	0.65–1.00	0.50–0.80	0.45–0.75
Old asphalt	0.50–0.80	0.35–0.70	0.30–0.80	0.25–0.75
Gravel	0.40–0.85	0.40–0.80	0.45–0.80	0.45–0.60
Cinders	0.50–0.70	0.50–0.70	0.65–0.75	0.65–0.75
Ice	0.10–0.25	0.07–0.20	0.05–0.10	0.05–0.10
Snow	0.10–0.55	0.10–0.55	0.30–0.60	0.30–0.60

the third property of friction according to classical mechanics. However, the listed values of the coefficient of friction generally do not vary by more than 0.05 under or over 30 mph. From a realistic engineering standpoint, the percent error introduced into a speed equation by varying the kinetic coefficient of friction of 0.05 is insignificant as will be shown in the next section. The models that we use in engineering design yield answers within engineering accuracy. Engineering accuracy is a measure of acceptable error in the computations. In most instances an error of 5% is quite acceptable when performing engineering calculations. Certain simplifying assumptions are always made when solving engineering problems. The assumptions should meet the following criteria: the methodology is proper and acceptable and the calculations reflect the accident scenario to within engineering accuracy.

After an appropriate selection for the coefficient of friction has been chosen, we can proceed with the development of the critical speed equation as follows. Suppose that the vehicle in Figure 4.4 is given an initial velocity V_i in the x-direction. The force **F** is taken in this case to be zero. The only force acting on the vehicle in the x-direction is the force of kinetic friction. From

Newton's second law (Equation 2.16) and a modification of Equations 4.10 or 4.11 with $\theta = 0$ we obtain

$$\begin{aligned} \mathbf{F} - f_k &= ma_x = 0 \\ N - W &= ma_y = 0 \end{aligned} \tag{4.17}$$

Thus, $N = W$ and $f_k = \mathbf{F}$.

Static friction is more complicated because it does not have a fixed value. In fact, as long as the vehicle in Figure 4.4 does not move, a_x and a_y are zero, and Newton's second law again gives Equation 4.17 with f_k replaced by f_s to indicate static friction. Now all we can say is

$$\mu_k = \frac{f_k}{N} = \frac{\mathbf{F}}{W} \tag{4.18}$$

$$\begin{aligned} f_s &= \mathbf{F} \\ N &= W \end{aligned} \tag{4.19}$$

We do not have a law for f_s like Equation 4.16 for f_k. Experiments show, however, that the force

$$f_{s\max} = \mu_s N \tag{4.20}$$

F can only grow so large before the vehicle breaks free and starts to slide, which shows that the force of static friction has a maximum value. The maximum force of static friction $f_{s\max}$ has the following two simple properties.

a. The maximum force of static friction is proportional to the normal force. The constant of proportionality is called the coefficient of static friction and is denoted by μ_s. We write

$$\mu_s > \mu_k \tag{4.21}$$

b. The coefficient of static friction is independent of the surface area of contact.

Again, as with kinetic friction, the coefficient of static friction depends on the nature of the two surfaces in contact. However, for a given pair of materials, the two rules above are found to be valid to a reasonable degree of engineering certainty. In typical cases of automobile rubber on concrete or asphalt, μ_s is about 0.9 on a good dry surface, about 0.4 on a wet slippery surface, and 0.2 or lower on ice. Experimentation has shown that the coefficient of static friction is always greater than the coefficient of kinetic friction. In mathematical terms an important application of this principle is the antilock brake system. Antilock brakes will be discussed in later sections.

4.4 Stopping Distances

Suppose the vehicle in Figure 4.4 is given an initial velocity V_i in the x-direction. Again, the force **F** is taken in this case to be zero. The only force acting on the vehicle in the x-direction is the force of kinetic friction. A simple modification of the first part of Equation 4.17 yields

$$a_x = -\frac{f_x}{m} \tag{4.22}$$

The second part of Equation 4.17 gives $N = W = mg$. Then $f_k = \mu_k N = \mu_k mg$. Using the results in Equation 4.21, we obtain

$$a_x = -\mu_k g \tag{4.23}$$

Applying the work energy principle as described in Equation 4.4, we may say

$$\int_{x=0}^{x=D} F\,dx = \frac{1}{2}mv_f^2 - \frac{1}{2}mv_i^2 \tag{4.24}$$

or when $v_f = 0$,

$$FD = -\frac{1}{2}mv_i^2 \tag{4.25}$$

Applying Equations 4.23 and 4.1 to Equation 4.15 yields

$$m(-\mu_k g)D = -\frac{1}{2}mv_i^2 \tag{4.26}$$

or

$$v_i = \sqrt{2\mu_k g D} \tag{4.27}$$

An alternate form of Equation 4.27 is

$$D = \frac{v_i^2}{2\mu_k g} \tag{4.28}$$

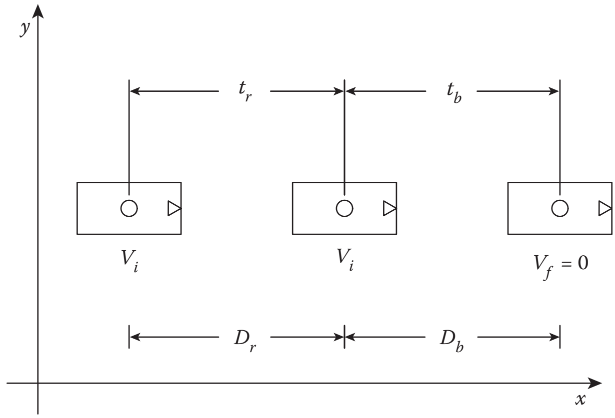

Figure 4.5 Reaction and stopping.

In Equations 4.27 or 4.28, D represents the braking distance. The term stopping distance is usually reserved for the total distance traveled by the vehicle. Included in the stopping distance is the distance traveled during the driver's reaction time. Let t_r be the reaction time, which is required for the driver to recognize the problem, decide to apply the brakes, and perform the braking maneuver. A general range of reaction time is between 0.5 and 1.5 seconds. The total stopping distance can then be calculated from

$$D_s = D_r + D_b \tag{4.29}$$

or

$$D_s = v_i t_r + \frac{v_i^2}{2\mu_k g} \tag{4.30}$$

The total time may be computed from

$$t_T = t_r + t_b \tag{4.31}$$

Figure 4.5 summarizes the results of Equations 4.29 through 4.31.

Next, we introduce some refinements and expand on how friction affects the speed of a vehicle.

4.5 Friction and the Speed of a Vehicle

Accident reconstructionists sometimes manipulate the equations that govern the critical speed of a vehicle based on the coefficient of friction and the length of the skid. One would hope that this manipulation is due to ignorance rather than due to deception in order to skew results in a particular direction. Skid tests have been performed by numerous investigators to validate the critical speed equation. These tests have generated a plethora of well documented data on the coefficient of friction under varying conditions. This data allows a reconstructionist to more precisely refine the coefficient of friction in a particular accident scenario. However, there is no scientific validity from an experimental or a theoretical viewpoint to manipulate the coefficient of friction based on the number of skid marks made by a vehicle under heavy braking conditions. Two theoretical arguments against the manipulation of the friction or "drag" coefficient based on the number of skid marks are provided.

The study of friction is referred to as "tribology" by physicists. Friction or tribology at the atomic scale is called nanotribology. Nanotribology can also be considered as friction at the microscopic level. In contrast, the friction encountered by accident reconstructionists is at the macroscopic level. In order to understand the frictional forces that affect the behavior of vehicles, some background and differences between friction at the microscopic and macroscopic levels should be explained.

Nanotribologists have found that friction at the atomic (microscopic) level differs significantly from the observations at the macroscopic (real world) level. For example, surface roughness at the microscopic level has little correlation with friction, and sometimes wet surfaces are stickier than dry ones. Automotive engineers and other investigators have found that surface roughness could not explain real world friction experienced in their designs. In some instances, friction between two surfaces decreased if one surface is smoother than the other. Two highly polished metals will adhere very firmly as in the case of "cold welding." Friction has been found to be proportional to true contact area in the microscopic level but independent of the macroscopic area as defined in classical physics. Over the past few years researchers have found that "phonons" or sound waves are generated when two surfaces slide relative to each other. The mechanical energy needed to slide the surfaces is converted to sound energy and subsequently into heat. The amount of mechanical energy that must be added to keep the motion going depends on the nature of the sliding surfaces. The resonant frequencies excited during the sliding action are a direct consequence of the mechanical energy consumed. Clearly, accident reconstructionists cannot attempt to determine the true contact area between a vehicle's tires and the road or the true contact within the brakes of the vehicle. At best, they can perform a skid test with a sled or with an accelerometer. Another surprising discovery by nanotribologists is that the frictional force is related to how easily two surfaces become stuck relative to becoming unstuck. The discrepancy of friction at the microscopic and macroscopic levels diminishes when one realizes that the true contact area is proportional to the force that squeezes the objects together. At the macroscopic level, this force is produced by the mass of the vehicle and the subsequent forces that are imparted on the tire road interface.

These forces are often misunderstood by accident reconstructionists. When a vehicle is being decelerated by braking and before the tires lose traction, the forces of static friction are in effect between the tire/road interface. At the same time, the forces of kinetic friction are acting on the rotors, drums, and brake shoes. Many times during heavy braking, one or more of the brakes will lock. When the brakes of one wheel lock, the forces of static friction are acting upon those brakes while the forces of kinetic friction affect the tire/road interface. The tire/road friction utilization is concerned with the maximum deceleration when the wheels are unlocked relative to the lowest tire/road friction coefficient with which the deceleration can be achieved. When actual braking forces equal optimum braking forces, then tire/road friction is used for vehicle deceleration. The maximum wheels-unlocked deceleration yields the minimum stopping distance of a vehicle. The effect on the road/tire/brake system of that particular wheel is reversed from the effect of a wheel that is not losing traction. However, in all instances, except when defective brakes are present, the forces of friction are all working on all wheels to stop the vehicle.

One of the pieces of evidence that reconstructionists use is the length of skid marks to determine vehicle speeds. Skid marks are probably the most misunderstood and most abused evidence used by reconstructionists. There is no question that steering input, weight shift, torsion, and wheel lock up determine the shape, length, and number of skid marks deposited by vehicles under heavy braking. Similarly, in many collisions, the metal deformation will lock one or more wheels so that postcollision skid marks are deposited on the road surface. Simply because only one wheel deposits skid marks does not mean that frictional forces are not affecting the entire vehicle.

Let us consider a vehicle that deposits only one skid mark either under preimpact conditions or under postimpact conditions. Some reconstructionists use the number of skid marks deposited by a vehicle to adjust the coefficient of friction or “drag coefficient” used in their calculations. For example, when $\mu=0.8$ with one wheel skidding, they will adjust the coefficient by dividing by four so that they use $\mu=0.2$. In other instances, when two skid marks are deposited, one longer than the other, they will average the length of the skid marks and use this value as the skid distance. In both cases they are affecting the equation used to calculate the minimum speed from skid marks, namely

$$v_s = \sqrt{2g\mu D} \tag{4.32}$$

where

v_s=minimum speed (ft/sec)

g=acceleration due to gravity (32.2 ft/sec^2)

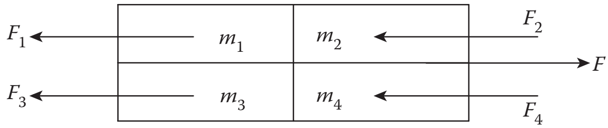

Figure 4.6 Vehicle masses.

μ = coefficient of friction or "drag coefficient"
D = skid distance (ft)

The number 2 and g cannot be manipulated, however, μ and D can, and are manipulated many times, as in the examples above to affect speed calculations. Two mathematical arguments are presented below to show that manipulation of μ and D, as explained above, violates fundamental laws of physics. Consider Figure 4.6, which represents a vehicle divided into four masses and forces affecting each wheel.

The total force **F** is produced by the motion of the vehicle. The forces F_1, F_2, F_3, and F_4 are deceleration forces affecting each wheel. Summing forces, we obtain

$$\mathbf{F} = F_1 + F_2 + F_3 + F_4 \tag{4.33}$$

4.6 Newton's Second Law Argument

By Newton's second law, we may say

$$F_1 = m_1 a_1, \quad F_2 = m_2 a_2, \quad F_3 = m_3 a_3, \quad F_4 = m_4 a_4 \tag{4.34}$$

Substituting Equation 4.34 into 4.33 we obtain,

$$F = m_1 a_1 + m_2 a_2 + m_3 a_3 + m_4 a_4 \tag{4.35}$$

If the vehicle remains together, the acceleration of each mass component must be the same

$$a = a_1 = a_2 = a_3 = a_4 \tag{4.36}$$

therefore

$$\mathbf{F} = (m_1 + m_2 + m_3 + m_4)a \tag{4.37}$$

Since weight W and mass m are related by gravity g

$$W = mg \tag{4.38}$$

and the frictional force f is related to weight W by the coefficient of friction μ

$$f = \mu W \tag{4.39}$$

We can find the total frictional force by summing the frictional forces on each wheel, namely

$$f = f_1 + f_2 + f_3 + f_4 \tag{4.40}$$

By substituting Equations 4.38 and 4.39 into Equation 4.40, we obtain

$$f = m_1\mu_1 g + m_2\mu_2 g + m_3\mu_3 g + m_4\mu_4 g \tag{4.41}$$

For simplicity's sake, let us assume that the coefficient of friction affecting each wheel is constant so that

$$\mu = \mu_1 = \mu_2 = \mu_3 = \mu_4 \tag{4.42}$$

Then

$$f = (m_1 + m_2 + m_3 + m_4)\mu g \tag{4.43}$$

From the basic definitions of Equations 4.1, 4.37, and 4.43, we see that

$$a = \mu g \tag{4.44}$$

Adjusting the masses in Equation 4.37 requires making the same adjustment in the masses of Equation 4.43. Even if a weight displacement during acceleration or deceleration causes a shift in the mass, the adjustment must be made to both sides of Equation 4.1. This effect is represented as follows

$$(m_1 + m_2 + m_3 + m_4)\mu g = (m_1 + m_2 + m_3 + m_4)a \tag{4.45}$$

or

$$(\Delta m)\mu g = (\Delta m)a \tag{4.46}$$

where Δm = mass shift or displacement.

4.7 Work–Energy Argument

This argument centers on the work done, or kinetic energy expended during acceleration or deceleration of a vehicle, namely

where

K_e = kinetic energy (ft-lb)

m = mass (lb-sec^2/ft)

ν = speed (ft/sec)

f = frictional (lb)

D = skid distance (ft)

In this argument, we use the same representation as in Figure 4.6 to find the total kinetic energy at each wheel, namely

$$\text{Work} = K_e = \frac{1}{2}mv^2 = f \times D \tag{4.47}$$

$$K_e = K_{e1} + K_{e2} + K_{e3} + K_{e4} \tag{4.48}$$

or

$$K_e = \frac{1}{2}m_1v_1^2 + \frac{1}{2}m_2v_2^2 + \frac{1}{2}m_3v_3^2 + \frac{1}{2}m_4v_4^2 \tag{4.49}$$

Similarly, the total work done by the frictional forces is

$$\text{Work} = f_1D_1 + f_2D_2 + f_3D_3 + f_4D_4 \tag{4.50}$$

Substituting for the frictional forces, we obtain

$$\text{Work} = W_1\mu_1D_1 + W_2\mu_2D_2 + W_3\mu_3D_3 + W_4\mu_4D_4 \tag{4.51}$$

for a constant coefficient of friction of Equation 4.15 and since each wheel of the vehicle travels the same distance

$$D = D_1 = D_2 = D_3 = D_4 \tag{4.52}$$

then

$$\text{Work} = (W_1 + W_2 + W_3 + W_4)\mu D \tag{4.53}$$

Equating Equations 4.49 and 4.53 under Equation 4.47 and realizing that $v = v_1 = v_2 = v_3 = v_4$ yields

$$\frac{1}{2g}(W_1 + W_2 + W_3 + W_4)v^2 = (W_1 + W_2 + W_3 + W_4)\mu D \tag{4.54}$$

Of course, Equation 4.54 reduces to Equation 4.32. We can again assume that a weight shift, torsion, steering input, or some other anomaly causes less than four equal length skid marks so that Equation 4.54 is represented as

$$\frac{1}{2g}(\Delta W)v^2 = (\Delta W)\mu D \tag{4.55}$$

The inescapable conclusions of the arguments summarized in Equations 4.46 and 4.55 are as follows:

1. The coefficient of friction or "drag factor" cannot be varied according to the number or length of the skid marks without violating fundamental laws of physics.
2. Simply because a tire does not leave a skid mark does not mean that frictional forces are not in effect. Actually, the braking efficiency of a wheel that does not skid is greater than the wheel that does skid across the pavement.
3. The longest skid mark is evidence that the vehicle was traveling at a minimum speed and that it was accelerating or decelerating. When calculating this minimum speed, it is improper to randomly vary the coefficient of friction based on the number or length of skid marks.
4. Adjustments to one side of Equations 4.46 or 4.55 require adjustments to the other side. Analysis of Equations 4.35, 4.41, 4.49, and 4.51 explain this effect in greater detail.
5. Simple adjustments to the coefficient of friction and the length of skid marks requires careful analysis of Equations 4.35, 4.41, 4.49, and 4.51. This analysis and data are seldom available in an accident reconstruction.
6. Calculating minimum speeds in pre- or postimpact phases of collisions by randomly varying the coefficient of friction or the skid distance often yields erroneous results. All calculations should be checked by independent second methods such as crush deformation analysis or various other techniques available to accident reconstructionists. The adage, "garbage in equals garbage out," rings true.
7. It must be recognized that when brakes are applied, the vehicle decelerates before any skid marks are deposited so that the actual speed of the vehicle is greater than that calculated from the minimum speed formulas.
8. Modifying the coefficient of friction depending on how many tires deposit skid marks is equivalent to adjusting the apparent area of

contact and is therefore, in violation of the classic laws of physics relative to the frictional force.

4.8 Critical Speed—Curved Trajectory

Another consequence of a vehicle depositing skid marks on a road surface occurs when the vehicle loses traction while rounding a curve. The motion of such a vehicle is more complicated than realized at first glance. The trajectory of the vehicle may simply cause a yawing motion, or it could produce a spinning motion. The trajectory may be a combination of two paths and may include some rolling motion toward the end of the trajectory. Subtle differences are observed in the equations of motion under all these cases.

Let us describe some basic equations of motion. In order to describe the motion of a vehicle, a proper frame of reference must be established. Chapter 2 describes several coordinate systems that uniquely determine the position of the vehicle relative to its motion. Using a right handed Cartesian coordinate system, which consists of three mutually perpendicular axes intersecting at some specified field point, 0 (origin), the distance from a point P to the origin is given by

$$D=\sqrt{x^2+y^2+z^2} \tag{4.56}$$

Similarly, the distance from point P_1 to point P_2 is described as

$$D_{12}=\sqrt{(x_1-x_2)^2+(y_1-y_2)^2+(z_1-z_2)^2} \tag{4.57}$$

In general the quantity D_{12} is a vector so that a more generalized form of the vector equation would be

$$D_{12}=D_xA_x+D_yA_y+D_zA_z \tag{4.58}$$

Therefore, Equation 4.58 represents the magnitude of the vector distance D_{12}. Suppose in the above discussion that a vehicle travels from P_1 to P_2 in a straight line in two dimensions (x,y). The average velocity of the vehicle is defined as

$$\boldsymbol{v}=\frac{\Delta(x,y)}{\Delta t}=\left(\frac{\Delta x}{\Delta t},\frac{\Delta y}{\Delta t}\right)=\left(\frac{dx}{dt},\frac{dy}{dt}\right)=(\boldsymbol{v}_x,\boldsymbol{v}_y) \tag{4.59}$$

The extension of Equation 4.59 into three dimensions should be obvious to the reader. The average velocity is a vector. There are many instances when it makes sense to talk about the average velocity of the vehicle or for lack of a better term, the average speed. The average speed is a scalar quantity given by

$$s = \frac{D}{\Delta t} \tag{4.60}$$

where D is the total distance traveled by the vehicle between P_1 and P_2. In the simple case in which the vehicle travels in a straight line and does not stop and turn around or otherwise retrace its path, the average speed is simply the magnitude of the average velocity, i.e.,

$$s = \sqrt{v_x^2 + v_y^2} \tag{4.61}$$

If the vehicle stops and turns around, or if it moves with a variable speed in the same direction, or if it moves along a curved path; it is said to have acceleration. The description of the motion of such a vehicle requires the use of calculus. As a general rule in the case where acceleration is a constant, the velocity of the vehicle increases or decreases at a constant rate.

$$\begin{aligned} x &= x(t), \qquad v_x = \frac{dx}{dt} \\ v_x &= v_x(t), \qquad a_x = \frac{dv_x}{dt} \end{aligned} \tag{4.62}$$

With variable acceleration, the rate of change of the velocity would not be constant. Such a scenario might exhibit itself when a vehicle is performing complex maneuvers such as braking, acceleration, or turning. Most of these cases can be dealt with easily by analyzing each component separately. The total reconstruction can then be determined by a step-by-step analysis of the total scenario. For convenience, we list the general equations of motion in one dimension (x-direction) as derived from basic calculus.

In the case of constant acceleration we obtain

$$v_x = v_{ox} + a_x t \tag{4.63}$$

$$x = x_o + v_{ox} t + \frac{1}{2} a_x t^2 \tag{4.64}$$

$$v_x^2 - v_{ox}^2 = 2a_x (x - x_o) \tag{4.65}$$

Equations 4.62 through 4.65 are used extensively to determine time, distance, velocity, and acceleration of vehicles in an accident reconstruction.

The derivation of Equations 4.63, 4.64, and 4.65 from Equation 4.62 is left as an exercise for the reader. The reader, as an engineering level accident reconstructionist, should not have any trouble performing those derivations. In fact, during trial or deposition testimony, many attorneys ask that the expert derive the equations used in the reconstruction. Similar equations hold for the y and z directions.

Let us now return to our original development of the curved trajectory. The simplest curved trajectory is that of a circle. The acceleration of a vehicle moving in a circle can be resolved into components normal and tangential to the path. Figure 4.7a represents a vehicle moving in a circular path of a radius R with center at the origin. Vectors $\mathbf{v}_1$ and $\mathbf{v}_2$ represent the velocity of the vehicle at points P_1 and P_2, respectively. The vector change in velocity, $\Delta\mathbf{v}$, is obtained in Figure 4.7b. Vectors $\Delta\mathbf{v}_n$ and $\Delta\mathbf{v}_t$ are the normal and tangential components of $\Delta\mathbf{v}$.

Triangles OP_1P_2 and $OP'_1P'_2$ in Figure 4.7 are similar triangles because both are isosceles and their long sides are mutually perpendicular. We may then say,

$$\frac{\Delta s}{R} = \frac{\Delta v_N}{v_1} \tag{4.66}$$

By definition, the magnitude of the average normal acceleration $|\mathbf{a}_N|$ is

$$|\mathbf{a}_N| = \frac{\Delta \boldsymbol{v}_N}{\Delta t} = \frac{\boldsymbol{v}_1}{R}\frac{\Delta s}{\Delta t} \tag{4.67}$$

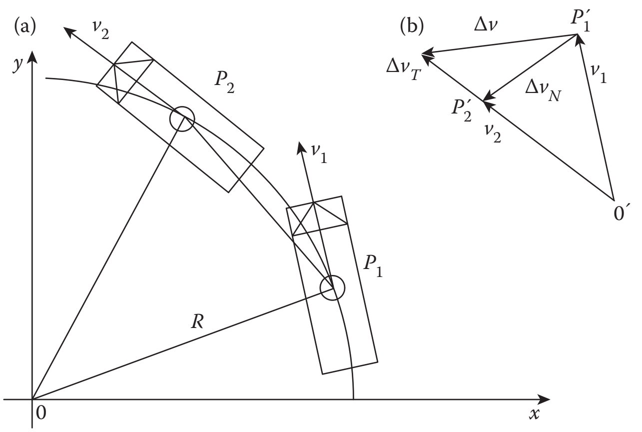

Figure 4.7 (a), (b) Vehicle in a circular path.

Taking the limit, we obtain

$$\mathbf{a}_N = |\mathbf{a}_N| = \lim_{\Delta t \to 0} \frac{\mathbf{v}_1}{R} \frac{\Delta s}{\Delta t} = \lim_{\Delta t \to 0} \frac{\Delta s}{\Delta t}\left(\frac{\mathbf{v}_1}{R}\right) \tag{4.68}$$

In the above equation, we recognize the basic calculus definition of the speed v_1 to be the limit of $\Delta s/\Delta t$. Thus

$$\mathbf{a}_N = \frac{\boldsymbol{v}^2}{R} \tag{4.69}$$

Thus, the magnitude of the instantaneous normal acceleration is inward and is referred to as the centripetal acceleration. Associated with the centripetal acceleration is the force according to Newton's second law. Since the magnitude of the centripetal acceleration equals v^2/R, and its direction is toward the center, the magnitude of the centripetal or radial force on a vehicle traveling in a circle is

$$F = \frac{m\boldsymbol{v}^2}{R} \tag{4.70}$$

The term "centripetal" refers to the effect of the force on a body moving in a circular path. In other words, the effect of the force results in a change in the direction of the velocity of the vehicle upon which it acts. Note that the force does not change the magnitude of the velocity. The term centripetal means center seeking. In fact, when a vehicle negotiates a circular path, it is accelerated toward the center as long as the frictional forces on the tires are not exceeded. Once the frictional forces are exceeded, the vehicle will lose control around the turn and may spin, yaw, or roll. Therefore, the critical speed at which this event occurs can be simply computed by analyzing the free body diagram in Figure 4.8.

While the vehicle remains under control we may write

$$\sum F_r = 0: F - f = 0 \tag{4.71}$$

or since

$$F = ma_N = \frac{w}{g}\frac{v^2}{R}, \qquad f = \mu w \qquad \text{then} \qquad \frac{w}{g}\frac{v^2}{R} - \mu w = 0 \tag{4.72}$$

Thus the critical speed around a turn is

$$\boldsymbol{v} = \sqrt{\mu g R} \tag{4.73}$$

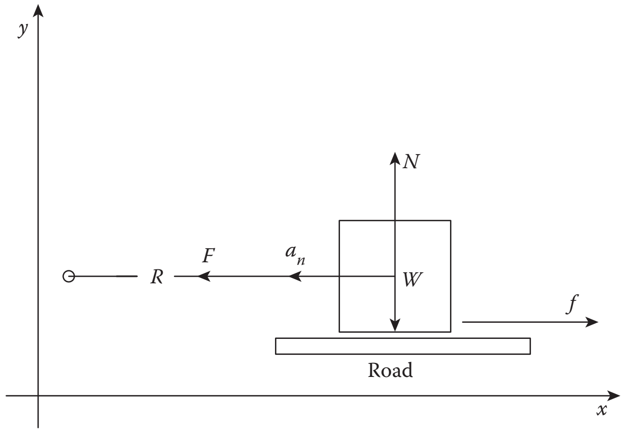

Figure 4.8 Critical speed in a turn.

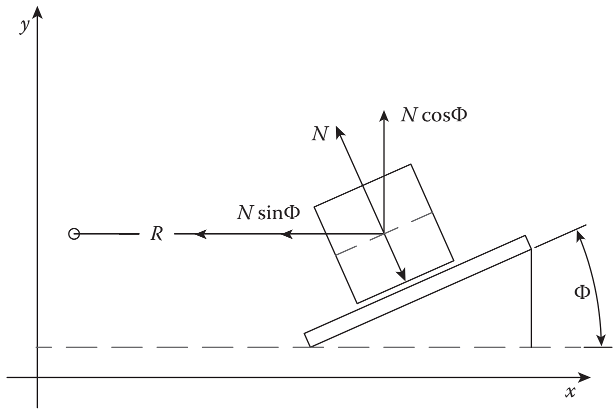

Figure 4.9 Superelevated turn.

The development of Equation 4.73 indicates that the forces acting on a vehicle that is rounding a curve are its weight *W*, the normal force *N*, and the centripetal force *F*. The centripetal force must be provided by friction. In order to minimize the effect that friction has to play on keeping a vehicle on track around a curve, many roads are banked. This banking is commonly known as "superelevation" of the roadway. Figure 4.9 shows a banked roadway and the forces affecting the vehicle.

In Figure 4.9 it is evident that the normal force *N* has a horizontal and a vertical component. The horizontal component $N\sin\Phi$ provides the centripetal force. Thus, applying Newton's second law, we obtain

$$N\sin\Phi = \frac{mv^2}{R}$$

while there is no vertical acceleration W = N cos Φ, then

$$\frac{N \sin \Phi}{N \cos \Phi} = \frac{mv^2}{WR}$$

or

$$\tan \Phi = \frac{v^2}{gR} \tag{4.74}$$

In Equation 4.74 for a given radius R there is no one speed that satisfies the angle criteria. Road designers have thus superelevated highways according to the average speed of the vehicles that traverse that particular section of roadway.

4.9 Critical Speed to Negotiate a Turn Including Superelevation

In some accident reconstructions, it is necessary to determine if the superelevation of a road surface is within design specifications for the radius of a curve that a vehicle is to maneuver safely. This section is devoted to the determination of the proper superelevation for varying a radii corresponding to varying speeds.

Normally curved road surfaces are designed as shown in Figures 4.10 and 4.11. Figure 4.10 represents a top view of a curved road surface, while Figure 4.11 shows a cross-section of a superelevated road surface. Complex curves necessitate a transition region before and after the curve is negotiated. These transition regions involve spiral curves leading to or departing the main circular curve. We will restrict our analysis to the circular portion of the curve where the loss of control of a vehicle occurs in many accidents. The circular portion of the curve has a smaller radial distance than the transition spiral and thus yields a slower design speed.

Definition of terms:

Transition region = uniformly increasing or decreasing superelevation and widening

Curves of $< 1°$ of arc require no superelevation

Curves of $< 2°$ of arc require no transition region

θ_t = transition angle

θ_c = central angle of curve

w = widening

R = radius of curve in feet

C = crown (1/4″ to 1/2″:1′)

Φ = angle of superelevation

F = force

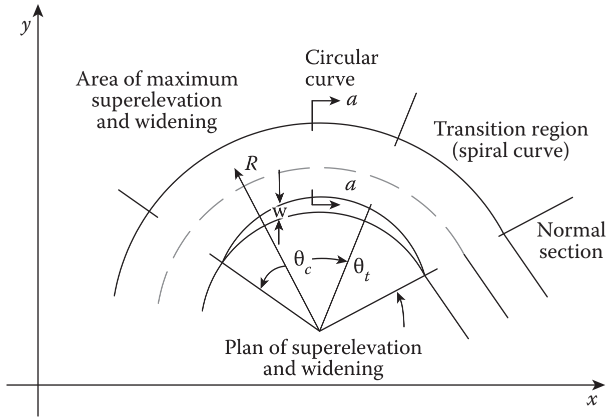

Figure 4.10 Typical road curve.

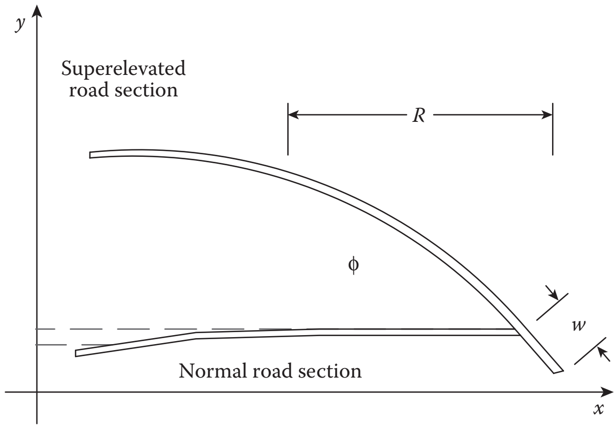

Figure 4.11 Road cross-section.

a = acceleration in ft/sec^2
W = weight
V = velocity in ft/sec
g = gravity = 32.2 ft/sec^2
f = side friction factor
S = superelevation
m = mass

Figure 4.12 shows a superelevated cross-section of road with a vehicle negotiating a curve of radius R. We will proceed with a different derivation than presented in Equation 4.69.

By Newton's second law,

$$\sum F = ma_r = \frac{W}{g}(a_r)$$

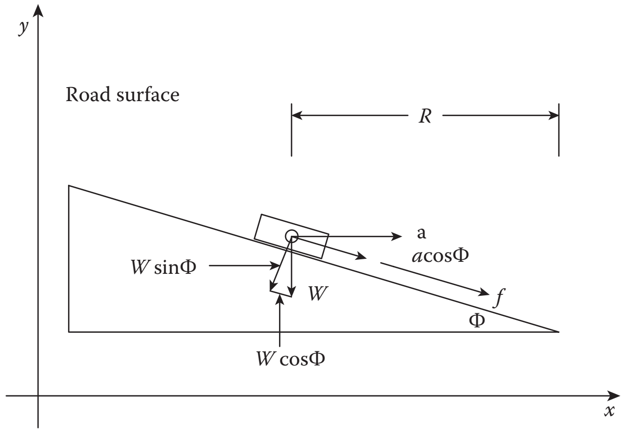

Figure 4.12 Superelevation section of road.

Centripetal acceleration is given by

$$a_r = \frac{V^2}{R}$$

The frictional force is

$$F = fW\cos\Phi$$

The component of the weight in the same direction as friction is

$$W\sin\Phi$$

The centripetal acceleration component of the superelevated road is

$$a_r = a\cos\Phi = \frac{V^2}{R}(\cos\Phi)$$

Summing forces

$$fW\cos\Phi + W\sin\Phi = m\frac{V^2}{R}\cos\Phi = \frac{W}{g}\frac{V^2}{R}\cos\Phi \tag{4.75}$$

$$f\cos\Phi + \sin\Phi = \frac{V^2}{gR}\cos\Phi$$

$$f + \frac{\sin\Phi}{\cos\Phi} = \frac{V^2}{gR}$$

$$\tan\Phi = \frac{\sin\Phi}{\cos\Phi} = S = \text{Superelevation}$$

$$S + f = \frac{V^2}{gR}$$

Thus

$$S = \frac{V^2}{gR} - f \tag{4.76}$$

Standard road design handbooks specify f as the side friction factor with a value of 0.16 for speeds of 60 mph or less or 0.14 for 70 mph speeds. Additionally, the speed V above is to be 75% of the design speed. Equation 4.76 becomes negative for values of

$$f > \frac{V^2}{gR} \tag{4.77}$$

Since negative values of S mean that the superelevation is inclined in the wrong direction, making it easier for vehicles to slide while negotiating a curve, a design standard lower limit of superelevation for different radii has been established and is reproduced in Table 4.3A and 4.3B.

4.10 Conservation of Energy Analysis

Many vehicular accident reconstructions can be performed with the use of the principle of conservation of energy. The total energy of the system is comprised of potential and kinetic energy. Since most accidents occur on nearly level surfaces, potential energy can be disregarded. Alternatively, if the road surfaces are not significantly level, an adjustment can be made to the frictional coefficient in order to incorporate any three dimensional effects. The basic premise states that the initial energy of the system must equal the final energy, or:

$$\frac{1}{2}m(v_i)^2 = \frac{1}{2}m(v_f)^2 \tag{4.78}$$

Table 4.3A Required Superelevation and Widening of Roads

		Design Speed (mph)															
		30		40		50		60		70		80		90		100	
R	*D*	*S*	*W*	*S*	*W*	*S*	*W*	*S*	*W*	*S*	*W*	*S*	*W*	*S*	*W*	*S*	*W*
5729.58	1	0.01	–	0.01	–	0.02	–	0.02	–	0.03	–	0.04	2	0.05	2	0.07	2
2864.79	2	0.01	–	0.02	–	0.03	–	0.05	–	0.06	–	0.08	2	0.10	2	0.125	2
1909.86	3	0.02	–	0.03	–	0.05	–	0.07	–	0.09	–	0.125	2	0.125	2		
1432.39	4	0.02	–	0.04	–	0.06	–	0.09	–	0.1	2						
1145.92	5	0.03	–	0.06	–	0.08	–	0.1	2								
954.93	6	0.03	–	0.06	–	0.10	2	0.10	2								
818.51	7	0.04	–	0.07	2	0.10	2										
716.2	8	0.05	2	0.08	2	0.10	2										
636.62	9	0.05	2	0.09	2	0.10	3										
572.96	10	0.06	2	0.10	2												
520.87	11	0.06	2	0.10	3												
477.46	12	0.07	3	0.10	3												
440.74	13	0.07	3	0.10	3												
409.26	14	0.08	3	0.10	3												
381.97	15	0.09	3														
358.10	16	0.09	3														
337.03	17	0.10	3														
318.31	18	0.10	3														

301.56	19	0.10	3
286.48	20	0.10	3
272.84	21	0.10	3
260.44	22	0.10	3
249.11	23	0.10	4
238.73	24	0.10	4

Legend:
R = *radius of curve in feet.*
D = degree of curve.
S = superelevation in feet per foot of width (for conversion: 0.01 = 1/8).
W = total widening in feet for 22′ two lane pavement.
Based on formula for superelevation: S = 0.067 V2/R–F where
S = superelevation in feet per foot.
V = 3/4 design speed mph.
R = radius of curve in feet.
F = side friction factor = 0.16 for 60 mph and less, 0.14 for 70 mph.
Example given: design speed 40 mph 8° curve.
Required: S, superelevation in feet per foot.
Solution: by table S = 0.08′.
Notes: 0.10 foot per foot is maximum superelevation in areas subject to ice and sleet. (0.08 per AASHO).
A maximum superelevation of 0.125 foot per foot is sometimes used in areas not subject to ice or sleet. (0.12 per AASHO).
For circular curves provide full superelevation and widening from PC to PT with minimum transition of at least 150 ft. For roads wider than 22 ft reduce figures in table by width minus 22 ft; i.e., a 9° curve on a normally 24 ft width, two lane, 50 mph road would be widened 3′-(24–22) or 1 ft.
For roads narrower than 22 ft increase figures in table by 22 ft minus width; i.e., an 8° curve on a normally 20 ft road width, two lane, 40 mph road would be widened 2 + (22–20) or 4 ft.
The Public Roads Administration recommends no widening of curves flatter than 4° on pavements designed for 70 mph, 5° for 60 mph, 7° for 40 mph and 8C for 30 mph.

Table 4.3B Minimum Curve Radii—"*S*" Not Over 0.10 Foot per Foot

	Design Speed (mph)							
	30	40	50	60	70	80	90	100
Min. safe radius "*R*"	232′	412′	644′	928′	1368′	1949′	2714′	3722′
Max. deg. of curve "*D*"	24.9	13.9	8.9	6.2	4.2	2.9	2.1	1.5

Source: Adapted from Joseph Barnett, *Concrete Pavement Manual*, Portland Cement Association; Seelye Elwin E. 1955. *Design*. 2nd Ed. NY: John Wiley & Sons.

For a system with two components such as two vehicles, Equation 4.1 becomes,

$$w_1(v_{1i})^2 + w_2(v_{2i})^2 = w_1(v_{1f})^2 + w_2(v_{2f})^2 \tag{4.79}$$

Equation 4.79 can be broken down into its components in order to solve for the initial velocities of the system. The initial velocities are then given by:

$$(v_{1i})^2 = ([\sin A_{2i})^2 - (\sin A_{1f})^2](v_{1f})^2 + R_{21}[(\sin A_{2i})^2 - (\sin A_{2f})^2](v_{2f})^2/[(\sin A_{2i})^2 - (\sin A_{1i})^2] \tag{4.80}$$

and

$$(v_{2i})^2 = ([\sin A_{2f})^2 - (\sin A_{1i})^2](v_{2f})^2 + (1/R_{21})[(\sin A_{1f})^2 - (\sin A_{1i})^2](v_{1f})^2/[(\sin A_{2i})^2 - (\sin A_{1i})^2] \tag{4.81}$$

In the above equations we define the following:

w_1 = weight of vehicle 1
w_2 = weight of vehicle 2
m = mass
μ = coefficient friction
g = acceleration due to gravity
R_{21} = ratio of vehicle weights
v_{1t}. = initial velocity of vehicle 1
v_2 = initial velocity of vehicle 2
V_{1f} = final velocity of vehicle 1; $v_{1f} = (2g\mu D_{1f})^{1/2}$
D_{1f} = vehicle 1 final distance
v_{2f} = final velocity of vehicle 2; $v_{2f} = (2g\mu D_{2f})^{1/2}$
D_{2f} = vehicle 2 final distance
A_{1i} = precollision angle of vehicle 1

A_{2_i} = precollision angle of vehicle 2
A_{1f} = postcollision angle of vehicle 1
A_{2f} = postcollision angle of vehicle 2

4.11 Generalized Critical Speed Analysis

A study of the previous sections reveals that when a vehicle's path is known whether traveling down a straight road, on a level or inclined surface, whether negotiating a curve, whether the curve is banked or inclined, a speed calculation can be made. Various equations have been developed in this chapter to compute stopping distance, critical speed, coefficient of friction, and acceleration to name a few. An entire section was devoted to arguments concerning the manipulation of the coefficient of friction in critical stopping distance calculations. Recent arguments in the accident reconstruction field concerning the validity of the critical speed equation in a turn have emerged. These arguments state that the critical speed equation cannot be used. However, the arguments do not state what techniques can be used to calculate the critical speed in a turn. In this section we will present mathematically the validity of the critical speed equation. As with any analysis tool, the critical speed equation depends on the judicious use of the appropriate radial distance. Critical speed tests performed by the authors have validated the critical speed equation. The experienced investigator knows how to measure the yaw marks that yield the correct solution.

The argument against the use of Equation 4.73 usually goes like this: An automobile does not behave like a rock on a string. They reason that while a vehicle is negotiating a turn and going into a yaw, part of the available tire-road friction is drag and part keeps the vehicle from turning over. In contrast, they reason that a rock on a string uses all available force to keep moving in a circle. Furthermore, they state that since the critical speed method is derived from a rock on a string, the critical speed derivation is improper. Another corollary argument deals with the coefficient of friction used. They reason that since the value of the coefficient of friction is derived from skid tests, these values are improperly applied in critical speed calculations. These erroneous arguments will be dispelled in this section and the next. In the previous sections we derived the critical speed-curved trajectory in terms of a circular path. In the last section it was pointed out that curves are complex, including sections of spirals and circles. However, the circular portion of a curve is the sharpest, and therefore, using the radius of the circular portion of the road will lead to the lowest solution of the critical speed in a turn equation. The derivations in the previous sections made no mention of rocks on a string. The equations that were developed arose from equilibrium or loss of equilibrium equations. The equations were derived from basic statics and their respective free body diagrams. Free body diagrams are acceptable analysis aids in engineering and physics. A proper free body diagram yields correct solutions and should not be construed as improper simply because it represents a static condition.

Figure 4.13 represents a vehicle on a curved trajectory. At any particular point in time *P*, the section of the trajectory has a radial distance *R*. Keep in mind that the development presented here is not static. We will develop a time varying equation for the critical speed in a curved path where control of the vehicle is lost.

From basic definitions we know that *R* is the radius at the point *P*, *S* is the arc length and ω is the angular velocity. The condition for loss of control can be gleaned from the vector accelerations, namely.

$$|\boldsymbol{a}| = |\boldsymbol{a}_n + \boldsymbol{a}_t| \geq \mu g \tag{4.82}$$

In Equation 4.82 we consider the normal and tangential components of acceleration which cause the vehicle to leave its intended path. Note that there are no rocks or strings, only real forces that affect the vehicle. Since $S = R\theta$,

$$v = ds/dt = Rd\theta/dt = R\omega \tag{4.83}$$

and

$$v^2 = R^2(d\theta/dt)^2 \tag{4.84}$$

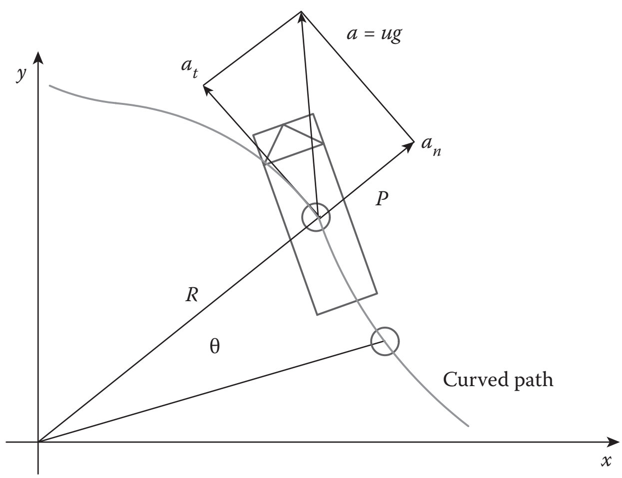

Figure 4.13 Critical speed—curved path.

By definition, the normal component of acceleration is,

$$\mathbf{a}_n = v^2/R = R(d\theta/dt)^2 \tag{4.85}$$

Again, by definition, the tangential component of acceleration is,

$$\mathbf{a}_t = dv/dt = d/dt(ds/dt) = d/dt(Rd\theta/dt) = Rd^2\theta/dt^2 \tag{4.86}$$

At the inequality, from Equation 4.82 we may write,

$$(\mathbf{a}_n)^2 + (\mathbf{a}_t)^2 = (\mu g)^2 \tag{4.87}$$

Substituting and separating the variables we obtain,

$$\frac{dv}{\sqrt{k^2 - v^4}} = \frac{dt}{R} \tag{4.88}$$

where $k = \mu g R$.

We are interested in the left side of the equation which involves an elliptic integral of the first kind. The solution to this integral is given by,

$$\frac{i\sqrt{-1/k}\, k\sqrt{1 - v^4/k^2}\; F[\varphi|m]}{\sqrt{k^2 - v^4}} \tag{4.89}$$

where

$F[\varphi/m]$ = elliptic integral of the first kind

$$i = \sqrt{-1} \quad m = -1$$

$$\varphi = i\ \sinh^{-1}\left[\sqrt{-1/k}\, v\right]$$

We can simplify Equation 4.89 to

$$F[\varphi|-1] = -\sqrt{\frac{\mu g}{R}}\, t \tag{4.90}$$

Note that $v = \sqrt{\mu g/R}$ is a solution to Equation 4.88. Let us now turn our attention to the value of the argument φ. We know that v will be a value in the neighborhood of $\sqrt{\mu g/R}$ so the argument of φ is

$$\varphi \cong i \sin h^{-1}[\sqrt{-1}] \tag{4.91}$$

The plot of the absolute value of the function on the left side of Equation 4.90 is shown in Figure 4.14.

The analysis above illustrates that the solution for the critical speed equation is accurate to within 10% and is, therefore, within engineering accuracy. The variability in the actual coefficient of friction and the approximation of the radial distance play a more critical role in the solution for the loss of control around a curve. It should be pointed out that there is no unique solution to Equation 4.88. Instrumented tests performed by the authors validate the critical speed equation and reaffirm that the proper values of radial distance and coefficient of friction play a more critical role than the use of the critical speed equation. We can summarize the generalized critical speed analysis above as follows.

1. The analysis was based on a generalized curved path, irrespective of whether it was a circle, ellipse, parabola, hyperbola, or any number of spirals.
2. The analysis was dependant on the normal and tangential components of velocity and acceleration as their position changed with time.
3. The radius of the curve does not need to be constant over the entire path. The radius need only be determined at the point of loss of control.
4. The critical speed equation is valid for the design of highways because roads are constructed of circular and spiral sections.

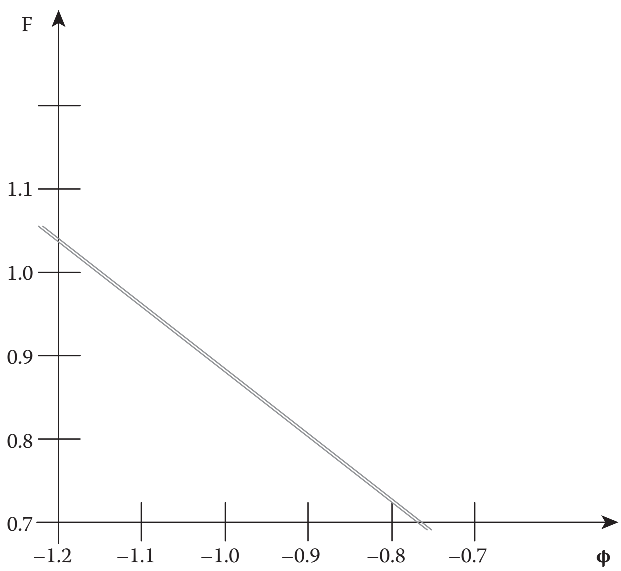

Figure 4.14 Plot of absolute value.

5. Skid marks produced by yawing or spinning vehicles are in the shape of curves and at the point of loss of control the skid marks have a mean radius and a normal and tangential component.
6. The development above was based on a valid free body diagram at the point of loss of control about an arbitrary curved path and yields a general solution of motion where the loss of control occurs.

As previously mentioned, vehicles losing control around a turn may yaw, spin, roll, or flip over. Yaw marks are deposited when a rolling tire is also sliding sideways. For most passenger cars the darkest or heaviest yaw mark is made by the outside front tire. The outside rear tire runs outside the front tire and its mark is generally less heavy. In contrast, when a vehicle is spinning, the tire marks will cross at least at one point. For large angles of spin rotation the tire marks may cross over more than once.

4.12 Critical Speed from Yaw and Rollover

Many single vehicle automobile accidents are characterized by the driver losing control over steering and over braking, causing the vehicle dynamics to yaw and then skid or roll to a stop. In a yaw, it is hard to tell which wheels are laying down the rubber. Many experts disagree on the actual tires that are producing one, two, three, or even four yaw marks. It is generally known, however, that the rear wheels track outside the front wheels. Many researchers pay too much attention to the radius of the individual yaw marks when, in fact, the important radial distance is that through which the center of mass of the vehicle traveled. The following speed calculations are in no way connected to which tires laid down the yaw marks. In fact, the center line through the yaw marks is a sufficiently accurate record of the path of the center of mass of the vehicle through the yaw and does not depend on which tires laid down the tracks. The yaw marks approximate sections of circles and the path drawn through the center of these yaw marks is also a section of a circle, which we take to be the path of the center of mass of the vehicle through the yaw. Since this type of accident occurs at high speeds, which corresponds to large radial distances, the arcs are relatively straight, making our assumptions valid.

Definition of terms:

V_a = average velocity through the yaw
V_c = critical speed of a vehicle in a yaw
V_i = speed entering the yaw
V_f = speed leaving the yaw
μ_a = average drag factor
μ_k = total vector coefficient of kinetic friction

μ_t = transverse drag factor in the yaw
μ_l = longitudinal drag factor in the yaw
D = distance of skid or roll after the yaw
R = radius of the yaw arc
S = arc length
L = length of the cord making up the yaw arc
h = rise of the arc above the cord
g = acceleration due to gravity

The radius R of the arc is related to the length L of the cord and the rise h of the arc above the cord by

$$R = \frac{4h^2 + L^2}{8h} \tag{4.92}$$

while the length of the arc S may be computed by

$$S = 2R\cos^{-1}\left(1 - \frac{h}{R}\right) \tag{4.93}$$

The critical speed of a vehicle in a flat turn of radius R is

$$V_c = \sqrt{\mu_t gR} \tag{4.94}$$

The speeds of the vehicle entering and leaving the yaw are related to the arc length S of the yaw by

$$V_i = \sqrt{V_f^2 + 2\mu_t gS} \tag{4.95}$$

The speed of the vehicle leaving the yaw and skidding or rolling to a stop through a distance D can be computed using the speed to stop formula.

$$V_f = \sqrt{2\mu_a gD} \tag{4.96}$$

Finally, the average velocity through the yaw is given by

$$V_a = \frac{V_i + V_f}{2} \tag{4.97}$$

Since the average speed through the yaw equals the critical speed,

$$V_a = V_c \tag{4.98}$$

substituting the above equation in accordance with Equation 4.97 yields

$$\sqrt{2\mu_t R} = \sqrt{\mu_a D} + \sqrt{\mu_a D + \mu_\ell S} \tag{4.99}$$

solving for μ_t yields

$$\mu_t = \frac{\mu aD}{R} + \frac{\mu_l s}{2R} \pm \sqrt{\frac{(\mu_a D)^2}{R^2} + \frac{\mu_a D}{R}\frac{\mu_\ell S}{R}} \tag{4.100}$$

which is of the form

$$\mu_t = a + \frac{b}{2} \pm \sqrt{a^2 + ab} \tag{4.101}$$

Completing the square within the radical

$$\mu_t = a + \frac{b}{2} \pm \sqrt{\left(a + \frac{b}{2}\right)^2 - \frac{b^2}{4}} \tag{4.102}$$

Since $\mu_t < 1$ and $R > S$, then $b \ll 1$.

$$\frac{b^2}{4} \ll \left(a + \frac{b}{2}\right)^2 \tag{4.103}$$

Thus, the only reasonable solution is

$$\mu_t \approx 2a + b = \frac{2\mu_a D}{R} + \frac{\mu_\ell S}{R} \tag{4.104}$$

It is now easy to choose μ_a and μ_k. We must not choose the longitudinal and transverse drag factors independently of one another. The total kinetic vector frictional force is the vector sum of the longitudinal and transverse frictional forces. Therefore, μ_k is given by

$$\mu_k = \sqrt{\mu_\ell^2 + \mu_t^2} \tag{4.105}$$

Choosing different values of the coefficient of kinetic friction μ_k yields values of μ_t in terms of μ_t in Equation 4.105. Additionally, choosing values of μ_a and substituting into Equation 4.104 allows us to choose a suitable value of the transverse drag factor μ_t which yields the critical speed of the vehicle in Equation 4.94.

4.13 Extension on Minimum Speed Calculations When Radius Cannot Be Determined Uniquely

In some reconstructions the yaw marks from a collision following loss of control, the tire marks have degraded to the point where they cannot be recognized. However, often, the beginning and end of the yaw was marked by the investigating officer. If these two points are known and the road geometry is known, then a minimum speed calculation can be made. In this analysis it is assumed that the vehicle did not leave the road surface. Figure 4.15 represents two points along a road where the points A and B are known as measured from the roadway. The separation of the points *L* along the road is also known. The arc is assumed to be tangent to the edge of the roadway on the *x*-axis.

Graphical or numerical solutions can be found that meet the requirements that have been specified. However, a general mathematical procedure will be outlined that lends itself to a variety of problems. To begin the analysis we construct a more general diagram as specified in Figure 4.16.

Figure 4.16 shows an arbitrary location for the center of the circle which produces the arc. We can write two equations for the radius in terms of the known quantities *A*, *B*, and *L* and the unknown center defined by x_c and y_c.

$$(y_c - B)^2 + (L - x_c)^2 = R^2 \tag{4.106}$$

$$(y_c - A)^2 + x_c^2 = R^2 \tag{4.107}$$

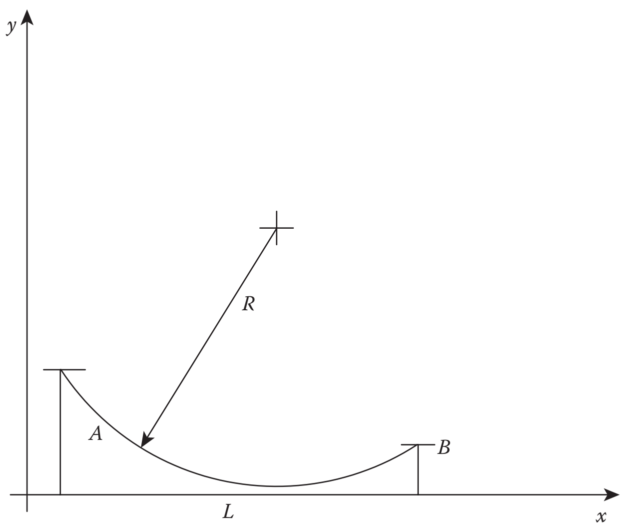

Figure 4.15 Unique radius.

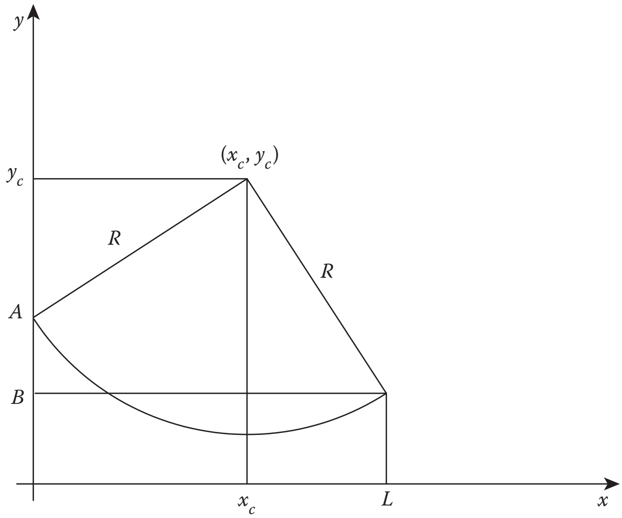

Figure 4.16 Unique radius—general solution.

Solving for the coordinates of the center of the circle yields,

$$x_c = ay_c + b \tag{4.108}$$

$$y_c = \frac{-(ab - A) \pm \sqrt{(ab - A)^2 - (1 + a^2)(A^2 + b^2 - R^2)}}{(1 + a^2)} \tag{4.109}$$

where $a = \dfrac{(A - B)}{L}$ and $b = \dfrac{(L^2 + B^2 - A^2)}{2L}$

The circle can be described as

$$(x - x_c)^2 + (y - y_c)^2 = R^2 \tag{4.110}$$

The condition that the arc AB. Lie entirely within the road is that R^2 be less than or equal to y_c^2. The radius of the circle that is tangent to the x-axis is,

$$R_x = \frac{-(ab - A) \pm \sqrt{(ab - A)^2 - (A^2 + b^2)a^2}}{a^2} \tag{4.111}$$

This equation yields two real solutions and never a complex conjugate pair. The reason that the equation never yields a complex conjugate pair is that for real and positive values A, B, and L, the radicand is always greater than zero. It is obvious that the equation is not valid for L equal to zero, a nonphysical case. The physically acceptable solution is the smaller of the two real solutions because we are looking for the smaller radius that corresponds to a minimum speed from yaw marks. The arc with the corresponding smaller value of R is tangent to the x-axis within the distance L, while the larger value of R corresponds to an arc tangent to the x-axis outside of the range of L.

The general equation as has been formulated, placed restrictions on the radius of the arc that may be tangent to the y-axis. Figure 4.17 shows a hypothetical road intersection with two vehicles approaching the intersection.

Vehicle 2 proceeds to run a stop sign forcing vehicle 1 to steer sharply to the left in order to avoid the collision. In doing so, the yaw marks deposited on the road may intersect the y-axis at one point or be tangent to the y-axis. These restrictions may yield a different solution for the minimum radius.

It is possible that a circle of radius larger than the radius of the circle that is tangent to the x-axis will be tangent to the y-axis. This circle that is tangent to the x-axis may or may not cut the y-axis at two points with point A being the higher point as shown in Figure 4.18.

In this case, the minimum radius, determined by the conditions on the x-axis, should be rejected because a new radius tangent to the y-axis yields a larger value of minimum radius, which translates to a higher speed. Because the car is traveling parallel to the road and steering sharply to the left, it would not cut the y-axis in two places. It is also a more reasonable solution because as shown in Figure 4.17, vehicle 1 would not normally cross the y-axis at two points. The condition for a circle tangent to the y-axis is that $X_c = R$ and $Y_c = A$. Applying this condition to Equation 4.108 yields,

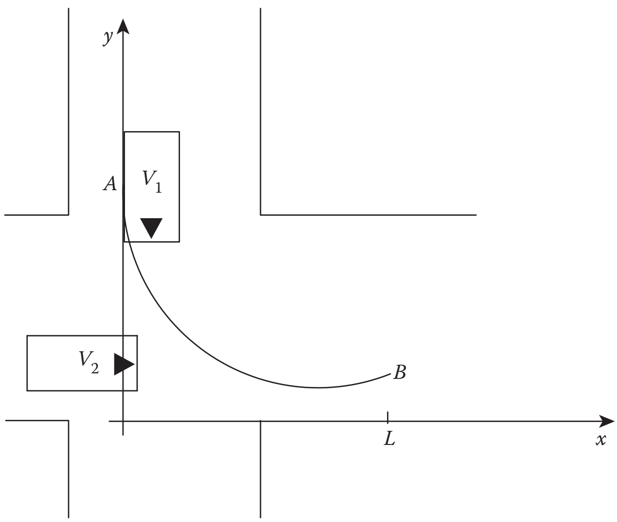

Figure 4.17 Intersection near collision.

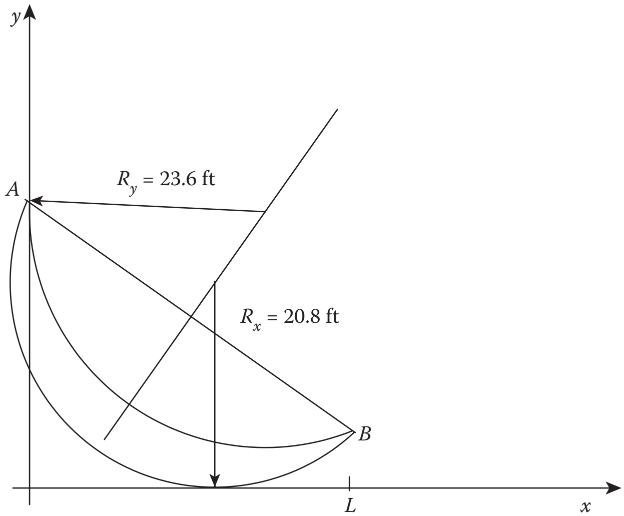

Figure 4.18 Possible solutions.

$$R_y = \frac{(A-B)^2 + L^2}{2L} \tag{4.112}$$

As an example, if we assume $A=28$ ft, $B=8$ ft, and $L=36$ ft, the radius of the circle tangent to the x-axis has two solutions, 20.8 ft and 131.8 ft. The radius of the circle tangent to the y-axis is 23.6 ft. The solution 20.8 ft is rejected because is cuts the y-axis in two places and is the smaller value. Please refer to Figure 4.17. Thus, the correct solution is the radius tangent to the y-axis.

4.14 Crush Analysis

Vehicle crush was first investigated in the 1970s by developing a correlation between damage to the vehicle and the related change in velocity, or ΔV. This analysis determined that there was a linear relationship between the impact speeds of vehicles into rigid barriers and the resulting crush from these collisions. From this data, mathematical models, known as algorithms, were developed to correlate vehicle damage measurements to accident reconstructions. The National Highway Traffic Safety Administration (NHTSA) developed the CRASH3 program. The crush behavior used in the CRASH3 program is modeled as a linear spring with characteristics as shown in Figure 4.19.

Based on this linear spring model the crash coefficients A, B, and G are given by NHTSA from their crash tests. Generally, these crash tests are conducted against rigid barriers at 30–35 mph. The tests include frontal, offset

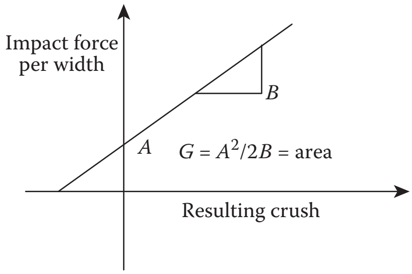

Figure 4.19 Crush model.

frontal, angled frontal, rear, and side impact tests. Since the relationship between the impact force per width and the resulting crush on the vehicle is linear or nearly linear, it is possible to extrapolate the data to speeds lower and higher than the test speeds.

An argument made by some experts is that the NHTSA crash tests are not valid at lower and higher speeds. Thus, they argue that reconstructing accidents based on crush at lower speeds is not valid. This argument is simply not noteworthy for the following reasons: First, we must ask why the crash tests are conducted at around 35 mph. The answer is simple, because it is well documented through legitimate research, human tolerance, and experimentation that severe injuries begin to occur at those speeds. Second, the error published by developers of crash data state that it may vary from about 3 to 7% based on the amount of crush and therefore, impact speed. For example, let us assume that very slight crush yields an impact speed of 7 mph. Let us further assume that the error is 15% so that the actual speed may vary between approximately 6 and 8 mph. For a higher collision speed we may determine from crush that the impact speed is 63 mph. If we assume an error of 5%, the actual speed may vary from approximately 60–66 mph. Certainly, in both the lower and higher speed calculations, the range of speeds are acceptable and within the accuracy that is possible in a properly executed accident reconstruction. In a study conducted by Prasad, the energy dissipated in vehicle crush utilizing a repeated test technique essentially validated the linear relationship of crush deformation for modern cars and began the tests at speeds of 10–35 mph. The coefficients of crush, the "*C*" values, ranged from 1 to 46 inches for the various speeds and vehicles tested. The absorbed energies ranged from approximately 8800 to 139,000 ft lbs.

The important point to make is that experts who attempt to discredit the relationship between vehicle crush and speed calculations cannot point to scientific or engineering studies that show the inappropriateness of the technique. The simple fact is that crush deformation is an acceptable method in accident reconstruction if properly utilized within the accuracy of the technique. Since crush deformation measurements are subjective to a certain extent, they have the potential for misuse. It is in the measurements of the crush values where the reconstructionist can distort and influence the outcome of the calculations. There are standards for crush measurements developed by the SAE. Please refer to Chapter 15 for the SAE standards. These standards guide the investigator and help to reduce the potential of misuse of the technique. It should be pointed out that the authors have used crash deformation and validated the technique with a crush data retrieval (CDR) tool, and standard energy and momentum methods. When used properly, crush deformation is an excellent method in accident reconstructions.

Since crush energy dissipation can be accurately correlated to vehicle speeds and change in velocity, the total energy dissipated in the collision between two vehicles can be computed as follows. The crush energy dissipation (CED) goes mainly into the deformation of the vehicles. Some energy such as that translated to sound or heat cannot be determined. The CED can be computed by taking the difference between the total initial and final kinetic energies. Thus,

$$CED = \frac{W_1}{2g}[(V_{1i}^2 + R_{2vl}V_{2i}^2) - (V_{1f}^2 + R_{2vl}V_{2f}^2)] \qquad (4.113)$$

The parameters in Equation 4.113 are detailed in Chapter 5. The change in velocity calculations are detailed in Chapter 2.

One area of crush deformation that has produced considerable error from the published data from NHTSA is with pole impacts. Every year many injuries and deaths occur from collisions with poles and trees. In reconstructing these accidents it is desirable to determine the vehicle speed prior to impact. Originally two methods were employed to determine vehicle speed. One method employed observed crush geometry and the other utilized maximum crush. The method used commonly to estimate impact speed from observed crush was developed by Campbell and has been incorporated into a variety of CRASH programs. In 1981, the National Transportation Safety Board (NTSB) released a report devoted to collisions with trees. The report recommended the method employing the *A* and *B* parameters as the most accurate method available to estimate impact speed from measured crush.

In 1983, Jones reported on an analysis of crush test data. That analysis found that using *A* and *B* stiffness parameters obtained from flat barrier tests under-predicted pole test speeds by approximately 67% of the actual test speed. In 1987, Smith et al., reported on tests with narrow object impacts. They found that the use of *A* and *B* parameters underestimated the speed by between 57 and 82%. Morgan and Ivey in 1987 developed an alternative formula which allows one to calculate the approximate impact speed given the maximum crush and vehicle weight. In 1992, Nystrom and Kost developed a formula based on regression analysis of actual staged tests and curve fitting techniques. The three methods outlined above are summarized in the equations below:

$$V_1 = \text{BPO}_1 + \text{BPI}_1 \cdot \text{CRM} \tag{4.114}$$

$$V_2 = 395D_2 - 0.062W \tag{4.115}$$

$$V_3 = \text{BPO}_3 + \text{BPI}_3 \cdot \text{CRM} \tag{4.116}$$

In the equations above the following parameters are defined as,
V_1 = preimpact speed according to NTSB (mph)
V_2 = preimpact speed according to Morgan and Ivey (mph)
V_3 = preimpact speed according to Nystrom and Kost (mph)
BPO_1 = speed at which no crush is expected (2.46 mph)
BPI_1 = slope of speed vs. crush (0.648 mph/inches)
CRM = maximum crush on vehicle (inches)
D_2 = maximum residual deformation (ft)
W = weight of vehicle (lbs)
BPO_3 = speed at which no crush is observed (5 mph)
BPI_3 = slope of speed vs. crush (mph/inches)
where

$$BPI_3 = 0.964 - (3.51 \times 10^{-5}) \times W \tag{4.117}$$

As an example, a vehicle weighing 2550 lbs had a maximum crush of 36.4 inches with a residual deformation of 0.468 ft from an impact with a rigid pole. The maximum crush extended to the front axle. The analysis from crush gives a median speed of 23 mph. The NTSB and Morgan equations yield a speed between 18 and 28 mph The Nystrom and Kost equation produces a speed between 42 and 48 mph. Based on the severity of the impact it was deemed the speed was in the range calculated by the Nystrom and Kost equation and was the most accurate. In this example we see that calculations performed by different investigators can yield significantly different results when collision with poles are analyzed. The crush analysis of 23 mph is near the center of the results from the NTSB and Morgan and Ivey equations between 18 and 28 mph. All three of these methods produce speeds significantly different than the median value of 45 mph from Nystrom and Kost.

4.15 Tree Impacts

In the previous section we saw how pole impacts can be analyzed through crush. In this section we offer an alternate solution when a vehicle impacts a tree. This type of collision can be treated as a strength of materials problem. We will assume that the tree is modeled as a cantilever beam of circular cross-section. This type of analysis lends itself to problems where a small tree is broken by the impact with a car or where the crush on the car is in question as a result of an alleged collision with the tree. Figure 4.20 is relevant to the analysis.

For cylindrical shapes such as trees with diameter D, we define the following parameters. Moment of inertia,

$$I = \frac{\pi D^4}{64} \tag{4.118}$$

section modulus,

$$S = \frac{\pi D^3}{32} \tag{4.119}$$

area,

$$A = \frac{\pi D^2}{4} \tag{4.120}$$

The maximum shear is equal to the applied force F. If we know the modulus of elasticity E, we can compute the deflection at the load from Equation 4.121.

$$X = \frac{FY^3}{3EI} \tag{4.121}$$

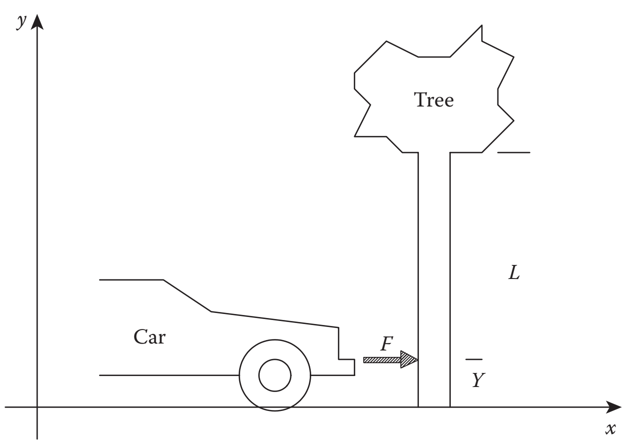

Figure 4.20 Tree impact.

The deflection end slope is then,

$$\varphi = \frac{FY^2}{2EI} \quad (4.122)$$

The shear stress is,

$$f_v = F/A \quad (4.123)$$

The maximum moment is,

$$M = FY \quad (4.124)$$

The actual bending stress is then given by,

$$f_b = M/S \quad (4.125)$$

For oak, the bending strength f_b is 800 psi, the shear strength f_v is 85 psi, and the modulus of elasticity is 900,000 psi. If f_v is greater than F_v, yield due to shear stress occurs. If f_b is greater than F_b, yield due to bending stress occurs.

Momentum Methods

5

5.1 Introduction

Probably the most powerful technique used in accident reconstruction is that of the conservation of momentum. Momentum may also be the most underused technique because of its subtleties and sensitivity. In Chapter 2 we devoted an introduction into the conservation of momentum. In this chapter we will explore the techniques available in momentum solutions. Momentum can be subdivided into elastic and inelastic collisions and recoil. Conservation of momentum allows for the solution of velocities before or after a collision. Figure 5.1 represents a collision between two vehicles showing their pre- and postimpact paths for the solution based on momentum.

The basic equation of conservation of momentum is then

$$m_1V_{1i} + m_2V_{2i} = m_1V_{1f} + m_2V_{2f} \tag{5.1}$$

where

m_1 = mass of vehicle 1
m_2 = mass of vehicle 2
V_{1i} = precollision velocity of vehicle 1
V_{2i} = precollision velocity of vehicle 2
V_{1f} = postcollision velocity of vehicle 1
V_{2f} = postcollision velocity of vehicle 2

5.2 Elastic and Inelastic Collisions

A completely elastic collision is one in which the two vehicles come together, collide and separate. In the elastic collision, the forces of interaction between the vehicles are conserved, the total kinetic energy is the same before and after the collision. Completely elastic collisions never occur when two vehicles have an accident. However, for many collisions an elastic model is a sufficient solution of the event. At the opposite end of an elastic collision is one in which the two vehicles become coupled and move in unison after the collision. Such a collision is completely inelastic. Most vehicles collisions range from elastic to inelastic to some degree. In those cases, a coefficient of restitution is

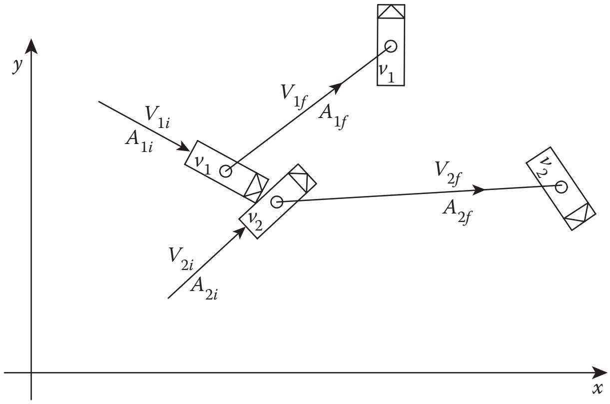

Figure 5.1 Conservation of momentum.

introduced into the conservation of momentum solutions. Before we develop specific equations, we wish to generalize conservation of momentum equations in terms of their elastic and inelastic qualities.

5.3 Elastic Collisions

In a perfectly elastic collision, the center of mass of the vehicles is central. After the collision, the vehicles separate at different velocities, and since kinetic energy and momentum are both conserved, we may write two equations. The first equation is given by 5.1 and the energy equation is

$$\frac{1}{2}m_1 V_{1i}^2 + \frac{1}{2}m_2 V_{2i}^2 = \frac{1}{2}m_1 V_{1f}^2 + \frac{1}{2}m_2 V_{2f}^2 \tag{5.2}$$

If the masses and the precollision velocities are known, the postcollision velocities are known. The postcollision velocities are given by

$$V_{1f} = \frac{2R_{2v1}V_{2i} + (1 - R_{2V1})V_{1i}}{(R_{2V1} + 1)} \tag{5.3a}$$

$$V_{2f} = \frac{2V_{1i} + (1 - R_{2V1})V_{2i}}{(R_{2V1} + 1)} \tag{5.3b}$$

If the masses and the postcollision velocities are given, the precollision velocities are given by

$$V_{1i} = \frac{2R_{2v1}V_{2f} + (1 - R_{2V1})V_{1f}}{(R_{2V1} + 1)} \quad (5.4a)$$

$$V_{2i} = \frac{2V_{1f} + (R_{2V1} - 1)V_{2f}}{(R_{2V1} + 1)} \quad (5.4b)$$

$$\text{where } R_{2V1} = \frac{W_2}{W_1} \text{ is the ratio of the masses} \quad (5.5)$$

In the case where one vehicle is at rest initially, say $V_{2i} = 0$, Equations 5.3 reduce to

$$V_{1f} = \frac{(1 - R_{2V1})V_{1i}}{(R_{2v1} + 1)} \quad (5.6a)$$

$$V_{2f} = \frac{2V_{1i}}{(R_{2v1} + 1)} \quad (5.6b)$$

If the weight of one vehicle is much more massive than the other, i.e., $W_1 >> W_2$ such as in a train-vehicle collision, Equations 5.6 reduce to

$$V_{1f} \approx V_{1i} \quad (5.7a)$$

$$V_{2f} \approx 2V_{1i} + V_{2i} \quad (5.7b)$$

It has been previously inferred that the energy may not always be conserved but that momentum is always conserved. Therefore, the equations developed above may not always hold true. In those cases, a more general solution of the conservation of linear momentum may be obtained by expanding Equation 5.1 into its appropriate components. This type of analysis is reserved for the next section. Before we leave this section, there are a couple of topics that need to be addressed. For the special case of the elastic collision in which one vehicle is at rest before the collision, $V_{2\text{i}} = 0$.

$$V_{1f} = \frac{(1 - R_{2V1})V_{1i}}{(R_{2v1} + 1)} \quad (5.8a)$$

$$V_{2f} = \frac{2V_{1i}}{(R_{2v1} + 1)} \quad (5.8b)$$

If the masses of the vehicles are equal and we know the final velocities of the vehicles, Equation 5.4 reduces to

$$V_{1i} = V_{2f} \tag{5.9a}$$

$$V_{2i} = V_{1f} \tag{5.9b}$$

5.4 Conservation of Linear Momentum

With reference to Figure 5.1 and given the pre and post impact angles of the vehicles as A_{1i}, A_{2i}, A_{1f}, and A_{2f} we can again define the ratio of the masses in terms of the ratio of weights. Thus, in the collision between V_1 and V_2, the weight ratio is defined as follows where W_1 and W_2, are the weights of vehicles V_1 and V_2, respectively. In a collision between two vehicles, conservation of momentum states that the total initial momentum is the same as the total final momentum. Momentum is an additive vector quantity defined as the product of mass and velocity.

$$R_{2v1} = \frac{W_2}{W_1} \tag{5.10}$$

Since the mass of a vehicle is its weight divided by the acceleration due to gravity, weight may be used in place of mass in the momentum equation. Setting up an (x,y) coordinate system in the usual fashion and measuring angles positive counterclockwise from the x-axis, allows the x and y components of the initial and final momentum to be expressed as

$$\begin{aligned} P_{ix} &= W_1 V_{1i} \cos A_{1i} + W_2 V_{2i} \cos A_{2i} \\ P_{iy} &= W_1 V_{1i} \sin A_{1i} + W_2 V_{2i} \sin A_{2i} \end{aligned} \tag{5.11}$$

$$\begin{aligned} P_{fx} &= W_1 V_{1f} \cos A_{1f} + W_2 V_{2f} \cos A_{2f} \\ P_{fy} &= W_1 V_{1f} \sin A_{1f} + W_2 V_{2f} \sin A_{2f} \end{aligned} \tag{5.12}$$

The equations of conservation of momentum

$$\begin{aligned} P_{ix} &= P_{fx} \\ P_{iy} &= P_{fy} \end{aligned} \tag{5.13}$$

may then be solved in a number of ways.

In this particular case, the angles and the final speeds will be taken as known quantities, and the initial speeds will be determined by the equations, producing the following results:

$$V_{1i} = \frac{V_{1f}\sin(A_{2i} - A_{1f}) + R_{2v1}V_{2f}\sin(A_{2i} - A_{2f})}{\sin(A_{2i} - A_{1i})}$$
$$V_{2i} = \frac{V_{1f}\sin(A_{1i} - A_{1f}) + R_{2v1}V_{2f}\sin(A_{1i} - A_{2f})}{R_{2v1}\ \sin(A_{1i} - A_{2i})} \tag{5.14}$$

If the initial and final coordinates of the centers of mass of the two vehicles are known, the post-collision angles and distances may be computed using

$$A_{1f} = \tan^{-1}\left(\frac{Y_{1f} - Y_{1i}}{X_{1f} - X_{1i}}\right)$$
$$A_{2f} = \tan^{-1}\left(\frac{Y_{2f} - Y_{2i}}{X_{2f} - X_{2i}}\right) \tag{5.15}$$

and

$$D_{1f} = \sqrt{(X_{1f} - X_{1i})^2 + (Y_{1f} - Y_{1i})^2}$$
$$D_{2f} = \sqrt{(X_{2f} - X_{2i})^2 + (Y_{2f} - Y_{2i})^2} \tag{5.16}$$

The postcollision speeds are determined from the postcollision distances and the coefficient of kinetic friction using

$$V_{1f} = \sqrt{2\mu_k g D_{1f}}$$
$$V_{2f} = \sqrt{2\mu_k g D_{2f}} \tag{5.17}$$

Similarly, if the preskid and initial coordinates of the centers of mass of the two vehicles are known, the preskid angles and distances may be computed using

$$A_{1i} = \tan^{-1}\left(\frac{Y_{1i} - Y_{1o}}{X_{1i} - X_{1o}}\right)$$
$$A_{2i} = \tan^{-1}\left(\frac{Y_{2i} - Y_{2o}}{X_{2i} - X_{2o}}\right) \tag{5.18}$$

and

$$D_{1i} = \sqrt{(X_{1i} - X_{1o})^2 + (Y_{1i} - Y_{1o})^2}$$
$$D_{2i} = \sqrt{(X_{2i} - X_{2o})^2 + (Y_{2i} - Y_{2o})^2} \tag{5.19}$$

The preskid speeds may then be computed using

$$V_{1o} = \sqrt{V_{1i}^2 + 2\mu_k g D_{1i}}$$
$$V_{2o} = \sqrt{V_{2i}^2 + 2\mu_k g D_{2i}} \tag{5.20}$$

Finally, it is useful to compute the total energy dissipated in the collision. It is called the Crush Energy Dissipation (CED) because most of the dissipated energy goes into the deformation of the vehicles. We may then compare the CED to the results of EDCRASH or other computer programs that calculate the energy based on crush. The computer program EDCRASH computes this quantity based on the class of the vehicles and the damage to the vehicles. Please refer to the EDCRASH program for more details. Here, the CED is computed by taking the difference between the total initial and final kinetic energies. Thus,

$$\text{CED} = \frac{W_1}{2g}\left[(V_{1i}^2 + R_{2v1}V_{2i}^2) - (V_{1f}^2 + R_{2v1}V_{2f}^2)\right] \tag{5.21}$$

5.5 Conservation of Linear Momentum with Restitution

The beginning of this analysis is the same as the analysis of the conservation of linear momentum. It is repeated for clarity, and to emphasize the theoretical underpinnings. In the collision between V_1 and V_2, the weight ratio is defined as follows:

$$R_{2v1} = \frac{W_2}{W_1} \tag{5.22}$$

where W_1 and W_2 are the weights of V_1 and V_2, respectively. In a collision between two vehicles, conservation of momentum states that the total initial momentum is the same as the total final momentum. Momentum is an additive vector quantity defined as the product of mass and velocity. Since the mass of a vehicle is its weight divided by the acceleration due to gravity, weight may be used in place of mass in the momentum equation. Setting up an (x,y) coordinate system in the usual fashion and measuring angles positive counterclockwise from the x-axis, allows the x and y components of the initial and final momentum to be expressed as:

$$P_{ix} = W_1 V_{1i} \cos A_{1i} + W_2 V_{2i} \cos A_{2i}$$
$$P_{iy} = W_1 V_{1i} \sin A_{1i} + W_2 V_{2i} \sin A_{2i} \tag{5.23}$$

$$P_{fx} = W_1 V_{1f} \cos A_{1f} + W_2 V_{2f} \cos A_{2f}$$
$$P_{fy} = W_1 V_{1f} \sin A_{1f} + W_2 V_{2f} \sin A_{2f} \tag{5.24}$$

The equations of conservation of momentum:

$$P_{ix} = P_{fx}$$
$$P_{iy} = P_{fy} \tag{5.25}$$

may then be solved in a number of ways.

In a standard momentum analysis, the angles and the final speeds are taken as known quantities. Energy methods are used to compute the postcollision velocities. These results are employed into the momentum equations to determine the impact speeds. The postcollision velocities are determined from the post-collision distances and the coefficient of kinetic friction using:

$$V_{1f} = \sqrt{2\mu_k g D_{1f}}$$
$$V_{2f} = \sqrt{2\mu_k g D_{2f}} \tag{5.26}$$

In some cases, the scene data is unreliable, which makes determining the impact location difficult. Even small changes in the impact point will have significant effects on the post-impact distances and angles. As such, there will be a level of uncertainty with the final velocity calculations. Usually, an accurate determination of the post-impact phase of at least one vehicle can be made. However, the limited confidence in the scene data requires an analysis of the impact phase.

In an impact between two vehicles (V_1 and V_2), the impact phase can be separated into two periods. Following the initial contact, a short period of increasing deformation takes place until the contact area between the vehicles ceases to increase. During this instant, the vehicles are moving at the same velocity (V_0). During the remainder of contact, a period of restoration occurs during which the contact area is reduced to zero. The relationship between the restoration and deformation phases of impact is called the coefficient of restitution (e), which reflects the capacity of the contacting bodies to recover from the impact.

For each vehicle, e can be defined by the following ratios: where F_r and F_d are the contact forces during the restoration and deformation periods. Combining the two expressions in Equation 5.28 eliminates V_0 and provides an equation for e.

The coefficient of restitution depends on the impact velocity, geometry of colliding objects, and given combination of contacting materials. The value of e will lie between 1.0 and 0. An e of 1.0 denotes a purely elastic impact where the energy loss through heat, deformation, and sound is negligible. The value $e = 0$ represents an inelastic, or plastic, impact where the vehicles cling together after colliding and the energy loss is maximum. In the purely plastic case ($e = 0$), the postimpact velocities (V_{1f} and V_{2f}) of the two vehicles will be equal.

$$\text{for}\quad V1: e = \frac{\int_{t_0}^{t} F_r dt}{\int_{0}^{t_0} F_d dt} = \frac{V_0 - V_{1f}}{V_{1i} - V_0}$$

$$\text{for}\quad V2: e = \frac{\int_{t_0}^{t} F_r dt}{\int_{0}^{t_0} F_d dt} = \frac{V_{2f} - V_0}{V_0 - V_{2i}} \tag{5.27}$$

$$e = \frac{V_{2f} - V_{1f}}{V_{1i} - V_{2i}} \tag{5.28}$$

For a given case, it may be found that V_{1f} can be more accurately determined from Equation 5.26. Then, V_{2f} can be described as follows:

$$V_{2f} = V_{1f} + e(V_{1i} - V_{2i}) \tag{5.29}$$

Substituting Equation 5.29 into Equation 5.25 yields:

$$V_{1i} = V_{1f}\frac{\sin(A_{2i} - A_{1f}) - R_{2v1}\sin(A_{2f} - A_{2i}) + e\sin(A_{2f} - A_{1f})}{\sin(A_{2i} - A_{1i}) + R_{2v1}\sin(A_{2f} - A_{2i}) + e\sin(A_{2f} - A_{1i})}$$

$$V_{2i} = \frac{V_{1f}}{R_{2v1}}\frac{\sin(A_{1f} - A_{1i}) + R_{2v1}\sin(A_{2f} - A_{1i}) + R_{2v1}e\sin(A_{2f} - A_{1f})}{\sin(A_{2i} - A_{1i}) + R_{2v1}\sin(A_{2f} - A_{2i}) + e\sin(A_{2f} - A_{1i})} \tag{5.30}$$

For the alternate case, V_{2f} may be more accurately determined from Equation 5.26. Then V_{1f} can be described as follows:

$$V_{1f} = V_{2f} - e(V_{1i} - V_{2i}) \tag{5.31}$$

Then substitution of Equation 5.31 into Equation 5.25 provides:

$$\begin{aligned} V_{1i} &= R_{2v1} V_{2f} \frac{\sin(A_{2i} - A_{1f}) - R_{2v1}\sin(A_{2f} - A_{2i}) + e\sin(A_{2f} - A_{1f})}{R_{2v1}\sin(A_{2i} - A_{1i}) + e\sin(A_{1i} - A_{1f}) + R_{2v1}e\sin(A_{2i} - A_{1f})} \\ V_{2i} &= V_{2f} \frac{\sin(A_{1f} - A_{1i}) + R_{2v1}\sin(A_{2f} - A_{1i}) + R_{2v1}e\sin(A_{2f} - A_{1f})}{R_{2v1}\sin(A_{2i} - A_{1i}) + e\sin(A_{1i} - A_{1f}) + R_{2v1}e\sin(A_{2i} - A_{1f})} \end{aligned} \tag{5.32}$$

Comparison of results from Equations 5.30 and 5.32 will determine which postimpact speed (V_{1f} or V_{2f}) is more reliable. Finally, the preskid speeds may be computed using:

$$\begin{aligned} V_{1o} &= \sqrt{V_{1i}^2 + 2\mu_k g D_{1i}} \\ V_{2o} &= \sqrt{V_{2i}^2 + 2\mu_k g D_{2i}} \end{aligned} \tag{5.33}$$

5.6 Conservation of Rotational Momentum

Solutions using the conservation of linear momentum are sufficient for most kinds of collisions. However, errors are introduced when the impact load is directed at a considerable distance away from the vehicle's center of mass. Examples of such collisions are frontal-offset impacts or T-bone collisions centered at the front or rear of the target vehicle. In a collision between two vehicles, denoted as V_1 and V_2, Figure 5.2 details the impact configuration.

In this diagram, the preimpact velocities are denoted V_{1i} and V_{2i} and the postimpact velocities are denoted V_{1f} and V_{2f}. These velocity vectors are directed at the respective angles denoted A_{1i}, A_{2i}, A_{1f}, and A_{2f} based on the Cartesian coordinate system. The rotational velocities are defined as ω_1 and ω_2. As the position and direction of the impact forces are located away from the center of mass, especially with vehicle 1 (V_1) in this example, moment arms l_1 and l_2 are defined. As shown in the figure, these moment arms can be broken down into their Cartesian components.

$$\begin{aligned} l_1 &= \sqrt{l_{1x}^2 + l_{1y}^2} \\ l_2 &= \sqrt{l_{2x}^2 + l_{2y}^2} \end{aligned} \tag{5.34}$$

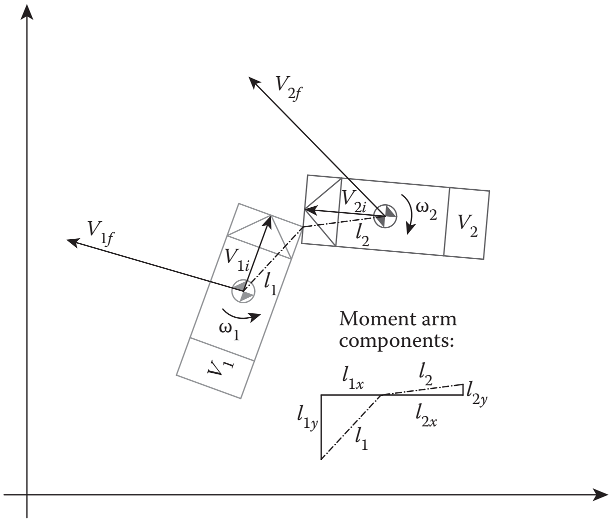

Figure 5.2 Rotational momentum.

Conservation of rotational momentum is given by the following equation, where "I" denotes the moment of inertia of the vehicles.

$$I_1\omega_{1i} + I_2\omega_{2i} = I_1\omega_{1f} + I_2\omega_{2f} \tag{5.35}$$

Solving this equation requires computing the angular velocities of the vehicles before and after the impact. Unless a vehicle is yawing at a significant rate prior to a collision, the left side of the equation can be considered as zero for most cases. Thus, we will only consider angular velocities resulting from impact. The postimpact rotational momentum of each vehicle is given by the following:

$$\begin{aligned} I_1\omega_{1f} &= m_1 \Delta V_1 l_2 \\ I_2\omega_{2f} &= m_2 \Delta V_2 l_1 \end{aligned} \tag{5.36}$$

Here, speed changes incurred by both vehicles as a result of the impact are defined as ΔV_1 and ΔV_2. The terms m_1 and m_2 refer to the masses of each vehicle. The ratio of the masses, or weights, is given by the following:

$$R_{2v1} = \frac{W_2}{W_1} = \frac{m_2}{m_1} \tag{5.37}$$

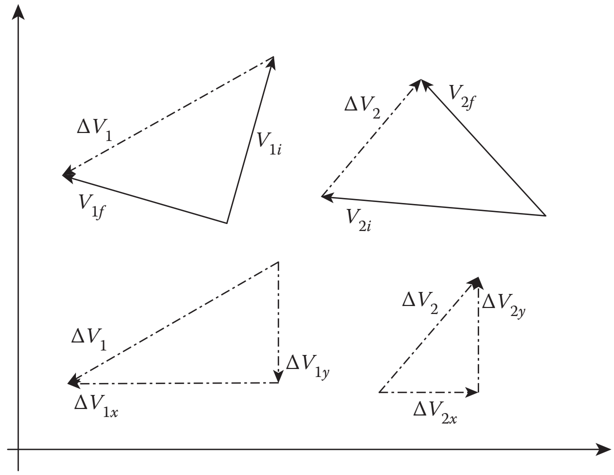

Figure 5.3 Speed change relationships.

The speed changes are defined by the following relationships and Figure 5.3:

$$\Delta V_1 = \sqrt{\Delta V_{1x}^2 + \Delta V_{1y}^2} = \sqrt{(V_{1ix} - V_{1fx})^2 + (V_{1iy} - V_{1fy})^2} \tag{5.38}$$

$$\Delta V_2 = \sqrt{\Delta V_{2x}^2 + \Delta V_{2y}^2} = \sqrt{(V_{2ix} - V_{2fx})^2 + (V_{2iy} - V_{2fy})^2} \tag{5.39}$$

Note that the x and y components of the pre and postimpact velocities are based on the specified angles gathered by the accident site information. By implementing these definitions for speed change into the governing equation, the following equations are generated:

$$\begin{aligned} 0 &= R_{2v1}\Delta V_{2x} l_{1y} + \Delta V_{1x} l_{2y} \\ 0 &= R_{2v1}\Delta V_{2y} l_{1x} + \Delta V_{1y} l_{2x} \end{aligned} \tag{5.40}$$

Organization of this equation is performed to place the unknown variables (V_{1i} and V_{2i}) on the left side.

$$\begin{aligned} V_{2i}R_{2v1}l_{1y}\cos(A_{2i}) + V_{1i}l_{2y}\cos(A_{1i}) &= V_{2f}R_{2v1}l_{1y}\cos(A_{2f}) + V_{1f}l_{2y}\cos(A_{1f}) \\ V_{2i}R_{2v1}l_{1x}\sin(A_{2i}) + V_{1i}l_{2x}\sin(A_{1i}) &= V_{2f}R_{2v1}l_{1x}\sin(A_{2f}) + V_{1f}l_{2x}\sin(A_{1f}) \end{aligned} \tag{5.41}$$

Conservation of energy principles for the postimpact translational and rotational movement yield the following equations for postimpact speeds.

$$V_{1f} = \sqrt{2\mu_{1f} g\left(\beta_1 \mathrm{WB}_1 \frac{\pi}{360} + D_{1f}\right)}$$
$$V_{2f} = \sqrt{2\mu_{2f} g\left(\beta_2 \mathrm{WB}_2 \frac{\pi}{360} + D_{2f}\right)} \tag{5.42}$$

Here, μ is the coefficient of friction, g is the acceleration due to gravity, β is the magnitude of the postimpact rotation, WB is the vehicle's wheelbase, and D_f is the postimpact skid distance. The postimpact rotation is taken as the absolute difference of the final heading angles (α_1 and α_2) to the initial heading angles (A_{1i} and A_{2i}). Note that it is assumed that the vehicle's preimpact heading corresponds with its direction, which is derived from the assumption that there is negligible rotational momentum prior to impact.

$$\beta_1 = |A_{1i} - \alpha_1|$$
$$\beta_2 = |A_{2i} - \alpha_2| \tag{5.43}$$

Once the unknowns are reduced to the preimpact speeds (V_{1i} and V_{2i}), the governing equation can be solved by several methods. Solving the two governing equations simultaneously provides satisfactory answers but is not conducive to coding. These equations have been organized for implementation into direct or iterative solutions for linear algebraic equations ($AX = b$). Cramer's rule can also be applied for implementation into spreadsheet programs.

5.7 Combined Linear and Rotational Momentum

Linear and rotational momentum may be combined in those reconstructions that combine both effects in the pre- or postphases of the collision. Each section of the collision may be solved piece-wise and then the two solutions may be then combined through superposition. Such solutions can be quite complex and can involve translation and rotation of the axes. In these types of reconstructions two sets of coordinates may need to be established to find the complete solution. For example, the linear momentum portion of the solution may utilize rectangular coordinates while the rotational portion of the solution may encompass cylindrical coordinates. These types of solutions also lend themselves to collisions involving more than one impact.

For instance a first impact may occur between two vehicles where the solution to the velocities is found from linear momentum. A third vehicle may then strike one of the original vehicles causing the vehicle to spin from the second impact.

5.8 Rotational Momentum—Alternate Solution

Another method of analysis for the solution of rotational momentum problems may be obtained by considering the vector moment of torque produced by a force **F**, consider Figure 5.4.

Recall from Chapter 2 that the vector moment is given by

$$\Gamma = \mathbf{r} \times \mathbf{F} \tag{5.44}$$

The vector angular momentum is defined as

$$\mathbf{H} = \mathbf{r} \times m\mathbf{v} \tag{5.45}$$

The vector angular momentum is also defined as the momentum of momentum. The magnitude of angular momentum is given by

$$|\mathbf{H}| = H = I\omega \tag{5.46}$$

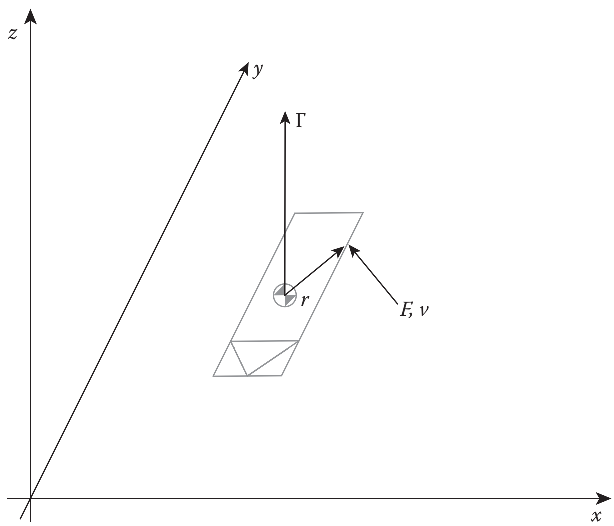

Figure 5.4 Rotational momentum.

where I = moment of inertia and ω is the angular velocity. For Figure 5.4 we may express the vectors as

$$\mathbf{r} = x\mathbf{a}_x + y\mathbf{a}_y \tag{5.47}$$

$$\mathbf{F} = F_x\mathbf{a}_x + F_y\mathbf{a}_y \tag{5.48}$$

$$\mathbf{v} = v_x\mathbf{a}_x + v_y\mathbf{a}_y \tag{5.49}$$

then from Equation 5.44

$$\Gamma = (xF_y - yF_x)\mathbf{a}_z \tag{5.50}$$

and from Equation 5.45 we obtain

$$\mathbf{H} = m(xv_y - yv_x)\mathbf{a}_z \tag{5.51}$$

where $\boldsymbol{a}_x$, $\boldsymbol{a}_y$, and $\boldsymbol{a}_z$ are unit vectors in the respective directions. Now consider the collision between two vehicles as shown in Figure 5.5.

The governing equations for vehicle 1 are

$$\Gamma_1 = \mathbf{r}_1 \times \mathbf{F_2} \tag{5.52}$$

$$\mathbf{H}_1 = r_1 \times m_1\mathbf{v_2} = I_1\omega_1 \tag{5.53}$$

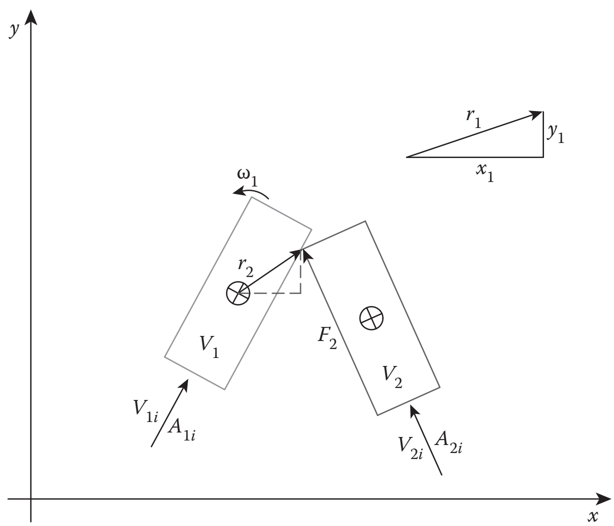

Figure 5.5 Collision between two vehicles.

For vehicle 2

$$\Gamma_2 = \mathbf{r}_2 \times \mathbf{F}_1 \tag{5.54}$$

$$\mathbf{H}_2 = \mathbf{r}_2 \times m_2 \mathbf{v}_1 = I_2 \omega_2 \tag{5.55}$$

The angular velocity of each vehicle's rotation may be determined from

$$\omega = \frac{2v_r}{\text{WB}} \tag{5.56}$$

where WB is the wheelbase of the vehicle and v_r is the velocity of rotation. The velocity of rotation is dependent on the total angle of rotation so that

$$v_r = \sqrt{2g\mu s} = \sqrt{2g\mu\left(\frac{\text{WB}}{2}\right)\theta} = \sqrt{g\mu\text{WB}\theta} \tag{5.57}$$

Thus, the angular velocity of each vehicle becomes

$$\omega_1 = \frac{2v_{r1}}{\text{WB}_1} = \sqrt{\frac{4g\mu\theta_1}{\text{WB}_1}} \tag{5.58}$$

$$\omega_2 = \frac{2v_{r2}}{\text{WB}_2} = \sqrt{\frac{4g\mu\theta_2}{\text{WB}_2}} \tag{5.59}$$

where θ is the angle of rotation of the vehicle. As in the previous sections, we assume that there is negligible preimpact rotation. Applying Equation 5.46 to the conservation of rotational momentum equations developed above, we obtain

$$(|H|)_{\text{initial}} = (I\omega)_{\text{final}} \tag{5.60}$$

or

$$V_{1i} = \frac{2gI_2}{W_2(x_2 \sin A_{1i} - y_2 \cos A_{1i})}\sqrt{\frac{g\mu\theta_2}{\text{WB}_2}} \tag{5.61}$$

and

$$V_{2i} = \frac{2gI_1}{W_1(x_1 \sin A_{2i} - y_1 \cos A_{2i})}\sqrt{\frac{g\mu\theta_1}{\text{WB}_1}} \tag{5.62}$$

On a final note, it is sometimes useful to determine the kinetic energy of rotation which is given by

$$E_{kr} = \frac{1}{2} I\omega^2 \tag{5.63}$$

The power is given by

$$P_r = \Gamma\omega \tag{5.64}$$

The torque vector moment is also related to the vector angular momentum as

$$\mathbf{\Gamma} = \frac{d\mathbf{H}}{dt} \tag{5.65}$$

5.9 Parametric Analysis for Left of Center Collisions

Momentum methods can be used effectively to determine whether a particular vehicle was left of center in a collision where two vehicles approach each other from opposite directions. The following example shows how Equations 5.14 through 5.20 are used by varying certain parameters, in particular, the preimpact angles to determine which vehicle was left of center. Figure 5.6 shows the geometry in a collision involving a dump truck and a Mustang. The Mustang is labeled vehicle 1 and the dump truck is labeled vehicle 2.

In this collision the exact weight of the dump truck was not known. However, it was determined that it weighed between 22,000 and 24,000 lbs.

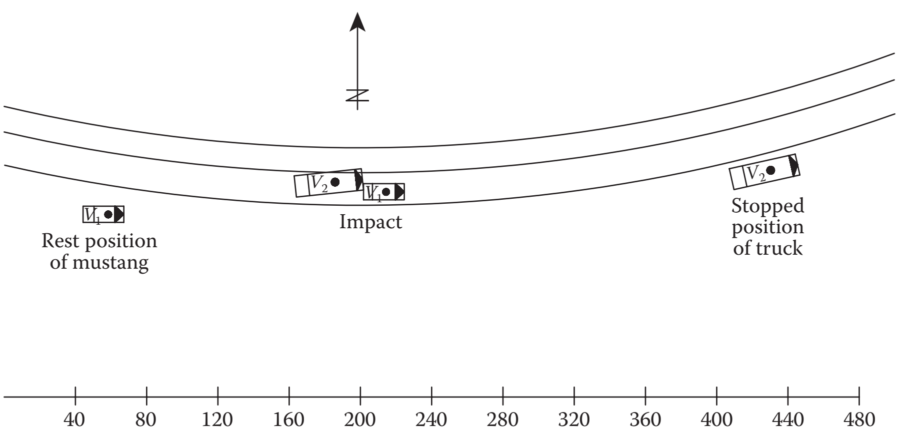

Figure 5.6 Left of center collision.

The dump truck was headed east, and the Mustang was headed west. The driver of the dump truck reported that the driver of the Mustang was passing another vehicle heading west and encroached into the eastbound lane. In order to prove that the Mustang was left of center at the point of impact, a parametric analysis was performed varying the weight of the dump truck and the precollision angle of the Mustang. Based on the variability of these parameters, the speeds of the Mustang and of the dump truck were calculated. Table 5.1 and the accompanying Figure 5.7 show the vehicle speeds as the preimpact angle of the Mustang is varied from 168 to 172 degrees. Note that as the preimpact angle of the Mustang increases toward 180 degrees, the speed of the Mustang becomes unreasonably fast. Since a reasonable speed for the Mustang would be less than approximately 90 mph, the preimpact angle of the Mustang would have to be less than 180 degrees so that the Mustang was, in fact, left of center and attempting to reenter its lane of travel. As the driver of the Mustang attempted to re-enter the west bound lane, the Mustang spun clockwise so that the near of the Mustang collided with the part of the dump truck. This example, from an actual case, shows the power of the conservation of momentum

Table 5.1 Vehicle Speeds Dependence on Weight of Dump Truck (W_2) and Preimpact Angle of Mustang (A_{1i})

W_2	22,000		23,000		24,000	
A_{1i}	V_{1o}	V_{2o}	V_{1o}	V_{2o}	V_o	V_{2o}
168	59.4	55.8	63.1	56.3	66.8	56.8
169	64.3	56.6	68.2	57.1	72.2	57.6
170	70.0	57.5	74.3	58.0	78.6	58.6
171	76.8	58.6	81.6	59.2	86.3	59.7
172	85.2	60.0	90.5	60.6	95.7	61.1

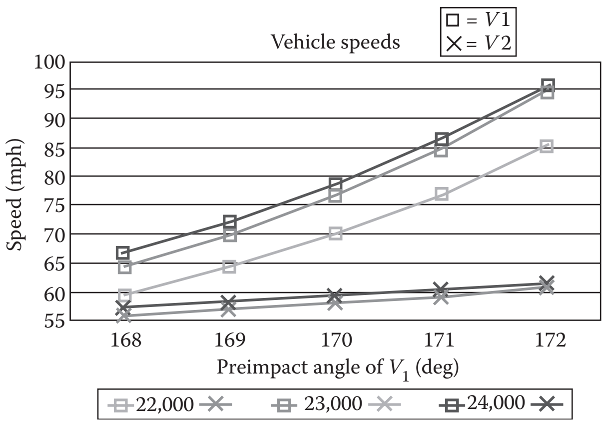

Figure 5.7 Vehicle speeds.

techniques. These solutions lend themselves to programming in spread sheets where the parameters can be varied. By varying the parameters, unknowns can be ascertained through trial and error until a reasonable solution is obtained.

5.10 Plastic—Elastic Analysis

This example shows how a reconstruction can take place when the amount of vehicle coupling after the collision is not known. The development is in general terms with no actual values given. Two vehicles collided nearly head on. A car (V_1) was traveling east and a pickup (V_2) was traveling west when they collided as shown in Figure 5.8. At the accident location the road is slightly uphill going east at an angle θ.

The force of kinetic friction is given by

$$f = \mu N \tag{5.66}$$

Newton's second law perpendicular and parallel to the incline gives

$$N - Mg\cos\theta = 0 \tag{5.67}$$

$$Mg\sin\theta - f = Ma \tag{5.68}$$

Solving Equations 5.66 through 5.68 yields

$$a = -(\mu\cos\theta - \sin\theta)g \tag{5.69}$$

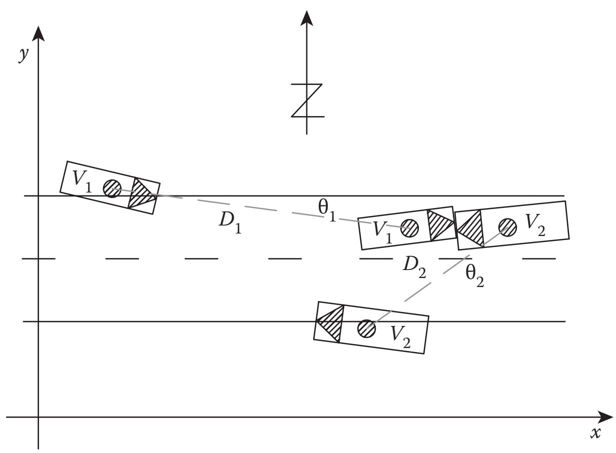

Figure 5.8 Plastic—elastic analysis.

This shows that the effective coefficient of static friction is

$$\mu_e = \mu\cos\theta - \sin\theta \tag{5.70}$$

The velocities of the vehicles immediately after the collision can be obtained from the stopping distance and the effective coefficient of friction. From basic kinematics, one obtains

$$V_{1f} = \sqrt{2g\mu_{e1} D_1} \tag{5.71}$$

$$V_{2f} = \sqrt{2g\mu_{e2} D_2} \tag{5.72}$$

The inspection of the accident site revealed that the vehicles did not separate immediately. Upon impact the front wheels of the car were locked as a result of frame intrusion into the tires. Thus, the car slid to a stop under the full effect of kinetic friction. On, the other hand, the site inspection indicated that the truck was partially under control of the driver after the collision. Effectively, the full effect of kinetic friction was negated for the truck. Thus, it was considered that the effective coefficient of friction for V_2 was unknown. However, conservation of momentum perpendicular to the road allows us to express the velocity of the truck immediately after the collision in terms of the velocity of the car immediately after the collision. The component of momentum was zero before the collision, hence it must have been zero after the collision. Thus,

$$M_2 V_{2f} \sin\theta_2 = M_1 V_{1f} \sin\theta_1 \tag{5.73}$$

Defining the mass ratio

$$R = M_1 / M_2 \tag{5.74}$$

we get

$$V_{2f} = R\left(\frac{\sin\theta_1}{\sin\theta_2}\right) V_{1f} \tag{5.75}$$

Now

$$U_1 = V_{2f}\cos\theta_2 + RV_{1f}\cos\theta_1 \tag{5.76}$$

$$U_2 = \sqrt{V_{2f}^2 + RV_{if}^2} \tag{5.77}$$

Conservation of momentum parallel to the road gives

$$V_{2i} = RV_{1i} + U_1 \tag{5.78}$$

while conservation of energy gives

$$V_{2i}^2 + RV_{1i}^2 = U_2^2 + 2Q/M_2 \tag{5.79}$$

where Q is the energy absorbed by the collision.

In order to obtain an expression for Q, consider the idealized case of a totally inelastic collision. In such a collision the vehicles move together as a single unit of mass $M_1 + M_2$ with velocity V after the collision. Then,

$$V_{2i} - RV_{1i} = (1+R)V \tag{5.80}$$

$$V_{2i}^2 + RV_{1i}^2 = (1+R)V^2 + 2Q_0/M_2 \tag{5.81}$$

Solving these equations for Q_0 gives

$$Q_0 = \frac{M_2}{2}\frac{R}{1+R}(V_{2i} + V_{1i})^2 \tag{5.82}$$

The amount of energy absorbed in a particular inelastic collision cannot exceed Q_0, thus

$$Q = \frac{M_2}{2}\frac{RF}{1+R}(V_{2i} + V_{1i})^2 \tag{5.83}$$

where F is a number between 0 and 1. F represents the coefficient of inelasticity. For a perfectly elastic collision $F = 0$. For a perfectly inelastic collision $F = 1$. Using Equations 5.78 and 5.83 in Equation 5.79 gives

$$V_{1i}^2 + 2\frac{U_1}{1+R}V_{1i} - \frac{U_2^2 - \left(1 - \frac{RF}{1+R}\right)U_1^2}{R(1+R)(1-F)} = 0 \tag{5.84}$$

Solving Equation 5.84 for V_{1i} gives

$$V_{1i} = \frac{U_1}{1+R}\left[\sqrt{1+\frac{(1+R)U_2^2-(1+R-RF)U_1^2}{R(1-F)U_1^2}}-1\right] \tag{5.85}$$

In Equation 5.85 the accident site determines the values of U_1 and U_2, so that a solution may be obtained by varying F.

Vehicle Specifications 6

6.1 Introduction

Vehicle specifications are an integral part of reconstructions of vehicular crashes. The vehicle specifications that may be of interest include basic dimensions such as length, width, height, wheelbase, front and rear overhangs, and track width. Most commercial programs for reconstructions require at least these minimum dimensional specifications. When performing low speed impacts and impacts with pedestrians, it is useful to know bumper, hood, and trunk heights. For biomechanical calculations interior dimensions may need to be taken of the vehicle or of an exemplar vehicle. When rotation of the vehicles is considered, the yaw moment of inertia is required. For rollover cases, the roll moment of inertia and the tip-over stability ratio of the vehicle are often required. The weight of the vehicle is almost always required in order to perform basic momentum calculations. For common passenger vehicles, the parameters listed above are readily available through a variety of commercial sources. For tractor-trailers, construction vehicles, off-road vehicles, motorcycles, and four wheelers, these parameters are not available and must be measured or calculated. This chapter deals with the techniques that are available to perform such calculations.

6.2 Calculation of Center of Mass Techniques

The forces acting on a vehicle do not all pass through one point. For example, each of the tires has a gravitational component. Those tire forces are distributed throughout the vehicle depending on factors such as the vehicle design and the velocity of the vehicle. These forces are said to be noncurrent so that the vehicle is generally subject to rotation and translation. In many reconstructions, the rotation of the vehicle is not necessarily pertinent to the solution of the velocities and the translations that occur from the collision. In engineering reconstructions of vehicular events it is important to calculate the forces acting on the vehicles. This process is established by determining the free body diagram for all the vehicles.

A critical force that acts on a vehicle is the weight of the vehicle that is produced by the acceleration due to gravity. As will be shown, the force of gravitational attraction exerted on the vehicle passes through the center of gravity or mass of the vehicle. Every portion of a vehicle is attracted to the center of the earth as a result of the gravitational force. Since every portion of the vehicle is made up of individual particles, each particle has a force directed to the center of the earth. However, since the distance to the center of the earth is much greater than the distance between the individual particles, the forces exerted on each of the particles are essentially parallel to each other. Thus, the resultant of all the forces on the particles is the weight of the vehicle and that force passes through the center of gravity or mass of the vehicle.

The center of mass of a vehicle can be determined from the area moment of inertia. The area moment of inertia is defined as the second moment of an area around a given axis. Figure 6.1 shows an area A on the x-y plane. The center of mass of the area is denoted as C and there is a translation of the axes corresponding to the center of mass.

In general the area moment of inertia is given by,

$$I_{Aa} = \int_A r_a^2 dA \tag{6.1}$$

where,

I_{Aa} = second moment of area around axis a

A = total area

r_a = distance from the differential element of area dA to the axis of rotation a

The mass moment of inertia is defined as,

$$I_{Va} = \rho \int_V r_a^2 dV \tag{6.2}$$

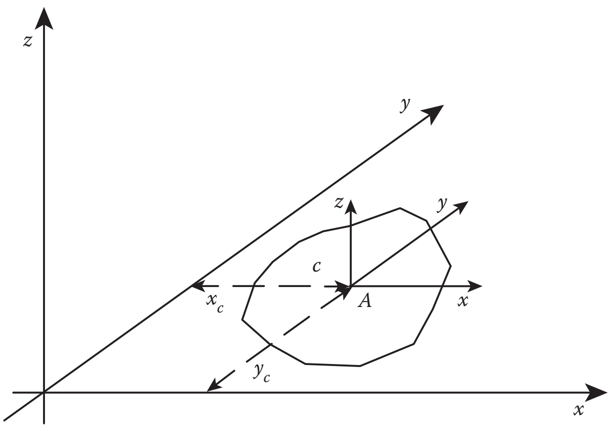

Figure 6.1 Area moments.

where,

I_{Va} = mass moment of inertia around axis a

r_a = distance from the differential element of volume dV to the axis of rotation a

ρ = density of the solid

In a planar mass distribution with mass m that is uniformly distributed over the area A so that the mass density is constant, we define the area and volume densities as,

$$\rho_A = \frac{m}{A}; \qquad \rho_V = \frac{m}{V} \tag{6.3}$$

The mass moment of inertia is related to the area moment of inertia as follows:

$$I_{Va} = \rho_V \int_V r_a^2 dV = \rho_V \int_V r_a^2 dA dh = \rho_V h \int_A r_a^2 dA = \rho_A \int_A r_a^2 dA = \rho_A I_{Aa} \tag{6.4}$$

Again, for a planar distribution of mass that is rotating about an axis in the plane of the mass, we can define the radius of gyration as the distance from the axis where the mass is concentrated and produces the mass moment of inertia. In this context, the radius of gyration becomes the rotation of the planar region and may be determined by a manipulation of Equation 6.1 as,

$$r_a = \sqrt{\frac{I_{Aa}}{A}} \tag{6.5}$$

As an example, let us determine some parameters for a van that can be approximated as a rectangular solid as shown in Figure 6.2. For ease of computation we will assume that the center of mass of the vehicle is at the geometrical center and we will neglect the effect of the tires.

At first glance it might seem that the rectangular solid we have chosen as a model for our cargo van could not possibly represent the vehicle with sufficient accuracy. We will show with this example that this model is sufficiently accurate and that some basic revisions allow us to calculate the yaw moment of inertia quite accurately. We have chosen the vehicle specifications for a 1990 Dodge B150 SWB, three door cargo van. The length is 178 inches, the width is 79 inches, and the height is 80 inches. The hood measures 40 inches from the ground and the base of the windshield is 15 inches from the front bumper. The curb weight is 3600 lbs, the yaw moment of inertia is 2365 lb-ft-sec^2. The roll moment of inertia is 557 lb-ft-sec^2. Let us

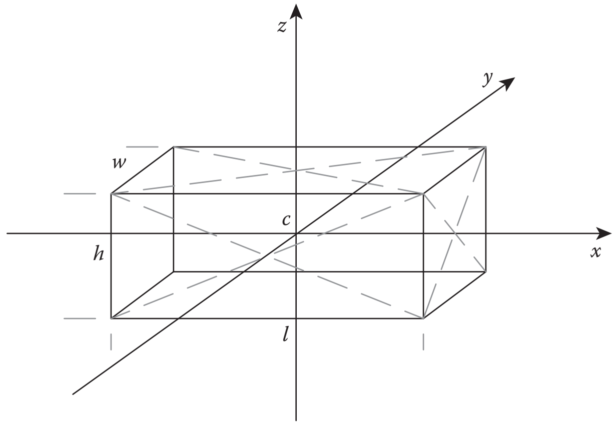

Figure 6.2 Cargo van.

now calculate the moment of inertia from the equations developed above. The area and the volume are given by,

$$A = wl; \qquad V = wlh \tag{6.6}$$

The area and mass densities are,

$$\rho_A = h\rho_V; \qquad \rho_V V = \rho_V wlh = \frac{W}{g} = m \tag{6.7}$$

where

W = weight of the vehicle
g = acceleration due to gravity
m = mass

The area and mass moments are

$$I_{Az} = \int_A (x^2 + y^2)\,dx\,dy = \frac{wl}{12}(w^2 + l^2) \tag{6.8}$$

$$I_{Vz} = \rho_V \int_V (x^2 + y^2)\,dx\,dy\,dz = \rho_v h \frac{wl}{12}(w^2 + l^2) = \rho_A I_{Az} \tag{6.9}$$

The radius of gyration is

$$r_z = \frac{1}{2}\sqrt{\frac{(w^2 + l^2)}{3}} \tag{6.10}$$

If we substitute the dimensions of the vehicle we compute the yaw moment of inertia to be 2454 as compared to a value of 2365. The percent error is 3.75% which is within engineering accuracy. We can make a simple modification because the vehicle is not quite as boxy in the front. Note that the hood is 40 inches above the ground and the windshield is 15 inches from the front bumper. We can now recompute assuming a length of 170 inches and obtain a value of 2275, and if we average this value with the previous value, we obtain a value of 2364.5 for the yaw moment of inertia. This simple example shows how powerful and accurate the technique can be when applied properly. Most vehicles can be approximated as a conglomeration of box elements for the computation of moments of inertia. It is apparent that tractor trailers are especially suited for this type of analysis because of their boxy shapes. The astute reader will realize that the assumption of the location of the center of mass is irrelevant for the analysis above.

6.3 Rollover/Tipover

Most often, the dynamic factors that determine the rollover of a vehicle are extremely difficult to determine in a reconstruction. There are several reasons for this statement. The exact steering and braking inputs of the driver are usually unknown. The amount of brake pedal force exerted by the driver is difficult to assess. Correspondingly, the amount of suspension depression or sway cannot be determined. The air pressure in the tires may not be known because some of the tires were deflated as a result of the rollover. The condition of the springs and shocks may not be known because the vehicle is no longer available. For these reasons and because the accident scene may not have been properly documented, the dynamics of the rollover may not be obtainable. However, some basic computations are possible from a static point of view. Generally, the static conditions for rollover are more restrictive. To analyze the static conditions for rollover we refer to Figure 6.3 where the analysis is carried out in cylindrical coordinates.

The distance from the center of mass of the vehicle to the edge of the tire is represented by the vector $\boldsymbol{r}$. The force that is creating the rollover is $\boldsymbol{F}_1$ and the force that is retarding the rollover is $\boldsymbol{F}_2$. These vectors are given by,

$$\mathbf{r} = \rho \mathbf{a}_\rho - z \mathbf{a}_z \tag{6.11}$$

$$\mathbf{F}_1 = F_{1\rho} \mathbf{a}_\rho + F_{1z} \mathbf{a}_z \tag{6.12}$$

$$\mathbf{F}_2 = F_{2\rho} \mathbf{a}_\rho + F_{2z} \mathbf{a}_z \tag{6.13}$$

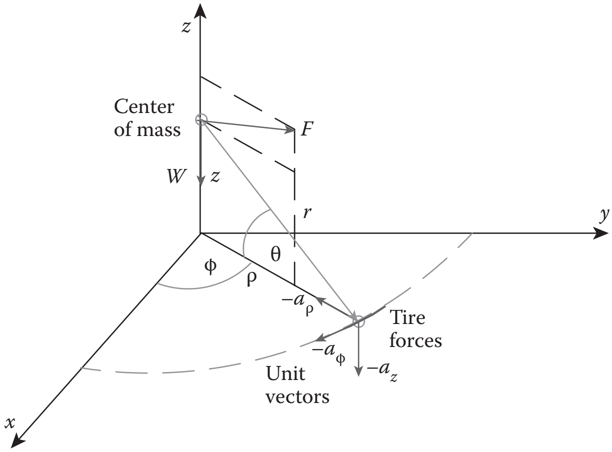

Figure 6.3 Rollover analysis.

The corresponding moments are $\mathbf{M}_1$ in the direction of travel of the vehicle and $\mathbf{M}_2$ attempting to resist the rollover motion of the vehicle. These are given by,

$$\mathbf{M}_1 = \mathbf{F}_1 \times \mathbf{r} \tag{6.14}$$

$$\mathbf{M}_2 = \mathbf{F}_2 \times \mathbf{r} \tag{6.15}$$

Summing moments and forces we obtain,

$$z\frac{w}{g}\left(\frac{v^2}{R}\right) = zW\cos\theta \sin\theta \tag{6.16}$$

or

$$v = \sqrt{\frac{g\rho zR}{\rho^2 + z^2}} \tag{6.17}$$

where

v = lateral velocity that causes the rollover
g = acceleration due to gravity
ρ = distance from the projection of the center of mass to the ground and the tire about which the rollover is occurring
z = vertical distance to the center of mass
R = radius of the yaw that produces the rollover.

For example a 2005 Chevrolet Impala has a width of 73 inches, a front track of 62 inches, and the center of mass is 42.18 inches behind the front axle and 22.77 inches above the ground. If the rollover occurs at a radius of 100 ft, the lateral speed that causes rollover is 24.7 mph neglecting loading and suspension effects. Loading, weight shift, under inflated tires, and soft suspensions tend to decrease this speed.

6.4 Gouge Spacing

Large trucks have significant front wheel lugs that attach the front wheels to the axle assemblies. If those attachments protrude beyond the outer surface of the tire while the vehicle is rolling over, then gouges are produced on the road surface. The spacing of the gouges that are produced can be analyzed according to the lug distribution and the velocity of the vehicle. Vehicle specifications can be used to determine whether a particular vehicle produced a set of gouges on the pavement. This analysis is based on an actual case where there was a difference of opinion concerning which vehicle produced the gouges. One vehicle had five lugs while the other had ten lugs. Consider the wheel shown in Figure 6.4 with an impending lug moving toward the creation of a gouge.

The angular velocity of the wheel is given by

$$\frac{S_A}{2\pi R_2} = \frac{\theta_A}{2\pi} \Rightarrow S_A = R_2\theta_A \tag{6.18}$$

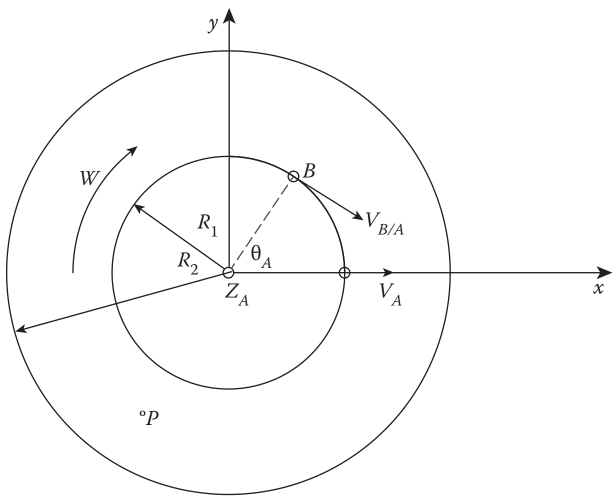

Figure 6.4 Wheel lugs.

Differentiating with respect to time yields

$$\mathbf{v}_A = R_2 \frac{d\theta}{dt} = R_2 \mathbf{w} \tag{6.19}$$

where

$$\mathbf{w} = \frac{\mathbf{v}_A}{R_2} \frac{(\text{inches/sec})}{\text{inches}} = \frac{\mathbf{v}_A}{R_2} \mathbf{a}_z (\text{rad/sec}) \tag{6.20}$$

where $\boldsymbol{w}$ = angular velocity
R_2 = tire radius
R_1 = lug radius
$\mathbf{a}_x \; \mathbf{a}_y \; \mathbf{a}_z$ = Cartesian unit vectors

$$\mathbf{v}_{P/A} = \mathbf{w} \times \mathbf{R}_{P/A} \tag{6.21}$$

Velocities of rolling motion must be resolved into two components, translation with the center at "*A*" and rotation about the center at "*A*." In translation, all points of the wheel move with the same velocity $\boldsymbol{v}_A$. In rotation, each point of the wheel moves about "*A*" with a relative velocity where

$\boldsymbol{R}_{P/A}$ = position vector of "*P*" relative to "*A*"

Accordingly, the velocity at a point "*P*" can be determined from the vector sum

$$\mathbf{v}_P = \mathbf{v}_A + \mathbf{v}_{P/A} = \mathbf{v}_A + \mathbf{w} \times \mathbf{R}_{P/A} \tag{6.22}$$

The velocity $\boldsymbol{v}_A$ of a moving vehicle whose wheel lugs create gouges on the pavement surface can therefore be analyzed in the following manner according to Figure 6.5.

$$\mathbf{v}_B = \mathbf{v}_A + \mathbf{v}_{B/A} = \mathbf{v}_A + \mathbf{w} \times \mathbf{R}_{B/A} \tag{6.23}$$

where

$$\mathbf{v}_{B/A} = R_1 (\cos\theta \boldsymbol{a}_x + \sin\theta \mathbf{a}_y) \tag{6.24}$$

or

$$\mathbf{v}_B = \mathbf{v}_A + \left(\frac{v_A}{R_2} \mathbf{a}_z \right) \times \left[R_1 (\cos\theta \mathbf{a}_x + \sin\theta \mathbf{a}_y) \right] \tag{6.25}$$

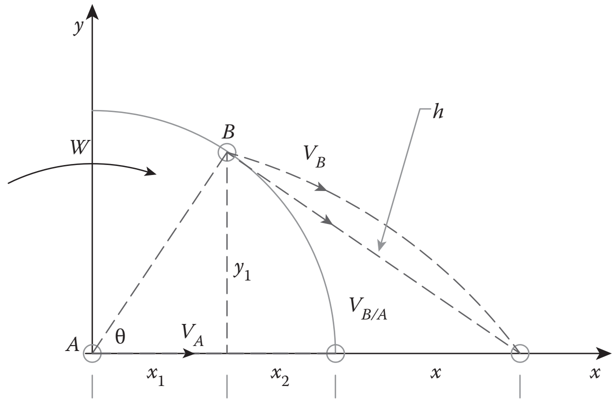

Figure 6.5 Wheel lug analysis.

where

$x_1 = R_1 \cos\theta$

x = gouge spacing

$\theta = 2\pi/5$ for five lugs

$\theta = 2\pi/10$ for ten lugs

For a wheel consisting of five lugs

$$\mathbf{v}_B = \mathbf{v}_A(1.38\mathbf{a}_x - 0.124\mathbf{a}_y) \tag{6.26}$$

or

$$|\boldsymbol{v}_B| = 1.385|\boldsymbol{v}_A| \tag{6.27}$$

for a wheel consisting of 10 lugs

$$\boldsymbol{v}_B = \boldsymbol{v}_A(1.324\mathbf{a}_x - 0.245\mathbf{a}_y) \tag{6.28}$$

$$|\boldsymbol{v}_B| = 1.35|\boldsymbol{v}_A| \tag{6.29}$$

From Figure 6.5, the hypotenuse can be determined as follows

$$y_1 = R_1 \sin\theta \tag{6.30}$$

$$h = \sqrt{y_1^2 + (x + x_2)^2} \tag{6.31}$$

$$h = \sqrt{R_1^2 \sin^2 \theta + \left(x + R_1 \left(1 - \cos\theta\right)\right)^2} \tag{6.32}$$

In Equation 6.32 we can approximate the hypotenuse as $h \approx v_B\theta/w$, so

$$x \approx -R_1 \left(1 - \cos\theta\right) \pm \sqrt{(v_B\theta/w)^2 + R_1^2 \sin^2 \theta} \tag{6.33}$$

The lug spacing then becomes

$$\left(v_B\theta/w\right)^2 = R_1^2 \sin^2 \theta + \left(x \ + R_1 \left(1 - \cos\theta\right)\right)^2 \tag{6.34}$$

Calculations for five lug and ten lug wheels at velocities ranging from 20 mph to 70 mph can then be carried out. Additionally, if the wheel rotation slips by 10% from its nominal value, i.e.,

$$\mathbf{w}_s = 1.1\mathbf{w}$$

The wheel spacing calculations can also be carried out. This analysis reveals that five lug wheels produce gouges 32 inches apart with no slip and 28.3 inches apart with 10% wheel slip. Similarly, ten lug wheels produce gouges varying between 16.6 and 14.8 inches apart. Note that the gouges are irrespective of vehicle's speed. The analysis can prove conclusively whether five lug or ten lug wheels created the gouges.

Vehicle Performance Characteristics

7

7.1 Introduction

In many reconstructions, the performance characteristics of the vehicles come into question. When failure analysis is considered as the cause of the collision or contributory to the collision, or affecting the occupants, the systems that may be responsible are braking, steering, acceleration, seatbelts, air bags, crash worthiness issues, tires, maintenance, recent repairs, or integrity of structural elements. Thus, in order to assess the potential for the involvement of these systems in a crash, a brief explanation of some of these systems follows. The most common systems that are involved or blamed for causing a crash are discussed. These generally are brake failure, steering failure, air bag deployment, seat failure, tire failure, electrical failure, or engine failure. Electrical failures are generally attributed to the computer control of the various vehicle systems.

7.2 Systems and Performance Characteristics

The performances of braking systems are covered under the appropriate sections of the Code of Federal Regulations (CFR). Please refer to Chapter 15 for the applicable sections pertaining for the performance regulations of various vehicles.

7.2.1 Braking

The basic functions of a brake system are to slow a vehicle's speed, to maintain its speed during downhill operations, and to hold a vehicle stationary after it has come to a complete stop. These basic functions must be performed during normal operation of the brakes. Additionally, a certain amount of braking effectiveness, during a brake system failure is needed for vehicle control. A typical automotive, small truck hydraulic brake system is illustrated in Figure 7.1.

All brake systems can be divided into four basic subsystems as follows. These four basic subsystems apply to all the braking systems in passenger, commercial, or specialty vehicles. The difference between brakes for tractor

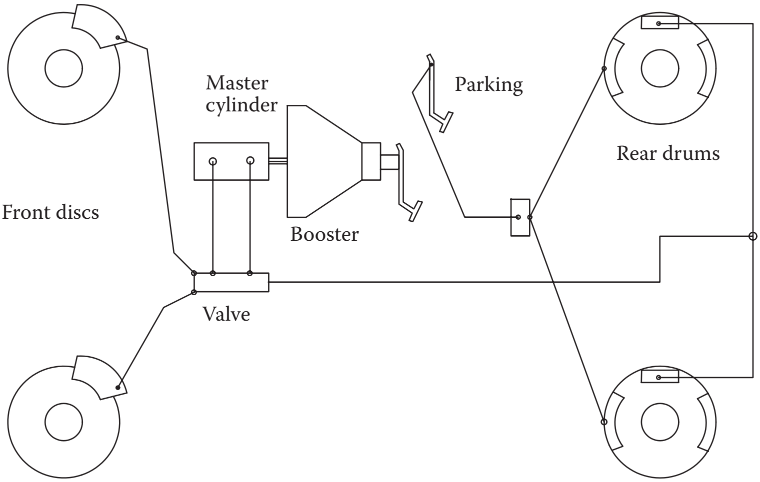

Figure 7.1 Typical automotive brakes.

trailers and passenger vehicles, for example, is in the design and execution of the various systems but not in the classification of the subsystems. The systems identified in this section relate to the common passenger vehicle and are not typical of braking systems for large commercial vehicles such as tractor trailers, or industrial vehicles. Braking systems for specialty vehicles vary greatly in design and complete coverage of these systems is beyond the scope of this book. According to Limpert, these systems are

1. Energy source system—includes the components that produce, store, and make available the energy required for braking.
2. Activation system—the components that are used to modulate or regulate the level or intensity of braking.
3. Transmission system—the components through which the braking energy travels from the activation system to the wheel brake systems.
4. Wheel brake system—the components that apply the forces to the wheels that retard the vehicle through the force of friction.

7.2.1.1 Vacuum Assisted Brake Booster

Vacuum assisted hydraulic brakes, also called power brakes, use a vacuum booster as illustrated in Figure 7.2 to assist the driver's effort in pressing the shoes against the drum.

The common car or small pickup system, sometimes called the mastervac system, is mounted directly against the fire wall opposite the driver's foot. It is mounted between the foot pedal and the master cylinder. The assist force, acting on the push rod which activates the master cylinder piston, is

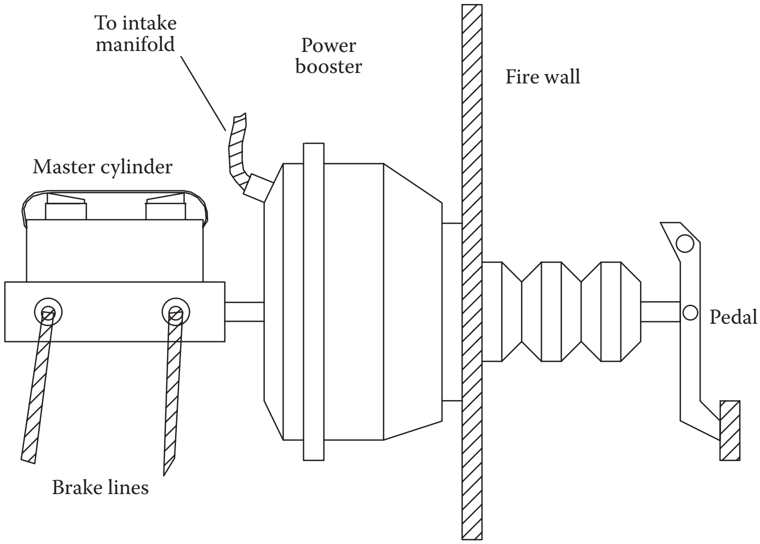

Figure 7.2 Power brakes.

produced by the difference in pressure across the booster piston or diaphragm with the vacuum or low pressure on the master cylinder side, and the atmospheric or high pressure on the input side. The low pressure is caused by the engine operation via a connection to the intake manifold of the engine. The intake manifold's low pressure is created as the engine draws air for the detonation of the fuel in the cylinders.

7.2.1.2 Brake Line Pressure Control Devices

There are two basic types of brake line pressure valves, the brake pressure limiter and the brake pressure reducer. Each of these devices can be activated either by brake line pressure or by vehicle deceleration. In many cases, two or three different functions are combined into one valve, commonly called a combination valve as shown in Figure 7.3.

The valve to the left is the metering valve, and the valve to the right is the reducer or proportioning valve discussed earlier. The switch in the center is the differential pressure switch, which is activated in the event of a hydraulic leak in one of the dual brake circuits. Metering valves are used primarily for rear wheel driven vehicles, using the front disc/rear drum system.

7.2.1.3 Step Bore Master Cylinder

The brake line pressure valves discussed earlier are typically installed between the master cylinder outlet and the rear brake wheel cylinders. With the standard dual or tandem master cylinder design shown in Figure 7.4, both pistons have the same diameter.

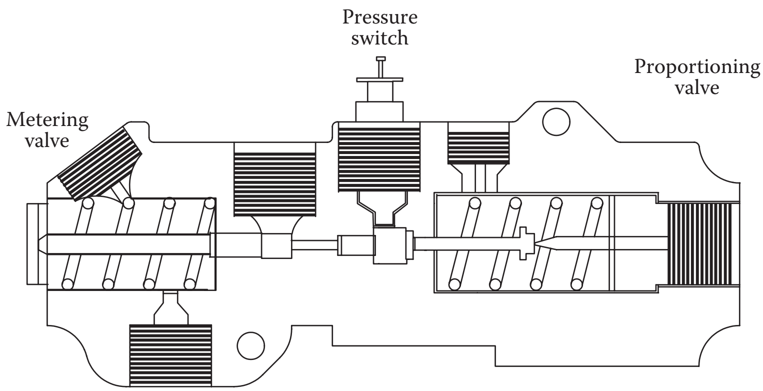

Figure 7.3 Combination valve.

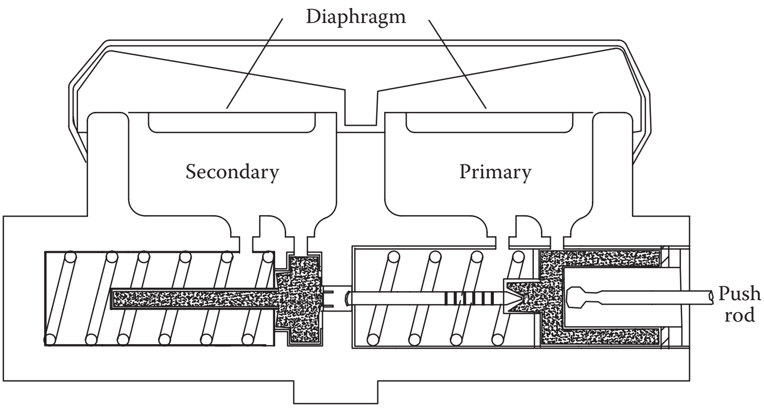

Figure 7.4 Master cylinder.

In a step or adjustable step bore master cylinder, the pistons are of different diameters and therefore produce varying pressure.

7.2.1.4 Brake Designs

Friction brakes used in automotive applications can be divided into radial or drum and axial or disc brakes. Drum brakes subdivide into external haul and internal shoe brakes. Typical shoe brakes subdivide further according to the shoe arrangement into leading/trailing, two leading or duo-servo brakes. Drum brakes may be further divided according to the shoe abutment or anchorage into shoes supported by parallel or inclined sliding abutment, or pivoted shoes. The brake shoe activation may be grouped into hydraulic wheel cylinder, wedge, cam, screw, and mechanical linkage activation. Disc brakes may be either a fixed or floating caliper design. Fixed caliper disc brakes have either two or four pistons that push the pads out on either side of the disc. In contrast, floating caliper disc brakes have one or two pistons on the inboard side only. The actual brake designs vary greatly in design and construction depending on the manufacturer or the application. However, in all the systems the braking action is produced by creating friction between the brake shoes or pads and the wheel attachment whether disc or drum.

7.2.1.5 Large Vehicles

The predominant large vehicle in the United States is the tractor/trailer combination. Vehicles with hydraulic brake systems, as with passenger motor vehicles, employ the components listed in the previous sections to control the braking performance. Those vehicles are subject to Federal Motor Vehicle Safety Standard (FMVSS) 105. Large vehicles are generally equipped with pneumatic (air brake) systems and are subject to FMVSS 121. Since March 1, 1997 all new tractor/trailers have been required to have antilock brake systems. Buses and other large vehicles were subject to this requirement effective March 1, 1998. The antilock brake systems on large vehicles behave just as they do for smaller vehicles. That is, they do not necessarily stop the vehicle any faster, but they allow for control of the vehicle as the brakes are applied because they do not lock the brakes.

The basic components of air brake systems include an air compressor that behaves as the energy source. The compressor is governed by controls that maintain a pressure between 100 and 125 pounds per square inch (psi). The air is stored in tanks that vary in number and size according to the design. However, the reserve capacity of these tanks is sufficient to allow the brakes to be used over several cycles even if a compressor failure occurs. A safety valve set at 150 psi is generally installed on the tanks, and the tanks have drains to rid them of water. Some systems have an alcohol evaporator that reduces the risk of ice forming in the brake valves during cold weather.

The brake pedal, which is often referred to as the foot valve or more accurately known as a treadle valve, activates the brakes and controls the air pressure in the system. Applying the brake pedal activates the foundation brakes which may be of three basic designs—the S-cam, wedge, or disc brake designs. The most common is the S-cam design. The front brakes of tractor/trailers generally have a brake chamber with a single air chamber with no spring. The rear brakes of the tractor and the trailer have a brake chamber with two air chambers. Associated with these basic components are various valves, fittings and lines. A typical single circuit air brake system is shown in Figure 7.5.

7.2.2 Steering

All of us have driven a variety of vehicles and noted that the steering systems of those vehicles vary widely. The actual steer angles are a function of the type of steering mechanism employed, the suspension system, the linkages,

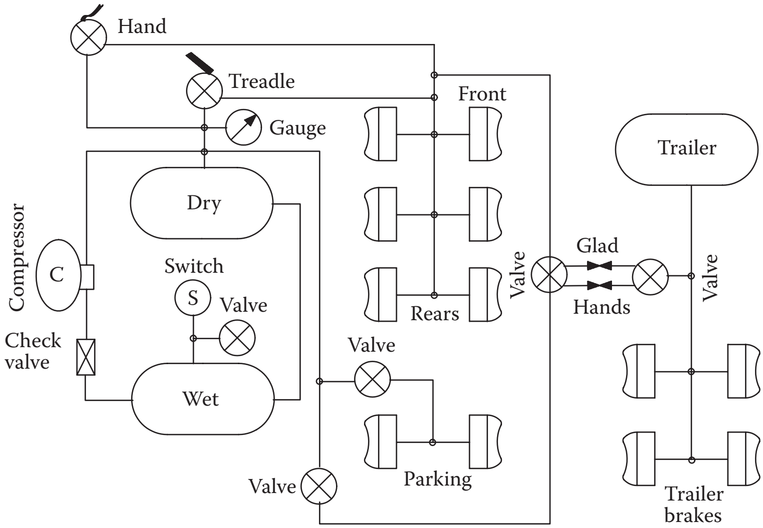

Figure 7.5 Air brake system.

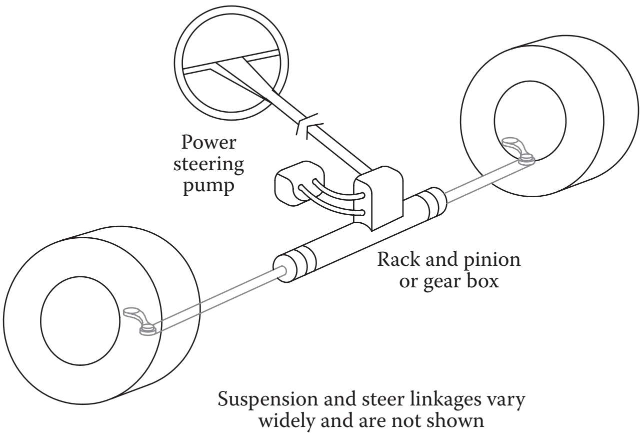

Figure 7.6 Steering system.

and whether the vehicle is front wheel drive. The actual conversion of the steering wheel input to the steer angles imposed on the wheels is achieved by two basic mechanisms, the steering box or the rack and pinion steering system. Figure 7.6 shows a generalized diagram of the steering system employed in most passenger vehicles.

The steering wheel is connected to the steering box or the rack and pinion gears through the shaft, universal joints, and vibration dampers. The rack or steering box transfers the rotational motion of the steering wheel to lateral translational motion that affects the steer angles of the wheels. From the rack or the gear box, there are a variety of linkages and joints that tie the system together. According to Gillespie, if the steer linkages connect to the rear of the wheel centers, the configuration is called rear-steer and if connected to the front, it is forward-steer. For heavy trucks the steering arrangement is similar utilizing a gear box and a connection to the left wheel. The left wheel is then connected to the right wheel through appropriate linkages. The output shaft of the gear box, whether for a truck or a passenger vehicle, is connected to a pitman arm that activates the linkages. The geometrical configuration of the linkages produces unequal steer angles between the inner and the outer turn wheels. This "Ackerman" geometry is shown in Figure 7.7.

Note from Figure 7.7 that the front track radiuses are greater than the rear track radiuses. The front outer and the front inner radiuses are also slightly greater than the rear outer and rear inner radiuses. Thus, the rear wheels of all vehicles off-track the front wheels to the inside of the turn. This effect is more pronounced the larger the vehicle. Tractor-trailers off-track to a much greater degree than solid frame uncoupled vehicles. The outer and inner steer angles are given by

$$\theta_o \cong \tan^{1} \frac{\mathrm{WB}}{R + \mathrm{TW}/2} \tag{7.1}$$

$$\theta_i \cong \tan^{1} \frac{\mathrm{WB}}{R - \mathrm{TW}/2} \tag{7.2}$$

In the equations above, R is the mean radius passing through the center of mass of the vehicle with respect to the center of the turn.

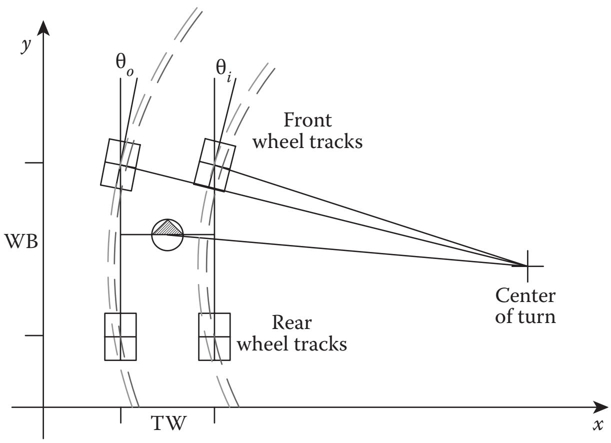

Figure 7.7 Ackerman geometry.

Coupled vehicles behave somewhat differently from what is presented above. Coupled vehicles must be analyzed by the method above for the tractor and by tractrix equations as described below for the trailer. Thus, the off-tracking is the summation of that produced by the Ackerman geometry and the tractrix displacement. The Ackerman offset relates to the front wheel of the tractor with respect to the tractor axle or tandem axles. The tractrix equations relate to the relative displacement between the king pin on the tractor and the axle or tandems on the trailer. Consider Figure 7.8 which represents the path followed by the trailer as it follows the tractor around a curve.

The paths of the front wheels of the tractor, the rear wheels of the tractor, and the wheels of the trailer will all follow different paths. As previously mentioned, the difference in the paths of the tractor can be analyzed by the Ackerman formula. The path difference between the rear wheels of the tractor and the wheels of the trailer follow a curve known as a catenary involute. The catenary is the tractrix evolute so that the tangent of the curve is described by the differential equation,

$$\frac{dy}{dx} = -\frac{\sqrt{L^2 - x^2}}{x} \tag{7.3}$$

The solution to the equation is

$$y = -L\log\left(\frac{L + \sqrt{L^2 - x^2}}{x}\right) + \sqrt{L^2 - x^2} \tag{7.4}$$

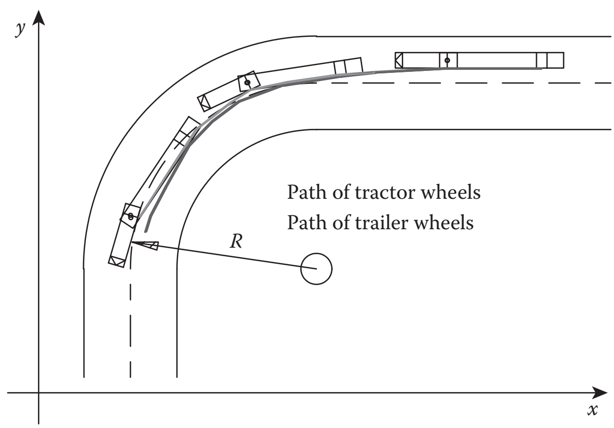

Figure 7.8 Trailer off-tracking.

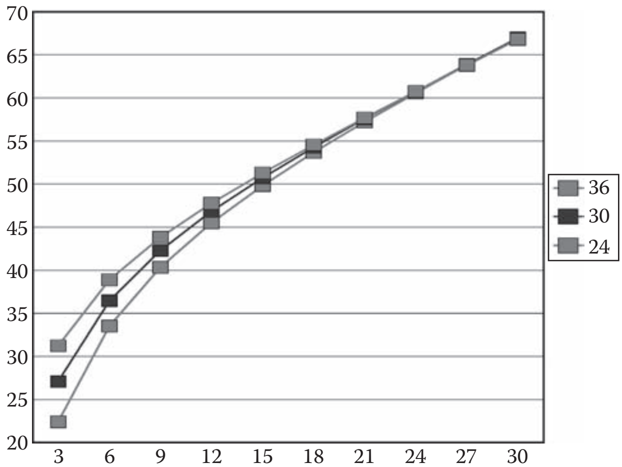

Figure 7.9 Relative off-tracking displacement.

L represents the distance from the kingpin to the rear wheels of the trailer. Figure 7.9 shows the relative displacement of the rear wheels for distances of 24, 30, and 36 ft at a given radius produced by the tractrix equation. These relative curves reveal, as would be expected, that the longer the trailer, the more severe the off-tracking that occurs as an articulated vehicle rounds a curve.

Road designers have recognized the effect of off-tracking and have developed standards for the widening of the curves. Off-tracking may be produced inside the turn radius or outside the radius at higher speeds. In both cases, the amount of off-tracking and the necessary widening depends on the characteristics of the vehicle and the radius of the curve. According to American Association of State Highway Officials (ASSHTO) the track width or sweep path width is given by,

$$\mathrm{SP} = \mathrm{tw} + R - \sqrt{R^2 - \Sigma L_i} \tag{7.5}$$

where

SP = sweep path width on curve in feet
tw = track width of vehicle, either 8.0 or 8.5 ft
R = radius of curve or turn in feet
L_i = wheelbase of vehicle between axles or articulation points in feet

Equation 7.5 can be used for any combination of radius, number, and length of wheelbases. For most designs, the radius is taken at the centerline of the highway.

In some reconstructions where the road is narrow, is traversed by an articulated vehicle, and was never corrected for the off-tracking effect, the articulated tractor trailer traversing this road may be forced to intrude into the opposing lane. In such an event, an opposing vehicle may have been struck by the tractor-trailer combination. Detailed measurements of the highway and the vehicle would then reveal the amount of off-tracking that took place. Such analysis in combination with standard reconstruction techniques will reveal if the off-tracking effect was instrumental in the collision.

7.2.3 Acceleration

One of the most fundamental movements of a vehicle includes the effect produced by acceleration. Acceleration affects braking, turning, ride, and forces imparted on the vehicle or its occupants during a crash. In this section we will only consider the acceleration as it applies to the performance of the vehicle resulting from the application of the accelerator pedal. As we have developed in previous sections, we will consider the vehicle to be a lumped mass system with the effects of acceleration being manifested on the center of gravity. In vehicle design, and in particular when the ride of the vehicle is analyzed, the wheels of the vehicle are treated separately and are referred to as unsprung masses.

When a vehicle accelerates, its performance is limited by two effects. At lower speeds, the acceleration is generally limited by the tire road interaction. At higher speeds the power available in the engine limits the acceleration. The performance of the vehicle is also restricted by the type of engine, either gasoline or diesel. Gasoline engines are capable of higher revolutions than diesel engines by a factor of about two to one. Diesel engines have a flatter torque curve over the operating range and develop more power at lower rpm's than gasoline engines. Friction in the internal combustion engine can never be eliminated and causes wear. Since diesel engines operate at reduced revolutions, they also last longer than gasoline engines. The lower rotational speed of diesel engines is attributed to two effects, compression and volatility of the fuel. Ignition of the fuel is achieved in the gasoline engine by an electrical spark whereas in the diesel engine by compressing the fuel in the cylinder to the ignition point. From basic thermodynamics we know the relationship between pressure, volume, and temperature for an ideal gas as,

$$pv = nRT \tag{7.6}$$

where

p = pressure in dynes/cm^2
v = volume in cm^3
n = constant number usually between 1 and 2

R = universal gas constant = 8.314 joules/gmol-°K
T = temperature in °K

Thus, as the pressure in a cylinder of an engine increases, the temperature in the cylinder increases and ignites the gas in the cylinder. That is why diesel engines do not have spark plugs. They operate at higher pressures in the compression range of 18–1. In comparison, gasoline engines have compressions in the 10–1 range. At those pressures, gasoline has not reached the ignition temperature, and thus requires an ignition from the spark plug. Within the compression range of the diesel engine, sufficient temperature is reached to ignite the diesel fuel without the need for a spark source such as a spark plug. The power that an internal combustion engine provides is a function of the torque it develops and the speed of rotation, or

$$P = \Gamma S \tag{7.7}$$

where

P = power in ft-lb/sec
Γ = torque in ft-lb
S = speed in rad/sec

From Newton's second law and since the power available to the wheels of the vehicle is the product of the force times the speed of the vehicle, we can express the acceleration as,

$$\mathbf{a} = 550\frac{g\,\mathrm{HP}}{WV} \tag{7.8}$$

In Equation 7.8 we define

g = acceleration due to gravity in ft/sec^2
V = vehicle speed in ft/sec
W = weight of vehicle in lb
HP = horsepower of the engine

The distance traveled from a stop by a given vehicle at a given acceleration and horse power rating over a specific time can also be determined by a manipulation of Equations 7.8 and

$$D = \frac{1}{2}\mathbf{at}^2 \tag{7.9}$$

Since the work or energy per unit time is measured in horsepower, we may write

$$D = \sqrt{\frac{550\,g\,\mathrm{HP}\,t^3}{2W}} \tag{7.10}$$

We may compute the time required for a vehicle of a given weight and horsepower to travel a given distance from Equation 7.10 as

$$t = \left[\frac{2WD^2}{550g\mathrm{HP}}\right]^{1/3} \tag{7.11}$$

As an example, a 3000-lb vehicle that develops 200 horsepower will travel from a stop a distance of 50 ft in 3.485 sec. The acceleration of the vehicle is then 8.23 ft/sec^2. The vehicle's speed at 50 ft is then 19.5 mph.

7.2.4 Electrical Systems

Modern passenger vehicles and commercial vehicles have complex electrical circuits and components that monitor and control performance. These include engine control, ride control, braking action, and air bag status and deployment. The systems also monitor parameters that may be of interest in a reconstruction. Virtually all vehicles over the last 10 years have a "black box" recorder or more properly called electronic control units that are monitored by the air bag module. At the present time only the three major American manufacturers of automobiles make the interrogation of many of their vehicles available to investigators. Foreign manufacturers of automobiles do not make interrogation of the air bag module available to be investigated by noncompany representatives. Additionally, commercial tractor's engine control modules may be interrogated with the proper equipment from the manufacturer.

If an electrical malfunction is suspected as having caused a collision, the status of the electronic systems can be evaluated through the use of a diagnostic tool. There are many of these tools available from a variety of manufacturers. These tools vary in complexity and some of the access only domestic vehicles. Some vehicles have proprietary tools while others do not allow their interrogation except by trained factory representatives. Figure 7.10 shows a typical interrogation tool used to troubleshoot passenger vehicles. Similar tools are available to troubleshoot commercial vehicles such as tractors and trailers. A standard Volt-Ohm-Meter whether digital or analog can also be used to trace circuits in a vehicle if it is suspected that an electrical malfunction caused a collision.

Figure 7.10 Interrogation tool.

7.3 Failure Analysis

The most common failures involved in collisions include brake failure, steering failure, and tire failure. Steering failure is characterized by catastrophic separation of one of the steering components such as a pitman arm, a gear box, the rack and pinion, or one of the linkages that make up the steering system. Determination of these failures requires disassembly and mechanical testing of the components. Similarly, tire failure is usually represented by delamination of the treads or of the belts in a tire. Ragged boundaries at the tire failure are typical in such events. Similarly, brake failures require thorough inspection of the brake systems. In some instances of brake failure or purported brake failure, it may be necessary to perform brake tests while the vehicle is being operated. The next section describes a method for the analysis of brake testing. Seatbelts and airbags may also fail and can be evaluated through inspection and electrical interrogation.

7.3.1 Brake Performance Characteristics

Brake tests using an accelerometer reveal that the friction coefficient has a characteristic curve as a function of time approximated by the curve shown in Figure 7.11.

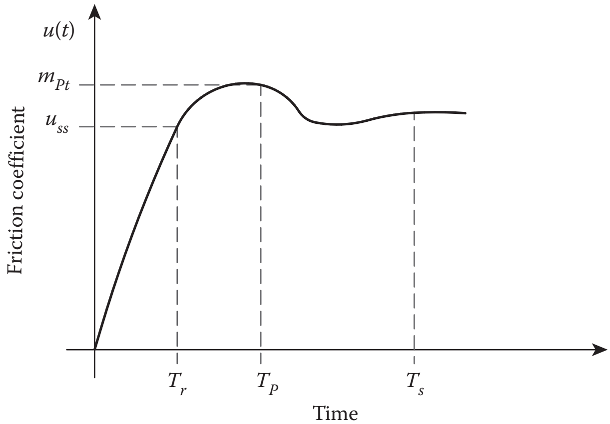

Figure 7.11 Brake response.

Figure 7.11 represents a typical response curve to a second order system when a step input is applied. Without question under hard braking conditions, the input is, in fact, approximately equal to a step input. Therefore, in the S-domain, the step response of the coefficient of friction is characterized by

$$\mathcal{L}\{u(t)\} = u(s) = \frac{w_n^2}{s\left(s^2 + 2\delta w_n s + w_n^2\right)} \tag{7.12}$$

The normalized time response is then

$$\mathcal{L}^{-1}\{u(s)\} = u(t) = u_{ss}\left[1 - \frac{1}{\beta}\varepsilon^{\delta w_n t}\sin\left(\beta w_n t + \varphi\right)\right] \tag{7.13}$$

where

$u(t)$ = friction coefficient for a step input
u_{ss} = steady state (or average) friction coefficient
M_{pt} = peak response or the friction coefficient
T_r = rise time of the response curve (sec)
T_p = peak time of the response curve (sec)
T_s = settling time required for the response to remain within 2% (sec)
δ = damping ratio
w_n = natural frequency (rad/sec)

$$\beta = \sqrt{1 - \delta^2}$$

$$\varphi = \cos^{-1}\delta$$

It can be shown that the percent overshoot is given by

$$\text{P.O.}\frac{M_{\text{pt}} - u_{\text{ss}}}{u_{\text{ss}}} \times 100\% = 100\varepsilon^{-\frac{\delta\pi}{\beta}} \tag{7.14}$$

while the settling time is

$$T_s = 4\tau = \frac{4}{\delta w_n} \tag{7.15}$$

The peak response is governed by

$$M_{\text{pt}} = u_{\text{ss}}\left(1 + \varepsilon^{\frac{-\delta\pi}{\beta}}\right) \tag{7.16}$$

and the peak time is

$$T_p = \frac{\pi}{\beta w_n} \tag{7.17}$$

From Equation 7.16, it can be shown that

$$\delta = \frac{-\ln\left[\dfrac{M_{\text{pt}} - u_{\text{ss}}}{u_{\text{ss}}}\right]}{\sqrt{\pi^2 + \left(\ln\left[\dfrac{m_{\text{pt}} - u_{\text{ss}}}{u_{\text{ss}}}\right]\right)^2}} \tag{7.18}$$

In order to describe the braking performance of a vehicle, braking tests should be performed using an accelerometer. When the braking performance $u(t)$ is tabulated and plotted for various speeds, an average curve of $u(t)$ can then be plotted and compared to the step response of a second order system. From the experimental data, M_{pt}, u_{ss}, T_p, T_s, and T_r can be inferred. From these values, δ and w_n, β, φ, and $u(t)$ can be compared to the average experimental curve of $u(t)$. The mathematical relationship that represents the data are commonly referred to as curve fitting.

The mathematical representation is the regression curve and equation which can then be evaluated by establishing an appropriate criterion such as least squares regression. The corresponding scatter diagram will look like Figure 7.12.

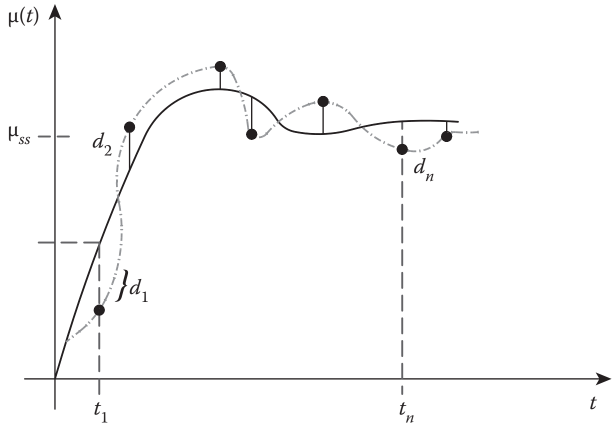

Figure 7.12 Comparison of theoretical and experimental data.

Least squares regression dictates that

$$d_1^2 + d_2^2 + \cdots + d_n^2 = \text{minimum} \tag{7.19}$$

As an example, Figure 7.13 shows various brake response curves for a 1990 Cadillac Deville. Figure 7.14 shows the average of the test results.

7.3.2 Seat Failure

In this reconstruction a vehicle lost control on an interstate highway as a result of wet roads. The vehicle skidded to the right berm area and as the driver attempted to reenter the travel lane, the vehicle rotated counterclockwise and struck a tree with the rear. The collision caused the driver's seat to fail rearward and produced the ejection of the driver through the rear window. The reconstruction and analysis were carried out in order to determine the strength of the seat and the velocity at which it would fail.

To produce the accurate speed of the vehicle as it left the highway (V_i), a survey of the path of the vehicle was taken. The energy lost with the tree impact was determined from a review of the manufacturer's video tape. The video tape revealed a change in velocity of approximately 20–25 mph for the barrier impact. A value of 25 mph was, therefore, used in this analysis.

The work–energy principle can be used to describe the energy losses as the vehicle left the road surface, slid down the ditch, up the embankment, hit the tree, bounced down the embankment, and came to rest. The work-energy principle is given by

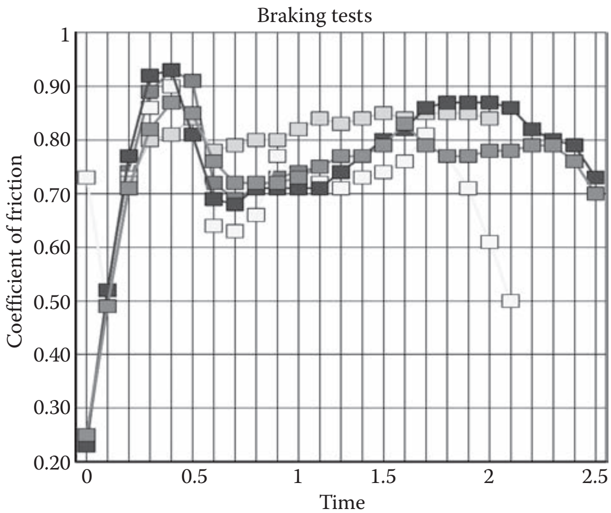

Figure 7.13 Brake performance tests.

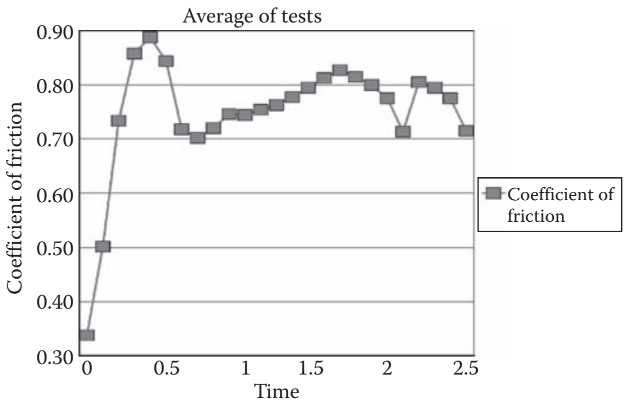

Figure 7.14 Average of tests.

$$Fl = \frac{1}{2} m v^2 \tag{7.20}$$

where

F = force applied
l = distance over which F is applied
m = mass of vehicle
v = velocity

Since there are five instances of energy loss, the total energy loss can be written as

$$E_i = E_1 + E_2 + E_t + E_3 + E_4$$

$$\frac{1}{2}mv_i^2 = \frac{1}{2}mv_1^2 + \frac{1}{2}mv_2^2 + \frac{1}{2}mv_t^2 + \frac{1}{2}mv_3^2 + \frac{1}{2}mv_4^2$$

or

$$v_i = \sqrt{v_1^2 + v_2^2 + v_t^2 + v_3^2 + v_4^2} \tag{7.21}$$

A vehicle skidding to a stop does so through the aid of friction. The equations can be derived from Figure 7.15.

$$\begin{aligned} \sum F_x &= F - f = 0 \Rightarrow F = f \\ \sum F_y &= N - W = 0 \Rightarrow N = W \end{aligned} \tag{7.22}$$

$$f = \mu N \tag{7.23}$$

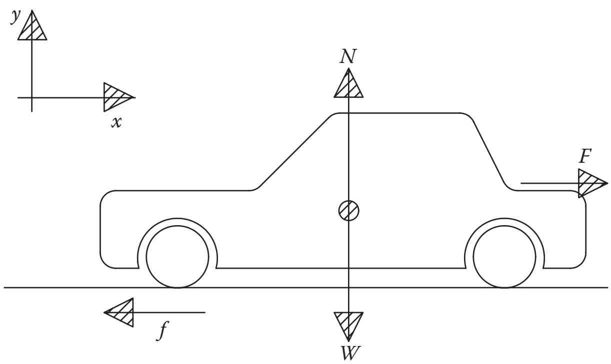

Figure 7.15 Vehicle skid. W = Weight of vehicle; N = normal force; f = frictional force; μ = coefficient of friction.

or

$$v_i = \sqrt{30\mu_1 l_1 + 30\mu_2 l_2 + v_t^2 + 30\mu_3 l_3 + 30\mu_4 l_4} \tag{7.24}$$

where

l_1 = distance from road to ditch; μ_1 = coefficient of friction for 1_1
l_2 = distance from ditch to tree; μ_2 = coefficient of friction for 1_2
l_3 = distance from tree to ditch; μ_3 = coefficient of friction for 1_3
l_4 = distance from ditch to rest; μ_4 = coefficient of friction for 1_4

Since the path was not level, the coefficient of friction values were corrected according to

$\mu_1 = \mu \cos t_1 - \sin t_1$
$\mu_2 = \mu \cos t_2 - \sin t_2$
$\mu_3 = \mu \cos t_3 - \sin t_3$
$\mu_4 = \mu \cos t_4 - \sin t_4$

where

t_1 = y-axis angle of l_1
t_2 = y-axis angle of l_2
t_3 = y-axis angle of l_3
t_4 = y-axis angle of l_4

From crush analysis, the vehicle struck the tree at approximately 25 mph. The seat obviously failed at this speed, but it is important to know the exact speeds required to deform the seat. The cross-section of the seat support at the point of failure was elliptical in shape and hollow. Certain sections of the seat frame were circular. For purposes of comparison and to completely analyze the seat, the hollow circular cross-section of the seat was also considered. The seat was measured using a set of calipers.

R_2 = outer radius of circular section
R_1 = inner radius of circular section
a = outer major axis of elliptical section
b = outer minor axis of elliptical section
c = inner major axis of elliptical section
d = inner minor axis of elliptical section

7.3.2.1 Analysis of the Circular Cross-Section

The work–energy principle is again implemented to determine the speed at which the seat fails. Since the equation for work is also a moment equation, it can be written as follows:

$$\text{moment} = Fd = \frac{1}{2} m v^2$$

Since the collision occurred at an angle, both bending and torsional effects on the seat must be taken into account. First the bending moments along each axis are determined. Since the dimensions are the same along the axes of a circle, only one moment is needed.

$$\frac{1}{2}mV_{b_1}^2 = M_{\text{bl}} = \frac{SI_{x,y}}{Y} \tag{7.25}$$

where

M_{bl} = circular bending moment
$I_{x,y}$ = circular moment of inertia about the x and y planes
S = permissible working stress
Y = circular distance to most remote fiber

The moment of inertia is derived using the equation

$$I_{x,y} = \int y^2 dA \tag{7.26}$$

The hollow circular section (Figure 7.16) is then drawn on a set of axes in order to set up the integration.

$$I_{x,y} = \int_{r=R_1}^{R_2}\int_{\varphi=0}^{2\pi} (r\sin\varphi)^2\, r dr d\varphi \tag{7.27}$$

$$I_{x,y} = \frac{\pi}{4}(R_2^4 - R_1^4) \tag{7.28}$$

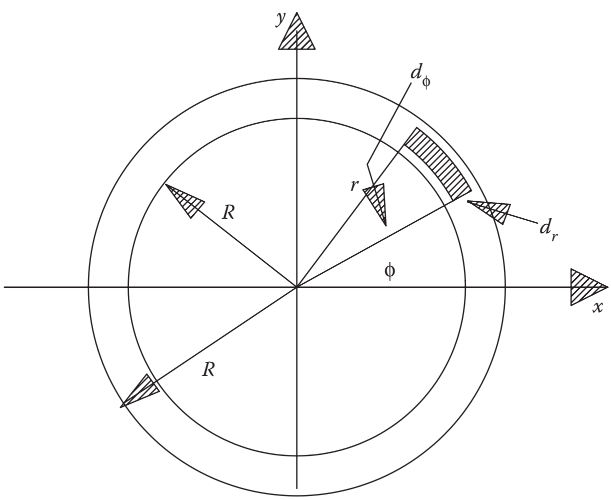

Figure 7.16 Circular section.

The equation for the torsional bending moment is very similar.

$$\frac{1}{2}mV_{\text{tl}}^2 = M_{\text{tl}} = \frac{SI_{\text{pl}}}{Y} \tag{7.29}$$

where

M_{tl} = torsional moment
I_{pl} = polar moment of inertia

Because of symmetry the polar moment of inertia reveals that it is the same as the moment of inertia about the x or y planes. And is given by,

$$I_{\text{pl}} = I_{\text{xy}} + I_{\text{xy}} \tag{7.30}$$

The moments are then combined to give a more accurate interpretation of the deformation of the seat. This combined circular moment M_{cl} and its corresponding velocity V_{cl} are determined from the following:

$$M_{\text{cl}} = \sqrt{M_{\text{bl}}^2 + M_{\text{tl}}^2} \tag{7.31}$$

$$\frac{1}{2}mV_{\text{cl}}^2 = M_{\text{cl}} \tag{7.32}$$

7.3.2.2 Analysis of the Elliptical Cross-Section

The analysis of the elliptical cross-section is quite similar to that of the circular cross-section. Again, the effects of bending and torsional moments on the seat support needed to be analyzed. However, each moment must be derived in each plane since the ellipse does not have radial symmetry.

$$\frac{1}{2}mV_{bx2}^2 = M_{bx2} = \frac{SI_x}{a} \tag{7.33}$$

$$\frac{1}{2}mV_{by2}^2 = M_{by2} = \frac{SI_y}{b} \tag{7.34}$$

where

M_{bx2} = elliptical bending moment about x-axis
M_{by2} = elliptical bending moment about y-axis
V_{bx2} = velocity determined by M_{bx2}
V_{by2} = velocity determined by M_{by2}

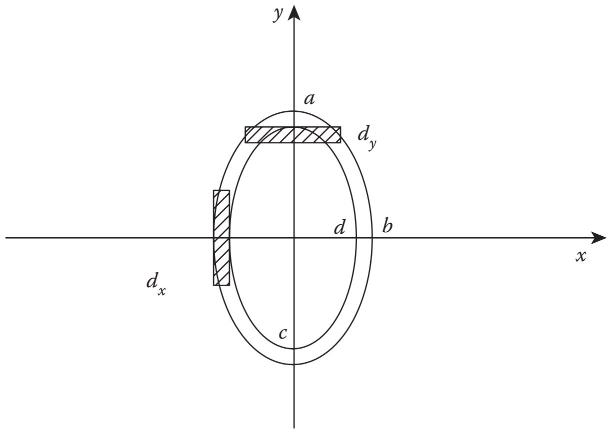

Figure 7.17 Elliptical sections.

$I_x = x$-axis elliptical moment of inertia
$I_y = y$-axis elliptical moment of inertia

Integration is needed to derive the moments of inertia for the elliptical cross-section (Figure 7.17).

$$I_x = \int y^2 dA$$

$$dA = 2x dy$$

$$\frac{x^2}{b^2} = \frac{y^2}{a^2} = 1 \tag{7.35}$$

$$\frac{x^2}{d^2} = \frac{y^2}{c^2} = 1$$

which yields

$$I_x = \frac{\pi}{4}\left(a^3 b - c^3 d\right) \tag{7.36}$$

Similarly,

$$I_y = \int x^2 dA$$

$$dA = 2y dx \tag{7.37}$$

$$I_y = \frac{\pi}{4}\left(ab^3 - cd^3\right) \tag{7.38}$$

Similarly, the torsional moment must be determined about both axes.

$$\frac{1}{2}mv_{tx2}^2 = M_{tx2} = \frac{SI_{p2}}{a} \tag{7.39}$$

$$\frac{1}{2}mv_{ty2}^2 = M_{ty2} = \frac{SI_{p2}}{b} \tag{7.40}$$

The polar moment of inertia is then

$$I_{p2} = I_x + I_y \tag{7.41}$$

where

M_{tx2} = elliptical torsional moment about x-axis
M_{ty2} = elliptical torsional moment about y-axis
V_{tx2} = velocity determined by M_{tx2}
V_{ty2} = velocity determined by M_{ty2}
I_{p2} = elliptical polar moment of inertia

As in the analysis of the circular cross-section, the moments are combined to provide for more accurate data. These combined elliptical moments (M_{cxa2}, M_{cxb2}, M_{cya2}, M_{cyb2}) and their respective velocities (V_{cxa2}, V_{cxb2}, V_{cya2}, V_{cyb2}) are given by the equations 7.42 and 7.43.

$$\begin{aligned} M_{cxa2} &= \sqrt{M_{bx2}^2 + M_{tx2}^2} \qquad M_{cxb2} = \sqrt{M_{bx2}^2 + M_{ty2}^2} \\ M_{cya2} &= \sqrt{M_{by2}^2 + M_{tx2}^2} \qquad M_{cyb2} = \sqrt{M_{by2}^2 + M_{ty2}^2} \end{aligned} \tag{7.42}$$

$$\begin{aligned} \frac{1}{2}mV_{cxa2}^2 &= M_{cxa2} \qquad \frac{1}{2}mV_{cxb2}^2 = M_{cxb2} \\ \frac{1}{2}mV_{cya2}^2 &= M_{cya2} \qquad \frac{1}{2}mV_{cyb2}^2 = M_{cyb2} \end{aligned} \tag{7.43}$$

In order to reiterate the findings from the analyses in the summary of results, several dimensional analyses were conducted. Two of these inquiries involved the determination of the velocity at departure from the road (V_i); the first of which examined its dependence on coefficient of friction (μ) and the velocity lost at tree impact V_t. These variables were varied around their central values at 0.50 and 25, respectively. The second analysis is the dependence on coefficient of friction and the distance from the ditch to the rest position of the vehicle (I_4). Both inquiries resulted in *V*, ranging between speeds of 52 and 58 mph (Tables 7.1 and 7.2).

The second set of dimensional analyses examined the speed at which failure would occur to the seat support with a cross-sectional shape similar to that of a hollow ellipse. Results from the determinations of bending and torsional moments about both the *x* and *y* axis provided velocities that would cause failure in the seat. These velocities were examined for their dependence on the length of the moment arm (*D*) and the weight of the driver (*W*).

Table 7.1 Velocity at Departure from Road (V_i)

Dependence on Coefficient of Friction (*u*) and Velocity Lost at Tree Impact (V_t)					
	0.40	0.45	0.50	0.55	0.60
V_t	V_i	V_i	V_i	V_i	V_i
20	48.2	50.7	53.0	55.2	57.4
21	48.6	51.1	53.4	55.6	57.7
22	49.1	51.5	53.8	56.0	58.1
23	49.5	51.9	54.2	56.4	58.5
24	50.0	**52.4**	**54.6**	**56.8**	58.9
25	50.5	**52.8**	**53.1**	**57.2**	59.3
26	51.0	**53.3**	**55.5**	**57.7**	59.7
27	51.5	53.8	56.0	58.1	60.2
28	52.0	54.3	56.5	58.6	60.6
29	52.6	54.8	57.0	59.1	61.1
30	53.1	55.4	57.5	59.6	61.6

Table 7.2 Velocity at Departure from Road (V_i)

Dependence on Coefficient of Friction (*u*) and Distance from Ditch to Rest Position (14)					
	0.40	0.45	0.50	0.55	0.60
14	V_i	V_i	V_i	V_i	V_i
10	49.7	52.0	I 54.2	56.3	58.3
12	50.1	**52.4**	**54.3**	**56.8**	58.8
14	50.5	**52.9**	**55.2**	**57.3**	59.4
16	50.9	**53.3**	**55.6**	**373**	59.9
18	51.3	53.7	56.0	58.3	60.4
20	51.7	54.1	56.5	58.8	60.9
25	52.6	55.2	57.6	60.0	62.2
30	53.6	56.2	58.7	61.1	63.5
35	54.5	57.2	60.0	62.3	64.7

The analyses produced a range of velocities between 7 and 12 mph for which the seat would deform. The computed velocities of deformation were consistent with the manufacturer's crash data that indicated a weak seat back.

7.3.3 Seat Belts and Air Bags

In some reconstructions the question of whether the seat belts or air bags failed may be pertinent to determine whether the occupants were properly protected. Seat belts and air bags have become more sophisticated and improved than when originally designed and installed in automobiles. The reader may recall the original seat belts installed in vehicles in the early 1960s as simply a mechanical device bolted to the frame of the vehicle, utilizing a fabric webbing, and secured with a latch. These first generation seat belts did not have a shoulder strap. It soon became apparent through crash testing and analysis of actual crashes that the lap belt was capable of producing serious injury in higher ΔV crashes. Furthermore, the upper torso was allowed to rotate significantly to the point that the chest and head of the occupants could strike surfaces such as the dash and the steering wheel. This research produced the introduction of the shoulder belt. Again, through testing and analysis of crash data, it was determined that pretensioners and load limiters were necessary in the seat belt design in order to mitigate the injuries of the occupants.

Seat belt designs vary according to the manufacturer but most have some common components. The seat belt webbing is attached to a retractor mechanism. The retractor mechanism is a spool of the belt with rächet gears and a spring attached to the spool shaft. The spring is pretensioned in order to keep the webbing wound around the spool. When the belt is pulled out, the spring is untwisted so that when the webbing is released, the belt will retract and the slack in the belt will be taken up. In the case of a sudden stop or a collision, the retractor mechanism has a locking device which keeps the belt from further outward movement. Two basic types of locking systems are commonly employed. One system locks the spool when the vehicle decelerates rapidly and is activated by a swinging pendulum attached to a pawl that locks the rachet gear. The other system is activated by a sudden jerk of the belt. When the belt is suddenly jerked, a centrifugal clutch drives a lever and cam into a pawl that locks the rachet gear.

Modifications on these two basic designs include pretensioners and load limiters. In the conventional locking mechanisms described above, the retractor does not allow the belt webbing from further extension. The pretensioner mechanisms actually pull the belt tighter to better secure the passenger. These devices work in consort with the conventional mechanisms. There are many designs of pretensioners on automobiles. Pretensioners are electrically connected to the air bag module. The air bag module, or black box, or more precisely known as the event data recorder, monitors motion sensors known as accelerometers in the event of sudden decelerations. Pretensioners may be activated by solenoids, electric motors, or by explosive charges.

Load limiters work by releasing the tension on the belt when a severe event is detected by the air bag module. There are two basic types of load limiters. One type includes a fold sewn into the belt webbing which is designed to break the stitches at a predetermined force. The other basic type of load limiter utilizes a torsion bar in the retractor mechanism. Under severe loading conditions, the torsion bar twists and allows the belt to lengthen slightly. Allowing the tension on the belt to release slightly in the event of a crash can significantly reduce the injuries sustained by the occupants.

Air bags are designed to work in conjunction with seat belts. Air bags are not designed to work without the security of the belt system. The dual purpose of the air bag belt system is to restrict the motion of the occupants and to soften the impact blow from the surrounding environment. When investigating crashes, a determination must be made, if possible on whether the seat belts were utilized and if the air bag system performed as designed. These findings are relevant in terms of the crashworthiness of the vehicle. Injuries sustained in a collision by the occupants may vary significantly when the air bags deploy and the seat belts are not secured. This evidence can be gleaned from first responders reports or from electrical interrogation tools.

Air bags are designed to slow and protect the occupant from frontal, side, or rollover type collisions. The air bag system is composed of three components—the bag itself, the sensors, and the system that inflates the bag. The bag is made of a nylon fabric laden with small holes designed to deflate the bag after the event. The interior of the bag has a talcum and cornstarch powder that keeps the bag lubricated and pliable. The sensors are mechanical switches that close electrical circuits when collisions or decelerations of significance are detected. Most sensors in vehicles are designed to activate when the velocity change is between 10 and 15 mph. The choice of the threshold speed change corresponds to the threshold for injury based on research. Please refer to Chapter 14. The inflation system is activated by a chemical reaction when sodium azide reacts with potassium nitrate. The chemical reaction releases nitrogen gas that inflates the bag. The inflation speed of the bag is approximately 200 mph. The time of inflation is approximately 40 milliseconds.

7.3.4 Light Bulbs and Filaments

The examination of light bulbs in vehicles that are involved in accidents to determine whether the bulbs were turned ON is not an exact science. However, depending on the conditions of the remains of the lights, it is sometimes possible to conclusively determine the ON/OFF status of the bulb. Under ideal conditions, the lamp should be examined immediately after the accident. But in reality, this is seldom possible because investigators are called upon to make a determination days, weeks, or years after the accident. Under these conditions, the evidence is often lost, damaged, or confused. Special care should be taken to correctly identify the bulbs closest to the point of impact and the type of filament associated with each bulb. It is also important to determine the location of all the exterior bulbs of the vehicle, their type, and function. However, even under ideal conditions, undisturbed bulbs and filaments give inconclusive results.

We may categorize this analysis by first determining whether the glass bulb is broken or not, whether the filament is broken or not, and whether the bulb is a single or double filament bulb. Within these categories there are degrees of certainty, which must be taken into consideration before reaching a conclusion.

1. Unbroken glass
   (a) If a single filament bulb is unchanged in shape, then it was probably not ON.
   (b) If a single filament is stretched and misshapen, then it may have been ON.
   (c) If one filament of a double filament light is slightly stretched, then the other filament may have been ON.
   (d) If one end of a filament of a double filament bulb has turned purple and the other end is bright silver, then the other filament was ON.

2. Broken glass
   (a) The color of a tungsten filament changes when the glass is broken if the filament is hot and therefore ON. Thus, if the filament has turned black, then the filament was ON.
   (b) Tungsten oxide deposits a white powder on glass or metal parts of the interior of the bulb. Thus, if white powder remnants are found inside the remains of a broken bulb, then the filament was ON.
   (c) If broken filament ends are rounded or beaded, then the filament was ON. However, if the broken ends of the filament are ragged, then the filament was probably OFF.
   (d) If the bulb contains two filaments, one with a white oxide deposit, then the other filament was ON.
   (e) If molten glass fragments are found on the filament or the brass portion of the light base, then the filament was ON.

3. Degrees of certainty
   (a) If a filament is black, white oxide covers the inside of the broken bulb glass, part of the filament is melted onto the glass, molten glass remains are found on the filament or the brass portion of the base, or the remaining filament length is stretched and the broken ends of the filament have large beads of molten metal; then the filament was ON when the bulb broke.
   (b) If the bulb has double filaments with the above conditions met and the second filament is purple at one end and silver at the other end; then the first filament was ON.
   (c) If the glass is unbroken and one filament of a double filament bulb is slightly stretched, then there is a chance that the first filament was ON.

4. Cautions
   (a) If the glass fractures while the light is OFF as a consequence of the wreck and someone turns the light ON after the crash; then the filament will burn out. Under these conditions, it is imperative to find the glass remnants and to look for the white deposit on the inside of the bulb pieces. Care should be taken to find broken filaments in order to determine whether the bulb was ON prior to or after the accident.
   (b) If glass fusion with or without molten filament pieces is present, then the filament was ON when the bulb broke. If there are tiny blobs of molten glass, then the filament was ON when it fractured.
   (c) If the filament fracture is clean and ragged, then the filament was cold at the time of the break and was OFF.

The guidelines listed above can often accurately determine whether the light bulbs were off or on and whether they are pertinent to a reconstruction. The examination of the remnants should be undertaken in a laboratory utilizing appropriate magnification and photography.

7.4 Testing of Components

Under certain circumstances it is imperative to notify all possible involved parties when examination and testing of components are to take place. For example, if a component of a brake system is suspected to have caused a crash, then the vehicle manufacturer, repair facility, or the component manufacturer may need to be notified. If brake failure occurred because the owner did not carry out preventive maintenance and the brake pads were simply worn, then there would be no need to notify other parties. When ample time and notification are given to other parties, and they choose not to attend, then there is no retribution available to the other party. Disassembly and testing should always be conducted in a systematic manner and properly documented. Proper documentation can take place through still or motion formats.

Spoliation of evidence is often raised when an involved party is not notified or fails to attend an inspection, disassembly, or testing of a component. Spoliation of evidence only applies when destructive testing or modification of the component takes place. Spoliation does not apply if, for example, an alternator is removed by taking bolts loose. The alternator can easily be remounted in its bracket without a loss or spoliation of the evidence. Generally, disassembly of components does not constitute spoliation because there is no material change of the evidence.

Testing of a component may also not constitute spoliation. For example, brake activation to determine if sufficient pressure is applied to the discs, does not constitute spoliation because there would be no material change to the evidence, assuming that the brake lines are intact and do not leak brake fluid. In instances where the evidence will be modified, a testing protocol should be established and agreed to by all parties. The basic guide to be used when establishing a testing protocol is to perform activities that scientifically and conclusively determine whether the component failed and contributed to the crash.

Some tests and disassembly require a modification of the evidence. For example a bearing may need to be cut in order to determine if the bearing failed. Evidence of the failure would be in the form of metal transfer in the raceway and galling of the bearings. This type of evidence can only be found by destructive testing involving cutting the bearing apart. When in doubt, always err on the side of caution and ensure that potentially involved parties are notified. The notification of involved parties is not the purview of the forensic reconstructionist. Usually, the assignment for the analysis comes from an attorney or an insurance adjuster. The responsibility of notification is only to the client and not to the other parties. It is the responsibility of the client to notify the other parties.

Bicycles, Motorcycles, and Pedestrians

8

8.1 Introduction

The collisions involving pedestrians, bicycles, scooters, motorcycles, and vehicles can be analyzed through standard Newtonian techniques or through equations developed from empirical data. This chapter outlines some of the basic principles involved in those collisions. But first it is relevant to consider some statistics with these types of collisions.

Motorcycle accidents include mopeds, three and four wheel motorcycles, minibikes, and off road motorcycles. In 2006 over 4900 people were killed on these types of vehicles. The National Highway Traffic Safety Administration funded a study by Harry Hurt that analyzed 4500 motorcycle accidents. Some of the findings include the following: three fourths of the accidents involved another vehicle, typically a passenger automobile. One fourth of the accidents involved collisions with fixed objects or the roadway. Vehicle failure represented 3% of those accidents with the most common failure a puncture flat on one of the tires. The failure of opposing motorists was the predominant cause of the accidents involving other vehicles. The most likely place for these accidents was at intersections where the automobile driver turned left in front of the motorcycle. Conspicuity of the motorcycle is a critical factor in these accidents, and accident involvement is significantly reduced by the use of motorcycle headlamps. Sixty percent of riders were not wearing helmets at the time of the accident. The helmet standard, FMVSS 218, provides a high level of protection in accidents. Table 8.1 summarizes motorcycle rider fatalities over a ten year period.

Pennsylvania motorcycle accidents increased from 3621 in 2004 to 4039 in 2005. The number of motorcycle accidents in Pennsylvania have increased steadily over this period. In 2000 there were 2837 motorcycle crashes in the Keystone state. The increase over the five year period is a substantial 42%. In comparison, the bicycle accident statistics show that 1353 crashes occurred with 18 deaths in 2005. Children ages 10–14 have the highest injury and death rate from bicycle accidents. This age group represents 26% of all injuries and 28% of all deaths from bicycle accidents. In 2005 there were 4763 accidents involving pedestrians in Pennsylvania, and 162 of those accidents were fatal. The majority of pedestrian accidents occurred during daylight hours.

Table 8.1 Motorcycle Rider Fatalities

Year	Registered Motorcycles	Vehicle Miles Traveled (Millions)	Motorcycle Rider Fatalities	Fatality Rate per 100,000 Registered Motorcycles	Fatality Rate per 100 Million VMT
1995	3,897,191	9797	2227	57.14	22.73
1996	3,871,599	9920	2161	55.82	21.78
1997	3,826,373	10,081	2116	55.30	20.99
1998	3,879,450	10,283	2294	59.13	22.31
1999	4,152,433	10,584	2472	59.53	23.46
2000	4,346,068	10,469	2897	66.66	27.67
2001	4,903,056	9639	3197	35.2	33.17
2002	5,004,156	9552	3270	65.35	34.23
2003	5,370,035	9577	3714	69.16	38.78
2004	5,780,870	10,048	4008	69.33	39.89

Table 8.2 NYC Pedestrian and Bicycle Fatalities

	1992	1991	1990	1989	1988	1987	1986
Bicycle–motor vehicle collisions	3520	3857	3356	3544	3661	4246	4313
Bicyclist fatalities	17	18	20	18	15	15	24
Pedestrian–motor vehicle collisions	13,599	14,732	15,109	14,552	14,043	14,304	14,347
Pedestrian fatalities	294	317	366	374	352	319	286
Pedestrian–bicycle collisions	298	258	351	327	430	511	63
Pedestrian fatalities	2	0	3	0	0	1	2

Table 8.2 is a compilation of bicycle and pedestrian fatalities in New York city from 1986 to 1992. The table shows a decline in bicycle motor vehicle collisions and in pedestrian motor vehicle accidents.

In 2004 the New York State Department of Motor Vehicles published a summary of pedestrian/motor vehicle accidents. In that study bicycles are excluded as a vehicle and bicyclists are excluded as drivers. Table 8.3 and the accompanying Figure 8.1 represent the results of that study. Note that the 30–39 age group has the most number of accidents, injuries and fatalities followed by the 40–49 age group. The graph follows a typical bell curve distribution. The New York study determined that the day of the week was not significant on the number of accidents but the time frame between 3:00 and 9:00 p.m. had the most accidents. The fewest pedestrian accidents occurred during the middle of the night. Sixty seven percent of all pedestrian/motor vehicle accidents occurred at intersections. The New York

Table 8.3 NY State Pedestrian/Motor Vehicle Accidents by Age

Drivers	Number	Fatalities	Injuries
Under 20	865	25	838
21–29	2603	54	2545
30–39	3019	74	2942
40–49	2979	62	2909
50–59	2102	54	2043
60–69	942	18	924
70–79	500	15	484
over 80	327	9	323
Totals	13337	311	13014

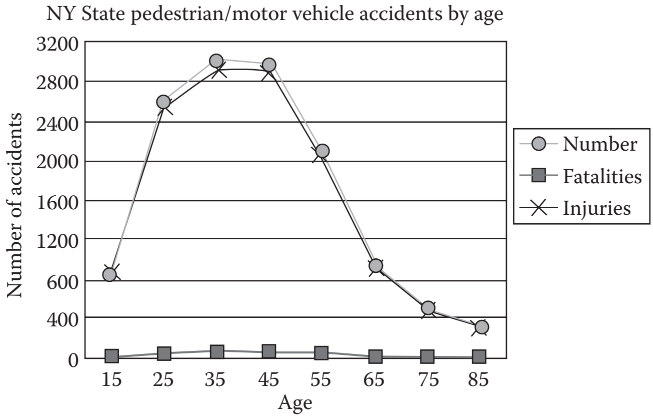

Figure 8.1 NY state pedestrian/motor vehicle accidents by age.

state study also revealed that contributing factors to the accidents included human factors at 60.4%, vehicular factors at 2.9%, and environmental factors as 8.2%. The results of these studies and many others indicate that pedestrian and bicyclist collisions with automobiles are decreasing but collisions with motorcycles are increasing. Improved signage and awareness by the driving public is attributed to the decrease in pedestrian and bicycle collisions with vehicles.

8.2 Gyroscopic Action in Two-Wheeled Vehicles

The effect that allows a bicycle or motorcycle rider to not topple over is gyroscopic action. Most of us who have ridden a bicycle realize that the cycle needs to be in motion in order to be stable. As the speed of the cycle increases, the system becomes more stable. When we slow down we need to steer the front

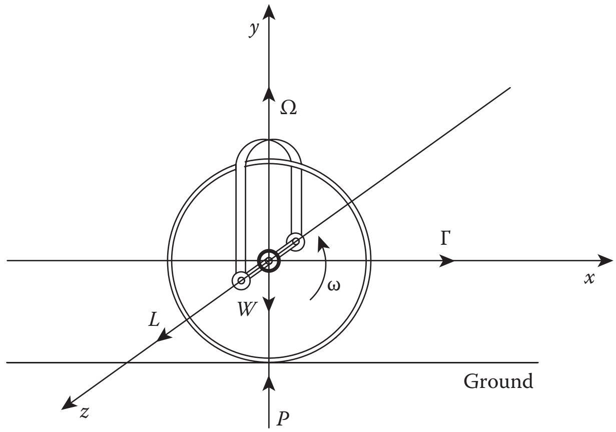

Figure 8.2 Gyroscopic action.

wheel to either side more and more as our speed decreases. Figure 8.2 shows a single wheel of a bicycle and the forces and torques that affect it.

In rectangular coordinates the equilibrium equations are

$$\mathbf{\Omega} = \Omega a_y \tag{8.1}$$

$$\mathbf{L} = L\mathbf{a}_z \tag{8.2}$$

$$\mathbf{W} = -W\mathbf{a}_y \tag{8.3}$$

$$\mathbf{P} = P\mathbf{a}_y \tag{8.4}$$

$$\Gamma = \Omega \times \mathbf{L} = \Omega I\omega\mathbf{a}_x \tag{8.5}$$

where

I = moment of inertia
ω = angular velocity
$\mathbf{L}$ = angular momentum
$\mathbf{W}$ = weight

Γ = torque
Ω = vector angular velocity of precession

As an example, we may calculate the angular velocity required of the front wheel of a bicycle to counteract the capsizing torque due to a weight of 120 lbs positioned 1 inch horizontally to the right or left of the line of contact of the wheels and the ground. If we assume that the moment of inertia of the front wheel is 0.25 slug-ft^2, its radius is 15 inches, and the forward speed of the bicycle is 20 ft/sec, we determine that the angular velocity must be 2.5 radians per second. Thus, riding a cycle at 20 ft/sec stabilizes the system quite well.

8.3 Vaulting of Pedestrians

The pedestrian motion as a result of the collision is of utmost importance in order to perform a proper reconstruction and speed determination. If the pedestrian is struck below his center of mass as shown in Figure 8.3, his body will rotate counterclockwise. This type of collision will cause the body to move upward over the hood and cause the pedestrian's head to strike the front windshield of the car. If the vehicle speed is high enough, the body may vault over the roof of the vehicle. Head injury in vehicle pedestrian accidents is the highest cause of death. Serious head injuries occur at vehicle impact speeds above 30 mph.

The pedestrian flight path over the vehicle is considered a vault as represented in Figure 8.3. If the pedestrian is struck at or above the center of mass he may be displaced and possibly run-over. Alternatively, the pedestrian may

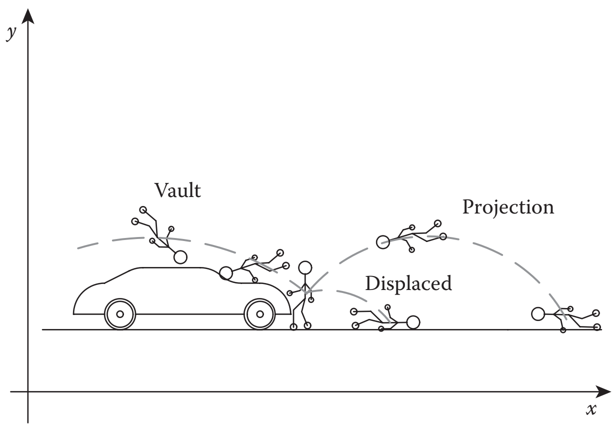

Figure 8.3 Pedestrian collision.

take a flight path similar to a projectile. Careful accident site measurements and vehicle damage measurements are required in order to properly assess the path of the pedestrian.

Vehicle speed estimates may be conducted in a variety of manners. Important information, such as the exact point of impact, may not be available. Sometimes ancillary information, such as remains of shoes or hats, help to locate the approximate point of impact. Sometimes the exact distance the body slid after the collision is difficult to determine. In many cases, the vehicle does not leave skid marks before or after the collision, which often happens when drivers are inattentive or when pedestrians dart in front of vehicles from obstructions to visibility, such as between parked cars. Another consideration involves the perception or visibility of the pedestrian to the driver at night. This visibility depends on several factors, such as the color of the clothing worn by the pedestrian, street lighting, and the intensity of the headlights. Pedestrian visibility at night for normal dark clothing is approximately 150 ft with low beam headlights.

Four methods are used in the analysis to estimate the vehicle velocity at impact. The first method involves the use of the vault equation. This equation is represented by

$$V_o = \sqrt{\frac{gD_1^2}{2\cos^2 A_v (D_1 \tan A_v + h)}} \tag{8.6}$$

A second method of analysis involves using the pedestrian sliding equation

$$V_s = \sqrt{V_f^2 - 2aD_2} \tag{8.7}$$

The third method of analysis involves an empirical equation developed by Limpert (1990).

$$V_e = 6.6\sqrt{8.4a^4 + aD} - 20a^2 \tag{8.8}$$

A fourth equation may sometimes be employed by solving for total stopping distance of the vehicle including reaction time. This equation is of the form

$$V_i = ga_2t_r\left[\sqrt{1 + \frac{2D_T}{ga_2t_r^2}} - 1\right] \tag{8.9}$$

For Equations 8.6 through 8.9, the following parameters are defined:

V_o = speed according to the vault equation (ft/sec)
V_s = speed according to the pedestrian sliding equation (ft/sec)
V_e = speed according to the empirical equation (ft/sec) developed by Limpert
V_i = speed according to total stopping distance (ft/sec)
g = acceleration due to gravity (ft/sec^2)
D_j = vault distance (ft)
A_v = vault angle (degrees)
h = vault height (ft)
V_f = final velocity (ft/sec)
a = acceleration of the body (ft/sec^2)
D_2 = distance the body slides (ft)
a_2 = vehicle deceleration in g units
t_r = driver reaction time (sec)
D_T = total stopping distance of vehicle

An average impact velocity (V_a) is used to give a median value for the velocities computed from Equations 8.6 through 8.9. This analysis can only be used as an approximation when considering side impacts. Frontal impacts account for approximately 75% of all vehicle/pedestrian accidents.

As an example we have calculated a pedestrian/vehicle collision from an actual accident where the approximate point of impact was known. A pedestrian was crossing a rural highway from a residence to her vehicle that was parked across the street. There was a bridge across a creek on the side of the residence and her vehicle was located directly across from the bridge. Thus, the impact point was within 10 ft of a direct line from the pedestrian bridge to her vehicle. Her body was projected from the line a distance of 91 ft according to police measurements. The vehicle that struck the pedestrian was a small pickup truck with a high front end. The lady was approximately 5 ft tall so that Equations 8.6 through 8.8 were used in the reconstruction. Although the police did indicate that skid marks were deposited on the road prior to and after impact, they did not measure or photograph the marks. The collision occurred at night.

The summary of results compare the three methods of analysis and yields a speed estimate of between 45 and 50 mph at impact. It should be pointed out that the vehicle stopping distance from Equation 8.9 using a conservative coefficient of friction of 0.65 (indicative of some skid marks) is approximately 58 mph. This analysis does not include any braking action prior to impact so that the actual vehicle speed would normally be greater. The results are included in Tables 8.4 and 8.5.

Table 8.4 Impact Velocity Dependence on Horizontal Distance

D	V_o	V_s	V_e
86	46.5	48.3	44.1
87	46.8	48.6	44.4
88	47.1	48.9	44.7
89	47.4	49.2	45.0
90	47.7	49.5	45.4
91	48.0	49.7	45.7
92	48.3	50.0	46.0
93	48.5	50.3	46.3
94	48.8	50.5	46.6
95	49.1	50.8	46.9

Table 8.5 Impact Velocity Dependence on Body Drag Factor and Horizontal Distance

	V_o			V_s			V_c		
f	$D=86$	$D=91$	$D=95$	$D=86$	$D=91$	$D=95$	$D=86$	$D=91$	$D=95$
0.7	46.5	48.0	49.1	42.6	43.9	44.8	42.4	43.9	45.0
0.8	46.5	48.0	49.1	45.6	46.9	47.9	43.5	45.0	46.2
0.9	46.5	48.0	49.1	48.3	49.7	50.8	44.1	45.7	46.9
1.0	46.5	48.0	49.1	51.0	52.4	53.6	44.3	46.0	47.3
1.1	46.5	48.0	49.1	53.4	55.0	56.2	44.2	45.9	47.3
1.2	46.5	48.0	49.1	55.8	57.4	58.7	43.9	45.6	47.0

8.4 Determination of Pedestrian Speed from Vehicle Damage

Damage on a vehicle can aid in the determination of the speed of the pedestrian. In some instances, the points where certain body parts of the pedestrian impacted the vehicle are determinable. For example, the impact with the front bumper of the vehicle and a fractured tibia along with an indentation of the front windshield and a fractured cranium is shown in the diagram of Figure 8.4.

If the dimensions of the vehicle are known so that an accurate measurement of the damage points on the vehicle can be determined, and if the speed of the vehicle can be calculated or approximated, then the speed of the pedestrian can be calculated from

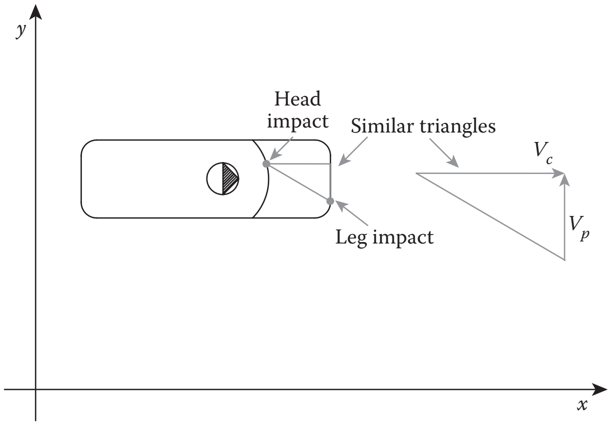

Figure 8.4 Vehicle—pedestrian impact damage.

$$V_p = V_c \frac{\nabla y}{\nabla x} \tag{8.10}$$

where

V_p = pedestrian speed
V_c = car speed
∇y = measurement along pedestrian path
∇x = measurement along vehicle path

It should be noted that the speed of the pedestrian is limited to within certain ranges. Walking speeds for healthy pedestrians range from 4 to 6 ft/sec. Olympic sprinters can cover 100 yards, or approximately 300 ft in 10 seconds or less or approximately 30 ft/sec. It is reasonable that healthy pedestrians can sprint at a speed approaching 20 ft/sec. It is also possible that the pedestrian was standing when struck by the vehicle. These guidelines for pedestrian speed give a reasonable measure of the calculations that are expected from this type of analysis. As with any analysis, care must be taken to ensure that the values obtained are within the capabilities of the pedestrian. For example, it would not be reasonable for an elderly female pedestrian to be sprinting at a speed of 15 ft/sec unless she had been an olympic athlete in her youth.

8.5 Vehicular Collisions with Pedestrians or Cyclists

Many of the methods outlined in this chapter or in other chapters can be employed in the reconstruction of collisions involving vehicles and pedestrians, bicycles or motorcycles. In particular, when properly employed, momentum techniques can yield accurate solutions to such reconstructions. An argument that is commonly employed against the use of momentum techniques is that it does not apply when there is a large discrepancy in the masses of the two objects. Recall that the theoretical development in Chapter 5 on momentum methods made no mention of mass differential. In fact, the equations of elastic collisions may be applied.

Before the development of modern sophisticated measurement techniques, muzzle velocities of bullets were conducted utilizing conservation of momentum. Recall that the total energy of a system is conserved, but the kinetic energy may not be conserved. Whether the collision is elastic or not, momentum is always conserved. This is the principle utilized in the ballistic pendulum that determined muzzle velocity of bullets. The experimental setup for these tests allowed a small mass object, the bullet, to make a completely inelastic collision with a body of considerably greater mass, a large block of wood. Before the collision, the momentum of the block of wood is zero because it is at rest. The momentum of the system after the collision must equal the momentum of the bullet before the collision. The velocity of the system after the collision is much smaller because of the large differential in mass and, thus can be determined much more easily than the velocity of the bullet. In Figure 8.5, the experimental setup for the computation of the bullet velocity is detailed. It should be noted that the masses of the bullet and the block of wood need to be known. It is also necessary to measure the vertical distance that the block of wood is displaced from the collision. As will be shown, these basic measurements are the only parameters that are required to give an accurate determination of the velocity of the bullet.

Since the bullet travels at a fast rate, the supporting ropes on the block remain essentially vertical upon impact. Thus the external forces in

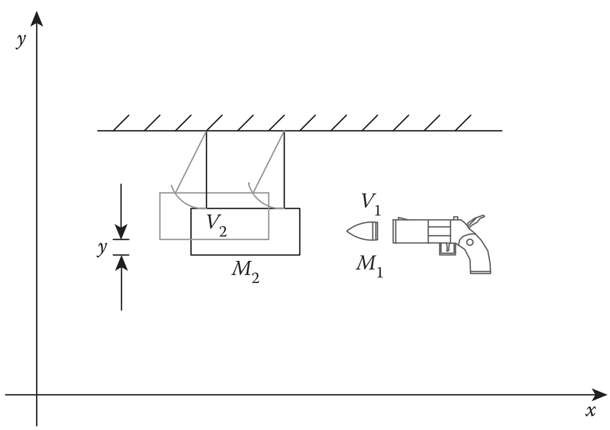

Figure 8.5 Bullet velocity.

the horizontal direction can be neglected and horizontal momentum is conserved. Then

$$M_1V_1 = (M_1 + M_2)V_2 \tag{8.11}$$

The kinetic energy just after the collision is,

$$E_{k2} = \frac{1}{2}(M_1 + M_2)V_2^2 \tag{8.12}$$

After impact, the pendulum swings until the kinetic energy is converted to gravitational potential energy, or

$$\frac{1}{2}(M_1+M_2)V_2^2 = (M_1 + M_2)g\,y \tag{8.13}$$

Solving the equations for V_1, we obtain,

$$V_1 = \frac{M_1 + M_2}{M_1}\sqrt{2gy} \tag{8.14}$$

As an example of how conservation of momentum can be used in pedestrian collisions let us assume the following scenario. A man is crossing a street with two lanes at a crosswalk. There is a large box truck stopped in the outside lane of traffic because the light is red. An inattentive driver in the inside lane does not realize that the light is red and continues to travel along the road not realizing that the pedestrian is crossing the street. Just as the pedestrian appears in front of the car, he sees the car and freezes in place. Unfortunately, the driver of the car is text messaging on his cell phone but sees the pedestrian. The driver reacts and applies the brakes at the point of impact. The car weighs 2000 lbs and the pedestrian weighs 200 lbs. After impact the car skids for a total distance of 10 ft with a frictional coefficient of 0.7. The pedestrian is immediately knocked to the ground and slides a distance of 20 ft with a sliding coefficient of 0.5. After impact, the car and the pedestrian both travel in a straight line. If we apply the momentum equations to this problem we find that after impact, the car was traveling 14.5 mph and the pedestrian was accelerated to 17.3 mph. At impact the car was traveling 16.23 mph and did not run over the pedestrian.

If we apply Equation 8.8 using the same value of 0.5 for the deceleration under sliding conditions, we obtain a car speed of 11 mph. Remember that Equation 8.8 is empirical and may not apply under all cases. Since the pedestrian was accelerated to 17.3 mph according to momentum, the car speed may be lower than the calculated speed of 16.23 mph. We might say that the car was traveling the average of the two calculations or approximately 13.6 mph. If we further assume that the speed limit along this street was 25 mph we could say to a high degree of engineering certainty that the car was not speeding but that the driver was inattentive. For the momentum example, if the car skidded for 10 ft before impact, the car was traveling approximately 21.8 mph and was still not speeding.

Geometrical Characteristics of Highways

9

9.1 Introduction

Most highways have been and are properly designed and constructed. The federal highway system, the various states, and municipalities have ongoing programs that maintain our highways. In some instances, the design, construction, and maintenance of a highway can play a role in the cause of a vehicular collision. It should be emphasized, however, that this is seldom the case. The type of highway is of upmost importance in the determination of contributory circumstances relative to the reconstruction.

The simple fact is that highways are designed for the terrain, traffic flow, and utilization of the particular artery. As such, slope, elevation, cross slope, width, drainage, curvature, visibility, and surface type, as well as other factors, determine the signage and speed limits imposed on the particular highway. In certain circumstances, the design of the road elements may be improper, the construction may be substandard, or the maintenance may be faulty. Only when one or more of these items can be related to an event such as a collision should they be considered as contributory. For example, if the pavement drop-off is excessive, according to recognized standards, but there is no evidence that the vehicle careened off the edge, overcorrected, and lost control causing an accident, then the pavement drop-off cannot be considered in the reconstruction. Note that emphasis is placed on recognized standards.

The three elements that must then be considered with respect to roads are design, construction, and maintenance. The questions that must be asked are: (1) was the roadway designed according to recognized standards, (2) was the road constructed in accordance with the design standards, and (3) was the road maintained according to recognized standards. Note that when we refer to the road we are speaking in terms of all the general characteristic elements of the road. These include geometrical considerations, signage, traffic control, visibility, and obstructions.

The first element deals with the design of the road. The American Association of State Highway and Transportation Officials (AASHTO) promulgates "*A Policy on Geometric Design of Highways and Streets*." The publication, which is often referred to as the "*Green Book*," is produced by a task force representing many of the states and some peripheral organizations and is updated on a regular basis. The policy is the design standard in the United States. The serious reconstructionist should be integrally aware of the standards.

Highway design must consider the following factors:

- Functional classification of the highway being designed
- Expected traffic volume and vehicle mix
- Design speed
- Topography for the selected highway location
- Level of service
- Funding safety
- Social and environmental concerns

While many of these factors are interrelated, there is a hierarchy when determining which factor will principally control the design. The list above is ordered in accordance with a "top-down" hierarchy.

The second element deals with the construction of the road. The design standards are generally on file with the appropriate regulatory agency. Accordingly, the as-built plans are also on file. If it is deemed that the design is proper but a question arises as to the construction, then an engineering survey can determine the suitability of the construction of the roadway and its conformance with the design.

Assuming proper design and construction, the third element involves maintenance operations that may be important in the reconstruction of an incident. In this instance each state has publications for maintenance operations and for traffic control during those operations. For any of the three elements listed above, there are three subelements that include geometrical considerations, visibility, and signage. Signage is generally regulated by the Manual of Uniform Traffic Control Devices (MUTCD).

9.2 Classification and Design Speed

In assessing a particular road, proper classification is essential. Requirements for a high volume road may not be applicable for a low volume road. Traffic demand is commonly referenced by the average daily traffic (ADT). A projected volume, referred to as the design hourly volume (DHV), is usually taken as a percentage of the expected ADT.

There are five major categories of highways. These are principal arterials, minor arterials, major collectors, minor collectors, and local roads and streets. Principal arterials, which generally include freeways and interstates, are interconnected with or augmented by the minor arterial system.

Collector systems convey traffic from local roads to the arterials. Rural and urban areas may have components of all five types of highways. Rural highways are normally characterized by lower traffic volumes, higher speeds, fewer turning conflicts, and fewer conflicts with pedestrians. In contrast urban areas are characterized by lower speeds, wide variations in traffic volume, narrower travel lanes, frequent intersections, significant numbers of pedestrians, reduced visibility, and more numerous roadside obstacles.

The design speed of a highway depends primarily on its classification and topography of the area. Design speed is defined as the "maximum safe speed that can be maintained over a specific section of highway when conditions are favorable such that the design features of the highway govern." These speeds range between 20 and 70 mph in 10 mph increments. The maximum design speed of 70 mph represents the highest speed that can be traveled under optimum conditions.

However, many drivers are oblivious to speed limits. Some assume that they are good drivers that can safely drive 10, 20, or 30 mph above the imposed limits. What these drivers fail to realize is that speed limits are determined after careful consideration, detailed scientific studies, and statistical analysis of human response. They also fail to realize that driving on the highway is a chaotic experience. There are too many unknowns so that predicting a particular outcome is practically impossible. On a congested highway it is not possible to determine what actions the drivers around your vehicle may make or if an unexpected event may occur. At best, the system is controlled chaos. There is no question that some drivers are better than others, that their reflexes are faster, their vision better, that they are more physically fit, and younger. The most gifted of these individuals are race car drivers or jet pilots. They are the exception rather than the norm. Highways are designed for the norm and not the exceptional driver and thus, speed limits are designed accordingly.

A truly exceptional human being in terms of reaction was the late Scott Crossfield. Scott Crossfield was deemed to be the fastest man on earth because he was a lead pilot on the X-15 project who flew faster than anyone else at that time to a speed of Mach 3. He was the designer and record setter for the X-15 project. For the younger generation or for those not aware of the X-plane projects we offer this brief explanation.

The X-plane projects began with the X-1 plane that broke the sound barrier and was piloted by legendary pilot Charles "Chuck" Yeager. At that time he was the fastest man on earth. Subsequent X-planes were designed and piloted to faster speeds culminating in the X-15 project. During the original flights of the X-15 project, when he flew in excess of 2000 mph, Scott Crossfield was "pushing the envelope" in the parlance of the test pilot. Many years later, in an interview about those record setting days, Scott Crossfield likened pushing the envelope to driving in excess of 70 mph. In essence, when we drive in excess of 70 mph we are taking unnecessary risks and exceeding the design characteristics of interstate highways.

9.3 Cross Sectional Elements

The basic cross sectional elements of a highway include the travel lanes, shoulders, and medians. Secondary elements include curbs, ditches, guardrails, and roadside barriers. Figure 9.1 details the typical elements of a two-lane highway (top of figure) and multilane highway (bottom of figure).

The width of the travel lane is dependent on its classification. Most arterials and high traffic volume (ADT) roads are 12 ft in width. Two lane rural roads may be reduced in width to 10 or 11 ft. However, reduced lane width is a contributing factor to higher accident rates and is therefore not employed unless the design speed is low.

Shoulders are the portions of the roadway that bound the edge of the travel lanes. Wide, paved shoulders are required for high ADT roads to facilitate emergency stopping. Narrow, gravel shoulders are common on two lane, rural roads. Shoulders are intended to be flush with the adjoining traffic lane and sloped to promote surface water drainage away from the road. Shoulders composed of gravel must be compacted and stable to support the load of a vehicle tire. If the gravel rapidly consolidates under the load of a moving wheel, the elevation drop may cause the vehicle to strike the exposed edge of the pavement and thereby cause the driver to lose control of the vehicle. As such, design and construction methods for

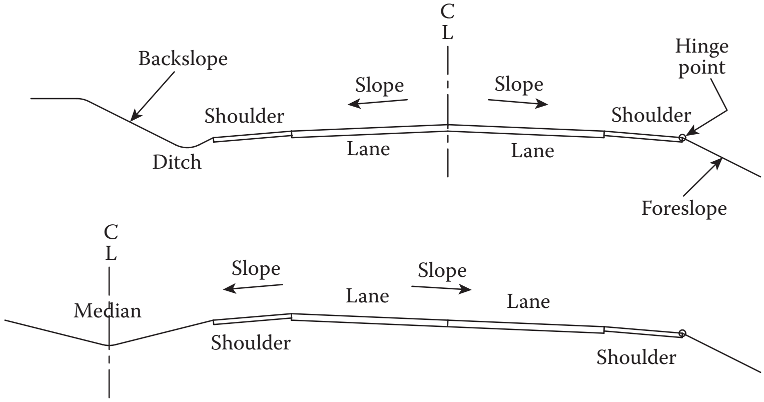

Figure 9.1 Highway elements.

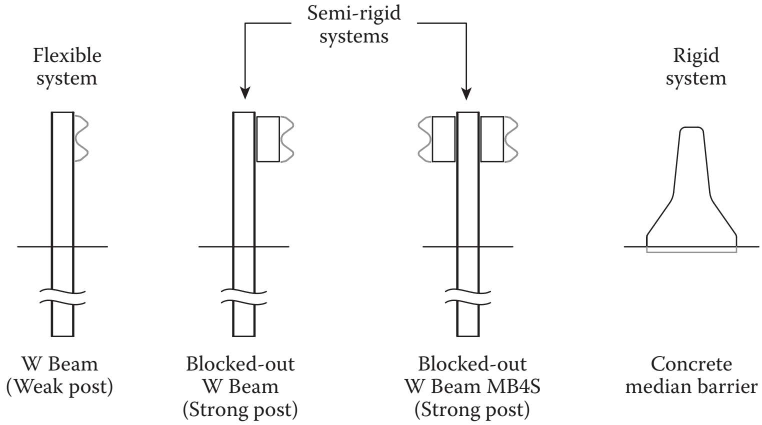

Figure 9.2 Barrier systems.

a shoulder are as important as ensuring adequate pavement strength for the traffic lane.

Medians are normally employed for high ADT roads and provide a variety of functions. Separating opposing lanes of traffic, providing an emergency stopping area, and mitigating headlight glare from opposing traffic are among the benefits of a median. The width of a median may range between 2 ft and in excess of 80 ft. In urban areas, the medians are typically narrow and flush or raised above the road, given the right-of-way restrictions. For multilane highways, the medians are normally depressed to provide drainage for surface water.

Roadside barriers are longitudinal systems that are used to protect vehicles from hazards on the roadside. These hazards may include a high wall or sharp drop off the side of the road. Guardrails are a subset of roadside barriers that are normally employed for sharp curves and large elevation changes at the edge of the roadway. Median barriers prevent a vehicle from crossing a divided highway into opposing lanes of traffic. Barrier systems may be flexible, semi-rigid, and rigid. Examples of these systems are shown in Figure 9.2. The selection, location, and designing of these systems depends on the road classification and hazards present. Standards such as the *Roadside Design Guide* base the selection of a system on a cost-benefit analysis.

9.4 Traffic Control Devices (TCDs)

Traffic control devices (TCDs) notify drivers of regulations and provide warnings and guidance to ensure safety and efficiency on the roadway. In general, these devices include road markings, signs, traffic signals, and controls.

The design, placement, operation, and maintenance of TCDs is governed by the MUTCD. The requirements set forth in the MUTCD vary depending on the road classification, design speed, and traffic volume. Additionally, specifications for school areas, bicycle facilities, and railroad crossings are covered in this standard. As indicated by the acronym, MUTCD was intended to ensure uniformity in the use of signs and markings.

Markings control traffic and encourage safe operation of vehicles. Pavement markings include centerline stripes, lane lines, and edge stripes. Crosswalk lines, stop bars, as well as words or symbols may also be used. Object markings are needed on physical obstructions that can not be feasibly removed. Reflective paint or the use of floodlighting may be employed to illuminate the obstruction. Delineators, whether post or road-mounted, are primarily used to guide nighttime traffic.

The three main types of signs are regulatory, warning, and guide. Regulatory signs indicate the rules for traffic movement, while warning signs reveal conditions that may involve risk. Guide signs are used to direct traffic along a specific route. Traffic signals control vehicle and pedestrian movement by assigning right-of-way. These signals may be timed or activated by the presence of traffic.

The effectiveness of TCDs depends on five requirements: that they fulfill a need, command attention, clearly and simply convey meaning, command respect from users of the road, and provide sufficient response time. For example, warning signs must be clearly visible to oncoming traffic and be positioned in such a way so that drivers can comprehend and react appropriately to the warning. This principle of sight distance is the topic of the following section.

9.5 Sight Distance

A basic principle of road design is sight distance relative to speed of travel. Safety and efficiency depends on a driver's ability to see oncoming traffic, pedestrians crossing the road, or potential hazards. Road curvature, intersections, and obstructions affect a driver's sight distance. In addition to these geometric factors, the design of a road must also consider stopping maneuvers, passing maneuvers, decisions for complex scenarios, and measurement criteria. A designer or forensic engineer may need to consider sight distance with respect to stopping, passing maneuvers, and more complex situations that involve gauging a driver's decision-making process.

In addition to the distance traveled by a vehicle while braking, stopping sight distance (D_{SSD}) includes the distance traveled by a vehicle immediately after the driver perceives a hazard to the point the driver applies the brakes. The initial process is based on the driver's perception and reaction time (t_R).

This time interval depends on the driver's ability to perceive and identify a stimulus, decide on the appropriate action to take, react to the stimulus, and execute a maneuver. Given an initial speed "v" and deceleration "a," the stopping sight distance is governed by:

$$D_{\mathrm{SSD}} = D_R + D_B = vt_R + \frac{v^2}{2a} \tag{9.1}$$

The acceleration is the product of the braking coefficient (μ) and acceleration due to gravity ($g = 32.2$ ft/s^2). Thus, Equation 9.1 can be expanded as follows:

$$D_{\mathrm{SSD}} = D_R + D_B = vt_R + \frac{v^2}{2\mu g} \tag{9.2}$$

This equation can be modified to include the effects of grade, whether the vehicle is traveling uphill or downhill. Reflecting grade in terms of a percentage "G" equal to the rise (or fall) of a road across a 100 ft distance, Equation 9.2 is modified as shown below:

$$D_{\mathrm{SSD}} = D_R + D_B = vt_R + \frac{v^2}{2(\mu \pm G)g} \tag{9.3}$$

According to the *AASHTO Green Book*, roads designed to include stopping sight distance are based on reaction times of 2.5 sec and decelerations of 11.2 ft/sec^2, or roughly 0.35 g's. These values are conservative and include a significant safety factor. Perception and reaction time studies referenced in the *Green Book* indicate that minimum brake reaction times vary between 0.64 and 1.64 sec. However, the recommended design value of 2.5 sec was chosen to include the reaction times needed by all drivers under most highway conditions. The design criterion exceeds the 90$^{\text{th}}$ percentile of reaction time for all drivers. Similarly, the 0.35 g deceleration level was chosen based on studies which showed that 90% of all drivers were able to decelerate at a greater rate.

Stopping sight distances are sufficient for most circumstances for alert drivers to come to a complete stop. A driver's ability to perceive and react is negatively affected for complex situations, such as those at multiphase intersections and ramp terminals. Where it is imperative to provide longer sight distances, the designer may implement decision sight distances, which provide drivers an additional safety factor. Additionally, the added time may provide an alternate maneuver to stopping, such as reducing speed or swerving. The *Green Book* identifies five alternate avoidance maneuvers when considering decision sight distance. For example, the perception/reaction time included in Equations 9.1 through 9.3 is increased to 3.0 sec for a stop on a rural road.

The *Green Book* also outlines criteria for ensuring adequate sight distance for passing scenarios. Passing sight distance (D_{PSD}) includes distances traveled in four stages of a passing maneuver. For a two-lane highway, these stages include:

d_1 = The distance traveled during the reaction phase and initial acceleration while encroaching to the left lane.
d_2 = The distance traveled while the passing vehicle is in the left lane.
d_3 = The distance between the passing vehicle at the end of its maneuver and the vehicle traveling in the opposing direction.
d_4 = The distance traveled by an opposing vehicle for two-thirds of the time the passing vehicle is in the left lane (two-thirds of d_2).

The distances traveled in the second, third, and fourth stages are based on studies performed for various highway speeds. These values are reflected in the *Green Book*. The governing equation for d_1 is dependent on the time of the initial maneuver (t_i), the average acceleration (a), the average speed of the passing vehicle (v), and the difference in speed between the passed and passing vehicles (m).

$$d_1 = t_i\left(v - m + \frac{1}{2}at_i\right) \tag{9.4}$$

The criteria for measuring sight distance includes the height of the driver's eye, sight obstructions, and the height of an object that must be viewed by the driver. A driver's eye is assumed to be at a height of 3.5 ft above the road surface, which is based on average vehicle heights. This height may be increased to 7.6 ft for larger trucks. The object criteria varies for stopping and passing sight distances. For instance, the stopping sight distance object is assumed to be 2.0 ft in height, which represents the size of an object that might potentially be encountered in the road. Consideration of smaller objects results in longer vertical crests without an appreciable increase in safety. A passing sight distance object is considered to be 3.5 ft in height. This height is based on a 15th percentile vehicle height minus an allowance, which results in a portion of the vehicle height that needs to be visible for another driver to properly identify the presence of a passing vehicle.

Sight obstructions must be considered for horizontal and vertical planes. Guardrails, telephone poles, and trees may encroach into the roadway so that the site distance across a horizontal curve is affected. For vertical curves, the curvature of the road across a crest or a low hanging tree or bridge across a sag may obstruct a driver's view. Frequently, a forensic engineer is asked to determine if obstructions hinder visibility for a particular road, which may indicate that the obstruction contributed to an accident. While less common, the design of the roadway itself (horizontal curvature and rate of vertical curvature) may also be called into question. The following sections will examine design requirements for horizontal and vertical alignment. As with road widths, alignment depends primarily on the design speed of the road.

9.6 Horizontal Curves

Horizontal curves are present in four forms: simple, compound, reversed, and spiral. In the interest of brevity, simple circular curves will be presented. With modern surveying and computer-aided drafting, the trigonometric equations are normally not of great concern to the forensic engineer. However, the following represents a primer for examining the design of a horizontal curve and its relationship to sight distance. Consider Figure 9.3.

Basic trigonometric relationships between the curve radius, chord length, deflection angle, and other variables are shown in Equations 9.5a through c.

$$T = R\tan\frac{\Delta}{2}$$

$$C = 2R\sin\frac{\Delta}{2} \qquad (9.5a–c)$$

$$M = R\left(1-\cos\frac{\Delta}{2}\right)$$

The length of the curve is defined as the sight distance (S) if the curve extends along the sight line of a driver.

$$S = \frac{R\Delta\pi}{180} \qquad (9.6)$$

The limiting requirements for the radius of a curve (R) depend on the design speed (v), super-elevation (e), and side friction factor (μ_S) as shown in Equation 9.7.

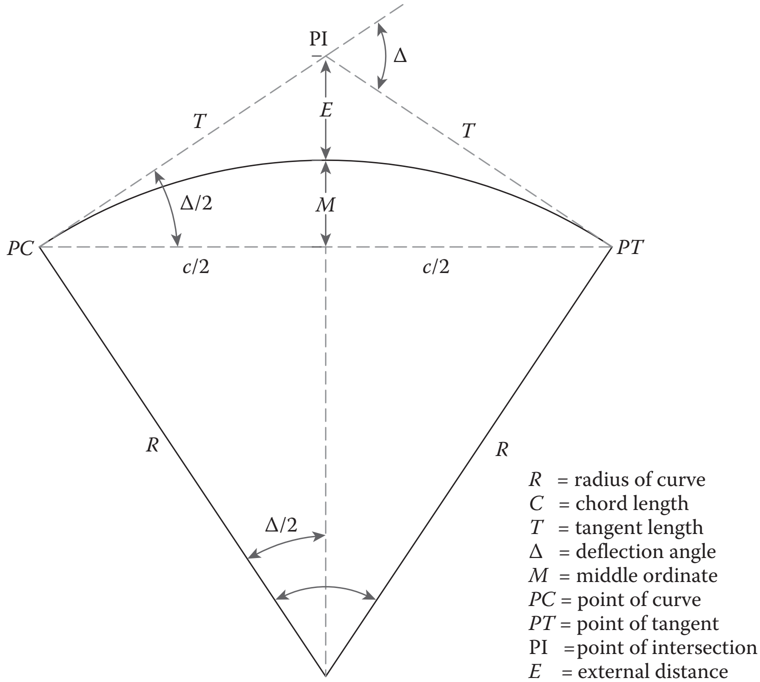

Figure 9.3 Typical layout of a simple horizontal curve.

$$R = \frac{v^2}{15(e + \mu_S)} \tag{9.7}$$

The conformance of a road's radius can be checked against known values at the right side of this equation. For example, an engineer may be asked to survey the site of an accident where the client's vehicle lost control through a simple horizontal curve. The survey revealed a super-elevation of 6.0% for the 50 mph road. The road radius was measured to be less than 750 ft. However, the minimum allowable radius based on Equation 9.7 and a limiting side friction factor of 0.14 is 835 ft. In this case, it can be concluded that the designer improperly selected a sharper curve radius than was allowed, which may have contributed to the accident. A proper design should have specified either a reduced speed or increased super-elevation.

The sight distance across a horizontal curve is depicted in Figure 9.4. As with the preceding example, the adequacy of a road design can be examined based on the minimum specifications and physical requirements. The aforementioned survey may have revealed a minimal sight distance in addition to an insufficient road radius. This survey revealed that a row of trees oriented close to the road presented an obstruction for vehicles traveling in the

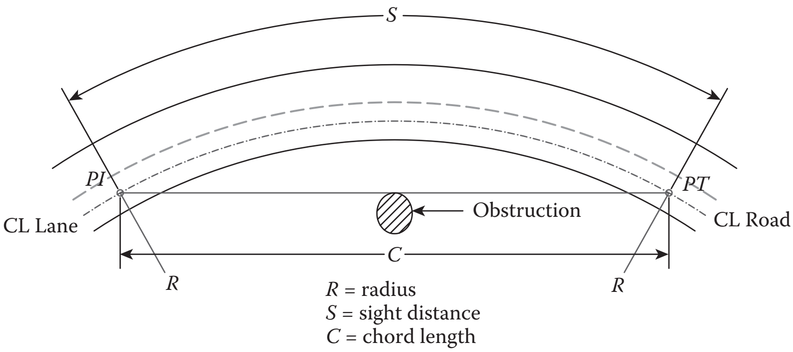

Figure 9.4 Sight distance across a horizontal curve.

inside lane. The estimated sight distance was determined to be roughly 350 ft. From Equation 9.2, the minimum stopping sight distance for a level road ($G=0$) and design reaction time (2.5 sec) is 425 ft for the 50 mph road. In this case, it would be revealed that the design was not performed in accordance with minimum standards with respect to radius and stopping sight distance.

9.7 Vertical Curves—Sag and Crest

Unlike horizontal curves, vertical curves are not circular in radius. Rather, they are intended to provide a gradual change in grade. The changing curvature is best described by a parabolic shape. Figure 9.5 outlines two types of vertical curves: crest and sag. Note that vertical curves may not change merely from uphill to downhill or vice-versa. For example, a vertical curve will be present when an uphill slope slightly increases or decreases but remains positively graded. An increase in grade will create a sag while a decrease in grade will form a crest, regardless of the initial slope.

In general, a designer should utilize graphical methods to check sight distances for alignment curves. Based on the simple equations for a horizontal circular curve, the equations to check for sight distance can be presented in closed form. Given the parabolic nature of vertical curves, graphical solutions are simpler to examine. Figure 9.6 demonstrates the sight distance across a crest in a vertical curve. Here, the sight distance (S) exceeds the length of the curve (L) between the two tangent points.

Since the vertical crest is approximated by a parabolic shape, the middle distance (X_3) is half of the curve length ($L/2$). The distances X_1 and X_2 can be found in terms of the respective grades and their algebraic difference. Graphical methods are utilized to find the sight distance (S) when it is exceeded by the curve length (L). Equations 9.8 and 9.9, respectively outline

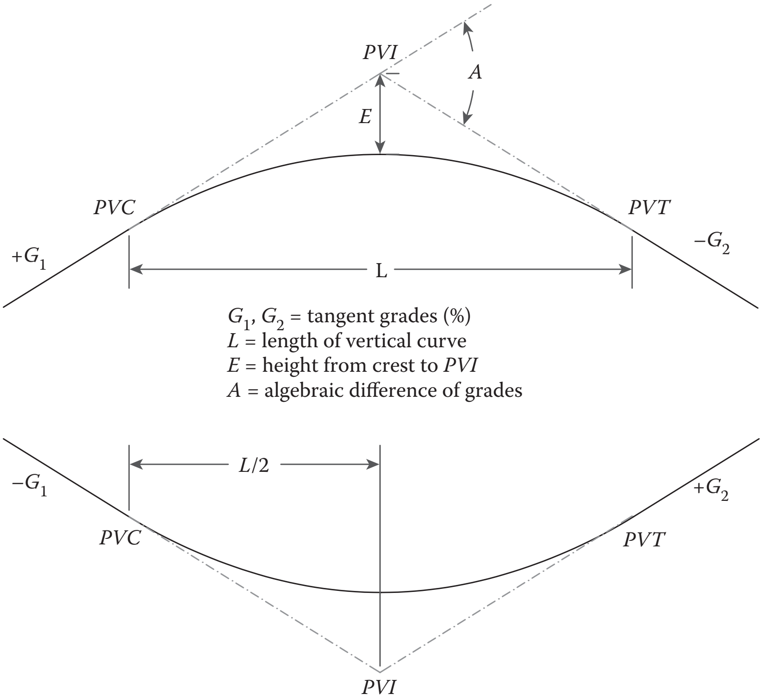

Figure 9.5 Vertical curves.

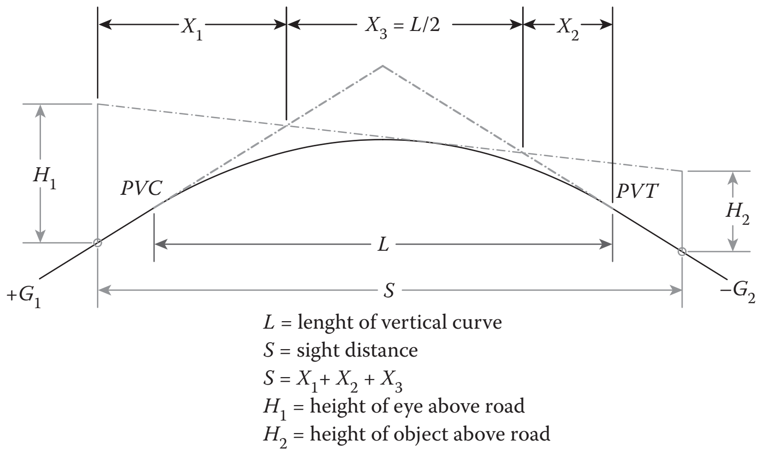

Figure 9.6 Sight distance across a vertical curve.

the minimum allowable length of vertical curves where the sight distance exceeds the length ($S > L$) and when it does not ($S < L$).

$$L_{\text{MIN}} = 2S - \frac{200\left(\sqrt{H_1} + \sqrt{H_2}\right)^2}{A} \quad (S > L) \tag{9.8}$$

$$L_{\text{MIN}} = \frac{AS^2}{100\left(\sqrt{2H_1} + \sqrt{2H_2}\right)} \quad (S < L) \tag{9.9}$$

9.8 Conclusions

This chapter represents a basic introduction to highway design and a few transportation engineering principles. While certainly not exhaustive, the referenced standards and equations provide the engineer with useful tools that are frequently utilized in a forensic investigation.

When conducting an investigation with regard to adequacy of the road, the first questions that must be asked are: what is the classification of this road and what are the applicable standards? The contribution of design, construction, or maintenance of a road to a specific accident is wholly dependent on answering these questions correctly.

The forensic engineer must keep in mind that the requirements of a high speed freeway are quite different than a low volume, rural road. Not only do the stopping distances increase in orders of magnitude with increased speed, regulations for high speed roads are also quite different. Thus, it is imperative that the engineer be intimately familiar with applicable and current standards.

Train Accidents

10

10.1 Introduction

Train accidents from a reconstructionists standpoint are limited to the interaction of the train with a vehicle, a pedestrian, a motorcycle, or a bicycle. It is not the purview of the reconstructionist to determine the factors affecting a train accident involving derailment, or collisions between trains. Those types of accidents are investigated by Federal agencies such as the National Transportation Safety Board (NTSB). In order to determine the interaction of the train with the vehicle or the pedestrian, it is necessary to quantify the speed of the train before braking and at impact. These calculations include train stopping distance and the time involved as well as many other factors that will be outlined in this chapter. Some of those factors include train design elements and the elements of rail-highway crossings. The calculations involving the other vehicle or pedestrian are extensively covered in other chapters.

Trains are allowed to move throughout the country at various speeds depending on the geometric design of the tracks and the particular section of the track through which they are traversing. Because trains are so significantly massive, can travel at fast speeds, and have low coefficients of friction for stopping, the most significant factors include the radius of the curve and the slope of the track. Generally, the slope of the track is limited to 5% and the radius of the curve to approximately 700 ft. According to the *Code of Federal Regulations* CFR 49, railroad tracks are divided into six classes as outlined in Table 10.1.

Trains are allowed to run according to an order, a time table, and a block through which the train is traversing. The train speed is determined from the class of the block though which the train travels. Each section of track can be different than the adjoining block of tracks. Consequently, the systems that signal the particular block specifies the maximum speed for that section.

The Association of American Railroads issues railroad operating rules which are referred to as *The Standard Code of Operating Rules*. These rules govern the activities of the train crew including crew members, the conductor, and the engineer. The rules also include the train operations while the train is approaching, passing though, or occupying the grade crossing. The use of headlights, bells, whistles, and horns at particular sections of the track is also specified. The train speed and the use of the brakes are also specified within these rules.

Table 10.1 Classification and Train Speed

Passenger Trains (mph)	Freight Trains (mph)	Track
N/A	10	Expected Track
15	10	Class 1
30	25	Class 2
60	40	Class 3
80	60	Class 4
90	80	Class 5

As previously mentioned, most of the information concerning a train accident is gathered by the NTSB and is beyond the scope of the private forensic engineer or accident reconstructionist. Considerations relative to the inspection and performance of the various systems of the train are beyond the scope of such investigators so that those factors can only be determined from the various reports issued by the investigating and regulatory agencies. However, there are calculations and determinations that can be performed by the reconstructionist.

10.2 Train Resistance and the Effect of Curvature and Grade

All trains are affected in their ability to brake because the coefficient of friction is between steel and steel, the wheels on the tracks, which is significantly lower than rubber on the road for motor vehicles. Please refer to Table 4.1. The curvature of the track increases the resistance to roll of the train while the grade may increase or decrease the coefficient of friction depending on whether the train is going up or down a grade. The effect of the grade is simply adjusted as determined in Chapter 4. The effect of track curvature on the grade resistance experienced by the train is determined from empirical relations as,

$$\text{Grade correction} = 0.04 \times \text{Degrees of curvature}$$

The resistance of the train on the track is determined from an equation attributed to W.J. Davis who performed the tests for General Electric. The Davis equation, as it is known, is given by

$$R = 1.3 + \frac{29}{W_a} + 0.045V + \frac{0.0005\,A\,V^2}{W_a N} \tag{10.1}$$

where

R = train resistence (lbs per ton of train weight)
W_a = train weight in tons per axle

V = train speed in mph
A = average car cross-sectional area in square feet
N = number of axles per car

The Davis equation applies to smaller cars weighing between 40 and 50 tons. For larger cars, weighing between 70 and 100, tons the modified Davis equation is used and is given

$$R = 0.6 + \frac{20}{W_a} + 0.01V + \frac{0.07V^2}{W_a N} \quad (10.2)$$

10.3 Computation of Train Speed

The determination of the speed of the train before brake application and the stopping distance are critical in the reconstruction of train vehicle collisions. Various methods for the determination of the train speed will be presented in this section. If a train is traveling along a set of tracks and the conductor sees an approaching vehicle at the crossing, he may apply the emergency brake system in the train. The train speed at impact may be calculated from Equations 4.27 through 4.31. It should be noted that corrections must be made to the coefficient of friction depending on the curvature and the grade of the track. The key in determining train speed and stopping distance by this method is to appropriately select the correct value of coefficient of friction. The coefficient of friction can be determined by consulting published values or it may be alternatively calculated. Published values of coefficient of friction can vary widely. Full service braking coefficients of friction vary from 0.07 to 0.14. In contrast, emergency braking coefficients of friction vary between 0.11 and 0.14.

The coefficient of friction may be calculated by multiplying the shoe/wheel coefficient of friction by the maximum net braking ratio. The shoe/wheel coefficient of friction is generally a function of the type of brake shoe used on the train. Cast iron shoes have a coefficient of friction against the wheels of approximately 0.15 while COBRA shoes have a value of approximately 0.3. For a train with an air brake system the coefficient of friction for the cars or locomotives is

$$\mu = \mu_{sw} B_{rm} \quad (10.3)$$

where

μ_{sw} = shoe/wheel coefficient of friction
B_{rm} = maximum net braking ratio

and

$$B_{\rm rm} = \frac{(0.79d^2)(N_c)(B_{cp})(R_l)(e)}{w} \tag{10.4}$$

In Equation 10.4, the following parameters are defined as

d = brake cylinder diameter in inches
N_c = number of brake cylinders
$B_{\rm cp}$ = brake cylinder pressure in pounds per square inch gage (psig)
R_1 = lever ration of the cylinders
w = car weight in pounds
e = efficiency of the rigging

The braking ratio as outlined above can vary widely. Typical variations are between 20 and 50%. Consequently, the methods outlined above are problematic in their implementation. Additionally, the investigation may not yield the necessary information in order to compute the coefficient of friction within engineering accuracy. A significant factor in the error can be due to the lack of information concerning the rigging efficiency of the train.

The speed of the train before brake activation can be determined from the approximate equation given below

$$V = \frac{21}{W}\left[F_R t_a + \sqrt{(F_R t_a)^2 + 0.065 D_b F_R W}\right] \tag{10.5}$$

where

$$t_a = \frac{t_s + t_b}{2}; \qquad t_s = \frac{L_t}{930\ \text{ft/sec}} \tag{10.6}$$

and

$$F_R = \sum\left(N_c B_{\rm rc} w_c f_c \left[\frac{B_{\rm cpc}}{50}\right]\right) + \sum\left(N_l B_{\rm rl} w_l f_l \left[\frac{B_{\rm cpl}}{50}\right]\right) \pm gW \tag{10.7}$$

In the equations above, the following parameters are defined as

t_a = half time for brake activation
t_s = signal time velocity
t_b = brake cylinder buildup time = 11 sec
D_b = train stopping distance in feet

L_t = length of train in feet
W = total train weight in tons
g = algebraic grade of the track including curvature correction
N_c. and N_1 = number of cars and locomotives
B_{rc}.and B_{rl} = car and locomotive net braking ratios at 50 psig
B_{cpc} and B_{cpl} = car and locomotive brake cylinder pressure (psig)
w_c and w_1 = car and locomotive tare weight in tons
f_c. *and* f_1 = car and locomotive brake/shoe coefficient of friction

The braking distance traveled by the train can be calculated from basic relationships developed in Chapters 2 and 4. We define,

$$D_b = D_{\text{bfb}} + D_s \tag{10.8}$$

where

D_{bfb} = braking force buildup time distance
D_s = stopping distance

The buildup time distance in feet is determined from the half time for the brakes to produce full pressure as defined in Equation 10.6, thus,

$$D_{\text{bfb}} = 1.466Vt_a \tag{10.9}$$

The stopping distance is developed from the work energy principle including a 5% increase in the stopping distance to account for the kinetic energy of the axles and wheels. Then,

$$\frac{1}{2}\left(\frac{W}{32.2}\right)V^2(1.466)^2(1.05) = F_R D_s \tag{10.10}$$

Substituting into Equation 10.8 we obtain the distance traveled by the train during braking as,

$$D_b = 1.466Vt_a + \frac{0.035WV^2}{F_R} \tag{10.11}$$

Train speeds and vehicle speeds can also be calculated by traditional methods outlined in Chapters 2, 4, and 5. For example, train speed can be calculated by momentum methods. Recall the section where one mass was significantly greater that the other mass. This analysis is summarized in Equations 5.7a and b. In some instances the crush deformation of the vehicle can be used to determine the change in velocity experienced by that vehicle and can then be used along with standard techniques to determine preimpact and postimpact speeds of the vehicle.

10.4 Train Manifest and Recorders

Trains in the United States are governed by general orders, schedule, and time tables within the blocks along the track. Once the section of the block where the accident occurred has been identified, information concerning the characteristics of the train can be gathered. This information includes the number and type of engines and cars in the consist. This information should also include the train manifest. Most trains including freight and passenger, have event recorders. These recorders vary in type, however they all log the train speed, the time, and the distance traveled. Some recorders may also include throttle position, load amperes, and brake pressure. These recorders may be electrical, hydraulic, or mechanical depending on the age of the locomotive. The display of the information of the recorders can also vary from strip chart types to magnetic or electronic types. The input to the recorders may be analog signals or digital data. The train manifest outlines the cargo that is being carried including the weight of the cargo. This information is necessary in order to calculate the train speed as outlined in the previous section. Generally, this information is not available without the involvement of legal action. Legal action may also be necessary in order to review the accident report by the railroad company or the accident investigation by the NTSB or other governmental agencies. Dispatchers' train sheets and transcripts of conversations with the train can also provide valuable information with respect to the activities surrounding the incident. Generally, police reports are readily obtained by the investigating reconstructionist or forensic engineer.

In railroad accidents it is important to accurately document the site through photographs, measurements, and possibly video. Video offers the opportunity to view how vehicles or pedestrians react to trains as they pass through the crossing. The measurements and photographs document the crossing geometry and whether signage and barriers affected the collision. Grade crossing accident data may also be available. The safety regulations and operating rules for railroads under the *Code of Federal Regulations* may also shed light and should be reviewed.

10.5 Train Crossings

Traditionally, the railroad tracks and the crossings are owned by the railroad. The standard track normally has a right of way of 60 ft for a single set of tracks. This right of way is measured on either side of the track for a distance of 30 ft. In the case of double tracks or multiple tracks, the right of way is generally measured from the center of the outermost tracks. In some instances, tracks may have been removed so that the right of way is not clearly determined. In those cases it may be necessary to request railroad right of way maps through the discovery process. There are some isolated incidents of collisions between pedestrians along the right of way and not within a designated crossing. However, most railroad incidents occur at rail grade crossings. Thus, special consideration is placed on the geometry of the crossing and the approach highway.

Approximately one third of the railroad crossings in the United States have active warning devices that inform the driver of a vehicle when a train is approaching the crossing. Two thirds of those crossings have passive warning devices. About 5% of all crossings had no warning devices as of 1990. The crossings without any warning devices are in rural areas where there is generally no obstruction to visibility. Since 1973 when the Federal Highway Safety Act was passed, federal funding has been earmarked for the improvement of railroad crossings including active warning systems and highway grade crossing realignment. The American Association of State Highway Officials (AASHTO) *A Policy on Geometric Design of Highways and Streets* and the Manual on Uniform Traffic Control Devices (MUTCD) formulate the standards relative to railroad crossings.

State highway agencies and the railroads have a duty to ensure the general safety of the public that uses the railroad crossings in the United States. This duty includes the clearance of obstructions to visibility, proper utilization and placement of warning devices, and design of relatively easy to traverse crossings. Irrespective of the propriety of the crossing, many motorists fail to obey warnings, signals, and gates. Therefore, there is also a legal requirement for the motorists in that they must follow the rules of the road.

The traffic control devices as outlined in the MUTCD are summarized as follows: The devices include signs, signals, and road markings along the road. Special consideration is placed on the avoidance of conflicts between the railroad signals and any highway signals and markings. Traffic control devices may be either passive or active. Passive traffic control devices include markings at pavement, signs, and illumination. The MUTCD lists all the different types of passive traffic warning devices required at railroad grade crossings. The most recognizable sign is the crossbuck. The crossbuck can become an active warning device with the addition of flashing lights mounted on the pole of the crossbuck. The flashing lights along with coordinated bells and the addition of gates at the crossing provide greater active warnings at railroad grade crossings. These active devices are controlled automatically and generally are activated 20 seconds before the arrival of the train at the crossing.

Figure 10.1 Conflicting signals.

In some instances traffic signals at highway intersections can conflict with the signals for the railroad grade crossing. Traffic signals on either side of the crossing can cause an entrapment of vehicles along the highway. The traffic signals may be on either side of the crossing or on both sides. This type of occurrence may only happen during certain times of the day at busy intersections and crossings. Generally engineering studies are required to determine if there is a conflict between the traffic signals and the railroad crossing signals. If the traffic signal is far enough away from the crossing, there may not be a conflict. However, if the traffic signal is near the crossing, especially in industrial settings where large vehicles predominate, particular attention is necessary. Large vehicles such as tractor trailers have lower values of acceleration and braking and are, therefore, more susceptible to the dangers of collisions with trains. Figure 10.1 shows a conflict between a railroad crossing and a traffic signal along the highway.

10.6 Sight Distance Triangle

In Chapter 9 we introduced the concept of the sight distance triangle. The triangle as applied to railroad crossings is essentially the same as developed in the previous chapter with the modifications for the parameters of the train crossing. Train and vehicle speeds determine the sight distance triangle. Please refer to Figure 10.2. Since trains require long distances to stop, it is not reasonable to expect the train to stop for oncoming traffic. Therefore, the triangle defines the distances along the highway and along the tracks corresponding to the train and vehicle speeds so that the vehicle can either stop

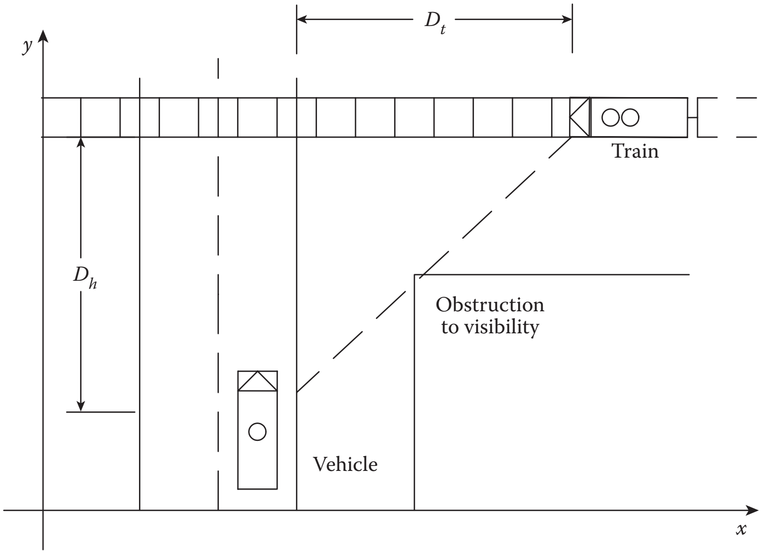

Figure 10.2 Sight distance.

before crossing or safely cross the tracks before the train arrives. The triangle assumes that an obstruction to visibility exists although that may not be the case. The distance along the highway is given by,

$$D_h = V_c T_r + \frac{V_c^2}{2g\mu} + D_c + D_v \tag{10.12}$$

and the distance along the tracks is

$$D_t = \frac{V_t}{V_c}\left[V_c T_r + \frac{V_c^2}{2g\mu} + 2D_c + \text{OAL} + D_{\text{tw}}\right] \tag{10.13}$$

If the vehicle is stopped at the crossing and decides to proceed forward as the train approaches, the distance from the crossing to the train for safe passage is given by,

$$D_{ts} = V_t\left[T_{ig} + T_r + \frac{\text{OAL} + 2D_c + D_{\text{tw}} - D_{1g}}{V_{1g}}\right] \tag{10.14}$$

In Equations 10.12 through 10.14 the following parameters are defined as:

D_h = distance along the highway
D_t = distance along the tracks
D_{ts} = distance along the tracks for a stopped vehicle
D_{lg} = distance traveled by vehicle to maximum speed in first gear
D_{tw} = track width distance = 5 ft for single tracks. For multiple tracks this distance must be measured
D_v = distance from the front of the vehicle to the driver. Assumed approximately 10 ft
D_c = distance from the front of the vehicle to the nearest rail. Assumed 15 ft for safety
OAL = overall vehicle length
g = acceleration due to gravity
μ = vehicle stopping coefficient of friction. Assumed to be between 0.3 and 0.5
T_r = reaction time of vehicle driver. Assumed to be 2.5 sec
T_{ig} = time required for vehicle to reach maximum speed in first gear
V_c = car or vehicle velocity
V_t = train velocity
V_{1g} = maximum speed of vehicle in first gear

Table 10.2 summarizes Equations 10.12 and 10.13 for coefficients of friction for the vehicle varying between 0.3 and 0.5. Those values apply to cars and large trucks with properly working brakes for normal application of the brake pedal. Those values do not reflect emergency braking conditions. As a rough estimate, in emergency full brake application, cars can easily obtain values of 0.8 and large trucks values of 0.45. Please refer to the Federal Motor Vehicle Standards in Chapter 15.

This chapter covers the basics of train/vehicle/pedestrian accident reconstructions. There are other factors that may impact the overall analysis of the investigation. These other factors may include the type of locomotives, the type of cars, whether passenger, freight, or fast speed commuter passenger cars, and particulars with respect to signage, signals, and the grade crossing itself. The actions of the train crew may also play a part in the reconstruction. Please refer to the appropriate sections of the *Code of Federal Regulations* for those particulars. The sections on rail grade crossings are fully described under the MUTCD. Factors that affect the performance of the drivers or pedestrians are covered in Chapters 7 and 8. The characteristics of the roads leading to the rail grade crossing are covered in Chapter 9 and the MUTCD. Additional pertinent information may be obtained from the Bibliography.

Table 10.2 Sight Distance Triangle Based on Coefficient of Friction and Train and Vehicle Speeds

	$V_t = 10$		$V_t = 20$		$V_t = 30$		$V_t = 40$		$V_t = 50$		$V_t = 60$	
V_c	D_h	D_t	D_h	D_t	D_h	D_t	D_h	D_t	D_h	D_t	D_h	D_t
						$\mu = 0.3$						
10	72.8	147.8	72.8	295.5	72.8	443.3	72.8	591.1	72.8	738.9	72.8	886.6
20	142.8	108.9	142.8	217.8	142.8	326.7	142.8	435.6	142.8	544.5	142.8	653.4
30	235.1	103.4	235.1	206.7	235.1	310.1	235.1	413.4	235.1	516.8	235.1	620.1
40	349.6	106.1	349.6	212 3	172.3	318.4	172.3	424.6	172.3	530.7	172.3	636. 9
50	486.3	112.3	486.3	224.5	486.3	336.8	486.3	449.1	486.3	561.3	486.3	673.6
60	645.4	120.1	645.4	240.1	645.4	360.2	645.4	480.2	645.4	600.3	645.4	720.4
						$\mu = 0.4$						
10	70.0	145.0	70	290.0	70	435.0	70	580.0	70	725.0	70	870.0
20	131.7	103.3	131.7	206.7	131.7	310.0	131.7	413.3	131.7	516.7	131.7	620.0
30	210.0	95.0	210	190.0	210	285.0	210	380.0	210	475.1	210	570.1
40	305.1	95.0	305.1	190.0	305.1	285.1	305.1	380.1	305.1	475.1	305.1	570.1
50	416.8	98.4	416.8	196.7	416.8	295.1	416.8	393.5	416.8	491.8	416.8	590.2
60	545.2	103.4	545.2	206.7	545.2	310.1	545.2	413.5	545.2	516.9	545.2	620.2
						$\mu = 0.5$						
10	68.3	143.3	68.3	286.6	68.3	430.0	68.3	573.3	68.3	716.6	68.3	859.9
20	125.0	100.0	125	200.0	125	300.0	125	400.0	125	500.0	125	600.0
30	195.0	90.0	195	180.0	195	270.0	195	360.0	195	450.0	195	540.0
40	278.4	88.3	278.4	176.7	278.4	265.0	278.4	353.4	278.4	441.7	278.4	530.1
50	375.1	90.0	375.1	180.0	375.1	270.1	375.1	360.1	375.1	450.1	375.1	540.1
60	485.2	93.4	485.2	186.7	485.2	280.1	485.2	373.5	485.2	466.8	485.2	560.2

As an example, we can calculate a variety of the parameters listed above concerning a particular accident. The following data was obtained from discovery and measurements.

V_t = velocity of the train from recorder = 34 mph
V_{1g} = maximum velocity of the vehicle in first gear = 8.8 ft/sec
a_t = acceleration of the vehicle in first gear = 1.47 ft/sec^2
OAL = length of the tractor trailer (vehicle) = 65 ft
D_c = distance from stop line to nearest rail = 15 ft
T_r = perception reaction time = assumed 2 sec
D_{tw} = distance between outer rails = measured 18 ft

The sight distance along the tracks for a stopped vehicle is 890 ft. The sight distance along the tracks for a moving vehicle traveling at 25 mph and the vehicle driver reacting in 2.5 sec is 350 ft and the distance along the highway is 170 ft. A coefficient of friction of 0.375 was utilized for the vehicle.

Commercial and Off-Road Vehicles

11

11.1 Introduction

Commercial vehicles are restricted to large frame trucks, buses, and articulated tractors and trailers. Recreational vehicles are not classified as commercial vehicles even though they are generally constructed from large truck or bus frames. Some recreational vehicles are constructed from small truck or van frames in the 3/4 to 1 ton category. Although large recreational vehicles have the same performance characteristics as buses or large trucks, they are not subject to the same federal regulations as commercial vehicles. The basic difference is that the driver of a commercial vehicle is required to have a commercial drivers license commonly referred to as a CDL. The general cut-off for the requirement of the driver to posses a CDL license is the weight of the vehicle at 26,001 lbs.

Operators of construction equipment such as dozers, end loaders, excavators, and fork trucks often require specialized training and certification. This is especially true for operators of cranes. Operators of these specialized types of equipment must have the appropriate certification according to rules and regulations promulgated by the Code of Federal Regulations (CFR). There are various sections of the code that apply to various industries such as 29CFR for construction and 30CFR for mining as well as 49CFR for transportation. Additionally, the Occupational Safety and Health Administration (OSHA) and the Mining Safety and Health Administration (MSHA) have rules and regulations pertinent to those industries. When performing reconstructions involving commercial, construction, or mining vehicles it is imperative that the reconstructionist becomes familiar with these rules, regulations, and standards.

11.1.1 Federal Motor Vehicle (FMV) Regulations *Title 49 Transportation*

Most reconstructions involving large vehicles involve either buses or large trucks such as tractor/trailers. These vehicles fall under certain sections of *Title 49 Transportation*. Title 49 is divided into nine volumes only some of which are pertinent to the reconstructionist. Volume 4 contains

Chapter II, Parts 200–299 under the regulatory entity of the Federal Railroad Administration, Department of Transportation. Volume 7 contains Chapter VII, Parts 700–799 under the regulatory entity National Railroad Passenger Corporation (AMTRAK). Certain of these parts may be pertinent in the case of a collision between a commercial or a construction vehicle and a train.

Volume 5 contains Chapter III, Parts 300–399 under the regulatory entity Federal Motor Carrier Safety Administration, Department of Transportation. Volume 6 contains Chapter V, Parts 500–599 under the regulatory entity National Highway Traffic Safety Administration (NHTSA), Department of Transportation. Volume 7 also contains Chapter VI, Parts 600–699, under the regulatory entity Federal Transit Administration, Department of Transportation. The pertinent sections of Volumes 5, 6, and 7 are the most important when performing reconstructions involving large or commercial vehicles. All of these publications are free and available through the web by simply typing CFR and following the instructions on the home page. The parts that are pertinent to reconstructions have been outlined in Chapter 15.

11.2 Tractor/Trailers

"Tractor/trailers are not just large vehicles." This statement has been used by other reconstructionists and presented in papers at conferences. Obviously, the authors take exception with this train of thought. Tractor/trailers are large vehicles, and the analysis of these vehicles follows the same principles that are applied to smaller vehicles. They differ in some respects in that the analysis also includes regulations and somewhat different vehicle response with respect to steering and braking. Of course physical laws apply equally to large and small vehicles. However, the analysis may be somewhat more complicated as will be shown in the analysis that follows. We wish to develop some equations for the loss of control of a tractor and trailer produced by a shift in the load. This load shift may produce an unstable situation as the vehicle rounds a curve, partially jack-knifes (yaws) and rolls over. Figure 11.1 represents a tractor and trailer rounding a curve in spherical coordinates as seen from above on the azimuth plane.

From Figure 11.1 we can define the following:

R = the average radius of the curve
v = the speed of the tractor/trailer
A_1 = heading angle of the tractor
A_2 = heading angle of the trailer
θ = the magnitude of the angle between the tractor and the trailer

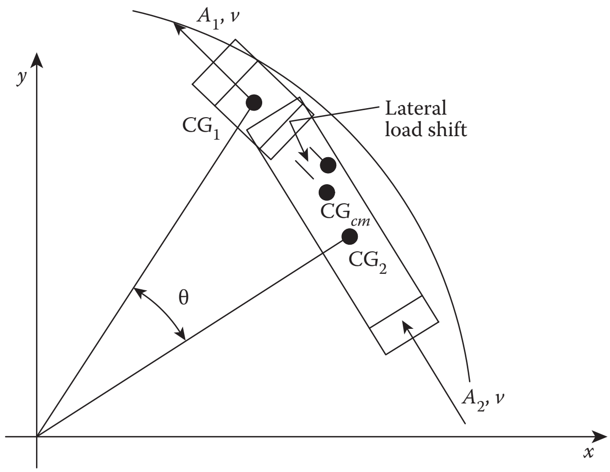

Figure 11.1 Azimuth plane.

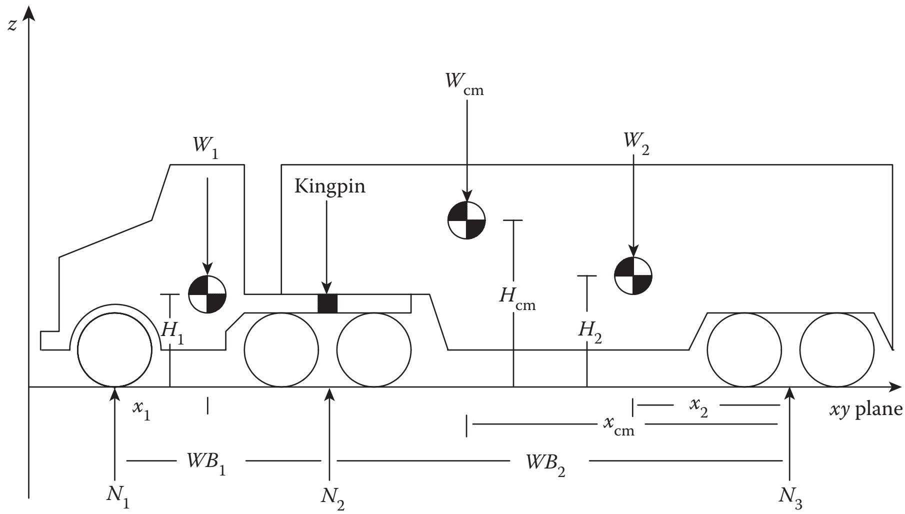

Figure 11.2 Elevation plane.

In the vertical plane as shown in Figure 11.2 we define the following parameters.

In order to simplify the analysis, the reaction at the tandems have been taken at the center. Summing forces we obtain.

$$\Sigma F_z = 0: \quad N_1 + N_2 + N_3 = W_t = W_1 + W_2 + W_{cm} \tag{11.1}$$

The road may be on a grade and may also be super-elevated, which must be accounted for. In order to analyze the conditions for loss of control as a result of the shift in the load we will look at the tractor and the trailer independently and then superimpose the solutions. We begin by looking at an orthogonal plane about the tractor as shown in Figure 11.3.

We define the following,

ε = superelevation of the road

TW_1 = track width to the center of the outer wheel

WW_1 = wheel width

F_1 = lateral force from the centripetal acceleration

a_c = centripetal acceleration = v^2/R

The lateral force is given by,

$$F_1 = m_1 a_c = \frac{w_1 v^2}{gR} \tag{11.2}$$

Summing forces in the x-direction,

$$\Sigma F_x = 0: \quad F_1 - w_1 \cos\varepsilon - f = 0 \tag{11.3}$$

Summing forces in the z-direction,

$$\Sigma F_z = 0: \quad N_1 - w_1 \cos\varepsilon = 0 \tag{11.4}$$

$$f = \mu_k N_1 = \mu_k w_1 \cos\varepsilon \tag{11.5}$$

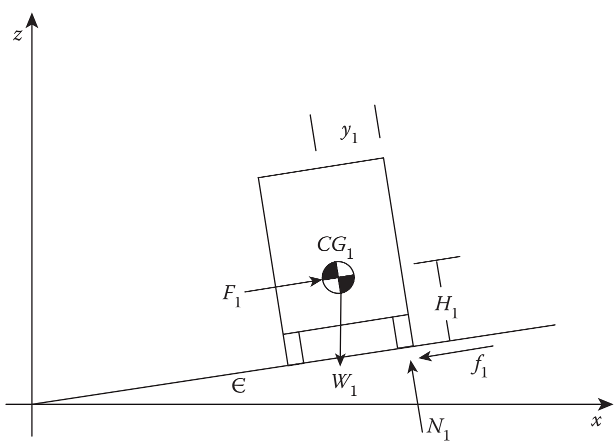

Figure 11.3 A_1 Orthogonal plane.

For stability, the yawing conditions are:

$$F_1 \leq w_1(\sin\varepsilon + \mu_k \cos\varepsilon) = \mu_{\text{eff}} w_1 \tag{11.6}$$

In the limiting case if the centripetal acceleration is greater than the frictional resistance, yaw loss of control occurs.

$$\text{if} \quad \mu_{\text{eff}} > \frac{v^2}{(gR)} \equiv \frac{(a_c)}{g}, \quad \text{no yawing occurs} \tag{11.7}$$

$$\text{if} \quad \mu_{\text{eff}} \leq \frac{v^2}{(gR)}, \qquad \text{yawing occurs} \tag{11.8}$$

For tipping conditions we sum the moments,

$$\Sigma M_{\text{over1}} = F_1 H_1 \tag{11.9}$$

$$\Sigma M_{\text{res1}} = w_1[y_1 \cos\varepsilon + H_1 \sin\varepsilon] \tag{11.10}$$

We now consider an orthogonal plane about the trailer, as shown in Figure 11.4.

As with the tractor, we define the following parameters for the trailer.

$$y_2 = \frac{\text{TW}_2 + \text{WW}_2}{2} \tag{11.11}$$

$$y_{\text{cm}} = \frac{\text{TW}_{\text{cm}} + WW_{\text{cm}}}{2} \tag{11.12}$$

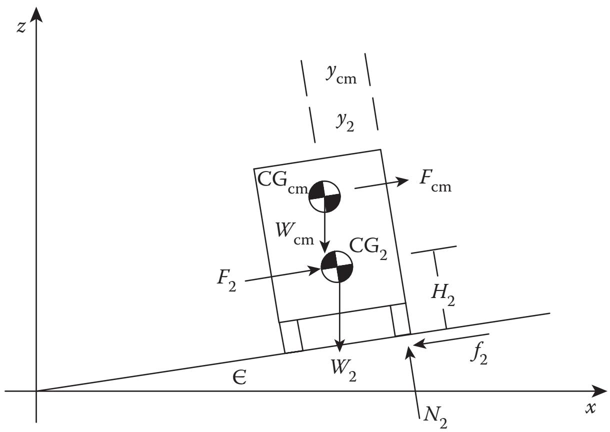

Figure 11.4 A_2 Orthogonal plane.

The load shift is created when,

$$y_{\mathrm{cm}}^{l} = y_{\mathrm{cm}} - D_{\mathrm{cm}} > 0 \tag{11.13}$$

$$F_2 = \frac{W_2 v^2}{gR} \tag{11.14}$$

$$F_{\mathrm{cm}} = \frac{W_{\mathrm{cm}} v^2}{gR} \tag{11.15}$$

We define the weight of the trailer as,

$$W_{\mathrm{tr}} = W_2 + W_{\mathrm{cm}} \tag{11.16}$$

Summing forces as before

$$\Sigma F_x = 0: \quad F_2 + F_{\mathrm{cm}} - W_{\mathrm{tr}} \sin\varepsilon - f_2 = 0 \tag{11.17}$$

$$\Sigma F_z = 0: \quad N_2 - W_{\mathrm{tr}} \cos\varepsilon = 0 \tag{11.18}$$

$$f_2 = \mu_k N_2 = \mu_k W_{\mathrm{tr}} \cos\varepsilon \tag{11.19}$$

For stability (yaw) the conditions are,

$$F_2 + F_{\mathrm{cm}} \le W_{\mathrm{tr}} \sin\varepsilon + \mu_k W_{\mathrm{tr}} \cos\varepsilon \tag{11.20}$$

$$\frac{W_2 v^2}{gR} + \frac{W_{\mathrm{cm}} v^2}{gR} \le W_{\mathrm{tr}}[\sin\varepsilon + \mu_k \cos\varepsilon] \tag{11.21}$$

$$W_{\mathrm{tr}}\left[\frac{v^2}{(gR)}\right] \le W_{\mathrm{tr}}[\mu_{\mathrm{eff}}] \tag{11.22}$$

$$\text{if } \frac{v^2}{(gR)} \ge \mu_{\mathrm{eff}} = \sin\varepsilon + \mu_k \cos\varepsilon, \qquad \text{yawing occurs} \tag{11.23}$$

The tipping conditions are determined from the sum of the moments.

$$\Sigma M_{\mathrm{over}\,2} = F_2 H_2 + F_{\mathrm{cm}} H_{\mathrm{cm}} \tag{11.24}$$

$$\Sigma M_{\mathrm{res}2} = W_2 H_2 \sin\varepsilon + W_{\mathrm{cm}} H_{\mathrm{cm}} \sin\varepsilon + W_2 y_2 \cos\varepsilon + W_{\mathrm{cm}} y_{\mathrm{cm}} \cos\varepsilon \tag{11.25}$$

The load shift D_{cm} reduces the value of y_{cm} *to the new value* y'_{cm}.

We can now couple the tractor and trailer together to determine the conditions for loss of control and possible roll over of the vehicle combination. In this analysis we assume that the fifth wheel that connects the rig does not fail and cause separation. If the system uncouples as the rollover takes place, the post-rollover velocities of the two sections can still be computed. By superposition, the total overturning moment becomes,

$$\Sigma M_{\text{overt}} = F_1 H_1 + F_2 H_2 + F_{\text{cm}} H_{\text{cm}} \tag{11.26}$$

$$\Sigma M_{\text{overt}} = \frac{v^2}{gR}[W_1 H_1 + W_2 H_2 + W_{\text{cm}} H_{\text{cm}}] \tag{11.27}$$

The total resistive moment is then,

$$\Sigma M_{\text{rest}} = \sin\varepsilon[W_1 H_1 + W_2 H_2 + W_{\text{cm}} H_{\text{cm}}] + \cos\varepsilon[W_1 H_1 + W_2 H_2 + W_{\text{cm}} y_{\text{cm}}] \tag{11.28}$$

Roll-over occurs if

$$\Sigma M_{\text{overt}} > \Sigma M_{\text{rest}} \tag{11.29}$$

Solving for the overturning conditions whether the load shifts or not, we obtain;

$$y_{\text{cm}} \leq \frac{W_t H_t}{W_{\text{cm}}}\left[\frac{v^2}{gR\cos\varepsilon} - \tan\varepsilon\right] - \frac{W_1 y_1}{W_{\text{cm}}} - \frac{W_2 y_2}{W_{\text{cm}}} \tag{11.30}$$

Now we can analyze the rollover conditions as follows:

If a load shift occurs, Equation 11.13 governs and D_{cm} is the weight shift distance.

For a stable load rollover occurs if the right side of Equation 11.30 $\geq y_{cm}$.

For a shifted load rollover occurs if the right side of Equation 11.30 plus $D_{cm} \geq y_{cm}$.

11.3 Off-Tracking for Coupled Vehicles

In Chapter 7 the effect of off-tracking was analyzed for both two axles and coupled vehicles. From the analysis in the previous section it must be noted that the radius of the curve, given by the letter *R*, was not distinguished whether it represented the radius of the front wheels, the radius of the tractor tandems, or the radius of the trailer tandems. Do not become confused and attempt to apply different values for the radius. Actually, the radius to be used in Equation 11.30 is the mean radius through the center of mass of the vehicle. The development of all motion equations in this book is with respect to the center of mass. Off-tracking is sometimes a byproduct of the loss of control of a vehicle that can lead to yawing or jack-knife conditions and eventual rollover. For the analysis of yawing or rollover we are not concerned with where on the road the wheels are, but rather that an unsafe condition can develop and cause an accident. The analysis for off-tracking is much more relevant when the rear tandems of a tractor/trailer cross over the center line of a highway and impact an approaching vehicle.

11.4 Construction Equipment

As a general rule, construction equipment seldom crashes against passenger vehicles mainly because of their respective locations of use. Construction equipment is normally operated in restricted zones where these types of operations take place. At times, construction or farm equipment travels or is carried on the highway. In these instances a collision with a motor vehicle may take place. The more common type of collision or accident involving construction equipment takes place at the job site. These types of events involve the failure or overturning of a particular type of equipment. A crane may fail by either overturning, or collapsing. A dozer may careen over an embankment, a dump truck may topple as it dumps its load, or a fork truck may overturn as it carries a load. These are a few examples of some common accidents or events that may require investigation or reconstruction.

The federal agencies and respective codes recognize the inherent dangers associated with construction and have regulatory authority for the practices employed in the use of such equipment. Additionally, the equipment manufacturers employ operating limits based on testing and engineering that restrict the usage of the equipment. Sometimes the failure of particular equipment is produced by a design flaw. More often the failure may be produced by inadequate or improper maintenance. Most often, the failure, accident, or event is caused by improper use and operation of the equipment beyond the design capabilities. These types of events produce loss of equipment, loss of production, injury, or the loss of life. From a monetary standpoint such events involve greater impact and require more careful and detailed analysis. However, the basic principles of analysis are utilized to determine the sequence of events in the reconstruction. One such case is described below.

A tractor trailer pulled into a rural road and the driver realized it was at the wrong location. There was a *y*-intersection where the driver decided to make his turn but could not negotiate the maneuver. Figure 11.5 shows the survey of the accident site.

A fork truck operator was near the site and offered to pick up the rear of the trailer and drag the unit in order to facilitate the maneuver that the tractor trailer driver was attempting. The lift was performed using a 3/8 inch chain 194 inches in length. The chain was looped over the forks and attached to the rear suspension hangers of the trailer. The forks of the machine were raised over the trailer and the fork truck began pulling the rig while negotiating the turn. Figure 11.6 shows scaled diagrams of the trailer and the fork

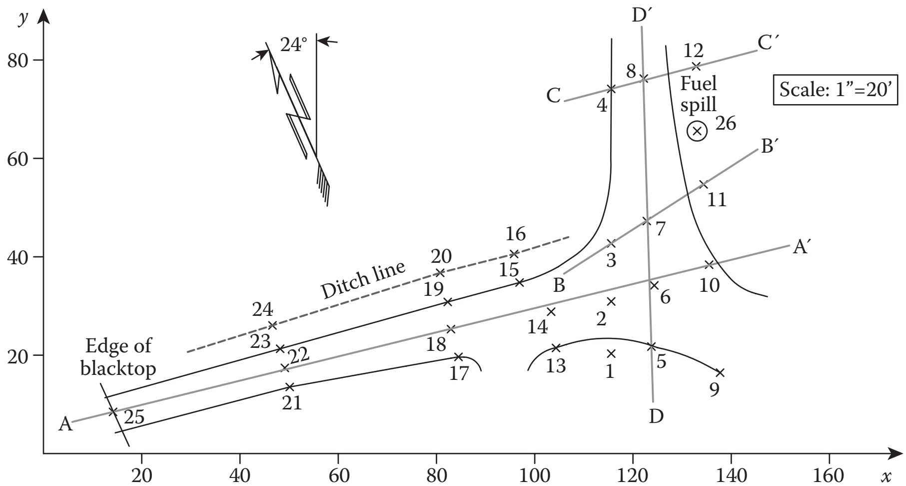

Figure 11.5 Survey of accident site.

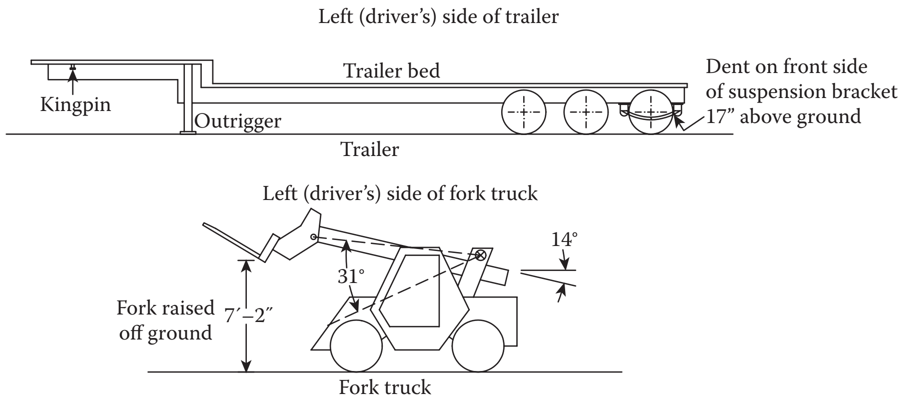

Figure 11.6 Scaled diagrams of vehicles.

truck. The angle and separation of the forks were measured by the investigating agencies. As the maneuver was carried out, the fork truck toppled over on its left side. The fork truck driver, who was not belted, fell to the left and was crushed by the fork truck.

Figures 11.7 through 11.10 show scaled diagrams pertinent to the reconstruction. The diagrams based on accurate measurements and computations of the road, the vehicles, and the rest positions summarize the physical evidence in this accident as outlined below.

1. The left rearmost suspension hanger on the trailer had been deformed, while the right side hanger was not. This deformation indicates that the greatest force was produced to the left side hanger as the turning maneuver was performed. The load would then be transferred to the left fork of the fork truck.
2. The forks were measured to be 7'–2" above the ground. This height corresponds to a boom elevation of approximately 14 degrees above level. These measurements reveal that the forks were raised to approximately 31 degrees above rest position.
3. The rest positions of the vehicles as measured by the police were verified by the survey as shown in the accompanying diagrams. The grade of the road indicated that the tractor trailer would have a tendency to move forward while in neutral gear.
4. The rest orientation of the vehicles shows that the rear of the trailer could only strike the chain prior to the fork truck rolling over. This orientation shows that the rear of the trailer could not have struck the fork truck body or tires. The height of the trailer bed was approximately 3 ft, while the forks were raised to a height of approximately 7 ft.
5. The OSHA report included a statement by a neighbor. This neighbor stated that "the fork lift was not leaning and that the right rear tire came off the ground first and then it laid over on its side." This statement indicated combined rolling and pitching of the fork truck about its left front tire. This motion was consistent with the application of the load through the left fork as detailed in point 1.
6. The OSHA report placed no fault on the actions of the tractor trailer driver.

In his deposition and statement to the police, the driver of the truck said that the fork truck was at all times pulling his tractor/trailer. A neighbor who witnessed the accident, said that either the bed of the truck was against the fork lift or that the chain used for the connection was pulling on one side. He further stated that something began pulling the fork lift to the right and that the fork truck was in a bind, and that the tractor trailer and the fork truck

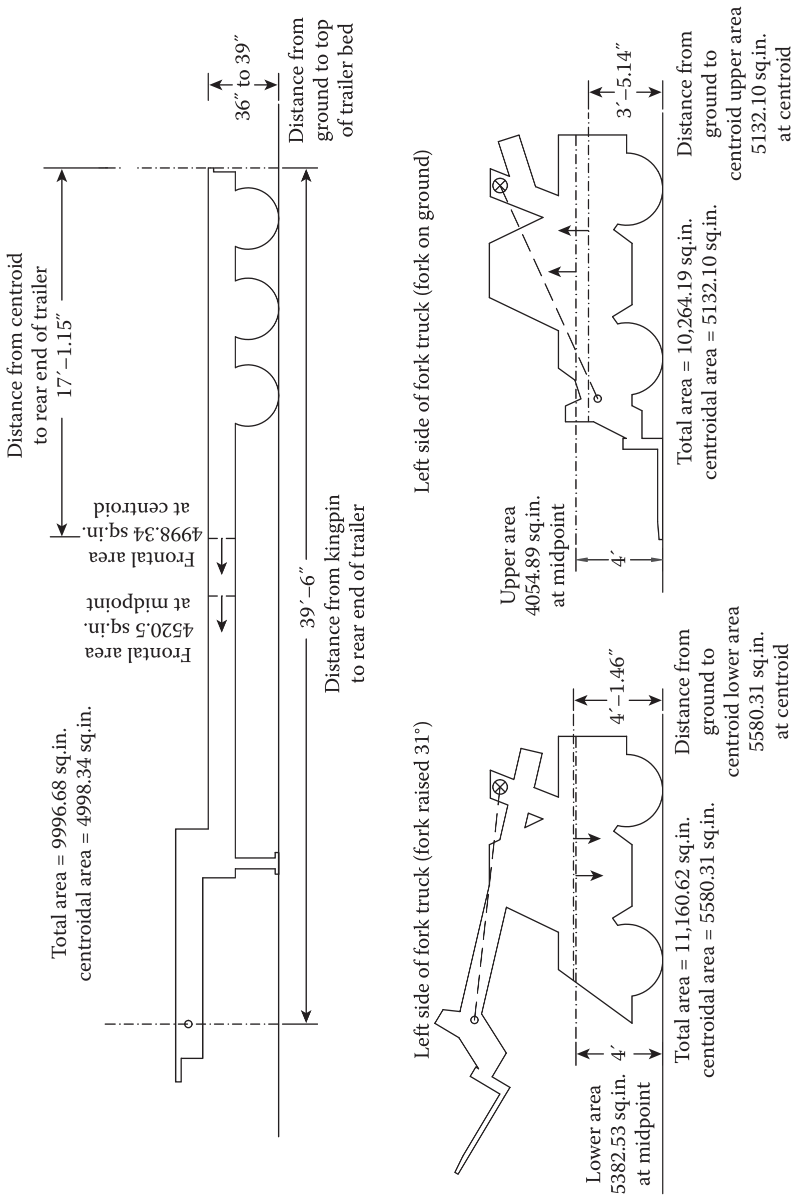

Figure 11.7 Center of mass calculations

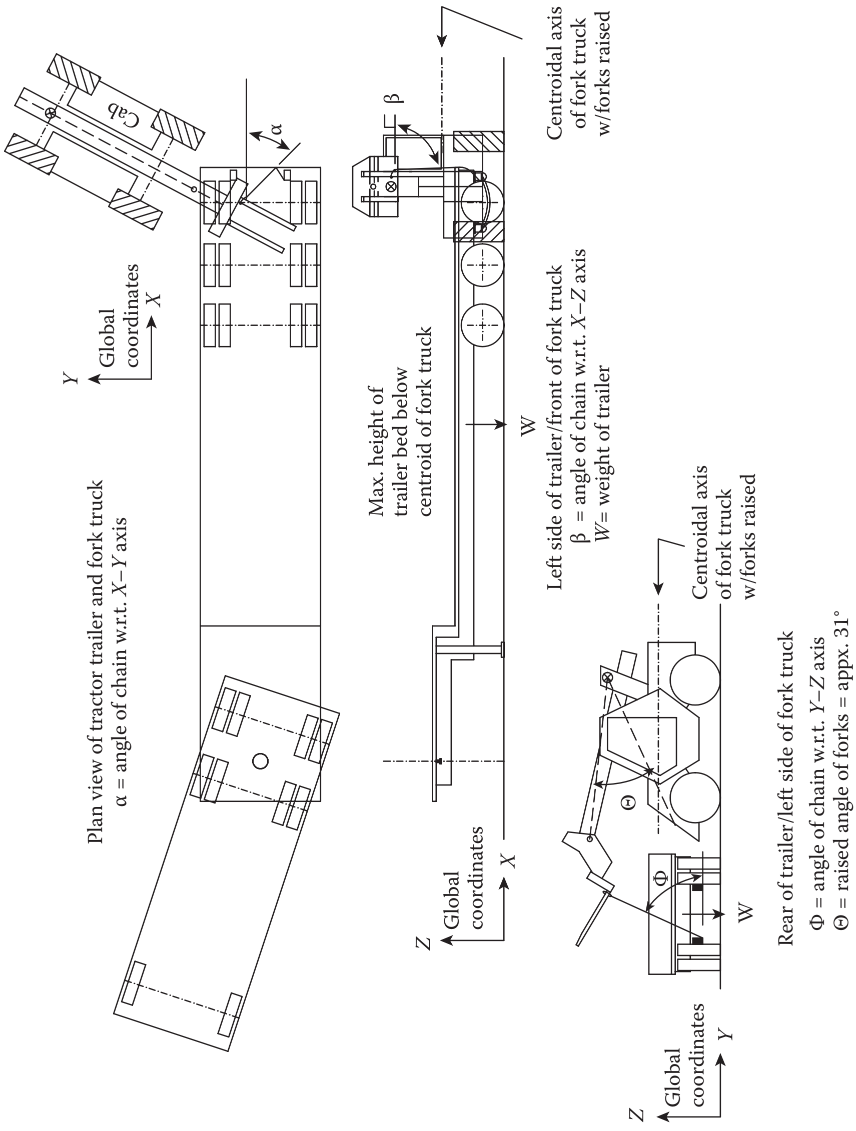

Figure 11.8 Conditions at tip-over.

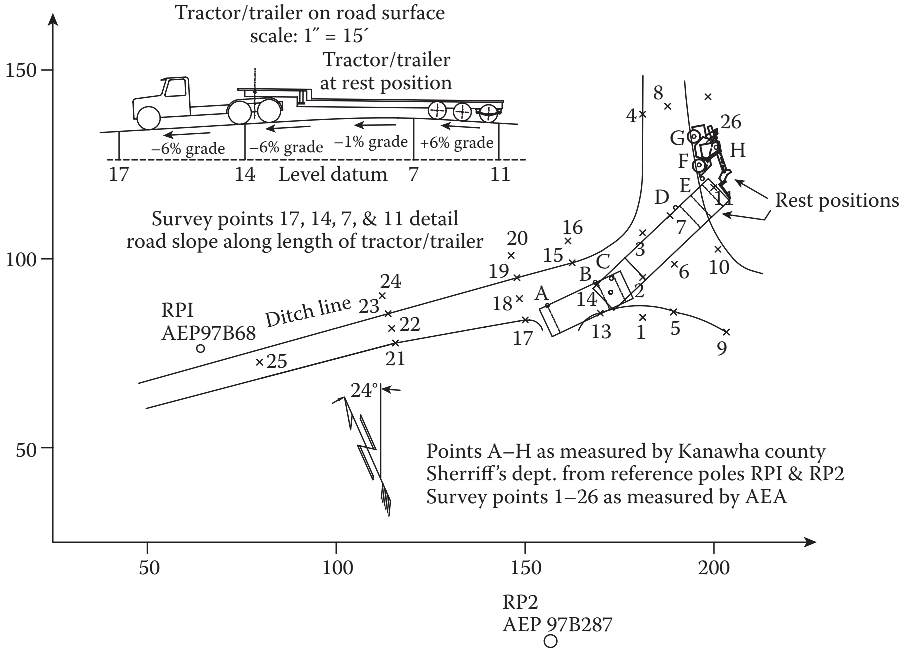

Figure 11.9 Tractor trailer rest position.

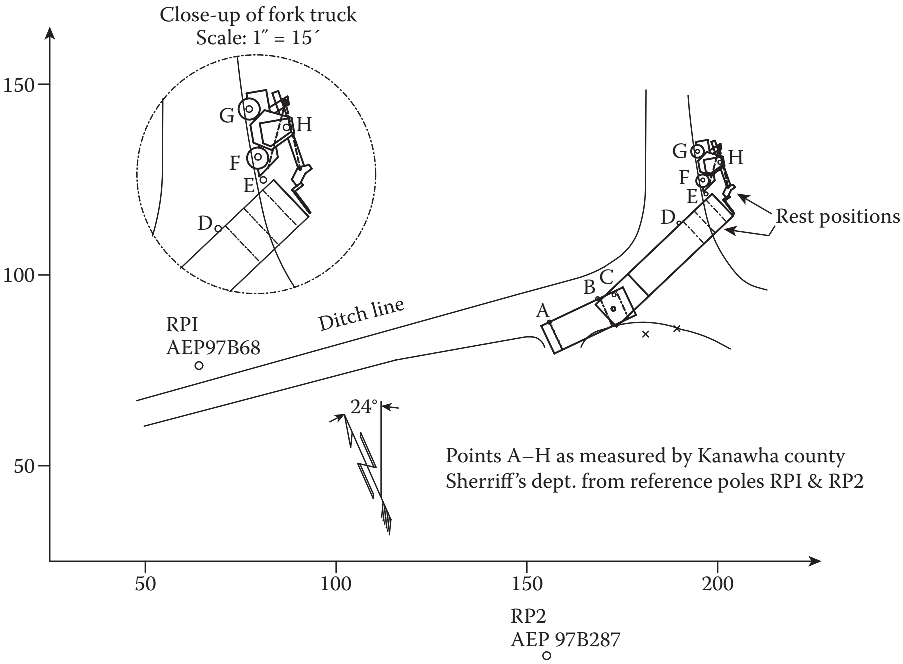

Figure 11.10 Fork truck rest position.

were in a continuous movement until the fork truck turned over. Finally, he stated that the forks were above the cab of the fork lift, that he saw the fork lift tilt before it turned over, and that he did not see the trailer come in contact with the fork lift.

The fork truck operating manual was reviewed. The manual discussed the required use of a seat belt, it indicated that extreme caution should be used when handling suspended, long, high, or wide loads and to always lower the boom (with or without load) before turning or traveling. It stated that one should never travel with a load raised or operate outside the capacity limits of the machine. It also said not to use the machine for lifting loads in tandem with other machines. The combined load, weight, and force of the other machine could exceed machine capacity and tip-over could result.

Applicable safety standards for fork truck operation were also reviewed. These standards are as follows: *ASME B56.6 Section 6.4.7(a)(l) do not exceed the truck manufacturer's capacity (2) only lift the load vertically and never drag it horizontally. 29 CFR 1910.178 (n) Traveling (6)(iii) on all grades the load and load engaging means shall be tilted back if applicable, and raised only as far as necessary to clear the road surface. Under (o) Loading (2) only loads within the rated capacity of the truck shall be handled.*

Figure 11.7 outlines the determination of the vehicles' centroidal axes. Given the centroid of the trailer through which its weight is transferred, it was calculated that approximately 8700 lbs of vertical lifting force would be necessary to raise the rear end of the trailer. At the known elevation of the forks and boom of the fork truck, the rated capacity of the fork truck was between 4200 and 4500 lbs depending on the moment created at the forks. Therefore, the vertical lift was approximately twice that of the rated capacity. An analysis of the longitudinal centroid of the fork was also performed given the raised or lowered position of the forks and boom. It was determined that raising the forks to the known elevation resulted in a centroid located over 49 inches above ground. It should be noted that the maximum height of the trailer's rear was measured to be 39 inches. If the trailer had struck the fork truck, it would have applied a lateral force below the centroid of the fork truck that would make it physically improbable for the application of such a force at low speeds to cause the fork truck to roll over on its left side.

Figure 11.8 illustrates various views for the orientation of the vehicles. Based on the orientations with respect to global coordinates, we determined the following:

1. By summing moments about the trailer kingpin, the Z-axis force, $F_z = 8700$ lbs.
2. Unit vector of force transferred through chain, $\mathbf{e} = 0.114\ \mathbf{e}_x + 0.398\ \mathbf{e}_y + 0.890\ \mathbf{e}_z$.
3. X-axis force, $F_x = 1090$ lbs. Y-axis force, $F_y = 3805$ lbs.

4. Resultant total force, $F = 9560$ lbs.
5. Forces F_x and F_z combined to produce roll-over moment, $M_R = 3889$ ft-lbs.
6. Forces F_y and F_z combined to produce pitch moment, $M_P = 100{,}182$ ft-lbs.

The roll-over moment was clockwise toward the left tires of the fork truck as seen from the front view of the fork truck. The pitch moment was counter-clockwise toward the front tires of the fork truck as seen from the left side view of the fork truck. These roll and pitch moments were consistent with the physical evidence and witness' statements of how the fork truck pitched and rolled over. This analysis revealed how the force on the chain was transferred to the left fork, causing the fork truck to overturn. Finally Figures 11.9 and 11.10 document the rest positions of the vehicles.

The analysis of this accident based on the physical evidence, the reports of regulatory agencies, police report, recognized standards, witness statements, depositions, and photographs indicated that no impact occurred between the trailer and the fork truck. The physical evidence, along with the direction of force and the moments that were created, indicated that the fork truck and chain were in a bind with the rear of the trailer. These moments caused the fork truck to pitch forward and roll toward its left side. This action raised the right rear tire causing the fork truck to overturn. The unbelted driver was killed in the accident. The analysis indicated that the rated capacity of the machine was exceeded, the roll and pitch moments were sufficient to overturn the machine, and that critical safety was disregarded. The combination of factors produced the event and indicates, as was pointed out at the beginning of the chapter, that tractors, trailers, and construction equipment are large vehicles that obey Newtonian mechanics. Accidents involving tractor-trailers, buses, large trucks, and construction equipment also involve various rules, regulations, and recognized standards that need to be addressed when performing such reconstructions. Most often, not following the recognized safety practices associated with these vehicles, in combination with other factors (such as operator error or equipment failure), leads to conditions that result in an accident.

Visibility, Perception, and Reaction

12

12.1 Introduction

The concepts of visibility, perception, and reaction of humans involved in accidents are areas of much debate. One other area of debate is conspicuity. In order to properly assess these terms, it is convenient to first define what we mean by these words. The definitions offered in this section are relative to an event such as a collision between two vehicles or an event such as an accident involving humans and their equipment. Visibility is the relative possibility of being seen under the conditions of distance, light, and atmosphere prevailing at a particular time. Another way of defining visibility is the maximum distance at which an object can be seen under the prevailing conditions, in other words, the range of vision.

Perception is the act of apprehension by the senses, or the ability to form a mental grasp of objects or qualities—the awareness, comprehension, insight, intuition, or the faculty for these objects or qualities. It is the understanding and knowledge of specific ideas, concepts, and impressions formed relative to the objects or qualities.

Reaction is the response to a stimulus or influence. Reaction can only occur when a particular event is seen or perceived. The reaction time is the lapse of time between stimulation and the beginning of the response. The stimulation cannot occur until the event is perceived by the senses.

Conspicuity is a term that has entered the science of visibility, perception, and reaction. What is exactly meant by the term conspicuity? At first thought one would think that the term is related to the word conspicuous. Conspicuous means it is open to view, that it is easy to see or perceive, that it is obvious. To be conspicuous is to attract attention by being unexpected, unusual, outstanding, striking, or egregious. Does conspicuity relate to an obvious, easy to see event or does it mean that the event must be unusual enough to shock our senses? Conspicuity can simply mean two very different scenarios according to the definition of conspicuous. For example, if a driver is following traffic on a busy freeway with the vehicles all traveling at about the same speed, is the traffic pattern conspicuous to an alert driver? Or does the traffic pattern have to change abruptly, such as with a speeding driver weaving dangerously through the traffic, for the traffic pattern to be conspicuous? This example also brings up another term that is introduced by human factors experts. This term is expectation. Does the driver expect the traffic to move in a uniform orderly manner with no surprises? Or is it reasonable under the circumstances described, to expect a potentially dangerous driver to perform his or her interpretation of a National Association Stock Car Racing (ANASCAR) racetrack?

Expectation and conspicuity are integrally related. Prudent and experienced drivers expect the unexpected and modify their driving accordingly. The driver's handbook for most states describes the rules of the road that drivers are to follow according to that paradigm. Drivers are supposed to be alert, drive according to established speed limits, decrease their speed according to road or weather conditions, obey all traffic laws, and be courteous at all times. Unfortunately, being human places significant restrictions on the way we behave while driving. Food, cell phones, a myriad of electronic devices, rudeness, and inattentiveness, to name a few, pose serious hazards while we drive and often lead to accidents. If we are inattentive, we cannot expect the unexpected event whether it is conspicuous or not. Thus, from a forensic engineering standpoint expectation, perception, and conspicuity are not factors that can be accurately quantified and properly measured. These terms and analyses are relegated to human factors sciences and are open to much question and debate. However, visibility and reaction are terms that can properly be quantified, defined, measured, and, therefore, used in accident reconstructions. We first wish to describe the limitations imposed by human factors analysis.

12.2 Limitations of Human Factors Analysis

An inordinate amount of effort has been devoted to the science of expectation, perception and conspicuity. The study of these terms is referred to as human factors analysis. Attempting to analyze how a particular person might react in a given situation is very complex and chaotic. There are simply too many variables to be considered and include mental processing, age, health, vision, hearing, gender, mental health, and distractions, to name a few. Human factors analysis is also subject to initial conditions which may not be the same for two drivers under the same set of conditions, events, or processes. Therefore, human response is actually truly chaotic and possibly beyond human scientific understanding. What is known is that no two humans perceive the same event in the same manner and therefore, cannot be expected to react in a scientifically validated way. At best, placing time frames and limits on expectation, perception, and conspicuity are conjectures without hard scientific basis. However, it is agreed that within certain bounds, time frames may be imposed on the terms of expectation, perception, and conspicuity. These time frames are a part of design standards of highways that have been developed for the construction of the road systems in this country.

12.3 Design Standards

A review of design standards for highways gives an insight into the reaction of drivers to unexpected events that may arise while driving. A *Policy on Geometric Design of Highways and Streets*, commonly referred to as the "*Green Book*" is the culmination of design standards that were begun in 1937. These standards along with many others relative to highways are developed by the American Association of State Highway officials (AASHTO).

A fundamental design criteria of sight distance on highways is the reaction time for the driver. This reaction time is associated with the ability of the driver to perform maneuvers in response to road and traffic conditions that arise. It is recognized that the complex maneuvers of driving require not only reaction but also perception of the events unfolding before the driver. Thus, the response time is generally referred to as the *perception-reaction time*. According to the *Green Book* a perception-reaction time of 2.5 sec is used in design. This time is based on the 85^{th} percentile reaction time based on numerous scientific studies. Drivers manuals for most states and in other countries indicate that reaction time for most drivers is approximately 1 sec and that the time may vary between 0.5 and 1.5 sec.

While driving, the operator must use various senses in order to gather sufficient information to make a decision. These senses are auditory, tactile, and most importantly visual. The visual sources of information that the driver receives are processed through the brain in a sequential order so that the response of the driver can only be sequential. As the complexity of the information increases, so does the time required to process the information and consequently react to the stimulus. In complex situations, where multiple visual information is presented, the driver has to sort the information and react to what is perceived as the best course of action based on experience and judgment. Therefore, more experienced drivers tend to make better decisions to complex stimulus. Many other factors such as age, health, and physical well being affect the time required for the driver to take action. According to the *Green Book*, when an event is expected, reaction time is approximately 0.6 sec and increases by 35% when unexpected events occur.

Stopping sight distance according to the *Green Book* is the distance along the highway that is available and visible to the driver. This distance should be such that it allows a driver traveling at the design speed limit to properly bring the vehicle under control or to a complete stop. This distance is the sum of the reaction time and the braking time, or,

$$t_{\text{ssd}} = t_r + t_b \tag{12.1}$$

where,

t_{ssd} = stopping sight distance time
t_r = reaction time
t_b = braking time

The reaction time includes the time required for the driver, after recognizing the necessity, to apply the brakes. Under most conditions the time needed for drivers to react varies with a variety of factors including distance, weather conditions, time of day, nature of the environment, and the characteristics of the driver. In studies by Johansson and Kumar, drivers expecting to apply the brakes responded in approximately in the range of 0.66–1.5 sec. Other studies according to the *Green Book* ranged from 0.64 to 1.64 sec. If the drivers did not expect to apply the brakes, the response time increased by approximately 1 sec. Thus, for design purposes, the *Green Book* utilizes a reaction time of 2.5 sec. This reaction time exceeds the 90$^{\text{th}}$ percentile reaction time and includes older drivers. Another way of looking at the design reaction time in the *Green Book* is to take the 1.64 sec reaction time and multiply by a safety factor of 1.5 (standard design safety factor) which yields a reaction time of 2.46 sec.

The braking distance in the standard is determined on a level road at the design speed for the road. The braking distance takes into account the deceleration rate of most drivers and assumes that it will be greater than 14.8 ft/sec^2 when confronted with an unexpected event or object on the road. Ninety percent of drivers decelerate at rates greater than 11.2 ft/sec^2. Thus, these braking decelerations are considered within the driver's capability to maintain control and steer properly on wet surfaces. Accordingly, the braking distance calculations for design of roads utilize this lower value of deceleration. Equation 12.2 is used to calculate the braking distance.

$$d = \frac{1}{2}\left(\frac{5280}{3600}\right)^2 \frac{V^2}{a} \tag{12.2}$$

where

d = distance in feet
a = acceleration in ft/sec^2
V = speed in feet per second

Table 12.1 shows the computation of the stopping distance and the time required to stop according to Equation 12.2 with the recommended design deceleration of 11.2 ft/sec^2.

Table 12.1 Stopping Distance and Time

V (mph)	*V* (ft/sec)	*d* (ft)	t_{ssd} (sec)
20	29.32	38.4	2.6
30	43.98	86.4	3.9
40	58.64	153.6	5.2
50	73.30	240.0	6.5
60	87.96	345.5	7.8
70	102.62	470.3	9.1

A review of Table 12.1 indicates that the design standards allow for ample time and distance to stop under the most adverse and convoluted of situations. We will next address the capability of drivers to react and stop under heavy braking conditions.

12.4 Capability of Drivers

According to Kosinski (2006) there are many factors that influence reaction time. These influences are based on different types of reaction time experiments. The reaction type experiments fall into three categories: (1) in simple reaction time experiments there is only one stimulus and one response, (2) in recognition reaction time experiments there are some stimuli that need to be responded to among several choices, (3) in choice reaction time experiments the response must correspond properly to the stimulus. These factors include the type of the stimulus, the intensity of the stimulus, arousal, age, gender, right vs left handedness, direction of the visual stimulus, practice, fatigue, distraction, alimentary content and dehydration, warning of impending stimuli, breathing, exercise, drugs and alcohol, personality, stress, intelligence, injury, and illness. Donders showed that simple reaction time is the shortest followed by recognition reaction time and choice reaction time. Many other investigators have expanded on this original work. Laming (1968) determined that the reaction times for the first two types of experiments varied from 220 to 384 milliseconds. Hicks determined that in choice reaction time experiments the time it takes to make a decision can be quantified by an equation. The family of techniques for modeling and representing the knowledge necessary for a person to perform a task is known as GOMS. The acronym stands for goals, operators, methods, and selection rules. Some of these methods are represented below.

Power law practice. This equation determines the time required to perform a task based on practice trials, stating that people improve in speed at a decaying exponential rate.

$$T_n = T_1 n^{-0.4} \tag{12.3}$$

where

T_n = time to perform a task after n-trials
T_1 = time to perform the task in the first trial
n = number of trials

Fitts' law. This equation determines the time it takes to point at an object and is logarithmic.

$$T_F = k\,\mathrm{Log}_2\left(\frac{D}{S} + 0.5\right) \tag{12.4}$$

where

k = 100 milliseconds
T_F = time
D = distance to target
S = size of target

Myer's law. This law is a refinement of Fitts' law.

$$T_M = A + B\sqrt{\frac{D}{W}} \tag{12.5}$$

where

T_M = time
A = 13 milliseconds
B = 108 milliseconds
D = distance to target
W = width of target

Hick's law. This law states the time it takes to make a decision.

$$\begin{aligned} T_H &= kH \\ H &= \mathrm{Log}_2(n+1) \\ H &= \Sigma p_i \mathrm{Log}_2\left(\frac{1}{p_i + 1}\right) \end{aligned} \tag{12.6}$$

where

H = information-theoretic entropy of a decision
n = number of probable alternatives
p_i = probability of alternative i for n alternatives of unequal probability.

Table 12.2 Braking Distance and Time

V (mph)	d (ft)	t_b (sec)	t_{ssd} (sec)
20	19.0	0.95	2.45
30	42.8	1.42	2.92
40	76.2	1.90	3.42
50	119.0	2.38	3.88
60	171.4	2.85	4.35
70	233.3	3.33	4.83

As an example, we may use Equations 12.4 through 12.6 to determine the reaction time of a vehicle operator to suddenly applying the brakes of the vehicle. Since the accelerator is next to the brake pedal, we can safely assume that the distance that the foot must travel to the target is approximately one foot. Further assume that the width or size of the brake pedal is approximately 4 inches. Fitts law calculates a reaction time of 293 milliseconds, Myer's law calculates 210 milliseconds, and Hick's law determines a reaction time of 240 milliseconds. This analysis shows that it would be safe to assume that the reaction time would be between 200 and 300 milliseconds in accordance with the values of scientific studies. If we then add 1 sec for the unexpected event, the result is a reaction time of between 1.2 and 1.3 sec.

We now make a comparison table for the same speeds as in Table 12.1, but now we apply a deceleration value of 22.5 ft/sec squared to correspond with a coefficient of friction of 0.7. This value of braking coefficient is certainly attainable for all manufactured cars. We also use a reaction time of 1.5 sec. Table 12.2 shows the results. A comparison of the values in both tables reveals the safety margin allowed by the design standards.

Computer Methods and Modern Reconstruction Tools

13

13.1 Introduction

The personal computer has been a useful, if not overused, tool in modem accident reconstruction. Applying generalized computer codes to a specific accident allows the engineer or reconstructionist to examine the effect of input changes on the result. For instance, performing a momentum analysis for a two-vehicle collision is simple enough to do by hand. However, an accurate result requires that there is little uncertainty in the input variables, especially impact and departure angles. If a reconstructionist wishes to determine if the speeds become unreasonable by a slight change in angle, he or she will need plenty of time, paper, and lead. With a properly written computer program, a parametric analysis becomes nearly instantaneous.

Another benefit of using software is based on the complexity of some accidents. Modeling vehicle crush, applying momentum analysis to a multi-vehicle pile-up collision, and three-dimensional models are almost certainly situations that cannot be solved without a computer. Added complexity to the code permits the elimination of some assumptions, and therefore creates a greater accuracy in the solution.

The pitfalls of applying computer programs to reconstruction work are such that the engineer becomes less involved in the basic principles and derivation of the governing equations. This is especially true when the engineer relies on commercially available programs, such as Engineering Dynamics Corporation Reconstruction of Accident Speeds on the Highway (EDCRASH) and PC Crash. While these are certainly well-made and reliable programs, relying solely on this software creates distance between the engineer and the math. Basic knowledge in computer coding is an overlooked skill for reconstruction work. By sacrificing some time and effort to develop a reconstruction program, money, and resources may be saved.

The primary intent of this chapter is to provide the reconstructionist with additional tools for applying the basic equations into a computer program. The first section will emphasize numerical methods, including direct and iterative solutions for systems of linear equations, as well as numerical differentiation and integration. A brief discussion in applying these methods to reconstruction cases will follow.

The second section will provide a brief introduction into some commercially available reconstruction programs. These programs are written by teams of computer engineers and are based on numerous studies and established data. Animations and simulations of accidents are tools that are increasingly in use for courtroom presentations. The difference in these will be discussed.

The final section involves a discussion of modern reconstruction tools, including black boxes, interrogation tools, and accelerometers. Occasionally, a case will warrant an investment into crash testing to compare competing hypotheses. Crash data yielded by installing accelerometers and black boxes into sacrificial vehicles can be more powerful than any printout from a computer program. Many modern vehicles are already equipped with black boxes, some of which can be examined by reconstructionists to gain indisputable conclusions into the causes of an accident. Injury severity and thresholds can be assessed by mounting sensors on dummies or live subjects. Actual testing of a subject vehicle, and documentation of its function with equipment, is often employed to determine if a vehicle component failed.

The mention of various computer programs and reconstruction tools in this section is by no means an endorsement or a criticism of any of them. The list of these tools is not all inclusive.

13.2 Numerical Methods

Engineers are often tasked with finding solutions to problems that cannot be easily solved in closed form. Solutions that require multiple equations, partial differential equations, as well as boundary and initial value problems are encountered in any engineering discipline. Numerical methods are oftentimes employed in these cases. Fortunately for accident reconstruction!sts, the problems that need to be solved and the numerical methods involved are relatively simple.

13.2.1 Systems of Linear Equations

Many problems in accident reconstruction involve systems of linear equations. Recall from Chapter 5 the governing equations for the conservation of linear momentum. Below, the equations are rewritten to reflect that the initial momentum is equal to the final momentum in each direction (x and y).

$$\begin{aligned} W_1V_{1i}\cos A_{1i} + W_2V_{2i}\cos A_{2i} &= W_1V_{1f}\cos A_{1f} + W_2V_{2f}\cos A_{2f} \\ W_1V_{1i}\sin A_{1i} + W_2V_{2i}\sin A_{2i} &= W_1V_{1f}\sin A_{1f} + W_2V_{2f}\sin A_{2f} \end{aligned} \tag{13.1}$$

Energy methods permit the final speeds (V_{1f} and V_{2f}) to be computed. Thus, the right side of the equations are known, whereas the left sides contain the two unknowns (V_{1f} and V_{2i}). This equation can be reduced to a more general description for the purposes of this chapter.

$$a_{11}x_1 + a_{12}x_2 = b_1$$
$$a_{21}x_1 + a_{22}x_2 = b_2 \qquad (13.2)$$

In matrix form, Equation 13.2 is reduced to the following basic equation.

$$A\boldsymbol{x} = \boldsymbol{b}$$

$$\begin{bmatrix} a_{11} & a_{12} \\ a_{21} & a_{22} \end{bmatrix} \begin{bmatrix} x_1 \\ x_2 \end{bmatrix} = \begin{bmatrix} b_1 \\ b_2 \end{bmatrix} \qquad (13.3)$$

Here, the matrix A represents the known quantities of the left side of the equation. For example, a_{11} is equal to $W_1\cos A_{1i}$. The vector **x** represents the unknown quantities of the left side of the equation. Namely, x_1, is V_{1i} and x_2 is V_{2i}. The vector **b** represents the right side of the equation, where the final velocities and departure angles are prescribed.

The 2×2 matrix A can be decomposed into the diagonal matrix D, the lower triangular matrix L, and upper triangular matrix U. It is also useful to define the identity matrix I, which is explained below for the 2×2 case.

$$D = \begin{bmatrix} a_{11} & 0 \\ 0 & a_{22} \end{bmatrix} \quad L = \begin{bmatrix} a_{11} & 0 \\ a_{21} & a_{22} \end{bmatrix}$$
$$U = \begin{bmatrix} a_{11} & a_{12} \\ 0 & a_{22} \end{bmatrix} \quad I = \begin{bmatrix} 1 & 0 \\ 0 & 1 \end{bmatrix} \qquad (13.4)$$

The determinant of a 2×2 matrix A is as follows:

$$\det(A) = |A| = a_{11}a_{22} - a_{21}a_{12} \qquad (13.5)$$

The above matrices and vectors can be examined for the three-dimensional case for conserving linear momentum. Here, the third equation would represent motion in the z-axis. However, there would remain essentially two unknowns and the added complexity is not applicable to the vast majority of two-vehicle accident reconstructions. For example, the pre- and postimpact motion of vehicles on a sloping road can be modeled by adjusting the friction factors (see Chapter 4 and Equation 4.14). With the 2×2 matrix, simultaneous solutions are possible if one wishes to solve it by hand. However, the sensitivity of the solution vector **x** to minor changes in A or **b** cannot be assessed this way and requires a numerical solution.

13.2.2 Direct Methods

There are numerous methods for directly solving systems of linear equations. These methods include Cramer's rule, elimination (Gauss and Gauss-Jordan), inversion of matrices, and factorization. These methods are less efficient than factorization and elimination methods. Although greater storage and an increase number of operations are required, this is not usually an issue when examining a 2×2 matrix. Only when the matrices become larger and more sparse do these issues arise.

Cramer's rule is a direct method that involves determining determinants. The solution vector **x** can be referred to as $x_j (j = 1,\ldots,n)$, where n represents the number of equations (or rows of the matrix A). The solution x_j is defined as:

$$x_j = \frac{\det(A^j)}{\det(A)} \tag{13.6}$$

where A^j is an $n \times n$ matrix. The j^{th} column in A is replaced by vector **b** to yield the matrix A^j. For example, the matrix A^2 would involve replacing the 2nd column of A with the vector **b**. The solution vector x_j, is thus, defined as follows.

$$x_1 = \frac{\begin{vmatrix} b_1 & a_{12} \\ b_2 & a_{22} \end{vmatrix}}{\begin{vmatrix} a_{11} & a_{12} \\ a_{21} & a_{22} \end{vmatrix}} \quad \text{and} \quad x_2 = \frac{\begin{vmatrix} a_{11} & b_1 \\ a_{21} & b_2 \end{vmatrix}}{\begin{vmatrix} a_{11} & a_{12} \\ a_{21} & a_{22} \end{vmatrix}} \tag{13.7}$$

Elimination methods are similar to simultaneous solutions in that they involve substitution of one unknown in terms of the remaining unknowns. These methods employ row operations where the following are permitted: scaling, pivoting, and elimination. Scaling permits the multiplication of any row by a constant integer. Pivoting involves the interchanging of the row order. Elimination involves the replacement of a row by a weighted linear combination of another row.

Gauss elimination is the general procedure described above. This method requires defining a $n \times n$ matrix A, a $n \times 1$ column vector **b**, and the $n \times 1$ solution vector **x**. Then, scale the k^{th} column ($k = 1\ldots,n{-}1$) and place the element with the largest magnitude in position a_{kk}. The third step employs an elimination procedure to create zeros in column k below the pivot element $a_{kk.}$

$$a_{ij} = a_{ij} - \left(\frac{a_{ik}}{a_{kk}}\right) a_{kj} \quad (i, j = k+1, \ldots, n)$$
$$b_i = b_i - \left(\frac{a_{ik}}{a_{kk}}\right) b_k \quad (i = k+1, \ldots, n) \tag{13.8}$$

This step results in an upper triangular matrix. The final step employs back substitution to yield **x**.

$$x_n = \frac{b_n}{a_{nn}}$$
$$x_i = \frac{b_i - \sum_{j=i+1}^{n} a_{ij} x_j}{a_{ii}} \tag{13.9}$$

To demonstrate this procedure, we will apply Equation 13.1, which represents the conservation of linear momentum for a two-vehicle collision, to an example problem. This problem involves two vehicles (V_1 and V_2) with identical masses, which permits elimination of the weights W_1 and W_2 from Equation 13.1.

$$V_{1i} \cos A_{1i} + V_{2i} \cos A_{2i} = V_{1f} \cos A_{1f} + V_{2f} \cos A_{2f}$$
$$V_{1i} \sin A_{1i} + V_{2i} \sin A_{2i} = V_{1f} \sin A_{1f} + V_{2f} \sin A_{2f}$$

The evidence indicates that the pre-impact angles A_{1i} and A_{2i} were 30 and 60 degrees, respectively. Conversely, the postimpact angles A_{1f} and A_{2f} were 60 and 30 degrees, respectively. Energy methods yielded a post impact speed of 40 mph for V_1 (V_{1f}) and 30 mph for V_2 (V_{2f}). The matrix A is represented by the cosines and sines of the preimpact angles. The unknown preimpact speeds (V_{1i} and V_{2i}) take the place of the solution vec.tor **x**. The right side of the equation, which represents the postimpact motion, takes the place of vector **b**. The matrix representation is shown below.

$$\begin{bmatrix} \cos A_{1i} & \cos A_{2i} \\ \sin A_{1i} & \sin A_{2i} \end{bmatrix} \begin{pmatrix} V_{1i} \\ V_{2i} \end{pmatrix} = \begin{pmatrix} V_{1f} \cos A_{1f} + V_{2f} \cos A_{2f} \\ V_{1f} \sin A_{1f} + V_{2f} \sin A_{2f} \end{pmatrix}$$

The row operations (scaling, pivoting, and elimination) associated with the Gauss procedure are shown below:

$$\begin{bmatrix} \frac{\sqrt{3}}{2} & \frac{1}{2} & 45.98 \\ \frac{1}{2} & \frac{\sqrt{3}}{2} & 49.64 \end{bmatrix} \text{Row}\#1 \times \frac{2}{\sqrt{3}}$$

$$\begin{bmatrix} 1 & \frac{1}{\sqrt{3}} & 57.32 \\ \frac{1}{2} & \frac{\sqrt{3}}{2} & 49.64 \end{bmatrix} \text{Row}\#2 - \frac{1}{2}\text{Row}\#1$$

$$\begin{bmatrix} 1 & \frac{1}{\sqrt{3}} & 57.32 \\ 0 & \frac{1}{\sqrt{3}} & 20.98 \end{bmatrix} \text{Row}\#2 \times \sqrt{3}$$

$$\begin{bmatrix} 1 & \frac{1}{\sqrt{3}} & 57.32 \\ 0 & 1 & 36.34 \end{bmatrix} \text{Row}\#1 - \frac{1}{\sqrt{3}}\text{Row}\#2$$

$$\begin{bmatrix} 1 & 0 & 36.34 \\ 0 & 1 & 36.34 \end{bmatrix}$$

The elimination procedure yields identical initial speeds (36 mph) for the two vehicles. Rather than performing this procedure by hand to examine the effects of changing the input variables, proper coding of Equations 13.8 and 13.9 is necessary.

If the matrix A is invertible, the matrix inverse method may be used. The inverse matrix A^{-1}, when multiplied by A, yields the identity matrix I.

$$\begin{aligned} &Ax = b \\ &A^{-1}Ax = Ix = x = A^{-1}b \\ &x = A^{-1}b \end{aligned} \tag{13.10}$$

Equation 13.10 becomes unusable if matrix A cannot be inverted. Singular matrices, whose determinant $|A|$ is zero, do not have inverses. As such, attempting to solve $A\mathbf{x} = \mathbf{b}$ with this method would not yield a unique solution.

Factorization methods involve decomposing the matrix A into lower diagonal *(L),* upper diagonal (U), and diagonal *(D)* matrices. One example of LU factorization, where the matrix A is decomposed into its lower and upper diagonal parts, will be presented. Other decomposition methods include the LU Crout method and the Choletsky LDL^T method, where L^T is the transpose of matrix L.

Once A is properly factored into the product LU, the governing equation can be manipulated as such.

$$\begin{aligned} &LUx = b \\ &L^{-1}LUx = IUx = Ux = L^{-1}b \\ &Ux = b' = L^{-1}b \\ &Lb' = LL^{-1}b = Ib = b \end{aligned} \tag{13.11}$$

The method is finalized by the following equation.

$$\begin{aligned} &Lb' = b \\ &Ux = b' \end{aligned} \tag{13.12}$$

For programing purposes, the Doolittle LU method involves performing the first three steps of the Gauss elimination method described previously. Storing the scaling, pivoting, and elimination information yields the L and U matrices. The $\mathbf{b}'$ and $\mathbf{x}$ vectors are then solved as follows.

$$\begin{aligned} &b_i' = b_i - \sum_{k=1}^{i-1} l_{ik} b_k' \\ &x_i = b_i' - \sum_{k=i+1}^{n} \frac{u_{ik} x_k}{u_{ii}} \end{aligned} \tag{13.13}$$

Elimination methods are sufficient for all nonsingular matrices. However, rounding errors and poorly conditioned matrices can affect the results of such an analysis. Rounding errors can be mitigated by performing iterative improvements. Conditioning refers to the sensitivity of a linear system to changes in the elements. Small changes in the input variables that produce large changes to the results indicate that the system is ill-conditioned and therefore more suitable to other solution methods.

13.2.3 Iterative Solutions

Large, sparse matrices require large amounts of storage space and operations when solved by direct methods. As such, iterative methods are often employed in these cases. Examples of iterative processes include the Jacobi method, Gauss-Seidel, successive-over-relaxation (SOR), and the conjugate gradient method. Preconditioning is frequently employed for matrices that are poorly conditioned as described above.

The linear system $A\mathbf{x} = \mathbf{b}$ can be displayed in index notation.

$$\sum_{j=1}^{n} a_{ij} x_j = b_i \qquad (i = 1, \ldots, n) \tag{13.14}$$

The Gauss–Seidel method involves making initial guesses to the solution ($x_i^{(0)}$ and $x_i^{(1)}$) and defining a residual vector $R\left(R_i^{(k)}\right)$.

$$\begin{aligned} x_i^{(k+1)} &= x_i^{(k)} + \frac{R_i^{(k)}}{a_{ii}} \qquad (i = 1, \ldots, n) \\ R_i^{(k)} &= b_i - \sum_{j=1}^{i-1} a_{ij} x_j^{(k+1)} - \sum_{j=1}^{n} a_{ij} x_j^{(k)} \qquad (i = 1, \ldots, n) \end{aligned} \tag{13.15}$$

The SOR method entails applying a relaxation factor ω that varies between 1.0 and 2.0.

$$\begin{aligned} x_i^{(k+1)} &= x_i^{(k)} + \omega \frac{R_i^{(k)}}{a_{ii}} \qquad (i = 1, \ldots, n) \\ R_i^{(k)} &= b_i - \sum_{j=1}^{i-1} a_{ij} x_j^{(k+1)} - \sum_{j=1}^{n} a_{ij} x_j^{(k)} \qquad (i = 1, \ldots, n) \end{aligned} \tag{13.16}$$

When $\omega > 2.0$, this method diverges. At $\omega = 1.0$, this method is equivalent to Gauss–Seidel. Where $\omega < 1.0$, the method is said to be "under relaxed." If the residual vector R is too large, an under-relaxation method is employed. An optimum relaxation factor is dependent on the size and nature of the system of equations. If a system is to be solved many times, determining this optimum value would be beneficial.

13.2.4 Polynomial Approximation and Interpolation

Occasionally, the forensic reconstructionist will be presented with sets of data to analyze. For example, pedal force and deceleration levels over time may be gathered from accelerometer data. Fitting curves to the set of data may be useful for the purpose of integrating or differentiating. (Methods of numerical integration and differentiation will be discussed in the next section.) Additionally, the value between adjacent data points may be desired, which will necessitate the approximation or interpolation of the function. Figure 13.1 depicts an arbitrary set of data points and a smooth function approximated between the points.

x	$f(x)$
0.5	0.30
0.7	0.50
1.0	0.75
1.2	0.70
1.4	0.65
1.6	0.85
1.9	0.80
2.2	0.80

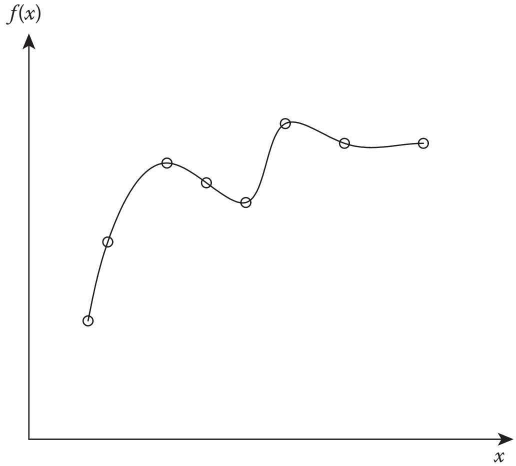

Figure 13.1 Arbitrary data points.

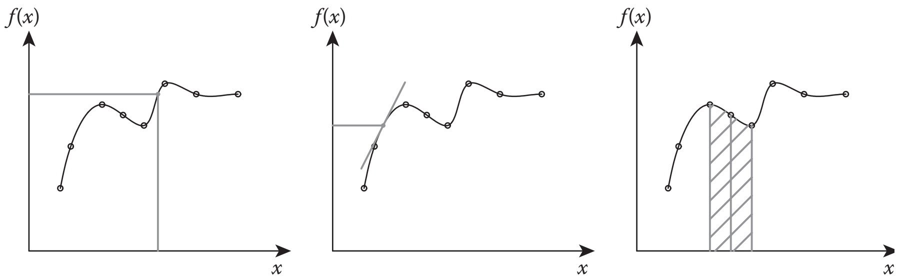

Figure 13.2 Approximating functions.

Figure 13.2 depicts applications of approximating functions, including interpolation, differentiation, and integration.

Typically, polynomial, trigonometric, and exponential functions will be chosen to match a set of data. These functions are representative of many physical processes and may be known to be applicable to a certain problem. Additionally, these functions are commonly chosen because they are smooth, differentiable, and can be easily integrated. Here, we will examine polynomial fitting.

There are two methods of fitting a polynomial to a set of data points: exact fits and approximate fits. Exact fits are created when the polynomial passes directly through each point. Direct fit polynomials, lagrange polynomials, difference formulas, and cubic splines are commonly used to precisely fit the function to the data points. Smooth data and smaller data sets are required for exact fits.

Approximate fits, such as the least squares method, pass the function through the data in the best possible manner. When the data sets are very large and rough, approximate fits are preferred. The manner through which the approximate fitting is made depends on the limitations on the error between the point and the function curve. Although various definitions of error limits exist, we will examine the least squares approach.

An n^{th} degree polynomial is defined as follows:

$$P_n(x) = a_0 + a_1 x + a_2 x^2 + \cdots + a_n x^n \tag{13.17}$$

Employing a nesting multiplication algorithm can assist in depicting the function in matrix form.

$$\begin{aligned} b_n &= a_n \\ b_i &= a_i + x b_{i+1} \qquad (i = n-1, n-2, \ldots, 0) \\ b_0 &= P_n(x) \end{aligned} \tag{13.18}$$

A procedure for deriving a direct fit polynomial is shown below. Here, $n + 1$ linear equations with $n + 1$ coefficients are generated. Direct methods for solving linear equations, such as Gauss elimination, can be implemented.

$$\begin{aligned} P_0(x) &= P_0 = a_0 + a_1 x_0 + a_2 x_0^2 + \cdots + a_n x_0^n \\ P_1(x) &= P_1 = a_1 + a_1 x_1 + a_2 x_1^2 + \cdots + a_n x_1^n \\ &\cdots\cdots\cdots\cdots\cdots\cdots\cdots\cdots \\ P_n(x) &= P_n = a_0 + a_1 x_n + a_2 x_n^2 + \cdots + a_n x_n^n \end{aligned} \tag{13.19}$$

The direct method outlined in Equation 13.19 is cumbersome and requires a considerable amount of time and effort. Lagrange polynomials provide a simpler means of fitting a curve to a set of data points. Lagrange polynomials can be expressed in linear terms (*P*,(*x*)), quadratic terms ($P_2(x)$), and so on. The linear polynomial that passes through two points [*a*,*f*(*a*)] and [*b*,*f*(*b*)] is as follows.

$$P_1(x) = \frac{(x-b)}{(a-b)} f(a) + \frac{x-a}{b-a} f(b) \tag{13.20}$$

$$\text{where } P_1(a) = f(a) \quad \text{and} \quad P_1(b) = f(b)$$

For higher order, n^{th} degree polynomials, a general procedure is described in Equation 13.21. Here, we are given $n + 1$ points $[a,f(a)]$, $[b,f(b)]$, ..., $[k,f(k)]$.

$$P_n(x)=\frac{(x-b)(x-c)\ldots(x-k)}{(a-b)(a-c)\ldots(a-k)}f(a)+\cdots+\frac{(x-a)(x-b)\ldots(x-j)}{(k-a)(k-b)\ldots(k-j)}f(k) \quad (13.21)$$

Neville's algorithm is based on the Lagrange interpolation and is given in general notation in Equation 13.22

$$f_i^{(n)}=\frac{(x-x_i)f_{i+1}^{(n-1)}-(x-x_{i+n})f_i^{(n-1)}}{x_{i+n}-x_i} \quad (13.22)$$

This algorithm is especially useful in determining the value of a function for a point x not in the data set x_i. For a set of $n + 1$ points, the interpolated value of an n^{th} order function can be calculated. Table 13.1 outlines Neville's algorithm for a set of four data points $[x_{1,}f_1],\ldots,[x_4,f_4]$.

The discussion to approximate fitting techniques will be limited to an introduction to the least squares approach. As previously stated, the intent of an approximate fit is to pass a polynomial through a set of points in the best possible manner. Here, an error e_i is introduced, which is the difference between the data point Y_i and approximated function point y_i.

$$e_i = Y_i - y_i \quad (13.23)$$

The notional form of the straight line approximation is as follows. Here, a is the y-intercept and b is the slope of the line.

$$y_i = a + bx_i \quad (13.24)$$

Table 13.1 Neville's Algorithm

x_i	$f_i^{(0)}$	$f_i^{(1)}$	$f_i^{(2)}$	$f_i^{(3)}$
x_1	$f_1^{(0)}$			
		$f_1^{(1)}$		
x_2	$f_2^{(0)}$		$f_1^{(2)}$	
		$f_2^{(1)}$		$f_1^{(3)}$
x_3	$f_3^{(0)}$		$f_2^{(2)}$	
		$f_3^{(1)}$		
x_4	$f_4^{(0)}$			

The least squares method involves minimizing the sum of the squares of the error values e_i. This sum is defined in Equation 13.25 below.

$$S(a,b)=\sum_{i=1}^{n}(e_i)^2=\sum_{i=1}^{n}(Y_i-a-bx_i)^2 \tag{13.25}$$

To minimize this function, the first derivative with respect to a and b is computed and set equal to zero.

$$\begin{aligned}\frac{\partial S}{\partial a}&=\sum_{i=1}^{n}2(Y_i-a-bx_i)(-1)=0\\ \frac{\partial S}{\partial b}&=\sum_{i=1}^{n}2(Y_i-a-bx_i)(-x_i)=0\end{aligned} \tag{13.26}$$

Algebraic manipulation of Equation 13.26 yields the general form of the linear least squares approximation.

$$\begin{aligned}an+b\sum_{i=1}^{n}x_i&=\sum_{i=1}^{n}Y_i\\ a\sum_{i=1}^{n}x_i+b\sum_{i=1}^{n}x_i^2&=\sum_{i=1}^{n}x_iY_i\end{aligned} \tag{13.27}$$

Higher-degree approximations are formulated in a similar manner. An n^{th} degree polynomial (as shown in Equation 13.17) will approximate a set of n data points, which involves computing $n+1$ equations described in Equation 13.28.

$$\begin{aligned}a_0n+a_1\sum_{i=1}^{n}x_i+\cdots+a_n\sum_{i=1}^{n}x_i^n&=\sum_{i=1}^{n}Y_i\\ a_0\sum_{i=1}^{n}x_i^{\,n}+a_1\sum_{i=1}^{n}x_i^{n+1}+\cdots+a_n\sum_{i=1}^{n}x_i^{2n}&=\sum_{i=1}^{n}x_i^{\,n}Y_i\end{aligned} \tag{13.28}$$

13.2.5 Numerical Integration and Differentiation

Differentiation and integration of functions are frequently employed in engineering analyses. Accident reconstruction techniques are largely based on the principles stated in Chapter 2, which are repeated here.

$$\boldsymbol{v} = \frac{dx}{dt}; \qquad \boldsymbol{a} = \frac{d\boldsymbol{v}}{dt} \tag{13.29}$$

$$\boldsymbol{v} = \int \boldsymbol{a}(t)dt; \qquad x = \int \boldsymbol{v}(t)dt \tag{13.30}$$

Typically, tabular data for a vehicle's position, velocity, and acceleration over time are not known unless the data are derived from a black box or performance testing. Despite the infrequency of possessing this data, the reconstructonist should be familiar with numerical integration and differentiation techniques when the occasion arises. Occasionally, the reconstructionist will attempt to solve an integral for which there is no closed-form solution. Equation 4.88 represents an example of this case, which is modified below to depict the bounds of integration.

$$\int_{v1}^{v2} \frac{dv}{\sqrt{k^2 - v^4}} = \int_{t1}^{t2} \frac{dt}{R} \tag{13.31}$$

Efforts made based on equations used in the previous section can yield an approximate or direct polynomial fit to a set of data.

Given an n^{th} degree polynomial $P_n(x)$ described in Equation 13.17, the first derivative and integrals are as follows.

$$\begin{aligned} &\frac{d}{dx}(f(x)) = f'(x) = f_x(x) \cong \frac{d}{dx}(P_n(x)) \\ &I = \int_a^b f(x)dx \cong \int_a^b P_n(x)dx \end{aligned} \tag{13.32}$$

$$\begin{aligned} &f_x(x) \cong P_n'(x) = a_1 + 2a_2x + 3a_3x^2 + \cdots + na_nx^{n-1} \\ &I \cong \int_a^b P_n(x)dx = a_0x + \frac{1}{2}a_1x^2 + \cdots + \frac{1}{n+1}a_nx^{n+1}\Bigg|_a^b \end{aligned} \tag{13.33}$$

Such an evaluation of a polynomial is trivial and need not be discussed further. Lagrange polynomials can be evaluated in a similar manner. For a second order Lagrange polynomial shown in Equation 13.34, the first order derivative is shown in Equation 13.35.

$$P_2(x) = \frac{(x-b)(x-c)}{(a-b)(a-c)}f(a) + \frac{(x-a)(x-b)}{(b-a)(b-c)}f(b) + \frac{(x-a)(x-b)}{(c-a)(c-b)}f(c) \tag{13.34}$$

$$f_x(x) \cong P_2'(x) = \frac{2x-(b+c)}{(a-b)(a-c)} f(a) + \frac{2x-(a+c)}{(b-a)(b-c)} f(b) + \frac{2x-(a+b)}{(c-a)(c-b)} f(c) \quad (13.35)$$

Divided difference formulas are also useful whether the data are equally or unequally spaced. Refer to Table 13.1 for a depiction of a divided difference table and description of the $f_i^{(j)}$ terms. A divided difference polynomial and its first derivative are shown below.

$$P_n(x) = f_i^{(0)} + (x-x_0) f_i^{(1)} + (x-x_0)(x-x_1) f_i^{(2)} + \cdots \quad (13.36)$$

$$f_x(x) \cong P_n'(x) = f_i^{(1)} + [2x-(x_0+x_1)] f_i^{(2)} + \cdots \quad (13.37)$$

Forward, backward, and centered difference formulas necessitate the construction of difference tables. Table 13.2 details a forward difference table based on the definition given in Equation 13.38.

$$\Delta f(x_i) = \Delta f_i = (f_{i+1} - f_i) \quad (13.38)$$

Here, the data are assumed to be equally spaced. The term h denotes the distance between adjoining points x_i and x_{i+1}. The interpolating parameter s is as follows.

$$s = \frac{x-x_0}{h} \rightarrow x = x_0 + sh \quad (13.39)$$

Table 13.2 Forward Difference Table

x_i	$f(x)$	Δf	$\Delta^2 f$	$\Delta^3 f$
x_0	f_0			
		$(f_1 - f_0)$		
x_1	f_1		$(f_2 - 2f_1 + f_0)$	
		$(f_2 - f_1)$		$(f_3 - 3f_2 + 3f_1 - f_0)$
x_2	f_2		$(f_3 - 2f_2 + f_1)$	
		$(f_3 - f_2)$		
x_3	f_3			

The Newton forward difference polynomial is described in Equation 13.40.

$$P_n(x) = f_0 + s\Delta f_0 + \frac{s(s-1)}{2}\Delta^2 f_0 + \cdots + \text{Error} \tag{13.40}$$

The first and second order derivatives corresponding to this definition are shown below. Higher order derivatives become less and less accurate with this method.

$$\begin{aligned} P_n'(x_0) &= \frac{1}{h}\left(\Delta f_0 - \frac{1}{2}\Delta^2 f_0 + \frac{1}{3}\Delta^3 f_0 - \cdots\right) \\ P_n''(x_0) &= \frac{1}{h^2}(\Delta^2 f_0 - \Delta^3 f_0 + \cdots) \end{aligned} \tag{13.41}$$

For the discussion of integration, we will concentrate on the Newton-Cotes formulas. The rectangle rule, a zeroth order formula, is self explanatory. The trapezoid rule, a first order formula that produces a second order error, is shown below. Here, a first degree polynomial is fitted to two data points.

$$\begin{aligned} I &= \frac{1}{2}h(f_0 + 2f_1 + 2f_2 + \cdots + 2f_{n-1} + f_n) \\ &\text{where:}\quad \Delta x_i = \Delta x = h \end{aligned} \tag{13.42}$$

Simpson's 1/3 rule involves fitting a second degree polynomial to three points that are equally spaced. The global error is of the order of h^4.

$$I = \frac{1}{3}h(f_0 + 4f_1 + 2f_2 + 4f_3 + \cdots + 4f_{n-1} + f_n) \tag{13.43}$$

Finally, a third degree polynomial using four data points can be integrated using the Simpson's 3/8 rule.

$$I = \frac{3}{8}h(f_0 + 3f_1 + 3f_2 + 2f_3 + 3f_4 + \cdots + 3f_{n-1} + f_n) \tag{13.44}$$

Evaluation of Equation 13.44 yields the same order of error as the Simpson's 1/3 rule and is slightly less accurate than the latter. Despite this loss in accuracy, Simpson's 3/8 rule is simpler to compute when the total number of increments is odd.

13.2.6 Programing

The numerical techniques described above can be used to solve a variety of problems in accident reconstruction. Computer software is an absolute necessity given the excessive time and effort involved in solving these problems by hand. There are a variety of commercial packages available for use by a reconstructionist.

Spreadsheet programs, such as Microsoft's Excel and Corel's QuattroPro, simulate paper worksheets by dividing the page into rows, columns, and individual cells. Spreadsheets are useful for direct solutions to algebraic equations that can be programed into cells. The cells and rows are helpful in visualizing problems that involve matrices, vectors, or computational grids. However, the larger and more complex a spreadsheet program becomes, the equations and relationships of each cell can become difficult to ascertain.

Programing languages such as C and Fortran are suited to numerical computation. However, these programs are scalar and non-interactive, which increases the time and effort involved in programming. Programs especially suited to engineers, such as MATLAB® and Maple, permit algebraic or symbolic manipulation of problems. MATLAB is especially useful for problems involving matrix and vector formulations. Maple is a symbolic computational system that allows users to produce exact analytical solutions to many problems. Another commonly used program, Mathcad, is oriented to engineers less familiar with programming languages.

13.3 Commercially Available Software

Computer software used in the accident reconstruction field can fit into three separate categories: reconstruction, simulation, and animation. The intent of this section is to provide a brief description of these types of software. This discussion should not be viewed as an endorsement of any specific computer program. However, many of these programs have been validated by independent organizations.

Reconstruction software is arguably the most intuitive and applicable in its procedure. These programs determine the conditions of a collision (i.e., speed and ΔV) from known parameters. As with the momentum analysis, the speeds at impact are determined from the known quantities; namely, impact configuration and rest position. Reconstruction software that includes energy analysis can quantify the magnitude of the collision (ΔV) based on the extent of crush damage and the stiffness of the vehicle. Equivalency between the momentum based ΔV and the damage based ΔV would be one criterion for arriving at a proper solution.

Programs such as EDCRASH, produced by Engineering Dynamics Corporation (EDCORP), utilize these basic principles. EDCRASH was validated during program development by staged collisions conducted at Calspan. Recent validation studies have revealed improved levels of accuracy for refined versions of this program.

Simulation software involves setting the initial conditions (impact speed and configuration) based on estimation or assumption, which permits the final outcome (trajectories, crush profiles) to be predicted. Solution convergence results when the initial conditions yield data that best matches physical evidence. Reconstruction programs may be first used to determine the best estimates, which can be used to corroborate the trajectories produced by the simulation software. Simulations may be employed prior to crash testing in order to better anticipate the post-impact trajectories.

Engineering Dynamics Corporation Simulation Model of Automobile Collisions (EDSMAC) and EDSMAC4, produced by EDCORP, and PC Crash, produced by MEA Forensic Engineers and Scientists, are two such simulation programs. Like EDCRASH, EDSMAC has been validated using the RICSAC collision experiments. PC Crash has been validated through numerous studies and is widely accepted in the forensic community.

Animations are distinct from reconstructions or simulations. Animation is defined as "*the act, process, or result of imparting life, interest, spirit, motion, or activity.*" The key word here is "*imparting*" as no solution or computation is produced in an animation. Rather, an animation depicts a scenario based on data *imparted* by the user. In other words, a reconstruction or simulation must first be performed to determine the motions of vehicles involved in a collision. Subsequently, an animation may be created to depict the motions based on the computations.

Animations are purely visual and intended only to show an audience what has been analyzed. Since numbers and tables are not as convincing to a jury, animations are useful in describing the events of a collision. While some of the reconstruction and simulation programs listed above have animation capabilities, the quality of the rendered scenes are somewhat lacking. This statement is not meant as a slight. The computational requirements of these programs are such that making movie-quality animations is not feasible.

Separate animation programs, such as 3DStudio Max produced by Autodesk, may be used to create a realistic, virtual world to recreate the collision. 3DStudio Max has been used to make numerous films and video games that have amazed audiences with their ability to create realistic images and motions. Fortunately for the forensic engineer, the requirements for realism in an animation displayed in a courtroom are not as high as a movie produced in Hollywood. Still, there is an immense time required to construct three-dimensional objects and vehicles, apply realistic surfaces and lighting conditions, and convert reconstruction data to create motion.

Measuring devices such as surveying total stations allow for a fast and accurate method of gathering information about a vehicle or a scene. Such data are readily downloaded to a computer with a program such as AUTOCAD so that an accurate three-dimensional map of the scene or the vehicle is created. This scene and vehicle can then be transferred to a program such as 3D Studio Max so that an animation of the event can be recreated. Additionally, the availability of satellite imagery and mapping software can aid the reconstructionist in the accurate assessment of the conditions pertinent to the reconstruction. There are also governmental agencies and various private data collection companies that can determine the weather, and lighting conditions at the time of the accident.

13.4 Reconstruction Tools

Some common arguments against a forensic engineer's conclusions are that they are based on estimations and computations involving some margin of error. As discussed in Chapter 16, small errors in independent variables can produce larger uncertainties in the dependant variables. While no engineer or scientist can claim to have an exact solution, an honest assessment of uncertainties can be used by an opposing party to imply that the solutions are unreliable. These errors are vastly reduced when the forensic engineer can refer to precise measurements of an accident. In this age of advanced technology, such measurements are frequently available. As it was pointed out in Chapter 3, the required accuracy of the measurement depends on the application rather than on the number of significant figures of the value.

Black box technology, originally a feature in aircrafts, has progressively been implemented into the automotive industry. The development of Electrically Erasable Programmable Read-only Memory (EEPROM) technology in automobiles permitted the storage of data in the event that power is disconnected. The application of nonvolatile electronic data storage has included antilock braking systems (ABS), cruise control, and supplemental restraint systems (SRS). The original intent of storing this data was to facilitate repair for the various electronic systems. However, the storage of collision data, especially in the air bag system (SRS), has also provided assistance to accident investigations.

Unfortunately for the majority of investigators, collision data stored in the SRS is unaccessible for all but the vehicle manufacturer. However, recent products have become available for the forensic engineer to access this data on a subset of vehicles. The Crash Data Retrieval (CDR) system, formerly manufactured by Vetronix Corporation and currently provided by Bosch

Diagnostics, permits users to access crash data stored in the SRS. A brief discussion of this system is included in Chapter 3. Data are stored in the SRS if a vehicle endures an event sufficient to “wake-up” the system. A low speed collision or curb impact that is not sufficient to trigger the air bags is defined as a non-deployment event. Such events are usually stored for 250 ignition cycles, when they are erased. Similarly, subsequent low speed collisions overwrite the preceding nondeployment event. Deployment events are those that produce ΔV’s of the order of 9–14 mph. When the air bags are deployed, data are permanently stored in the air bag module.

Among the vehicles included in the CDR system are many manufactured by General Motors (GM) since 1994, as well as some Ford, Chrysler, and Isuzu models. The CDR systems permit the investigator to access the data through the data link connector (DLC). If the vehicle is without power, as is often the case for high speed collisions, the CDR hardware can be linked via the air bag module. These modules are normally mounted to the floor pan or center console. Figure 13.3 depicts a typical CDR set-up. Figure 13.4 shows a crash pulse graph. The data made available by the manufacturer varies greatly with the model. An investigator may be able to determine impact speeds, lateral and longitudinal ΔV, status of the driver’s seatbelt, and vehicle performance for the 5-sec period preceding a collision.

A forensic engineer may perform crash testing, either as a research project or as a part of a legal case to assess his or her findings. Black box modules and accelerometers may be installed in a test vehicle to measure and record the crash data. Black boxes, such as those manufactured by Independent Witness Inc., are permanently installed on a subject vehicle. These modules have an independent power source and provide ΔVs and accelerations for each crash. Figures 13.5 through 13.11 depict a crash test involving an

Figure 13.3 Typical CDR set-up.

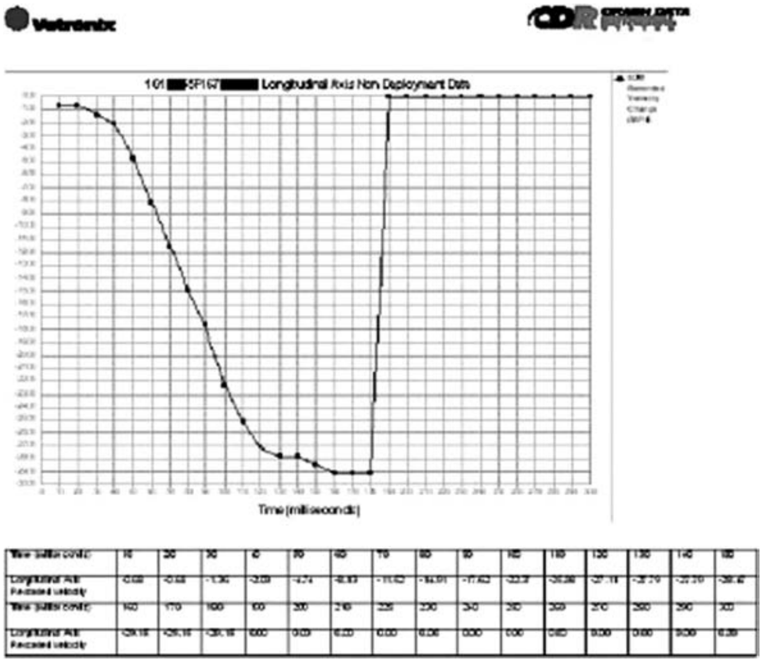

Figure 13.4 Crash pulse graph.

Figure 13.5 Crash test vehicle.

Figure 13.6 Crash test set-up.

Figure 13.7 Accelerometer in test vehicle.

Figure 13.8 Vehicles after impact.

Figure 13.9 Damage after impact.

exemplar pick-up truck striking the side of a large transport truck. The test pick-up was traveling at 25 mph while the transport truck was stationary. The crash test was performed to depict the difference in damage of the test vehicle to the more extensive damage incurred to a pick-up that had previously collided with the transport truck. The reconstruction revealed that the subject pick-up had impacted the transport truck at a speed of roughly 45 mph. The impact occurred between a steel storage box and the front tandem wheel along the driver's side of the transport truck. As shown, the black box module was installed in the center of the floor of the pick-up. The pick-up

Figure 13.10 Impact on tire.

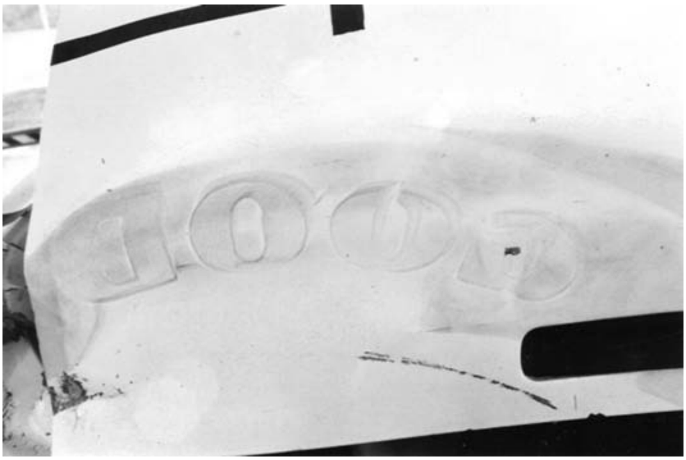

Figure 13.11 Impact on truck.

was dragged into the target vehicle at the test speed of 25 mph. While not pertinent to this chapter, Figures 13.10 and 13.11 reveal the precise impact location on the front of the test pick-up. When the performance of a vehicle is in question, and that vehicle is drive-able, accelerometers may be used to directly measure its operation. Accelerometers are composed of spring-mass sensing devices. Slight movement of the device is measured electronically to reveal changes in acceleration (G forces) over time. When an accelerometer is mounted to a vehicle, the inertial movement of the vehicle induces the motion of the sensor.

Figure 13.12 Accelerometer.

Figure 13.13 Closeup of Accelerometer.

Braking and acceleration tests are performed to assess whether claims of malfunctioning or defects have merit. Chapter 7 included a discussion of brake testing wherein deceleration levels were measured with an accelerometer. Lateral accelerations, commonly utilized in critical speed computations detailed in Chapter 4, may also be measured. Figures 13.12 and 13.13 detail an accelerometer manufactured by Vericom Computers that was mounted to a vehicle for acceleration testing.

Low Speed Impacts and Injury

14

14.1 Introduction

At first glance it might seem that the title of this chapter is inconsistent. What do low speed impact crashes have to do with injuries to the occupants of a vehicle or to pedestrians? Actually, there are low speed crashes that can injure pedestrians and cyclists. However, there is a limit on the speed that can injure the occupants of a vehicle. Let us analyze the two events separately because they are, in fact, subject to different forces, energies, and effects.

The first case to consider is that of a vehicle striking a pedestrian or a cyclist. It does not much matter if the cyclist is on a bicycle, a moped, or a motorcycle. At this point we will arbitrarily choose 10 mph as the collision speed of the vehicle. We will classify collisions less than 10 mph as low speed and collisions above 10 mph as higher speed. We will not differentiate collisions above 10 mph as medium or higher speeds. Later in this chapter we will discuss collision speeds with respect to injuries of the occupants. Right now we are discussing collision speeds of a vehicle relative to an unprotected pedestrian or cyclist.

To illustrate the principles of injury involved in a vehicle/pedestrian or cyclist collision let us assume that the vehicle and pedestrian are traveling at 15 and 4 ft/sec, respectively. Further assume that the two are traveling perpendicular to each other, the car at 0 degrees and the pedestrian at 90 degrees. The car weighs 4000 lbs and the pedestrian or cyclist weighs 200 lbs. Just before impact, the pedestrian stops directly in front of the car. If we apply conservation of momentum and conservation of energy to the problem, we calculate the post impact speed of the car at 14.6 ft/sec and the post-impact speed of the pedestrian at 7.6 ft/sec. The kinetic energy imparted on the pedestrian is 5776 ft-lbs. Although the car can easily absorb such energy, the human body cannot without considerable injury, which is especially true when the forces are concentrated over a small area of the body such as the leg or head. As an analogy for this type of collision, consider the case of a nail, a small mass, being driven by a 2-lb hammer. If we decide to use a 10-lb hammer instead, we find the task of driving the nail so much easier because the heavy hammer has five times the mass and therefore five times the energy. A small mass, the pedestrian, is being driven by a large mass, the car.

What is the difference if a person is in a car that gets rear-ended by another car? Let us assume that the first car and occupants weigh 4000 lbs and the second car and occupants weigh 3000 lbs. The striking car is traveling 15 ft/sec and the second car is stopped. If we apply conservation of momentum and energy to the problem, we calculate that the postimpact speed of the striking car is 2.14 ft/sec, and the postimpact speed of the stationary vehicle is 2.44 ft/sec. If an occupant in the stationary vehicle weighs 200 lbs and he is accelerated to the speed of the struck vehicle by the seat back and headrest, then the kinetic energy imparted on his back is 18.6 ft-lbs.

A comparison of the kinetic energy calculations in these simple examples show the large disparity between 18.6 and 5776 ft-lbs for the two types of collisions. In the second example, the masses in the collision were comparable and the occupant was protected at least at two levels. At the first level, the struck vehicle absorbed much of the energy. At the second level, the cushioning provided by the seat also absorbed energy. At the third level the biomechanical construction of the human also provided some level of protection for the components of the occupant. In this chapter we will discuss the methods of analysis and the tolerances of the human body to injury. It should be made clear that the data referred to in this chapter is based on sound scientific testing and not on opinions of experts that have no scientific underpinning.

14.2 Methods of Analysis

A common argument made in low speed impacts is that certain methods of analysis cannot be used to determine vehicle speeds. Two methods that come under attack are momentum and crush. Let us examine both of these methods individually. The argument that momentum cannot be applied to low impact collisions because the postcollision distances are not accurately known is actually a valid argument to a certain extent. However, boundaries can be applied to such collisions because the vehicles do not move a significant distance after impact. The vehicles may also roll to a stop. In most of these cases the impact is of a rear-end type where one vehicle is at a stop and the other vehicle fails to brake. Even in these collisions, the problem can easily be solved from Equations 5.3 through 5.9. These types of collisions are colinear, that is the pre and postimpact angles are essentially the same so that momentum equations tend to blow up because the argument in the denominator may go to zero. Please refer to the linear momentum equations of Chapter 5. However, the angles are never exactly the same so that a simple parametric variation of the angles will readily determine the solution. If one attempts to solve these problems with a hand calculator, the task is almost impossible and at the very least tedious. Thus, reconstructionists using calculators soon abandon the effort and label the solution as unsolvable or state that the method of analysis does not apply. Actually, these problems are easily solved in a spreadsheet program if the reconstructionist programs the equations properly. Then by varying the parameters individually and sequentially, the solution is readily obtained.

The reader is encouraged to study Chapter 16 on sensitivity analysis in order to fully appreciate the effects of parametric analysis of these problems. On a final note on momentum, one should review the development of the mathematical formulations of the various momentum equations. Those theoretical developments place no restrictions on the speed of the vehicles. Thus, momentum equations apply over the range of speeds that reconstructionists encounter. Recall from Chapter 2 that the concepts of impulse and momentum as well as energy were derived from Newton's second law. Thus, to imply that momentum techniques are not valid is paramount to stating that Newton's second law does not apply. For our observable universe, in the macro scale, to state that the second law does not apply is simply incorrect.

The other argument used in low impact collisions is that crush methods are not applicable at low speeds. The main reason for the argument is that crash tests are generally performed at the 30 to 40 mph range with barriers. Thus, these tests could not possibly represent collisions at lower speeds. The question is, can the tests represent within acceptable engineering accuracy collisions at lower speeds? The answer is yes. We begin the argument in the following manner. Thousands of crash tests have been performed by the National Highway Traffic Safety Administration (NHTSA). These tests date back more than 45 years. General Motors (GM) developed the first impact sled in 1962. As of the date of writing, since testing began and according to NHTSA, 577 tests have been performed on various vehicles at speeds between 0 and 16 kph. These tests fall into what we have defined as low impact collisions. In comparison 5,199 tests have been performed between 0 and 100 kph. As it was pointed out in Chapter 4 in the section on vehicle crush, there is a linear relationship between impact speed and crush deformation within limits of accuracy. The accuracy at the lower speeds is well within acceptable levels for engineering calculations. According to SAE Paper 900412 the vehicle crush behavior can be modeled as being linear in the range of 10–40 mph. This study found correlation values ranging from 0.97 to 0.99 to the linear model. The methods of analysis utilized for low velocity impacts and for the biomechanical calculations of injury are simply Newtonian mechanics as have been described in the chapters of this book. When biomechanical calculations are performed on various parts of the human body, the biological structures are simply treated as mechanics of material structures with the known parameters of those structures.

14.3 Biomechanics of Injury

14.3.1 Soft Tissue Injuries

The human body is no different from any other structure that is analyzed by engineers. When vehicular accidents are reconstructed, basic principles of physics and strength of materials are utilized. These principles include forces, moments, energy, stress, strain, and acceleration to name a few. Similarly, once the dynamic forces acting on the vehicles are determined, these forces impact the occupants so that the same principles apply with respect to the biomechanics of injury, the only difference being the materials studied are human body parts such as bones, ligaments, muscles, tendons, and soft tissues. The properties of human tissue are well known through experimentation as outlined in the references.

A basic premise of science is that theoretical and experimental results must agree. In other words, what we observe must be explained by the theories and equations that are developed to explain the processes we experience. The basic dynamic laws of physics are Newton's laws, which cannot be broken by the reconstructionist. The biological data on human injury analysis is gathered from *STAPP Car Crash Conferences* and from *Strength of Biological Materials* by Yamada (1970). This biological data obtained through experimentation places lower and upper limits on the forces, velocities, and accelerations necessary to injure the human body. One of the most violated principles of injury analysis is that of soft tissues. The U.S. Aerospace Medical Laboratory conducted numerous tests on monkeys and transposed that data to humans to determine the upper limit of human tissue to accelerations without the occurrence of injury. This upper limit has been placed at 12 g where g is the acceleration due to gravity. Similarly, at accelerations in the range of 125–150 g, there is a 99% probability of injury to human soft tissues.

Anteflex whiplash injuries have been extensively studied. Some of the most comprehensive studies were conducted by Clemens and Burrow in Berlin, Germany on 53 cadavers. These studies found three areas of the spine that are susceptible to injury. These areas are at the base of the cranium and C1, the region of C3 and C4, and the region of C6 and C7. These tests, in the range of 17 mph and decelerations in the range of 30 g, correlated to serious injury involving 90% of ruptures of discs and 30% fractures. The exact limit of vulnerability was found to be at 13 mph and 13 g. According to Damask (1990) there are four degrees of injuries associated with whiplash as shown in Table 14.1.

Note that in the above discussion there is excellent agreement on the accelerations required for the onset of injury as determined by the U.S. Aerospace Medical Laboratory and the studies conducted by Yamada (1970)

Table 14.1 Degrees of Injuries

Degree	Comments	Speed and Acceleration
1	Isolated fissures of discs without injury to the ligaments or bones	13–16 mph 13–15 g
2	Injury to discs, ruptures of interspinal ligaments, rupture of joint capsules, fractures of vertebral processes, but no rupture of the posterior longitudinal ligaments. Subluxation is possible and probable at the sixth vertebra as well as teardrop fractures	17 mph 16–30 g
3	Rupture of posterior longitudinal ligament, luxation of all vertebral joints, injury centered at C6, but increased vulnerability of C1/C2, possible basal skull fracture	34 g
4	Complete disconnection of the neck	42 g

and Clemens/Burrow. Therefore, at accelerations of 12 g or less, corresponding to speed changes less than 10 mph, no soft tissue injuries occur to the human body.

SAE Technical Paper 930889 states, "For rear end collisions within the velocity range included in our test series, the classic 'whiplash' injury mechanism, seems unlikely since no hyperextension or hyperflexion was observed in any of our test subjects." SAE Technical Paper 940532 states, "The present study enhances the existing data base of volunteer studies which support the premise that, for restrained occupants with a head restraint available, single exposure to a rear end collision with a Delta *V* of 8 kph or less is within human tolerance levels, and extends the data base to include females and those with some degree of pre-existing spinal pathology."

As an example, in a reconstruction of an accident based on crush and energy, the crush analysis indicated that the velocity changes experienced by the occupants were 4.0 mph for a Toyota and 2.0 mph for Dodge Durango. These computed values were consistent with the damage observed on the vehicles because the Durango showed no damage and the Toyota revealed very minor damage.

Assuming a worst case scenario of a Delta *V* of 5 mph or approximately 7.33 ft/sec, the accelerations experienced by the occupants can be calculated as follows: since for average humans the differential distance between the lower spine and the rest of the spine is approximately 2.5 inches or approximately 0.2 ft, we may calculate the acceleration from

$$a = \frac{v^2}{2x} = \frac{(7.33)^2}{2(0.2)} = 134 \text{ ft/sec}^2$$

This computed acceleration is approximately 4 g. For a 230-lb individual, the torso weighs approximately 115 lbs and the upper part of the torso is 5/6 of the weight or approximately 96 lbs. Therefore, the mass in slugs is

$$m = \frac{96}{32.2} \approx 2.98 \text{ slugs}$$

Thus, the total force exerted on the spinal column is

$$F = ma = (2.98)(134) = 399 \text{ lbs}$$

If we assume that the shearing force will be evenly distributed over the 15 disks, we obtain

$$\frac{399}{15} = 26.6 \text{lbs} = 12 \text{kg}$$

The ultimate tensile strength of disk cartilage is about 0.24 kg/mm^2. The cross-section of a disk in a human is approximately 660 mm^2. Thus, the tensile stress for this application is

$$\frac{12 \text{kg}}{660 \text{mm}^2} = 0.018 \text{kg/mm}^2$$

This value is approximately 7.6% of the ultimate strength. Therefore, some form of injury is not possible in the spinal column. If the weight of the occupants and their exact dimensions are not known, they can be varied as shown in Table 14.2 and Figure 14.1.

14.3.2 Occupant Kinematics and Vehicle Impacts

In the absence of direct physical evidence of injury to occupants of motor vehicles, the question arises as to the occurrence of soft tissue injuries. Soft tissue injuries involve a variety of ailments including whiplash and sprained backs as well as more serious injuries to the internal organs, such as the liver, spleen, lungs, and heart. Other less well known injuries include temporal mandibular joint (TMJ), carpal tunnel, and hernias of the abdomen. Many serious injuries to internal organs involve direct damage to the interior compartments of the vehicle, including head impacts on windshields, bent steering wheels, indentations on dash panels, indentations to the head liners or mirrors, and broken or bent seats.

Table 14.2 Biomechanical Spinal Injury Calculations Dependence on Weight and Disc Size

Weight of occupant (lbs)	100.00	150.00	200.00	250.00	300.00
Ultimate strength of disc cartilage (kg/mm/mm)	0.20	0.22	0.24	0.26	0.28
Disc size (mm sq)	640.00	650.00	660.00	670.00	680.00
Speed change (mph)	5.00	5.00	5.00	5.00	5.00
Acceleration (ft/sec/sec)	134.32	134.32	134.32	134.32	134.32
Mass (slugs)	1.29	1.94	2.59	3.23	3.88
Spinal column force (lbs)	173.81	260.72	347.62	434.53	521.44
Shearing force per disc (kg)	5.27	7.90	10.53	13.17	15.80
Tensile stress on disc (kg/mm/mm)	0.0082	0.0122	0.0160	0.0197	0.0232
Percent of ultimate strength (%)	4.11	5.52	6.65	7.56	8.30

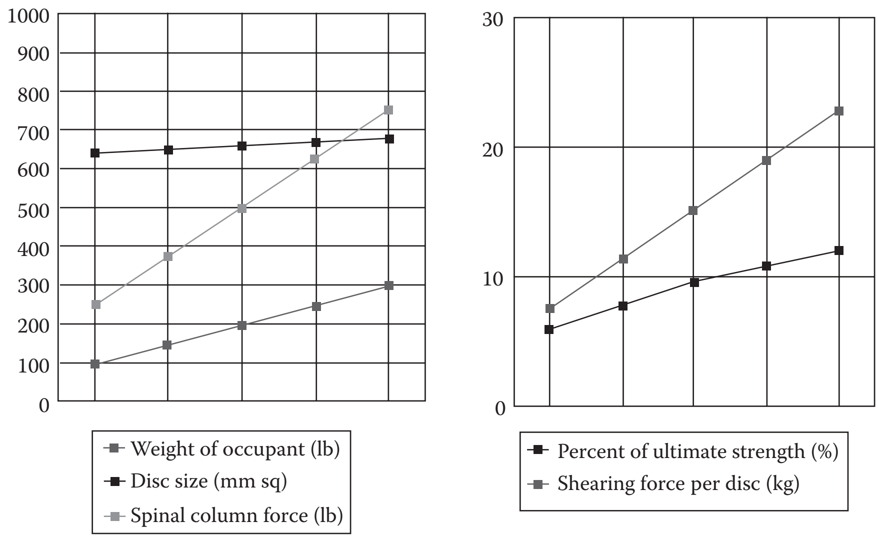

Figure 14.1 Biomechanical spinal injury calculations.

Injuries to soft tissues occur when rapid decelerations cause the tensile strength of the particular tissue to be exceeded. Consequently, internal organs, muscles, tendons, and ligaments can tear, abrade, bruise, and lacerate. Newton's second law states that the force exerted on a body of mass is equal to the product of the mass and the acceleration. This basic principle has been applied by various investigators to determine the acceleration necessary to produce injury to humans and animals. Damask states that there is a 5% probability of injury to humans at an acceleration of 12 g. For accelerations greater than 12 g, the risk of injury increases proportionally. At an acceleration of 17 g, the probability of injury to human soft tissues is approximately 99%. It is generally accepted that at accelerations in the range of 100–150 g the injuries to the soft tissues of humans and animals are catastrophic. One can, therefore, safely conclude that accelerations less than 10 g will not produce significant injuries to humans while accelerations greater than 100 g will almost always result in severe injuries of the soft tissue type. It should be noted that at the higher accelerations there will also be corresponding injuries such as fractures and lacerations. Injuries to the occupants associated with accelerations in excess of 100 g are always accompanied by significant physical damage to the interior and exterior of the vehicle and outward direct physical evidence of injury to the occupants.

Ogan et al. (1993) have shown that vehicle to curb impacts produce peak acceleration to humans that are less than 4 g. The peak accelerations in this research occurred at speeds of approximately 5 mph and decreased as speed increased. Ogan concluded that peak acceleration levels experienced by vehicle occupants when striking curbs are minimal.

Rear end collisions at low speeds using human subjects have been conducted by West et al. (1971). These tests revealed that at impact speeds of between 3 and 5 mph, the forces experienced by the vehicle occupants were sufficient to cause their heads to be displaced rearward and make contact with head supports at the rear top of the seats. The maximum levels of head acceleration for these tests were between 3.0 and 7.5 g. "*Neither the level of cervical bending nor the level of cervical torque measured in these tests reached the level at which injury to the vehicle occupant would be expected. Therefore, for an individual who does not have any predisposition to injury, a whiplash injury would not be expected for impacts of this magnitude…In our experiences, low back pain and injury to the temporal mandibular joint (TMJ) are often claimed as a result of minor low speed collisions. When seated normally within the vehicle seat, the thoracic and lumbar spines are fully supported by the seat back. Our testing has revealed that when exposed to a minor rear impact the seat back bends in response to the collision forces but maintains full support of the lower spine.*

A model has been proposed to explain how TMJ injuries may result from an excessive opening of the mouth induced during a rear end collision event. Review of the videotape records of the collision tests which have been conducted failed to demonstrate any opening of the jaw as a result of the impact forces. This is as expected as there are no forces present during the collision phase which would articulate the jaw, as suggested by the model…Even at the highest level of testing performed, significant relative movement between the thoracic and lumbar spine did not occur…Our tests indicate that singular low back strain is not expected as a consequence of low speed rear impacts."

Mertz and Patrick (1971) have established the noninjury level to the human neck and the kinematics of whiplash. The noninjury level for a 50th percentile male occurs when a human's head is subject to a torque of 35 ft-lbs. The torque level at which injuries to the neck ligaments occurred was 42 ft-lbs. The torques can be converted to accelerations of 14 and 16.8 g respectively, assuming a 0.25 ft displacement and head weight of 10 lbs. It is important to note that these studies by Mertz and Patrick (injury threshold of 14 g) when compared to Damask (injury to humans at 12 g) are in excellent agreement.

We may correlate the accelerations produced by low impact vehicular speeds to normal activities associated with every day living. As human structures evolved, structural resilience and strength of the soft tissues had to adapt to walking, running, jumping and falling. Humans would not have survived the evolutionary process if the structural components were subject to injuries from simple activities. Allen et al. (1994), have measured the accelerations produced on the heads of eight volunteers performing 13 daily activities. The measured values ranged from less than 1 g to as high as 8.5 g. These activities included head movements in various directions, sneezing, coughing, kicking, standing, hopping off steps, and plopping in chairs. Certainly, none of these activities producing accelerations in the 8 g category caused any injury to the test subjects. Humans are certainly capable of greater physical feats than those experienced in daily activities without sustaining injury.

When standard reconstruction techniques as outlined in the preceding chapters are coupled with occupant kinematics, the acceleration of the occupants can be calculated. Unless the occupants are subjected to accelerations greater than 10 g, no soft tissue injury can occur. The 10 g limit is very conservative because researchers have shown that the first indications of injury occur at between 12 and 14 g.

The threshold of injury is a widely debated topic in accident reconstructions. Some experts state that injuries can occur at any speed and acceleration. The scientific testing does not support those conclusions. As an example, let us calculate the speed that a human falls. One model for a human fall is that of a cylindrical object falling. Figure 14.2 represents a cylindrical object subject to falling.

The moment of inertia of the rod model for a human about the base of the cylinder is

$$I = \rho \int r^2 dV = \int z^2 dz = \frac{1}{3} m l^2 \tag{14.1}$$

To determine the speed at which the head strikes the ground we will use the conservation of energy principle. The conservation of energy principle states that the total potential energy must equal the total kinetic energy.

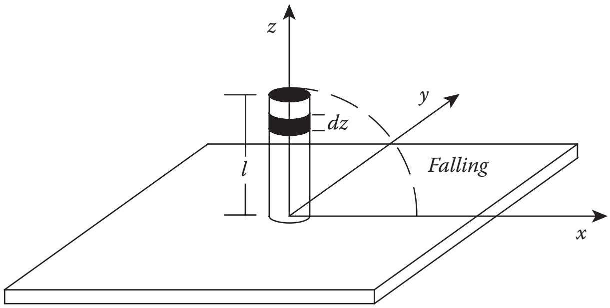

Figure 14.2 Cylindrical object falling.

The kinetic energy has two components, the translational energy and the rotational energy or,

$$mgl = \frac{1}{2}mv^2 + \frac{1}{2}\left[\frac{1}{3}ml^2\right]\left(\frac{v^2}{l^2}\right) \tag{14.2}$$

$$v = \sqrt{\frac{3}{2}gl} \tag{14.3}$$

We can now conclude that a human falling will achieve a speed between a free fall and Equation 14.3 or

$$\sqrt{\frac{3}{2}gl} < v > \sqrt{2gl} \tag{14.4}$$

As an example, an infant who is 2.5 ft tall, and whose head strikes the ground, will do so at between 7.5 and 8.6 mph. In contrast, an adult's head will strike the ground at speeds between 11.6 and 13.4 mph. As we will see in the last section, the computed speed for an adult fall may be sufficient to cause injury. However, we know from experience that babies and toddlers regularly fall as they learn to walk without permanent injury. We note that the speed at which a baby's head falls is less than what is required to produce spinal injuries in adults although the mechanism of injury is quite different.

14.3.3 Bone Fractures

Long bones are subject to fracture in cases where the applied forces exceed the strength of the bone structures. We can determine the fracture strength subject to transverse forces to their axis in terms of the ultimate tensile strength of the bone. Figure 14.3 represents a bone under pressure and subject to fracture. The bending moment necessary to break the bone is computed from the approximation of the bone as a hollow cylinder and the application of Young's

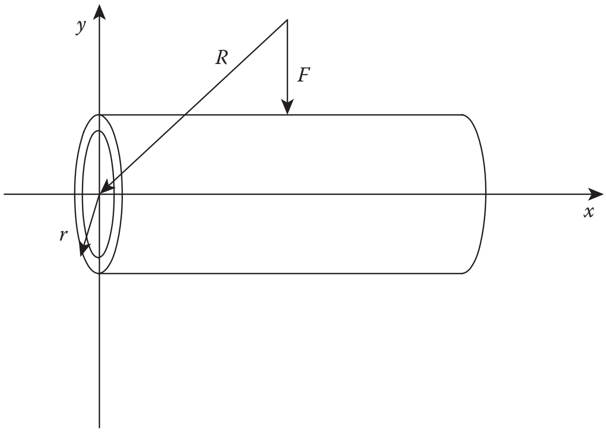

Figure 14.3 Bone fracture.

modulus of elasticity for the bone. We recall the basic definitions of stress and strain as,

ε = strain
σ = stress
Young's modulus $E = \sigma/\varepsilon$

The stress is related to the applied force F and the area A as,

$$dF = \sigma dA \tag{14.5}$$

The torque Γ exerted about the neutral axis of Figure 14.3 is

$$d\Gamma = \sigma y dA \tag{14.6}$$

However, by Young's modulus the stress is

$$\sigma = \frac{Ey}{R} \tag{14.7}$$

and

$$d\Gamma = \frac{Ey^2}{R} dA \tag{14.8}$$

The total torque about the neutral axis is called the bending moment M_b, so

$$M_b = \int d\Gamma = \frac{E}{R} \int y^2 dA \tag{14.9}$$

We recognize the integral of Equation 14.8 as the area moment of inertia I_a and then we can write

$$M_b = \frac{EI_a}{R} \tag{14.10}$$

The maximum stress, $\sigma_{\max}$ occurs at the radius r of the cylinder so that Equation 14.6 can also be written as

$$\sigma_{\max} = \frac{Er}{R} = Y_b \tag{14.11}$$

The term Y_b is called the ultimate bending stress for human long bones. The external bending moment or torque M_b can then be expressed in terms of the ultimate bending stress, the area moment of inertia, and the radius as

$$M_b = \frac{Y_b I_a}{a} \tag{14.12}$$

where a ir the radius of the bone at the breaking point.

As an example, a seven-year-old child darted in front of a vehicle in a school zone. The speed limit in the school zone was 15 mph. The vehicle's front bumper struck the child in the left femur but did not break the bone. The child did sustain contusions and abrasions from the collision. Is it possible that the vehicle was exceeding the speed limit as claimed by the child's parents and attorney? This question can be answered by a couple of methods. One method can be applied from the equations of Chapter 8. If the vehicle is equipped with an event data recorder as outlined in Chapter 13, then some information may be gleaned from the interrogation of the air bag module. Another method of analysis is detailed from biomechanical calculations outlined as follows.

The child weighed 65 lbs and the following parameters were determined from measurements:

$$I_a = 0.018\ \text{in}^4, \qquad Y_b = 3.4 \times 10^4\ \text{lb/in}^3, \qquad a = 0.5\ \text{in}$$

The bending moment is

$$M_b = \frac{(3.4 \times 10^4)(1.8 \times 10^{-2})}{0.5} = 1224 \quad \text{inch-lbs}$$

The leg of a human is approximately 15% of the total weight and the thigh represents approximately 2/3 of the total leg weight. So for the 65-lbs child the weight of the thigh is approximately (65)(0.15)(0.66) = 6.4 lbs. The most likely place along the length of the femur to break is in the middle. The thigh bone of the child was measured to be 12 inches long so that the force required to break the femur would be

$$F = \frac{M_b}{6} = \frac{1224}{6} = 204\ \text{lbs}$$

Using Newton's second law, we can compute the acceleration of the leg as it was struck by the front bumper of the vehicle.

$$a = \frac{F}{m}; \qquad m = \frac{6.4\ \text{lbs}}{32.2\ \text{ft/sec}^2} = 0.198\ \text{slugs}; \qquad a = \frac{204\ \text{lbs}}{0.198\ \text{slugs}} = 1030\ \text{ft/sec}^2$$

The distance that the muscles and tissue of the thigh compresses is approximately 1 inch or 0.0833 ft. Therefore, in order to break the femur bone of the child, the vehicle had to be traveling a speed of,

$$v = \sqrt{2ad} = \sqrt{(2)(1030)(0.08330)} = 13\ \text{ft/sec} = 8.9\ \text{mph}$$

Since the vehicle did not leave skid marks and had to be traveling at least 9 mph to break the child's femur bone, it was safely concluded that the vehicle was not speeding.

14.3.4 Head Injury Criterion (HIC)

One of the most catastrophic injuries, in terms of impairment, that vehicular collisions produce is concussion, commonly referred to as closed head injury. Closed head injury is characterized by injury to the brain as a collision produces damage to the lining, blood supply and brain itself. Before we begin a discussion of the Head Injury Criterion (HIC) and other injury criteria we need to historically relate these developments.

In 1970 the Highway Safety Act formed the NHTSA whose basic charter is provided by the National Traffic and Motor Vehicle Safety Act of 1966. The purpose of the NHTSA is "to reduce traffic accidents and death and injuries to persons resulting from traffic accidents." Congress legislated the authority to the Secretary of Transportation and the Secretary delegated to NHTSA the responsibility to issue Federal Motor Vehicle Safety Standards (FMVSS) including the authority to carry out the Safety Act. The Federal Register System contains the Code of Federal Regulations (CFR). Title 49, Transportation, of the code is the pertinent section dealing with various aspects relevant to accident reconstructions. Parts 571 and 572 contain various standards. Standard 208 deals with occupant crash protection. There is also a new experimental program that closely parallels FMVSS 208 under the control of NHTSA and is called the New Car Assessment Program (NCAP). The test programs for both FMVSS 208 and NCAP are based on barrier crash tests that include the use of Hybrid II and III dummies. The FMVSS 208 tests are conducted at 30 mph and the NCAP tests are conducted at 35 mph. Both tests have a margin of error in speed of approximately 1 mph. It should be noted that the energy calculations, because of the speed error in testing, can be approximately 1.5 times greater in the NCAP tests vs. the FMVSS 208 tests. Table 14.3 shows the current FMVSS 208 injury criteria for different parts of the body of occupants involved in motor vehicle collisions.

Data have been assembled through the years in concussion and other severe closed head injuries. These data have been arranged by scientists at Wayne State University and others, i.e., Lissner et al. (1960), into a curve as shown in Figure 14.4.

It is seen that the time of application of an acceleration to the head as well as the peak acceleration play a significant role in close head injuries. The HIC curve has been approximated by Versace (1971) by curve fitting techniques to be,

$$HIC = [t_2 - t_1]\left(\frac{1}{[t_2 - t_1]}\int_{t_1}^{t_2} a(t)dt\right)^{2.5} \tag{14.13}$$

In Equation 14.12 $a(t)$ is the head acceleration and the time element t_2–t_1 is set at ≤ 36 msec. The level of concussion is when the HIC number equals or exceeds 1,000. When the integral is evaluated we obtain,

$$\frac{1}{[t_2 - t_1]}\int_{t_1}^{t_2} a(t)dt = \frac{a}{2}[t_2 - t_1] \tag{14.14}$$

The acceleration value a is the maximum value. Given that the acceleration can be expressed as,

Table 14.3 FMVSS 208 Injury Criteria

Criteria	Hybrid II	Hybrid III
Head: HIC ≤ 1000	X	X
Chest: acceleration ≤ 60 G	X	X
Femur: force ≤ 2250 lbs	X	X
Chest: compression ≤ 3 in	N/A	X

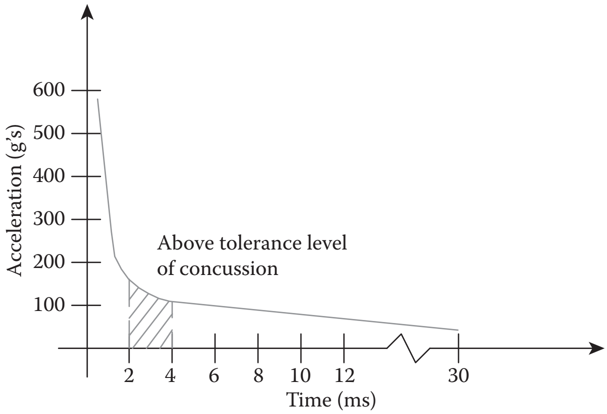

Figure 14.4 Tolerance curve.

$$a = \frac{\nabla v}{[t_2 - t_1]} \tag{14.15}$$

The ratio of the HIC can then be expressed as,

$$\frac{HIC_1}{HIC_2} = \left(\frac{\nabla v_1}{\nabla v_2}\right)^{2.5} \tag{14.16}$$

In 1977 Nahum and Smith performed experiments on cadavers to obtain pressure vs. acceleration data of the brain for frontal impacts to the skull. A typical plot of the linear data from these experiments is shown in Figure 14.5.

In 1980 Ward and his collaborators showed that the threshold intercranial pressure for brain injury is 24 lbs/in^2 or about 1,240 mmHg. Above 34 lbs/in^2 (1,758 mmHg) severe head injury results. Analysis from the representative data from Figure 14.5 the threshold for injury was determined to be at an acceleration of 1293 m/sec^2, and the condition for serious injury occurs at an acceleration of 1,758 m/sec^2 or above. From these experiments the existing HIC values were determined. A plot of the representative pressure vs. HIC values is shown in Figure 14.6.

The serious injury level of 34 lbs/in^2 (1750 mmHg) corresponds to a HIC of about 1000, the accepted value for the threshold of brain injury. We may make a rough estimate of the velocity of impact of the frontal skull against a rigid surface that will give a rise to a HIC of 1000. The associated acceleration is 1293 m/sec^2. Stalnaker et al. (1977) have used high speed radiography

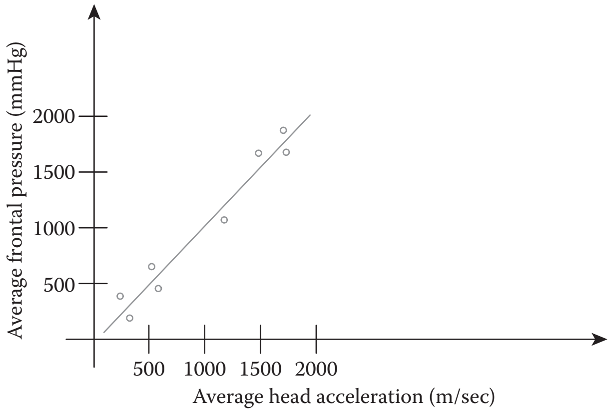

Figure 14.5 Pressure vs. acceleration.

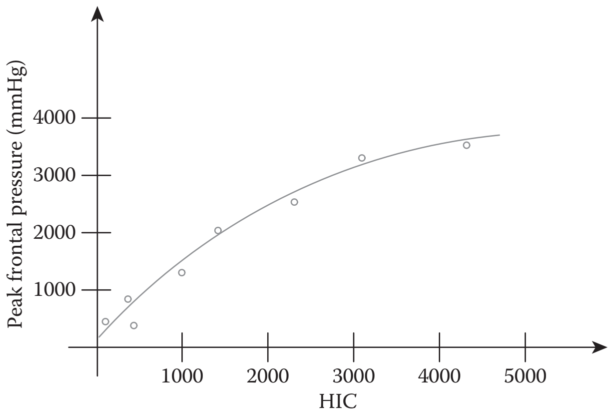

Figure 14.6 Pressure vs. HIC.

to x-ray the motion of the brain in frontal impacts to cadaver skulls. It appears that the brain moves approximately three centimeters forward. We may now calculate the associated velocity required to produce head injury as follows,

$$v = \sqrt{2ax} = \sqrt{(2)(1293)(0.03)} = 8.9\text{ m/sec} = 19.8\text{ mph} \tag{14.17}$$

Recent research has suggested that the threshold HIC value should be around 700 with a corresponding acceleration of about 1000 m/sec^2. For these values the velocity for brain movement of two centimeters is approximately 14 mph. Thus, we see that an adult falling on his head has a greater potential of sustaining head injury when compared to a child. Please refer to the references for the actual graphs of the tests mentioned in this chapter. FMVSS 208 also specifies that the tests for the acceleration of the chest region be restricted to 60 g and that the compressive force to the lower limbs cannot exceed 2250 lbs.

14.4 Staged Collisions

An alarming fact dealing with accident reconstructions is the ever growing incidence of staged collisions. A staged collision is one where the vehicles may or may not have collided. If they did collide, the collision is staged by the participants. If the vehicles did not collide, the damage to the vehicles is pre-existing. Sometimes the damage to the vehicles is pre-existing and is exacerbated by the collision. Generally, these types of collisions are at relatively low speed because the occupants are not willing to risk actual injury. Most of these collisions involve claims of injury to various parts of their anatomy. However, a basic characteristic of the injury claimed is to soft tissues. The most common soft tissue injury claimed is to the spinal column. The authors have also seen injuries involving the carpal tunnel and TMJ injuries claimed in these low impact or staged collisions. Carpal tunnel syndrome is when the transverse carpal ligament at the base of the wrist pinches the nerve along the flexor tendons. Repetitive motion causes the tendons to swell and thereby pinch the nerve. This syndrome cannot be caused by a single event such as gripping the steering wheel hard during a collision as claimed by the participants. Carpal tunnel is mostly associated with repetitive work such as typing or manual assembly of components. These alleged injuries are pre-existing and can easily be discounted as having arisen from a low impact collision. TMJ refers to the temporomandibular joint which allows the jaw to open. TMJ syndrome may be caused by trauma to the jaw, disease, wear, or bad habits such as grinding of the teeth. In a collision, TMJ injury cannot be caused unless there is a significant impact to the jaw of the occupant. Again, these injuries can be discounted in the reconstruction. In many staged collisions, reconstructionists are asked to assess the potential for injury based on the biomechanical movement of the occupants.

Staged collisions have a distinct signature. The list below is a compilation of the many characteristics of a staged collision. It is recognized that many legitimate collisions may exhibit some of these characteristics. However, a combination of several of these factors generally point to the collision being staged.

1. Time of day. Often the collision is reported to have occurred late at night.
2. Remote location. The location of the alleged collision may be in an industrial or residential area or a country setting.

3. Type of vehicle. Generally the vehicles are inexpensive older vehicles with high milage and in poor condition.
4. Phantom vehicle. Some staged collisions involve phantom vehicles that reportedly left the scene.
5. Moved vehicles. The vehicles have mostly been moved from the alleged collision point even if it was not necessary to do so because of the nature of the remote location.
6. Lack of a debris field. Collisions involving broken lights produce debris from those parts and dirt from under the vehicle chassis. These alleged impacts produce no debris.
7. Type of injury complaint. Most of these alleged collisions involve spinal injuries that are being treated at known "injury clinics."
8. Treating facility. The injury clinic has a track record for these types of treatments and is often located far from the claimants residence. Generally all the parties involved are treating at the same facility.
9. Tardiness of treatment. Most often, the claimants are not taken to the hospital and seek treatment days or weeks after the collision. The onset of injury almost always takes at least one day to manifest itself. Those of us who that have sprained our backs know who the pain is immediate and generally debilitating.
10. Multiple occupants. If you stage an accident, include all your relatives and friends. It does not matter that you don't know the friends name or where they live. Many times the alleged passengers are not listed in the police report. Many times there is no police report.
11. Mismatched horizontal damage. The horizontal profile of the damage to the vehicles does not match. One vehicle has narrow damage and the other has wide damage.
12. Mismatched vertical damage. One vehicle has low damage and the other high damage. The damage to both vehicles should be consistent in the vertical and horizontal planes.
13. Lack of paint transfer. When two vehicles collide, paint is generally transferred. Sometimes the color of the paint transfer does not match such as red paint from a green vehicle.
14. Energy imbalance. Energy calculations reveal a significant discrepancy in the calculated damage energies.
15. Momentum imbalance. If the description of events violates conservation of momentum such as the wrong direction of travel of the vehicles, then careful scrutiny must be considered.
16. Absence of road marks. These alleged collisions never involve pre or post impact skids or gouges on the road surface.
17. Inconsistencies in road geometry. Some collisions allege that a left turn was made when there is no street turning to the left. Participant statements can often doom the claim.

18. Inconsistencies in damage location. The participants claim that the vehicle approached from the right when, in fact, the damage tp the vehicle indicated that the PDOF came from the rear.
19. Inconsistencies in travel direction. Participants state that they were traveling home in a southerly direction when, in fact, they live north of the accident site.
20. Tool marks on vehicles. Close examination of the damage can often reveal tool marks made to simulate a collision. Sometimes the vehicles are precrashed against poles and then the crush profiles do not match the alleged accident scenario.
21. Unusual impact and damage to vehicles. Look for evidence that construction equipment or buildings were used to simulate the damage.
22. Lack of independent witnesses. There is never an independent witness available to corroborate the alleged collision.
23. Inconsistent paint transfer. The hue or color of the paint should be closely scrutinized. This may involve collections a sample and submitting it for laboratory analysis.
24. Violation of occupant kinematics. The occupants may claim that they were struck from the left side causing their bodies to move to the right.
25. Violation of physical laws. Newtonian dynamics should always be considered in order to determine if the collision makes sense.
26. Participant rings. Check for close associations between the parties involved.

Standards and Protocols 15

15.1 Introduction

During the years that the authors have been practicing forensic engineering and in particular in the area of accident investigation and reconstruction, it has become evident that there is a great need for standardization. However, there is great opposition to the development of standards. The primary reason for the opposition to standards in accident reconstruction is the diverse nature of the individuals and groups who perform accident investigations and reconstructions. There are three main groups of people performing investigations and reconstructions. One group may be classified as engineers or scientists who have formal training in mathematics and the sciences. Some of these individuals are members of or are represented by the National Association of Forensic Engineers (NAFE). The second group is comprised of individuals who have police or investigative backgrounds. Their level of training is generally associated with the Institute of Police Training and Management (IPTM) or the Northwestern University Traffic Institute. Many of these individuals may also have training associated with the National Association of Professional Accident Reconstruction Specialists (NAPARS) and the Accrediting Council for Traffic Accident Reconstruction (ACTAR). The third group of individuals consist mainly of professionals in the areas of visibility, reaction, and conspicuity. The level of expertise of those who practice in these endeavors is quite diverse.

Over the past few years there has been great conflict between the first two groups of individuals performing accident investigations and reconstructions. The conflict seems to be between NAFE and ACTAR over which group best represents the profession. The main complaint seems to come from the engineers who feel that the police trained individuals are not qualified to perform the investigations. Let us make the following point very clear. There are excellent investigators and reconstructionists who come from both backgrounds just as there are some from both camps who should not be practicing.

In this book the authors make no statement with regard to qualifications, experience, or determination as to the suitability of the experts. Simply, that is not the purview of either group. Neither group is the gate keeper of the system. It is not ethical for any group with vested interests to police another group with similarly vested interests. The vested interest is to keep the other group from practicing the profession of accident investigation and reconstruction. What these groups fail to realize is that the gate keeper is the judicial system. The court systems in this country have recognized experts in accident investigation and reconstruction from many backgrounds. The adversarial nature of the criminal and civil systems is designed to challenge experts as to their suitability to offer opinions on such matters. Judges and juries determine the qualifications and competency of the experts. It should also be recognized that the level of expertise required for these investigations varies with the complexity if the case. Many reconstructions require only minimal mathematical skills and a rudimentary knowledge of the physical principles involved. Some forms of analysis may require significant training in the physical sciences and mathematics that may be beyond the capabilities of some individuals including people with engineering degrees. Although this book tends to discuss the more complex physical principles and deeper mathematical basis, it should not be construed as an elitist publication in the context of excluding other experts. We simply elucidate the finer points and show how some experts bend or misuse the laws of physics. Experts from both camps bend the rules. Degrees or licenses are not adequate safeguards against charlatans and "snake oil salesmen or women."

Another reason for the opposition to standards is basic human nature. Most people, and in particular, experts, do not want to be told how to do things. After all, they are experts. They are also fallible. They forget to do certain things. They may even make mistakes in their calculations. There are any number of ways that their investigation may come into question. Many of the mistakes or omissions made by diligent investigators are minor or inconsequential, which simply do not affect the basic conclusions of the case. Sometimes the errors are deliberate and designed to skew the results toward their client. In those rare cases, the expert becomes an advocate, a role which the expert should not play in an ethical environment. Many times the expert is accused of skewing the data or advocating for his or her side although the analysis or opinions are proper. In these cases, the expert is not an advocate but must defend the conclusions. Such is the nature of the litigation system.

There are two goals in advocating the development of standards in accident investigations and reconstructions. These goals are (1) to develop procedures that help to keep the expert from making mistakes during the investigation and analysis and (2) to defend the actions taken. A set of procedures and protocols is not only the way of science but also the way of police investigations. Both areas of background from which accident investigators come are rooted in the scientific method. The scientific or engineering experts learned mathematics and science by following set procedures, or check lists. Engineering judgment does not allow one to bend the rules of science. The terms, art and science, are sometimes used in accident reconstructions. However, investigations and reconstructions are based on science only. Police training is based on specific procedures. Police agencies have been historically under much more intense scrutiny than experts in reconstructions who come from the sciences or engineering. Their training has required police experts to be "under the gun" and "take the heat" much more than engineers. For that reason alone, police trained reconstructionists are often much better expert witnesses. Police agencies have learned that procedures, standards, and protocols are not obstructions to investigations. Standards and protocols therefore, offer a two sided sword in accident investigations and reconstructions. They minimize errors to which humans are prone and provide a level of competence that is recognized in the industry. If activities are undertaken to the level of recognized standards, then those activities are much less likely to be questioned or criticized.

Some headway has been made in the development of standards and guidelines for accident investigations and reconstructions. There are some standards that have been developed by the Society of Automotive Engineers (SAE), Federal Motor Vehicle (FMV) publications, and the American Society of Testing and Materials (ASTM). More standards are necessary and will be developed over time. In the next sections of the chapter, we introduce our version of a protocol for inspections and reconstructions as well as the existing standards available.

15.2 Protocol for Inspections and Reconstructions

This section should not be construed to apply under all circumstances. Some of the material in this section is covered under SAE and ASTM standards and guidelines and may be considered repetitive. Please refer to the applicable standards in this chapter for more detailed explanations of procedural guidelines.

15.3 Standard Guide for Vehicular Accident Inspections and Reconstructions

15.3.1 Scope

This guide is for individuals who are investigating the events relating to vehicular incidents or accidents involving persons, vehicles, roadways, or sites where a loss of property, injury, or a loss of life has occurred. The purpose of this guide is to provide a compendium of information and practices, but not to establish a standard practice or recommend a specific course of action. The guide is intended to increase the awareness of information and approach in this area. The guide covers methodologies and practices for the recognition, documentation, reporting, collection, and preservation of potentially relevant physical items and information pertaining to a vehicular incident.

This guide is intended to serve as a reference rather than as a definitive standard. As such, a forensic practitioner may use other relevant standards and protocols to supplement the information in this guide. The guide outlines many courses of action so that the investigator may choose the appropriate course of action relative to the investigation. The nature of the incident and the employer's requirements will also generally dictate the scope of work and practices required. For example, in some instances the employer may require the investigator to work from existing evidence rather than collecting the evidence. Realizing that such restrictions tend to limit the scope and possibly the accuracy of the work, significant analysis can still be performed. Sometimes, the vehicles or equipment may no longer be available or the site may have been altered. Under such circumstances, photographs, data bases, and exemplars may be used to perform the analysis. Computer techniques may also be used to create a virtual scene based on measurements and photogrammetry.

15.3.2 Significance and Use

Every year, injuries, property damage, and business interruptions occur as a result of vehicular incidents. The recording of information, physical data, and evidence following a vehicular incident is important if the origins and causes of an incident are to be determined. This document can help convey forensic findings to both technical and nontechnical third parties. The documentary data, including reports and statements, are used to corroborate the findings.

Since the evidence at the scene of a vehicular incident is time sensitive, forensic investigations conducted as soon as possible after the incident often collect the most useful information. In most instances, the forensic practitioners are not afforded the privilege of investigating the vehicular incidents soon after they occur. Police or regulatory authorities investigate most incidents within minutes or hours. Police, fire departments, and other responding authorities having jurisdiction (AHJ) are required to document the incident scenes and often perform some of the most immediate site analysis and evidence collection. However, these authorities often have primary statutory responsibilities to protect life and property.

Therefore, it is recognized that the reports generated by these agencies, while important, may not include all relevant data. It is in a follow-up role that private forensic practitioners play a vital role as they often have greater collection resources and more time to spend on the investigation than the responding authorities having jurisdictions (AHJs).

Proper collection of incident details may allow for the replication or reconstruction of an incident. The reconstruction or replication of the incident may take many perfectly valid forms. The reconstruction can be performed by the application of basic physical laws such as conservation of energy and momentum. The reconstruction may be based on available crash data or on actual crash tests with exemplar vehicles or equipment. The reconstruction may be based on computer simulations and models. A combination of methods may be used to validate the results of the investigation and reconstruction. Wherever practical, it is suggested that more than one method of analysis be used to reach the conclusion of the forensic practitioner.

15.3.3 Equipment

Useful equipment for vehicular incident investigations and reconstructions include but are not limited to:

1. Measuring devices, total stations, transits, rolling tapes, measuring tapes, micrometers, calipers, dial indicators, feeler gauges, scales, pressure gauges, crush jigs, etc.
2. Vehicle diagnostic tools, Crash Data Retrieval (CDR) tools, volt–ohm meters, oscilloscopes, vacuum gauges, timing lights, calculators, and computers.
3. SAE standard and metric wrenches and tools, jacks, stands, and equipment lifts.
4. Mirrors, boroscopes, thermal imaging devices, microscopes, x-ray equipment, etc.
5. Cameras with micro and macro capabilities, video and audio recorders.
6. Maps, global positioning systems, aerial and satellite images.
7. Accident reconstruction and simulation software, vehicle specification data bases, crash test data, drawing software.

15.3.4 Procedure

The procedure outlined below is not to be construed as a sequence of events that are to be followed in order of appearance. It is realized that these procedures will generally overlap, intersect, and follow in a random sequence.

1. Historical and background data
   Police reports, emergency responders reports, fire department reports, vehicle repair estimates, police photographs, news coverage reports, photographs or video, adjuster photographs, injury or medical reports, witness statements, examinations under oath, depositions. Maintenance records or repair records. Weather and sun or moon position records. Illumination records.
2. On-site activities
   These activities include proper documentation of the site with measurements, photographs, or video. They may include the use of exemplar equipment, actors, or vehicles to demonstrate particular characteristics concerning the events of the incident. These activities may also include studies relative to perception, visibility, illumination and conspicuity.
3. Vehicle and equipment inspections
   During the joint inspection of vehicles or equipment or the retrieval of data from event recorders, protocols for those activities should be established. Measurements with appropriate equipment along with photographs and video recordings should document the activities. Disassembly of components should be systematically documented. Destructive testing may be agreed upon.
4. Postsite and postequipment inspection activities
   Interviews with police, Emergency Medical Service (EMS), fire department personnel, repair or maintenance facilities. Request for production of documents or evidence. Aerial or satellite imagery. Literature search. Policies, codes, and standards. Training records.
5. Exemplar and crash testing
   Useful information may be obtained from destructive and non destructive testing of exemplar equipment or vehicles. Such tests are often undertaken to determine crashworthiness or safety issues that may arise.
6. Standard analysis
   Conservation of energy. Conservation of momentum. Newtonian mechanics. Time motion analysis. Crush deformation. Damage analysis. Mathematical modeling of events. Photogrammetry. Vehicle or equipment performance characteristics. Roadway characteristics.
7. Simulations and computer models
   2D and 3D models and simulations utilizing commercial software.
8. Research activities

15.3.5 Reports

Over the course of a vehicular incident investigation and reconstruction, the forensic practitioner may be required to prepare multiple reports in various formats including but not limited to:

1. Verbal reports
2. Status reports
3. Preliminary reports
4. Draft reports
5. Interim reports
6. Final reports
7. Amendments to reports

The client may require the forensic investigation report to include where applicable the following information:

1. Signature and professional licensing or certification stamps
2. Credit given to any additional contributors
3. Sources of data relied on and list of references and appendices
4. Other reports, statements, or depositions used or referenced
5. Drawings and calculations
6. Opinions on origins and causes of the incident

15.4 American Society of Testing and Materials (ASTM) Standards

The following is a list of the ASTM standards and guides that may be applicable to accident investigations and reconstructions.

ASTM E 620 Standard Practice for Reporting Opinions of Technical Experts
ASTM E 678 Standard Practice for Evaluation of Technical Data
ASTM E 860 Standard Practice for Examining and Testing Items That Are or May Become Involved in Litigation
ASTME 1020 Standard Practice for Reporting Incidents
ASTM 1188 Standard Practice for Collection and Preservation of Information and Physical Items by a Technical Investigator
ASTM E 2292 Standard Practice for Investigation of Carbon Monoxide Poisoning Incidents
ASTM E 2332 Standard Practice for Investigation and Analysis of Physical Component Failures

ASTM E 2345 Standard Practice for Investigating Electrical Incidents
ASTM E 2493 Standard Guide for the Collection of Non-Volatile Memory Data in Evidentiary Vehicle Electronic Control Units

15.5 Federal Motor Vehicle (FMV) Standards

The CFR includes sections applicable to accident investigations and reconstructions. These are:

Title 23 Highways
Part 470 Highway systems
Part 625 Design standards for highways
Part 635 Construction and maintenance
Part 646 Railroads
Part 650 Bridges, structures, and hydraulics
Part 652 Pedestrian and bicycle accommodations and projects
Part 655 Traffic operations
Part 657 Certification of size and weight enforcement
Part 658 Truck size and weight, route destinations—length, width and weight limitations
Part 1235 Uniform system for parking for persons with disabilities

Title 49 Transportation
Part 213 Track safety standards
Part 214 Railroad workplace safety
Part 215 Railroad freight car safety standards
Part 217 Railroad operating rules
Part 218 Railroad operating practices
Part 221 Rear end marking devices—passenger, commuter and freight trains
Part 222 Use of locomotive horns at public highway-rail grade crossings
Part 224 Reflectorization of rail freight rolling stock
Part 225 Railroad accidents/incidents: Reports classification, and investigations
Part 228 Hours of service of railroad employees
Part 229 Railroad locomotive standards
Part 232 Brake system safety standards
Part 233 Signal systems reporting requirements
Part 234 Grade crossing signal system safety
Part 390 Federal motor carrier safety regulations
Part 392 Driving of commercial motor vehicles

Part 393 Parts and Accessories Necessary for Safe Operation
Part 395 Hours of service of drivers
Part 396 Inspection, repair, and maintenance
Part 563 Event data recorders
Part 569 Regrooved tires
Part 570 Vehicle in use inspection standards
Part 571 Federal motor vehicle safety standards
Part 574 Tire identification and recordkeeping
Part 581 Bumper standard
Part 605 School bus operations

15.6 SAE Standards

The SAE have also developed standards or recommended practices applicable to the forensic investigation of accidents as follows.

SAE J 98 Personnel Protection for General Purpose Industrial Machines
SAE J 224 Collision Deformation Classification
SAEJ231 Minimum Performance Criteria for Falling Object Protective Structures (FOPS)
SAE J 232 Industrial Rotary Mowers
SAE J 276 Steering Frame Lock Articulated Loaders and Tractors
SAE J386 Operator Restraint Systems for Off-Road Work Machines
SAE J 819 Engine Cooling System Field Test
SAE J 850 Fixed Rigid Barrier Collision Tests
SAE J 972 Moving Rigid Barrier Collision Tests
SAE J 1001 Industrial Flail Mowers and Power Rakes
SAE J 1040 Performance Criteria for Rollover Protective Structures (ROPS) for Construction
SAE J 1042 Operator Protection for General Purpose Industrial Machines
SAE J 1301 Truck Deformation Classification
SAE J 1308 Fan Guard for Off-Road Machines
SAE J 1388 Personnel Protection—Steer Skid Loaders
SAE J 1674 Early Acquisition and Preservation of Information in a Motor Vehicle Accident
SAE J 2314 Ethics for Accident Investigation and Reconstruction
SAEJ 2426 Occupant Restraint System Evaluation-Lateral Rollover System-level Heavy Trucks
SAE J 2505 Measurement of Vehicle-Roadway Frictional Drag
SAE J 2808 Road/Lane Departure Warning Systems
SAE CtRP 9,12,13 Heavy Truck Crashworthiness

Sensitivity and Uncertainty

16

16.1 Introduction

Once a reconstruction has been performed given the best available data, there is always a measure of uncertainty of some of the parameters. For example, the coefficient of friction is never exactly known but rather it is estimated. It may also be important to know how sensitive some of the parameters are to change, which may affect the equations that are used in the reconstruction. As an example, it is known that T-bone collisions are not very sensitive to preimpact angles and that collinear collisions are quite sensitive to these angles. Parametric analysis, the variation of a parameter from a known or estimated central value, allows for the sensitivity and uncertainty to be quantified. It is always important to perform these calculations because all of the parameters are not exactly known and the models used in the reconstruction cannot be entirely accurate. From a theoretical standpoint, we will define sensitivity and uncertainty in this chapter and see how they apply in accident reconstruction.

16.2 Sensitivity and Uncertainty

Let us assume that an equation is a function of several variables. For example, for the stopping distance equation

$$v = \sqrt{2g\mu D} \tag{16.1}$$

the speed v is a function of two variables, namely μ and D. Thus, we may write

$$v = f(\mu, D) \tag{16.2}$$

Thus, any equation dependent on n variables can be expressed as

$$P = f(x_1, x_2, \ldots, x_n) \tag{16.3}$$

First, let us consider the case where an equation is a function of only one variable, $P = f(x)$. The sensitivity of P to the variable x is defined as

$$S_x^P = \lim_{\Delta x \to 0} \frac{\Delta P/P}{\Delta x/x} = \frac{x}{P} \lim_{\Delta x \to 0} \frac{\Delta P}{\Delta x} = \frac{x}{P}\frac{\partial P}{\partial x} = \frac{\partial(\ln P)}{\partial(\ln x)} \tag{16.4}$$

Applying the basic definition of sensitivity, the following relationships may be developed.

$$S_x^{cx} = 1; \quad c = \text{constant} \tag{16.5}$$

$$S_x^P = -S_x^{1/P} \tag{16.6}$$

$$S_x^P = -S_{1/x}^P \tag{16.7}$$

$$S_x^{P_1 P_2} = S_x^{P_1} + S_x^{P_2} \tag{16.8}$$

$$S_x^{P_1/P_2} = S_x^{P_1} - S_x^{P_2} \tag{16.9}$$

$$S_{x^n}^P = \frac{1}{n} S_x^P \tag{16.10}$$

$$S_x^{P_1+P_2} = \frac{P_1 S_x^{P_1} + P_2 S_x^{P_2}}{P_1 + P_2} \tag{16.11}$$

Since most functions are in terms of various parameters, it is important to determine the multiparameter deviations. To do so we begin with the basic definition as expressed in Equation 16.4 so that for small deviations in x we can determine the change in the function due to one element as,

$$\Delta P \cong S_x^P \frac{\Delta x}{x} P \tag{16.12}$$

For multiple elements we may expand Equation 16.11 in a Taylor series to obtain

$$\Delta P \cong \frac{\partial P}{\partial x_1}\Delta x_1 + \frac{\partial P}{\partial x_2}\Delta x_2 + \cdots + \frac{\partial P}{\partial x_m}\Delta x_m + \text{higher order terms} \tag{16.13}$$

For small variations in ∇x_j we neglect the higher order terms so that

$$\Delta P \cong \sum_{x_j}^{m} \frac{\partial P}{\partial x_j}\Delta x_j = \sum_{x_j}^{m}\left(\frac{\partial P}{\partial x_j}\frac{x_j}{P}\right)\left(\frac{\Delta x_j}{x_j}\right)P = \sum_{x_j}^{m} S_{x_j}^{P}\, V_{x_j}\, P \tag{16.14}$$

where $V_{x_j} = \Delta x_j / x_j$ = per unit change in the parameter x and is known as the variability of x.

For Equation 16.1 we may determine, as an example, the sensitivity of the parameters μ and D by applying Equation 16.9. The sensitivity for these parameters is ½ for each. This result may also be verified by the application of the basic definition of sensitivity. Applying Equation 16.13 we can determine the per unit variation of the velocity with respect to the parameters μ and D.

$$\frac{\Delta v}{v} = \frac{1}{2}\left(\frac{\Delta\mu}{\mu} + \frac{\Delta D}{D}\right) \tag{16.15}$$

In terms of the root mean square variation Equation 16.15 becomes

$$\frac{\Delta v}{v}\Big|_{\text{rms}} = \frac{1}{2}\sqrt{\left(\frac{\Delta\mu}{\mu}\right)^2 + \left(\frac{\Delta D}{D}\right)^2} \tag{16.16}$$

Equations 16.15 and 16.16 give a measure of the uncertainty of the calculations.

This type of analysis can be used to determine the sensitivity of the momentum equations. Recall that the equations of linear momentum for the postimpact velocities are given by

$$V_{1i} = \frac{V_{1f}\sin(A_{2i} - A_{1f}) + R_{2v1}V_{2f}\sin(A_{2i} - A_{2f})}{\sin(A_{2i} - A_{1i})} = \frac{V_{1f}\sin\varphi_1 + RV_{2f}\sin\varphi_2}{\sin\varphi_5} \tag{16.17}$$

$$V_{2i} = \frac{V_{1f}\sin(A_{1i} - A_{1f}) + R_{2v1}V_{2f}\sin(A_{1i} - A_{2f})}{R_{2v1}\sin(A_{2i} - A_{1i})} = \frac{V_{1f}\sin\varphi_3 + R\,V_{2f}\sin\varphi_4}{R\,\sin\varphi_5} \tag{16.18}$$

For Equation 16.17 the sensitivity to φ_5 is:

$$S_{\varphi_5}^{V_{1i}} = \frac{-\varphi_5}{\tan\varphi_5} = \operatorname*{Lim}_{\varphi_5 \to 0} \frac{d/d\varphi_5(\varphi_5)}{d/d\varphi_5(\tan\varphi_5)} = -1 \tag{16.19}$$

Thus, when the approach angles are nearly equal or opposite, the momentum equations are very sensitive to the angles and are difficult to solve unless parametric studies are undertaken. Parametric studies lend themselves to be solved by spread sheets or computer programs where several parameters can be varied and their effect studied. It is generally found that some parameters do not affect the results from a particular equation as much as others. Therefore, we always encourage the use of parametric analysis in a reconstruction. When parametric analysis is performed, the uncertainty can be quantified and the effects observed. Again, for Equation 16.17 we may determine the sensitivity to the other parameters as

$$S_{\varphi_1}^{V_{1i}} = \frac{\varphi_1 V_{1f} \cos\varphi_1}{V_{1f}\sin\varphi_1 + RV_{2f}\sin\varphi_2} \tag{16.20}$$

$$S_{\varphi_2}^{V_{1i}} = \frac{\varphi_2 RV_{2f} \cos\varphi_2}{V_{1f}\sin\varphi_1 + RV_{2f}\sin\varphi_2} \tag{16.21}$$

$$S_R^{V_{1i}} = \sin\varphi_5 \tag{16.22}$$

$$S_{V_{1f}}^{V_{1i}} = S_{V_{2f}}^{V_{1i}} = 1 \tag{16.23}$$

We see that the initial velocity of vehicle 1 is directly proportional to the final velocities of vehicles 1 and 2 and that the sensitivity as a function of the ratio of the weights R is related to the sine of the difference between the preimpact angles.

Bibliography

Allen, M.E. et al. 1994. Acceleration perturbations of daily living, A comparison to whiplash. *SPINE* 19(11):1285–1290.

American Society of Testing and Materials (ASTM). *E 2493-07 Standard Guide for the Collection of Non-Volatile Memory Data in Evidentiary Vehicle Control Units.* West Conshohocken, PA 19428.

Beer, F. and E.R. Johnston, Jr. 1962. *Vector Mechanics for Engineers: Statics & Dynamics*. New York, NY: McGraw-Hill Book Co.

CFR49. *Code of Federal Regulations.*

Clemens, H.S. and K. Burrow. 1972. Experimental investigations on cervical spine at frontal & rear-end vehicle impacts. *Proceedings of the 16th STAPP Car Crash Conference.* 76–104.

Damask, A.C. and J. Damask. 1990. *Injury Causation Analysis: Case Studies and Data Sources.* Charlottesville, VA: The Michie Company.

Daryanani, G. 1976. *Principles of Active Network Synthesis and Design.* NY: NY John Wiley & Sons. 148–149.

Davis, W.J. 1926. Tractive resistance of electric locomotives & cars. *General Electric Review* 29:685–708.

Donders, F.C. 1868. On the speed of mental processes. *ACTA Psychologica* 30:412–431.

Dorf, R.C. 1980. *Modern Control Systems.* 3rd Ed. Reading, MA: Addison-Wesley.

Douglas, J.D. and R. Burden. 2003. *Numerical Methods.* 3rd Ed. Pacific Grove, CA: Thomson Brooks/Cole.

FMUSS 105. *Federal Motor Vehicle Safety Standard 105.*

FMUSS 121. *Federal Motor Vehicle Safety Standard 121.*

Garber, N.J. and L.A. Hoel. 1996. *Traffic and Highway Engineering.* 2nd Ed. Boston, MA: PWS Publishing.

Gillespie, T.D. 1992. *Fundamentals of Vehicle Dynamics.* Warrendale, PA: Society of Automotive Engineers.

Hicks, W.E. 1952. On the rate of gain of information. *Quarterly Journal of Experimental Psychology* 4:11–26.

Higdon, Archie, et al. 1968. *Mechanics of Materials.* New York, NY: John Wiley & Sons.

Hoffman, J.D. 2001. *Numerical Methods for Engineers and Scientists.* 2nd Ed. NewYork, NY: CRC Press.

Human Tolerance to Impact Conditions as Related to Motor Vehicle Design. April, 1980. Warrendale, PA: Society of Automotive Engineers J885.

Hurt, H. 2006. NHTSA Study. *Motorcycle Accident Cause Factors and Identification Countermeasures.* University of Southern California. Los Angeles, CA.

Johanson, G. and K. Rumar. 1971. Driver's brake reaction times. *Human Factors.* 13(1):23–27.

Jones, I.S. 1983. The effect of impact type and vehicle velocity on vehicle crush characteristics. *27th Proceedings of the American Association for Automotive Medicine*. Barrington, IL 60011.

Kazarian, L.E. et al. 1970. Biomechanics of vertebral columns and organ response to seated spinal impact on rhesus monkeys. *Proceedings of the I4th STAPP Car Crash Conference.* Warrendale, PA: Society of Automotive Engineers.

Kosinski, R.J. 2006. *A Literature Review of Reaction Time.* Clemson, SC: Clemson University.

Krim, J. 1996. Friction at the atomic scale. *Scientific American*, 275 Oct., 74–80.

Laming, D.R.J. 1968. *Information Theory of Choice-Reaction Times.* London, UK: Academic Press.

Limpert, R. 1990. Car-pedestrian accidents. *Accident Reconstruction Journal.* Volume 2 No: 3 May/June 16–18.

Limpert, R. 1992. *Brake Design and Safety.* Warrendale, PA: Society of Automotive Engineers, 255–258.

Lissner, H.R., M. Lebow, and F.G. Evans. 1960. Experimental studies on the relation between acceleration and intracranial pressure changes in man. *Surgery Gynecology, and Obstetrics* 111:329–338.

Loumet, J.R. and W. Jungbaure, 1994. *Train Accident Reconstruction and FELA and Railroad Litigation.* Tucson, AZ: Lawyers & Judges Publishing.

Manual on Uniform Traffic Control Devices for Streets and Highways. 2004. U.S. Department of Transportation Federal Highway Administration. Washington, D.C. 20590

McConnell, W.E. et al. 1993. *Analysis of Human Test Subject Kinematic Responses to Low Velocity Rear Impacts.* SAE 930889. Warrendale, PA: Society of Automotive Engineers.

Mertz H.J. and L.M. Patrick. 1967. *Investigation of the Kinematics and Kinetics of Whiplash.* SAE Paper 670919. Warrendale, PA: Society of Automotive Engineers.

Mertz H.J. and L.M. Patrick. 1971. *Strength and Response of the Human Neck.* SAE Paper 710855. Warrendale, PA: Society of Automotive Engineers.

Morgan, J.R. and D.L. Ivey. 1987. *Analysis of Utility Pole Impacts.* SAE Paper 870607.

Nahum, A.M. and R. Smith. 1977. Intracranial pressure dynamics during head impact. *Proceedings 21st STAPP Car Crash Conference*. Warrendale, PA: Society of Automotive Engineers. National Highway Traffic Safety Administration (NHTSA) Crash Tests.

New York State Department of Motor Vehicles. 2004. *Summary of Pedestrian/Motor Vehicle Accidents.*

New York City Department of Transport. 1991. *Traffic Fatalities Data in New York City.*

NHTSA, NCSA, FARS. 1995–2003 (Final) ARF. 2004. *Pennsylvania Crash Facts and Statistics Report.* 2005. Bureau of Highway Safety & Traffic Engineering, DA Dept of Transportation.

Nystrom, G.A. and G. Kost. 1992. *Application of NHTSA Crash Test Data to Pole Input Predictions*. SAE Paper 920605.

Ogan, J.S. T.L. Alcorn, and J.D. Scott. 1993. Acceleration levels and occupant kinematics associated with vehicle to curb impacts. *Accident Reconstruction Journal* May/June:22–26.

Penrose, R. 2004. *The Road to Reality.* New York, NY: Afred A. Knopf.

A Policy on Geometric Design of Highways and Streets. 2001. Washington, DC: American Association of State Highway and Transportation Officials.

A Policy on Geometric Design of Highways and Streets. 2004. Washington, DC: American Association of State Highway and Transportation Officials.

Prasad, A.K. 1990. *Energy Dissipated in Vehicle Crush—A Study Using the Repeated Test Technique*. SAE 900412. East Liberty, OH: Transportation Research Center of Ohio, Inc.

Roadside Design Guide. 2006. Washington, DC: American Association of State Highway and Transportation Officials.

Rosenbluth, W. 2001. *Investigation and Interpretation of Black Box Data in Automobiles*. West Conshohocken, PA: ASTM.

Sears, F. and M. Zemansky. 1964. *University Physics*. Reading, MA: Addison-Wesley Publishing Company, Inc.

Seelye Elwin, E. 1955. *Design*. 2nd Ed. NY: John Wiley & Sons.

Smith, G.C., M.B. James, T.R. Perl, and D.E. Struble. 1987. *Frontal Crush Energy and Impulse Analysis of Narrow Object Impact*. ASME Paper 87-WA/SAF-5. Boston, MA.

Sears, F. and M. Zemansky. 1964. *University Physics*. Reading, MA: Addison-Wesley Publishing Company, Inc.

Stalnaker, R.L., J.W. Melvin, and G.S. Nusholtz et al. 1977. Head impact response. *Proceedings 21st STAPP Car Crash Conference*. Warrendale, PA: Society of Automotive Engineers.

Steidel, R.F., Jr. 1989. *An Introduction to Mechanical Vibrations*. 3rd Ed. New York, NY: John Wiley & Sons.

Szaho, T.J. et al. 1994. *Human Occupant Kinematic Response to Low Speed Rear End Impacts*. SAE 940532. Warrendale, PA: Society of Automotive Engineers.

Triggs, T.J. and W.G. Harris. 1982. Reaction time of drivers to road stimuli. *Human Factors Report No. HFR-12*.

US Department of Transportation Federal Highway Administration. 2003. *Manual on Uniform Traffic Control Devices for Streets and Highways*.

Vehicle dynamics technology, 1976. *SAE Technical Report J670e*. Warrendale, PA: Society of Automotive Engineers.

Versace, J. 1971. A review of the severity index. *Proceedings 15th STAPP Car Crash Conference*. Warrendale, PA: Society of Automotive Engineers.

Ward, C., M. Chan, and A. Nahum. 1980. *Intercranial Pressure—A Brain Injury Criterion*. Warrendale, PA: Society of Automotive Engineers.

West, D.H. et al. 1993. Low speed rear end collision testing using human subjects, accident reconstruction journal. 5:226.

Yamada, H. 1970. *The Strength of Biological Materials*. Philadelphia, PA: Williams and Wilkins.

Index

G

O

P

R

T

U

V

W

X

Y

FORENSICS AND CRIMINAL JUSTICE

MATHEMATICAL METHODS FOR ACCIDENT RECONSTRUCTION

A FORENSIC ENGINEERING PERSPECTIVE

Over the past 25 years, Harold and Darren Franck have investigated hundreds of accidents involving vehicles of almost every shape, size, and type imaginable. In ***Mathematical Methods for Accident Reconstruction: A Forensic Engineering Perspective,*** these seasoned experts demonstrate the application of mathematics to modeling accident reconstructions involving a range of moving vehicles, including automobiles, small and large trucks, bicycles, motorcycles, all-terrain vehicles, and construction equipment such as hoists and cranes.

The book is anchored on basic principles of physics that may be applied to any of the above-named vehicles or equipment. Topics covered include:

- foundations of measurement
- energy methods used in reconstruction
- momentum methods
- vehicle specifications
- failure analysis
- geometrical characteristics of highways
- visibility, perception, and reaction
- crash data recorders
- low speed impacts
- standards and protocols

Exploring a broad range of accident scenarios and also acknowledging the limits of applicability of the various physical methods employed, the breadth and depth of the book's coverage makes it a critical reference for engineers and scientists who perform vehicular accident reconstructions.

88971

ISBN: 978-1-4200-8897-7
90000
9 781420 088977

CRC Press
Taylor & Francis Group
an **informa** business
www.crcpress.com

6000 Broken Sound Parkway, NW
Suite 300, Boca Raton, FL 33487
270 Madison Avenue
New York, NY 10016
2 Park Square, Milton Park
Abingdon, Oxon OX14 4RN, UK

www.crcpress.com